Aspects of Exotic Option Pricing Theory

by

Savina Kazantzaki

March 2006

A thesis submitted for the degree of Doctor of Philosophy of the University of London and for the Diploma of Imperial College.

Department of Mathematics,
Imperial College London,
180 Queen's Gate, London SW7 2BZ.

Abstract

A study is made of standard options (also known as *plain-vanilla* options) and derivatives with more complicated payoffs known as *exotic options*. Exotic options are interesting for several reasons. They are harder to price as sometimes being very model dependent. They also give the owner greater flexibility and protection against adverse movements of the asset. The valuation of vanilla and exotic options can be quite demanding and complicated when treated analytically, but can be pretty straightforward when done numerically.

We price European options with complicated barriers. Barrier options in general are cheaper than plain vanilla ones because of the risk of either not being knocked-in, allowing the option to become effective when the barrier is hit, or being knocked-out, resulting in the termination when the barrier is hit. How much cheaper a barrier option is compared to a plain vanilla option depends on the location of the trigger. We examine step barrier options in the Black-Scholes framework for single and multi-asset options. We value a single asset European double barrier step option using a Fourier series approach and introduce a moving barrier in time which acts as an upper bound to the step barrier. A series of double barrier problems are presented for three-, five- and multi-asset options.

We provide an analytical valuation method for European style Asian options with a double barrier using the WKB method and illustrate and develop the technique for the case where the barriers jump symmetrically inwards and outwards. We display a more realistic example of such an option, give bounds for the value and compare with the Black-Scholes model.

We also study the effect of transaction costs in the case of Asian options and suggest a procedure for determining the sign of the Gamma when the payoff is single signed. When the sign of the Gamma changes the problem is solved numerically using finite differences.

Acknowledgements

I would like to take this opportunity to express my sincere gratitude to my supervisor Prof C.Atkinson without whom this thesis would not have been possible. His continuous guidance and support has been very valuable.

I am grateful for the financial support from E.P.S.R.C. which funded my studies during the last four years. Also I would like to thank NATO and Embirikio Foundation for their financial support.

My greatest debt is to my parents for their continuous support, financial and emotional, throughout my Ph.D. life.

Finally I would like to thank all my friends and especially Anthoula Macha and Kostandinos Kostandinou for their daily comfort during this experience. Special thanks to Michael Benzinou for being a loyal friend and to Panorea Benatou for her comforting and at the same time entertaining emails from Athens.

Dedicated to my parents,
Nikos and Evanthia Kazantzaki

CONTENTS

LIST OF FIGURES

LIST OF TABLES

1. INTRODUCTION

1.1 Definitions - Background

This thesis focuses on the study of the valuation of exotic options under log-normal distributions and explores different aspects in option pricing theory.

During the last 50 years, derivatives have become increasingly important in the world of finance. The exotic options market has been mostly developed in the foreign exchange market. This has driven the academic interest, in studying exotic options, to a competitive level full of continuously derived models and methods in order to form a better understanding of the pragmatic world of trade.

A study is made of standard options, also known as *plain-vanilla* options, and derivatives with more complicated payoffs known as *exotic options*. Exotic options are interesting as they are harder to price, sometimes being very model independent and can give the owner greater flexibility and protection against adverse movements of the asset. The valuation of vanilla and exotic options can be quite demanding and complicated when treated analytically but can be pretty straightforward when done numerically although care has to be taken with regard to the speed and accuracy.

Derivatives are securities[1] whose value depend on or are derived from the price of some other time-varying quantity. Usually that other quantity is the price of some other asset such as bonds, stocks, currencies, or commodities. Derivatives were created to support an insurance market against fluctuations. An option is an instrument that gives the owner the right, but not the obligation, to buy or sell a specified number of an underlying asset at a specified price called the *exercise price* or the *strike price*, within a specified period of time called the *expiration date* or *maturity*. It is widely known that there are two types of options depending on whether the holder of the option wants to buy or sell an asset. A *call* option gives the holder of the option the right to purchase a particular asset for an agreed price at a specified time in the future, Hull [39]. A *put* option gives the holder of the option the right to sell a particular asset for an agreed price at a specified time in the future. If the option is exercised on its maturity date it is said to be *European*, while if it may be exercised anytime prior to

[1] Notes, bonds, stocks, futures contracts, options or any other interests or instruments are commonly known as *securities*.

expiry it is said to be *American.* A *long position* in the context of options, is when an investor buys the right to buy (call) or sell (put) an option at a specific price and date. For a *short position* its the opposite where the investor sells an options contract.

In European options one can exercise the option only on the expiration date itself. If we use S to denote the stock price of the underlying asset and K the strike price then the value (payoff) of a call option at the maturity date $t = T$ will be $\max(S - K, 0)$. This value is the *intrinsic value* of the call option and will be exercised at time $t = T$ if the stock price of the underlying asset S is bigger than the strike price K (*in-the-money option*), i.e. will take the value $S - K$ and won't be exercised if the stock price S is less than the strike K (*out-of-the-money option*), i.e. will take the value zero. The case where the stock price is equal to the strike price the option is said to be *at-the-money.* Therefore, the payoff function of a European option is

$$V_C(S,T) = \max(S - K,\, 0)\,,$$

for the case of a call and

$$V_C(S,T) = \max(K - S,\, 0)\,,$$

for the case of a put.

There are securities where the payoff depends on the average price of the underlying asset over a certain interval. Those securities are known as Asian options and are commonly traded in the over-the-counter market. The underlying asset can be anything like stocks, stock indices, foreign currencies, debt instruments, commodities and many different futures contracts. Such securities protect traders against the adverse movements of the market. Asian options are path-dependent options and are particularly difficult to value as their future value depends on the entire path of the stock price rather than just on its final price. They have a payoff that depends on the price history of the underlying via some kind of average. Different definitions use a continuous or a discrete sampling of the price history of the underlying asset and involve an arithmetic or geometric average. For the case of European type Asian options, if A is the average stock price and K the strike price, the payoff function of a call option is

$$V_C(S,T) = \max(A - K,\, 0)\,,$$

and for a put option is

$$V_P(S,T) = \max(K - A,\, 0)\,.$$

Asian options can be distinguished in two types, the fixed-strike and the floating-strike Asian options. For a *fixed-strike* Asian option the payoff is the difference between the average price of the underlying and the predetermined strike price, $A - K$, whereas for the *floating-strike* Asian option the payoff is the difference between the spot price[2] and the average price of the underlying, $S - A$. Average strike options can guarantee that the average price paid for an asset in frequent trading over a period of time is not greater than the final price. This makes them cheaper than other options. Finally there are two types of averaging; the *arithmetic average* which is the mean of the asset price, and the *geometric average* which is the exponential of the mean of the logarithm of the asset price. If S_t is the asset price corresponding to time t, then the average can be written as

$$A = \begin{cases} \frac{1}{t}\int_0^t S(u)\,du & \text{, if arithmetic} \\ \\ \exp\left(\frac{1}{t}\int_0^t \ln S(u)\,du\right) & \text{, if geometric} \end{cases} .$$

1.2 Asian options

There are various ways to price options and a considerable amount of analytical and numerical work has been done in valuing European type Asian options. The difficulty in pricing them is that one does not know how to describe analytically the distribution of the sum, if discrete, or integral, if continuous, of the logarithms. Some recent work has been done on the discrete problem, Atkinson and Fusai [3].

A quite popular method of pricing Asian options is by taking the Laplace transform of the value of the option. Geman and Yor [29] derived an analytic solution of the arithmetic Asian option, which is 'out of the money', in terms of the inverse Laplace transform of a confluent hypergeometric function. They used the method of the fast Fourier transform to calculate the inverse Laplace transform of the value of the Asian call option (Geman and Eydeland [27]). Even though the numerical inversion of the Laplace transform is a difficult task, Fu, Madan and Wang [23] investigated the Laplace transform inversion using Monte Carlo simulation to price continuous Asian options. Donati, Ghomrasni and Yor [20] priced Asian options by obtaining a closed formula for the Laplace transform of the first moment with exponentials of the Brownian motion with a drift. Fusai [24] priced Asian options by computing a Laplace transform with respect to the maturity and a Fourier transform with respect to the logarithm of the strike and numerically inverted the double transform using the multivariate version of the Fourier-Euler algorithm. Carr and Madan [10] used the fast Fourier transform to

[2] The present delivery price of a given financial instrument being traded on the spot market.

value options using the density function. Also, Fusai and Tagliani [25] inverted the Geman and Yor [29] Laplace transform using the trapezoidal rule and evaluated fixed strike Asian options using moments. Lipton [51] deduced an ordinary differential equation (ODE) by taking the Laplace transform of the value of the option and expressed it in terms of hypergeometric functions obtaining a complete solution. The Geman and Yor problem has been revisited by Carr and Schröder [12], [11].
Another approach is by approximating the density function for the distribution of the average by a lognormal function. Turnbull and Wakeman [69] and Ritchken, Sankarasubramanian and Vijh [59] use the Edgeworth series expansion to approximate the probability density function of the average rate. The former obtained a formula for European arithmetic options and deduced a closed-form for European geometric options, while the latter found exact formulas for the European geometric options. Marcozzi [53] formed an ultra-parabolic variational equation satisfying the value of an Asian option. Carverhill and Clewlow [13] used the convolution method as an efficient and flexible way of valuing Asian options. They mainly concentrated on the fixed-average options and employed the fast Fourier transform to compute the convolution of the summed densities.

A well known approach for valuing Asian options is the formulation of a parabolic partial differential equation (PDE) whose solution can be found analytically and numerically. A very popular method of pricing fixed-strike Asian options is by solving the formed PDE using numerical methods, most popular being Monte Carlo simulation (e.g. Kemna and Vorst [43], Rogers and Shi [62]) and finite difference methods (e.g. Alziary, Décamps and Koehl [2]). Rogers and Shi [62] were the first ones to find a scaling property to reduce the problem to a problem of solving a one-dimensional parabolic PDE for the floating and fixed strike Asian option. They provided a lower bound that turned out to be the true price for the option. Thompson [68] derived the bounds found by Rogers and Shi [62], by the use of one-dimensional integrals and showed numerical evidence for it.
The concept of using the similarity variable has been successfully used by Rogers and Shi [62], Ingersoll [41], Wilmott, Dewynne and Howison [73], Lipton [51]. Using the similarity variable to reduce the dimensionality of the problem decreases the computing time. A similar PDE approach for Asian options was produced by Barucci, Polidoro and Vespri [5] who derived a parabolic PDE for the case of the arithmetic average using the similarity variable. Alziary, Décamps and Koehl [2] derived a one-variable PDE whose solution gives the value of a European type Asian option and gave an analytical approach by comparing Asian and European options. Večeř [71] formed an average for both discrete and continuous arithmetic average types and formed a one-dimensional PDE for the price of the Asian option which accommodates continuous or

discrete dividends. Vecer [70] studied the arithmetic average Asian options by solving a one-dimensional PDE, applied to both continuous and discrete average Asian options. Zhang [75] presented a semi-analytical method to price the arithmetic average rate Asian option with continuous sampling. He derived a new analytical approximation formula by using a singularity removal technique governed by a PDE which was solved numerically accurately. In 2003 he studied the value of continuously sampled Asian options (both geometric and arithmetic) by solving the PDE with the perturbation method and obtaining an analytical solution in a series form. Hugger [35] formulated a PDE for the Asian call option and also provided boundary conditions for the Asian options.

The floating-strike Asian option has received far less attention in research as one requires to find a relationship between the underlying asset price S_t and the average A_t. Henderson and Wojakowski [33] presented a symmetry result between the floating and fixed-strike Asian options. It was shown by Rogers and Shi [62], Alziary, Décamps and Koehl [2], Ingersoll [41] and Večeř [71] that the floating-strike Asian option satisfies a one dimensional PDE. However this one-dimensional PDE is difficult to solve numerically as the diffusion term is very small for values of interest on the finite difference grid. The dirac delta function appears as a coefficient of the PDE in the case of the floating strike option. The PDE framework can also be applied for the case of discrete Asian options. Benhamou and Duguet [7] priced discrete Asian options with and without dividends using the PDE framework and gave numerical results using the Crank-Nicolson method.

Linetsky [50] formed a one dimensional diffusion equation and provided a series and an integral representation of continuously sampled arithmetic Asian options using the Sturm-Liouville problem. Fouque and Han [22] applied the asymptotic framework to derive two one-dimensional partial differential equations for pricing Asian options with stochastic volatility which they solved numerically. Matacz [54] gave an integral representation of the path-dependent option price by performing partial averaging on the underlying risk-neutral diffusion process. Večeř and Xu [72] priced Asian options in a semimartingale model, by removing the path-dependent variable in the payoff of all kinds of Asian options.

1.3 Barrier options

An appealing factor when studying exotic options is investigating the effect of barriers. There are various kinds of barrier options such as plain vanilla options, time-dependent barrier options, Asian barrier options or barrier options which depend on the average of the underlying asset prices, window or limited-time barrier options. In general they are called exotic barrier options. Barrier options, also called trigger options, are similar to standard options except that the options are eliminated or activated when the underlying asset price reaches a predetermined barrier or boundary price. Therefore they are path-dependent options since their value depends on the price movement of the underlying asset. Barrier options are very popular in the over-the-counter market as they are more cost effective than the standard options which are path-independent in which case it does not matter what path the underlying asset takes during the life of the option. There are two main types of barrier option, the *out* option, that only pays off if a level is not reached by the asset (*knock-out* option) and the *in* option, that pays off if the level is reached by the asset before expiry (*knock-in* option). For the latter definition see Wilmott [74]. Furthermore there is the characterization of the position of the barrier relative to the position of the initial value of the underlying. If the barrier is above the initial asset value then we have an *up* option, whereas if it is under the initial asset value we have a *down* option. The payoff at expiry can be any of the common contracts, like a call, put, binary. During the life of these contracts the position of the barrier could change as time evolves either discretely or continuously. In theory barrier monitoring is assumed to be continuous, but in practice it is often discrete. We will be examining continuously expanding barrier options, chapter 3.

A wide variety of literature exists in the case of single barrier options. Lo, Yuen and Hui [52] used a PDE for the square root constant elasticity of variance (CEV) to derive an analytical formula, in terms of the confluent hypergeometric function, to price up-and-out options using the eigenfunction expansion technique. Ritchken [60] used lattice procedures to price a wide range of single barrier options that are either at constant levels or they vary with time. The implicit method for solving PDE models presented by Zvan, Vetzal and Forsyth [78] accommodated the case for valuing options with barriers. They used the PDE method which was valid in pricing discrete Asian options with or without barrier features. Their method numerically can be used for pricing floating and fixed strike, American or European options. The binomial lattice model was used by Ritchken [60] who provided a simple and efficient algorithm to price and hedge options that have single or multiple barriers. Roberts and Shortland [61] price barrier options with time-dependent coefficients by using boundary-crossing time estimation techniques and obtain tight bounds on the price of the option. Kou [45] analyzes a big variety of one-dimensional single discrete barrier options by simplifying the barrier correction formula given by Broadie, Glasserman and Kou [9] who propose a continuity correction for the discretely monitored barrier option. The latter introduced a continuity correction for discrete barrier options. Hui, Lo and Yuen [38] used the square root constant elasticity of variance (CEV) process to derive an analytical solution for up-and-out European barrier options by applying

the eigenfunction expansion technique. They produced numerical results, which vary significantly as time to maturity and volatility increases and compared them with the corresponding Black-Scholes model. Heritage [34] approximated the price of an up-and-out call moving average barrier option in terms of the price of the corresponding standard barrier option on the Black-Scholes model.
There has also been work done for high dimensional radial single barriers by Firth and Dewynne [21]. They provide solutions for the case of multi-asset radial knock-in barrier in one, three and five dimensions. However, they consider a highly idealised relation between the assets so that they have radial symmetry. We shall also consider such special problems in sections 5.3 and 5.5.1. They use Laplace transform methods to find an analytical expression for valuing multi-asset barrier options. Also Linetsky [48] valued floating barrier[3] options using a path integral representation of the (transition) probability density function. He valued time-dependent ladder-like barriers using the density function obtained by using the convolution of two standard down-and-out densities.

An extension of single barrier options are double barrier options. These are options which have a barrier above and below the price of the underlying asset. In this case the option gets knocked in or out as soon as one of the two barriers is hit. Kunitomo and Ikeda [46] derive closed-form pricing formulae for curved boundaries by expressing the value of double-barrier knock-out put and call European options as an infinite series of weighted normal distribution functions. They also examine the convergence of the series, by using some numerical examples and discuss a more general case of curved boundaries. Upper and lower bounds in the form of double integrals were derived by Thompson [67] for pricing European options with a knock-out clause containing one or two curved boundaries. Schröder [64] constructed a pricing formula series for double-barrier options which converges much faster than the one given by Kunitomo and Ikeda [46]; he provides numerical evidence by introducing a convergence parameter. Rogers and Zane [63] find a method of simply transforming the knock-out moving barrier problem to a fixed barrier, which they numerically evaluate. Kolkiewicz [44] finds the values of different forms of European double barrier options with and without exponentially time dependent boundaries by representing the exit time densities as infinite series of exponential functions. Pelsser [57], [58] derived some pricing formulas for different kinds of basic double barrier options and expressed them in terms of trigonometric series. He used the Bromwich integral to invert the Laplace transform of the probability density function of the asset hitting the lower and upper barrier (double knock-out barrier). Hui, Lo and Yuen [38] used the method of reflection to express

[3] Floating barrier options (FBOs) are options on the underlying payoff asset with the barrier proportional to the price of the second barrier asset, Linetsky [48].

the value of a double barrier option as the sum of infinite series of the cumulative normal distribution. Roberts and Shortland [61] give simple and easy-to-use method for calculating barrier options with time-dependent coefficients by applying boundary-crossing time estimation techniques in order to obtain tight bounds on the option price. Haug [32] used a put-call transformation for valuing single barrier options to value double barrier options. Kolkiewicz [44] provided a pricing and hedging strategy using infinite-series representations of the density functions of the exit times through the upper and lower barrier.

Most of the solutions that exist on double barrier options are either expressed as the sum of infinite series or as inverse Laplace transforms. Geman and Yor [30] obtained a simple expression of the Laplace transform of the option price for the case of double barrier options with fixed boundaries, similar to the one they had for the Asian options and provided numerical evidence using Monte Carlo simulation. Craddock, Heath and Platen [15] evaluated double barrier options by Laplace inverting the value of a European call option using various numerical inversion schemes and compared them. They Laplace inverted the Geman and Yor [29] Asian Laplace transform call option solution after expressing it in terms of the confluent hypergeometric function and finally just in terms of the Gamma function. Sidenius [66] priced double knock-out options by finding the probability density of the asset conditioned if neither the two barriers are hit during the lifetime of the option and he took the Laplace transform of the densities and found them identical to Geman and Yor. Davydov and Linetsky [17] priced double barrier options by taking the discounted risk-neutral expectation of the payoff as the value of the option and represented the transition density as an inverse Laplace transform, as a series of normal densities and as a Fourier series. They used Euler's algorithm to invert the Laplace transform. Hui [36] valued a one-touch double knock-out barrier binary option using the Black-Scholes framework. He provided an analytical solution to both European and American options using Fourier series and estimated the convergence. Under the same framework, he studied the Black-Scholes equation by pricing rear- and front-end single and double barrier call options and also the effect on the Greeks[4] against the price and maturity, Hui [37].

Another method to approach the valuation of a double barrier option numerically is by using a partial differential equation. Zvan, Vetzal and Forsyth [78] value double barrier European options using a fully implicit method to solve the PDE numerically and compared it with the Crank-Nicolson method. They also considered the case of a two-asset barrier option and produced numerical evidence. Linetsky [49] studied barrier and arithmetic Asian options by using a PDE and taking eigenfunction expansions using the Liouville transformation. Similarly, Davydov and Linetsky [18] priced single

[4] Greeks are hedge parameters such as delta, gamma, vega, theta and rho.

and double barrier options using the linearity of the pricing operator and the eigenvector property of the eigen-securities and illustrated them numerically using the constant elasticity of variance process and the Cox-Ingersoll-Ross term-structure model. Costabile [14] priced European barrier options with time-dependent and multiple boundaries on a binomial tree. Broadie, Glasserman and Kou [9] used the pricing formula for continuous path-dependent options to approximate the price of discrete options and used the trinomial lattice method to price discrete barrier options.

The type of barrier that we will be examining is the double barrier, where the two barriers are positioned under and above the initial value of the asset. More precisely we will study the effect of double knock-out barriers for Asian options and down-and-in, up-and-out European options. The payoff of such an option is based on the history of the price of the underlying asset up to the expiration date.

1.4 *Basket options*

Another outlet of Asian options is where the payoff depends on the value of a portfolio of assets (multiple underlying assets). These options are known as basket options and are quite challenging to price. Dahl and Benth [16] express the value of the Asian basket option as multi-dimensional integrals and use quasi-Monte Carlo methods to value the option. Ju [42] uses the Taylor expansion around zero volatility to approximate the value of a basket option. Akcoglu, Kao and Raghavan [?] propose three techniques to price discrete European type Asian basket options whose underlying assets follow the binomial tree model. They use Monte Carlo simulation, a general recursive bucketing-based scheme and a combination of Fast Fourier Transform (FFT) and bucketing-based schemes to price European Asian basket calls.

1.5 *Transaction costs*

An interesting effect is the presence of transaction costs when valuing options. Leland [47] considered a model that allows transactions only at discrete times. By adopting a δ-hedging argument, he derived an option price that converges to a Black-Scholes price as transaction costs become arbitrarily small with an adjusted volatility. Barles and Soner [4] applied a utility function approach as well as an asymptotic analysis of a nonlinear PDE under the effect of transaction costs. Gondzio, Kouwenberg and Vorst [31] propose a stochastic optimization model for hedging contingent claims and take into account the effects of stochastic volatility and transaction costs. The presence of transaction costs affect the volatility and therefore the governing equation. Morozovsky [56] constructed a modified Black-Scholes equation with transaction costs and gave a solution to the equation for the case where the option was close to expiry and the case where the transaction costs were small. Dewynne, Whalley and Wilmott [19] constructed a PDE model for valuing exotic options with the possibility of a similarity solution. They used explicit finite differences to overcome the strong nonlinearity caused by the transaction costs term.

1.6 Numerical methodology

The most popular approach in valuing path-dependent options and specifically Asian options is numerically. The majority of the work done is based on the Monte Carlo simulation as well as on different models using the finite difference grid. One of the first well-known studies in that area is by Kemna and Vorst [43] who use Monte Carlo simulation to determine the price of an average value-option expressed as a PDE. They show that an out-of-the-money[5] standard option can be expected to be significantly more expensive than an average value option and they find an analytical value for a geometric average option. Monte Carlo simulation was also used by Ritchken, Sankarasubramanian and Vijh [59] to price a number of path-dependent contracts, average and lookback[6] option values, and Rogers and Shi [62] provided numerical results for the PDE with very good accuracy.

Benhamou and Duguet [7] derive a PDE for the Asian option which they solve quite efficiently with the standard Crank-Nicholson method. Zvan, Forsyth and Vetzal [77] explore the pricing of Asian options numerically by solving a one-dimensional similarity variable PDE and a two-dimensional PDE using finite differences. The two-dimensional PDE that rises for the case of the Asian option can be reduced to a one-dimensional one by introducing an appropriate similarity variable, Ingersoll [41], Wilmott and Dewynne [73], Rogers and Shi [62]. This can happen only when the payoff is of a particular form and is consistent with the similarity variable itself. However these kind of PDEs can apply only to European-style options and it is difficult to numerically solve them as the diffusion term is very small compared to the values taken on the finite difference grid. Alziary, Décamps and Koehl [2] derived a one-state variable PDE for pricing a European type Asian option (for both fixed and floating-strike) and solved it numerically by applying a modified explicit method (similar to the one used by Hull and White [40]). Fusai, Sanfelici and Tagliani [26] commented on the different numerical schemes used in solving PDEs in finance. They mainly focused

[5] An option is said to be out-of-the-money when either in the case of a call option the asset price is less than the strike price, or in the case of a put option the asset price is greater than the strike price (Hull [39]).

[6] Lookback options have a payoff that depends on the realized maximum or minimum of the underlying asset over some period prior to expiry.

on the finite difference and finite element approach. Linetsky [50] provided numerical examples using a series and an integral representation to compute continuously sampled arithmetic Asian options using the Sturm-Liouville property. Fouque and Han [22] solved with finite differences two one-dimensional partial differential equations using the asymptotic framework for pricing Asian options with stochastic volatility. As the biggest disadvantage of the explicit method is the lack of convergence, Hull and White [40] provided a systematic procedure for implementing a modified version of the method in such a way that convergence is guaranteed when Δt tends to zero.
The finite differences numerical method was used by Meyer [55] who solved the problem for the fixed-strike Asian call. Zhang [75] developed a fast and accurate method of pricing and hedging European average rate Asian options with continuous sampling by constructing a PDE using a similarity variable equivalent to that of Rogers and Shi [62] and solved it numerically using the Crank-Nicolson scheme. Later on Zhang [76] used the perturbation method to write the solution of the governing PDE in a series form and observed numerically that the series solution converges very quickly giving a good approximate value that is more accurate than any other approximate method.

Another method mentioned in earlier sections is the numerical inversion of the Laplace transform. Craddock, Heath and Platen [15] priced Asian options by using various numerical methods to invert the Laplace transform of Geman and Yor [29] after expressing it as a series of the Gamma function. Abate and Whitt [1] suggested numerical methods (Euler and Post-Widder) of inverting the Laplace transform of the probability distribution.

1.7 Structure of the thesis

The plan of the thesis is as follows. In chapter 2 we present the Asian option framework by deriving the governing two-dimensional PDE equation using the delta hedging framework. More specifically we derive a simpler one-dimensional PDE using the martingale method formed by Rogers and Shi [62] and by delta hedging with the underlying asset. Furthermore we discuss special cases by introducing two similarity variable frameworks adapted by Wilmott, Dewynne and Howison [73] and Rogers and Shi [62] (similar to the one introduced by Geman and Yor [29]).

In chapter 3 we examine step barrier options in the Black-Scholes framework for single and multi-asset options (basket options). We introduce a moving barrier in time which is a good bound for the step barrier found later in chapter 4. The moving barrier grows symmetrically in time creating a wedge which acts as a double barrier to the underlying. We generalise the method for baskets with N underlying assets and give examples of the problem in two, three and five dimensions.

In chapter 4, we value a single-asset European double barrier step option using the Black-Scholes equation, where the two barriers are knock-out. We use a Fourier series approach to address the nature of the problem. We assume that there is a symmetrically expanding barrier in time, wedge, which acts as an upper bound to the step barrier. Additionally, we assume there is another expanding barrier inside the wedge so that the step barrier moves between the two expanding barriers. We value the step barrier under the effect of the two wedges and give numerical evidence for the pricing as well as for the upper bound of the Fourier step barrier.

In chapter 5, the problem with the double knock-out barrier is extended to the case where there are N underlying assets in the option. We employ the Fourier series approach to express the solution in terms of Bessel functions of first and second kind and suggest that the WKB method can also be used to value the option accurately. As an example we value a basket option with three underlying assets which can be easily transformed to the classic heat equation. For the case where there are five underlying assets the Fourier series approach applies giving satisfactory results.
We study the effect of a double knock-out barrier for the three- and five-dimensional problem in which the upper barrier is far away from the lower barrier. We verify that this problem structure is equivalent to the single knock-in barrier problem treated by Firth and Dewynne [21]. For the three-asset option we apply the method of images to deduce the solution given by Firth and Dewynne [21] and extend the problem to the case where the barrier jumps. In the five-asset option we apply the Fourier series solution method to the problem of Firth and Dewynne [21]. The above problem is extended to one where an expanding barrier plays the role of the lower bound to the Fourier series step solution. Numerical evidence is given for the bound as well as for the value during the life of the option.

In chapter 6 we value European Asian options with the effect of double knock-out barriers. Because of the nature of the problem we value these options using the WKB method and present numerical evidence. In Appendix A we test the accuracy of the WKB solution against the exact solution of the PDE in terms of a conjugate pair of Bessel functions of first kind. We examine how the value of the option changes when the two barriers shrink and widen. We apply the method for a more realistic payoff than the one used to test the method and give bounds for the solution.

We study the price of Asian options with the effect of transaction costs in chapter 7. We take the one-dimensional similarity variable PDE for the case of a fixed- and floating- strike Asian option and suggest a method to determine the sign of the Gamma term according to the nature of the problem. The solution of the latter PDE is exploited numerically in chapter 8.

Finally, in chapter 8 we provide the framework of the numerical approach we utilise to value some of the problems we mentioned earlier. We use the explicit finite difference scheme to value PDEs for Asian options with the similarity variables with and without the effect of transaction costs. Even though the method requires some attention to maintain stability, it is easy and fast to implement.

2. FRAMEWORK AND FUNDAMENTAL EQUATIONS

2.1 Framework

We consider a standard complete market economy. The price of a stock option is a function of the underlying stock's price and time. Suppose that the price of some risky asset at time t is S_t. As its value changes over time in an uncertain way it is said to follow a stochastic process. We assume the underlying asset S follows the log-normal random walk

$$dS = \mu S\, dt + \sigma S\, dX_t, \tag{2.1}$$

where μ is the drift and σ is the volatility of the stock price. Both of these parameters are assumed constant (drawn from the normal distribution with mean of zero and standard deviation of 1.0). dX_t is the increment of the Brownian motion X_t [1]. Equation (2.1) is a Stochastic Differential Equation (SDE) and is a continuous-time model of the underlying asset price.
Most of the academic literature on path-dependent options follow the lead set by Black and Scholes [8] and assume that the underlying asset price follows geometric Brownian motion with constant volatility. This implies that the future asset prices are log-normally distributed which leads to tractable analytical formulae. By saying that a variable has a log-normal distribution means that the logarithm of the variable has a normal distribution. In order to change the measure, the normal distribution is transformed to a log-normal distribution by defining $x = \ln S$.

A Markov process is a particular type of stochastic process where only the present value of a variable is relevant for predicting the future.

Consider a small change in x as t goes to $t + dt$ (and so $S \to S + dS$) and taking in mind the properties of the Brownian motion, the price of the risky asset at time t

[1] Brownian motion or else Wiener process is the continuous-time equivalent of the Normal distribution with a mean change zero and a variance rate of 1.0 per year. One can think of dX_t being a random variable drawn from a Normal distribution with mean zero, $\mathbb{E}[dX_t] = 0$, and variance dt $\mathbb{E}[dX_t^2] = dt$

is given by the following equation,

$$S_t = S_o \exp\left[\left(r - \frac{1}{2}\sigma^2\right)t + \sigma X_t\right],$$

which can be considered as a model for a random walk[2] of the asset price.

Our aim is to compute the value of an Asian call option with maturity T, strike K written on a risky asset S_t. As we have no general analytical solutions for the price of the Asian options, a variety of techniques have been developed over the years to analyze this kind of path-dependent option.

In general, the value of an average value option depends on the average value of the stock I, the value of the stock S as well as on the time t, $V(I, S, t)$. Consider a small time-step $t \rightarrow t + dt$ where the value of the option changes by

$$dV(I,S,t) = \frac{\partial V}{\partial t}\,dt + \frac{\partial V}{\partial I}\,dI + \frac{1}{2}\frac{\partial^2 V}{\partial I^2}\,(dI)^2 + \frac{\partial V}{\partial S}\,dS + \frac{1}{2}\frac{\partial^2 V}{\partial S^2}\,(dS)^2 + \frac{\partial^2 V}{\partial I\,\partial S}\,dI\,dS\,,$$

where $I = \int_0^t S(\tau)\,d\tau$ is the average (running sum). Taking into consideration the properties of the Brownian motion, from equation (2.1) we have $(dS)^2 = \sigma^2 S^2 dt$, $dI = S\,dt$ and $dS\,dI = O(dt^{3/2})$ and the above equation can be rewritten as

$$dV(I,S,t) = \left(\frac{\partial V}{\partial t} + S\frac{\partial V}{\partial I} + \frac{1}{2}\sigma^2 S^2 \frac{\partial^2 V}{\partial S^2}\right)dt + \frac{\partial V}{\partial S}\,dS\,.$$

We construct a portfolio consisting of the value of the option V and a small amount Δ of the underlying S,

$$\Pi = V - \Delta S\,.$$

We consider a small change of the portfolio, Π, in a small time-step $t \rightarrow t + dt$ and we keep Δ fixed at the beginning of the time interval

$$d\Pi = dV - \Delta\,dS\,.$$

The portfolio changes by

$$d\Pi = \left(\frac{\partial V}{\partial t} + S\frac{\partial V}{\partial I} + \frac{1}{2}\sigma^2 S^2 \frac{\partial^2 V}{\partial S^2}\right)dt + \frac{\partial V}{\partial S}\,dS - \Delta\,dS\,.$$

The deterministic terms are the dt terms, whereas the random terms are the ones with

[2] A random walk has the property that it is a Brownian motion and is also normally distributed.

the dS where the risk lies. The risk in the portfolio can be eliminated by carefully choosing the value of the constant quantity Δ. By choosing

$$\Delta = \frac{\partial V}{\partial S},$$

the randomness is reduced to zero. This is called delta hedging and is achieved by exploiting the correlation between the option and its underlying. By choosing the value of Δ, the portfolio we hold changes by

$$d\Pi = \left(\frac{\partial V}{\partial t} + S\frac{\partial V}{\partial I} + \frac{1}{2}\sigma^2 S^2 \frac{\partial^2 V}{\partial S^2} \right) dt.$$

This change is completely riskless. The model taken into account contains a risk free cash account which is employed in the formation of self financing replicating portfolios from which we then obtain the various pde's we have to solve. If we have a complete risk-free change $d\Pi$ in the portfolio value Π then it must be the same as the growth we would get if we put the equivalent amount of cash in a risk-free interest-bearing bank account, i.e. set

$$d\Pi = r\Pi\, dt = r\left(V - S\frac{\partial V}{\partial S} \right)$$

to eventually get a partial differential equation which is similar to the Black-Scholes equation with the derivative of the average added;

$$\frac{\partial V}{\partial t} + S\frac{\partial V}{\partial I} + rS\frac{\partial V}{\partial S} + \frac{1}{2}\sigma^2 S^2 \frac{\partial^2 V}{\partial S^2} - rV = 0\,. \tag{2.2}$$

The continuously sampled arithmetic average $A = \frac{1}{t}\int_0^t S(\tau)\, d\tau$ can be written in terms of the running sum $I = \int_0^t S(\tau)\, d\tau$ as $A = \frac{I}{t}$. The equation (2.2) is a two-dimensional PDE given by Ingersoll [41] and the option value V depends on three variables, I, S and t. Note that neither dividends nor transaction costs are taken into account for the formulation of the above equation.

Therefore the payoff at expiry for a floating-strike call is

$$\max\left(S - \frac{1}{T}\int_0^T S(\tau)\, d\tau, 0 \right),$$

and for a floating-strike put (e.g. Wilmott, Dewynne and Howison [73]) the payoff is

$$\max\left(\frac{1}{T}\int_0^T S(\tau)\, d\tau - S\,, 0 \right).$$

For the case of a fixed-strike call and put option the payoff will be

$$\max\left(\frac{1}{T}\int_0^T S(\tau)\,d\tau - K\,,0\right) \quad \text{and} \quad \max\left(K - \frac{1}{T}\int_0^T S(\tau)\,d\tau\,,0\right),$$

respectively.

2.2 Special Case

There are special cases where different types of payoff can depend only on two variables. For those types of payoffs the PDE (2.2) can be written in terms of two variables only. In these special cases the average admits to have a similarity reduction using a similarity variable. The similarity variable is carefully chosen so that it is consistent with the payoff. The method of 'similarity variables' amounts to changing the numeraire Geman, Karoui and Rochet [28]. We examine the case of a call and a put Asian option with a floating-strike payoff which can be expressed in terms of the similarity variable R. The variable R in this case is equal to the running average of the asset over the price of the underlying, i.e.

$$R = \frac{\int_0^t S(\tau)\,d\tau}{S} = \frac{I(t)}{S}\,. \tag{2.3}$$

To check the consistency of the similarity variable with the payoff, we rearrange the payoff so that it can be written as a function of R only. Rearranging the payoff for a floating-strike Asian call option we find

$$\begin{aligned} V(S,I,T) &= \max\left(S - \frac{1}{T}\int_0^T S(\tau)\,d\tau, 0\right) = S\max\left(1 - \frac{1}{TS}\int_0^T S(\tau)\,d\tau, 0\right) \\ &= S\max\left(1 - \frac{R}{T}\right). \end{aligned}$$

A natural choice for an Asian call option is of the form

$$\max\left(S - \frac{1}{t}\int_0^t S(\tau)\,d\tau, 0\right),$$

where the running average is taken from time 0 to t. This also gives the correct payoff at $t = T$, known as the floating-strike call option (p. 27).
The intrinsic value for the floating-strike call option can be written as

$$S\max\left(1 - \frac{1}{St}\int_0^t S(\tau)\,d\tau, 0\right).$$

Define a similarity variable R to be

$$R = \frac{1}{S}\int_0^t S(\tau)\, d\tau\,,$$

which in terms of the running sum I becomes

$$R = \frac{I}{S}\,.$$

Therefore the intrinsic value takes the form

$$S \max\left(1 - \frac{R}{t}, 0\right) \quad \text{and} \quad S \max\left(1 - \frac{R}{T}, 0\right) \text{ at } t = T\,,$$

which looks more like the payoff for a put option.
In a small time interval, as t increases to $t + dt$, R changes as

$$\begin{aligned} dR &= \frac{1}{S + dS}\int_0^{t+dt} S(\tau)\, d\tau - \frac{1}{S}\int_0^t S(\tau)\, d\tau \\ &= \frac{1}{S}\left(1 + \frac{dS}{S}\right)^{-1}\left(\int_0^t S(\tau)\, d\tau + \int_t^{t+dt} S(\tau)\, d\tau\right) - \frac{1}{S}\int_0^t S(\tau)\, d\tau\,. \end{aligned}$$

Expanding and rearranging we end up with a stochastic differential equation for the similarity variable R which doesn't depend on S explicitly

$$dR = [1 + R(\sigma^2 - \mu)]\, dt - R\,\sigma\, dX\,. \tag{2.4}$$

The value of the option takes the form

$$V(I, S, t) = S\, H(R, t)\,,$$

and the PDE (2.2) in terms of the similarity variable becomes

$$\frac{\partial H}{\partial t} + \frac{1}{2}\sigma^2 R^2 \frac{\partial^2 H}{\partial R^2} + (1 - rR)\frac{\partial H}{\partial R} = 0\,, \tag{2.5}$$

assuming the underlying pays no dividend, with payoff

$$H(R, T) = \max\left(1 - \frac{R}{T}, 0\right)\,.$$

Equation (2.2) is reduced to a one-dimensional parabolic PDE (2.5) which depends only on the two variables R and t. This is possible because the average strike option admits similarity reduction. The value of the Asian option depending on three independent variables cannot always be reduced to a function of two variables, as there are options governed by different equations with different payoffs.

We can derive a similar PDE when applying this method for a similarity variable almost identical to the one introduced by Geman and Yor [29] and by Rogers and Shi [62]. We have a European Asian option governed by equation (2.2) with a fixed-strike payoff of the form

$$V(S,I,T) = \max\left(\frac{1}{T}\int_0^T S_\tau \, d\tau - K,\, 0\right), \tag{2.6}$$

for which we introduce the similarity variable

$$U = \frac{1}{S}(K_1 - I), \tag{2.7}$$

where $K_1 = K\,T$. The pde (2.2) takes the form

$$\frac{\partial W_1}{\partial t} + \frac{1}{2}\sigma^2 U^2 \frac{\partial^2 W_1}{\partial U^2} - (1 + rU)\frac{\partial W_1}{\partial U} + rW_1 = 0, \tag{2.8}$$

where $V(S,I,t) = \exp\left(-r(T-t)\right) V_1(S,I,t)$ and $V_1(S,I,t) = \frac{S}{T} W_1(U,t)$. At $t = T$, the payoff for a call option in terms of the similarity variable U will be

$$W_1(U,T) = \max(-U\,,0). \tag{2.9}$$

Equation (2.8) is identical to the equation found by Rogers and Shi [62] the derivation of which will be shown further on. From the payoff we see that U can have negative values as well. For negative U, the value of the option will be positive otherwise zero. The equation (2.8) can be without the rW_1 term just by taking $V(S,I,t) = S\,W(U,t)$

$$\frac{\partial W}{\partial t} + \frac{1}{2}\sigma^2 U^2 \frac{\partial^2 W}{\partial U^2} - (1 + rU)\frac{\partial W}{\partial U} = 0. \tag{2.10}$$

From the payoff (2.9)we can see that the similarity variable U takes negative values as well. The stochastic differential equation of the similarity variable U as t increases to dt is

$$dU = -\sigma U dX - [1 + (r - \sigma^2)U]\,dt, \tag{2.11}$$

which is explicitly independent on S. We must impose boundary conditions at both $U = 0$ and $U \to \infty$. From the definition of the variable $U = \frac{1}{S}(K_1 - I)$ for U to tend to infinity, S needs to tend to zero. In this case the option will not be exercised and hence will have the value zero, i.e.

$$W(U,t) = 0 \quad \text{as} \quad U \to \infty\,. \tag{2.12}$$

To examine the behavior of the option at $U = 0$ we look closely at the PDE (2.10) as well as at the SDE (2.11). For $U = 0$, from (2.11) we find that $dU = -dt < 0$, which implies that U does not remain zero, but moves away from $U = 0$ and becomes negative, $U < 0$. This can be seen from the payoff as well (2.9). Also by setting $U = 0$ in (2.10) we find that only the first derivative with respect to U and t is present making the option behave at zero like

$$\frac{\partial W}{\partial t} - \frac{\partial W}{\partial U} = 0 \quad \text{as} \quad U = 0\,. \tag{2.13}$$

For a put option, the governing equation is the same as (2.8) with payoff

$$W_1(U,T) = \max(U\,,0)\,. \tag{2.14}$$

Equation (2.8) can also be derived using the martingale method as mentioned by Rogers and Shi [62]. They assume the underlying asset follows the log-normal random walk

$$dS = c\,S\,dt + \sigma\,S\,dB_t\,, \tag{2.15}$$

where B_t is a standard one-dimensional Brownian motion, $\mathcal{F}_t$ is the natural filtration of B_t, c is the risk-less interest rate, whose notation is mostly well known as r, and σ is the volatility. By following the same procedure as mentioned in section 2.1, the price of the risky asset at time t is

$$S_t = S_o \exp\left[\left(c - \frac{1}{2}\sigma^2\right)t + \sigma B_t\right].$$

The price of a 'fixed-strike' Asian call option is expressed as the conditional expectation with respect to the filtration $\mathcal{F}_t$ (Rogers and Shi),

$$
\begin{aligned}
M_t &\equiv \mathbb{E}\left[\left(\int_0^T S_u\,\mu(du) - K\right)^+ \middle| \mathcal{F}_t\right] \\
&= \mathbb{E}\left[\left(\int_0^t S_u\,\mu(du) + \int_t^T S_u\,\mu(du) - K\right)^+ \middle| \mathcal{F}_t\right] \\
&= S_t\mathbb{E}\left[\left(\int_t^T \frac{S_u}{S_t}\,\mu(du) - \frac{1}{S_t}\left(K - \int_0^t S_u\,\mu(du)\right)\right)^+ \middle| \mathcal{F}_t\right] \\
&= S_t\,\phi(t,\xi_t)\,,
\end{aligned}
$$

where $\phi(t,\xi_t)$ is an auxiliary function and is continuous, decreasing in t and in ξ_t. ξ_t is defined as $\xi_t = \frac{1}{S_t}\left(K - \int_0^t S_u \mu(du)\right)$ and is the weighted payoff function depending on the history of the asset's value; μ is a probability measure with density ρ_t in $(0,T)$. Specifically, for a fixed strike option, $\rho_t = 1/T$ whereas for a floating strike option, $K=0$ and $\rho_t = 1/T - \delta(T-t)$, where δ is the Dirac delta function.
So for the case of a 'fixed-strike' Asian option, ξ_t will look like

$$
\xi_t = \frac{1}{S_t}\left(K - \int_0^t S_u\,\rho_t(dt)\right)\,. \tag{2.16}
$$

We consider a small change of ξ as $t \to t+dt$ and expand

$$
\begin{aligned}
d\xi_t &= \frac{1}{S_t + dS_t}\left(K - \int_0^{t+dt} S_u\,\rho_t(dt)\right) - \frac{1}{S_t}\left(K - \int_0^t S_u\,\rho_t(dt)\right) \\
&= \frac{1}{S_t}\left(1 + \frac{dS_t}{S_t}\right)^{-1}\left(K - \int_0^t S_u\,\rho_t(dt) - \int_t^{t+dt} S_u\,\rho_t(dt)\right) - \frac{1}{S_t}\left(K - \int_0^t S_u\,\rho_t(dt)\right)\,.
\end{aligned}
$$

Taking into account (2.16) and $(dS_t)^2 \sim \sigma^2\,S_t^2\,dt$ we can write

$$
\begin{aligned}
d\xi_t &= (\sigma^2\xi_t - \rho_t)\,dt - \frac{\xi_t}{S_t}\,dS_t + O(dt^{3/2}) \\
&= (-\rho_t + (\sigma^2 - r)\xi_t)\,dt - \sigma\xi_t\,dB_t\,,
\end{aligned} \tag{2.17}
$$

which is the stochastic differential equation for ξ_t.

By the martingale method: Earlier we found that $M_t = S_t\,\phi(t,\xi_t)$. In a similar way M_t changes by an amount

$$\begin{aligned} dM_t &= S\,d\phi + \phi\,dS + dS\,d\phi \\ &= S\left(\frac{\partial \phi}{\partial t}\,dt + \frac{\partial \phi}{\partial \xi}\,d\xi + \frac{1}{2}\frac{\partial^2 \phi}{\partial \xi^2}\,(d\xi)^2 + \cdots\right) + \phi\,dS + dS\,d\phi \\ &= \phi\,dS + S\,(\dot{\phi}\,dt + \phi'\,d\xi + \frac{1}{2}\phi''(d\xi)^2 + \cdots)\,. \end{aligned}$$

Using the equations (2.15), and taking into account that $(d\xi)^2 = \xi^2\sigma^2 dt$ and $dB = \epsilon\,dt^{1/2}$, where ϵ is a random variable drawn from the normal distribution $N(0,1)$, dM_t takes the form

$$dM_t = S\left[r\phi + \dot{\phi} - (\rho_t + r\xi)\phi' + \frac{1}{2}\,\sigma^2\xi^2\phi''\right]\,dt - \sigma^2\xi S\phi' dt\,dB + \sigma\phi S dB\,.$$

M_t is a martingale and its deterministic part should be equal to zero. This leads to a backward parabolic partial differential equation of the form

$$\frac{\partial \phi}{\partial t} + \frac{1}{2}\,\sigma^2\xi^2\frac{\partial^2 \phi}{\partial \xi^2} - (\rho_t + r\xi)\frac{\partial \phi}{\partial \xi} + r\phi = 0\,. \tag{2.18}$$

The above PDE is the same as the one we derived earlier using Geman and Yor's similarity variable U, (2.8), with $\rho_t = 1$.

Hedging with the underlying asset: For this method we follow the derivation used in section (2.1). Similarly in order to remove the risk, we construct a portfolio which includes V and a small amount Δ of the underlying S, i.e. $\Pi = V - \Delta S$. In a time step $t \to t + dt$, Π changes by $d\Pi = dV - \Delta dS$. The value V of the option is a function of ξ, S and t. Using Itô's lemma we have:

$$dV(S,\xi,t) = \frac{\partial V}{\partial t}\,dt + \frac{\partial V}{\partial S}\,dS + \frac{\partial V}{\partial \xi}\,d\xi + \frac{1}{2}\frac{\partial^2 V}{\partial S^2}\,(dS)^2 + \frac{1}{2}\frac{\partial^2 V}{\partial \xi^2}\,(d\xi)^2 + \frac{\partial^2 V}{\partial \xi\,\partial S}\,dS\,d\xi\,.$$

Using $(d\xi)^2 = \sigma^2\xi^2\,dt$, $dS\,d\xi = -\sigma^2\xi S\,dt$ and regrouping, the right-hand-side of dV becomes

$$\left(\frac{\partial V}{\partial t} + (\sigma^2\xi - \rho_t)\frac{\partial V}{\partial \xi} + \frac{1}{2}\,\sigma^2 S^2\frac{\partial^2 V}{\partial S^2} + \frac{1}{2}\,\sigma^2\xi^2\frac{\partial^2 V}{\partial \xi^2} - \sigma^2\xi S\frac{\partial^2 V}{\partial S\,\partial \xi}\right)\,dt + \left(\frac{\partial V}{\partial S} - \frac{\xi}{S}\frac{\partial V}{\partial \xi}\right)\,dS\,.$$

Thus the portfolio changes by

$$\begin{aligned} d\Pi &= \left(\frac{\partial V}{\partial t} + (\sigma^2\xi - \rho_t)\frac{\partial V}{\partial \xi} + \frac{1}{2}\,\sigma^2 S^2 \frac{\partial^2 V}{\partial S^2} + \frac{1}{2}\sigma^2\xi^2\frac{\partial^2 V}{\partial \xi^2} - \sigma^2 \xi S \frac{\partial^2 V}{\partial S\,\partial \xi}\right) dt \\ &+ \left(\frac{\partial V}{\partial S} - \frac{\xi}{S}\frac{\partial V}{\partial \xi} - \Delta\right) dS\,. \end{aligned}$$

To eliminate the risk in the portfolio we choose Δ to be

$$\Delta = \frac{\partial V}{\partial S} - \frac{\xi}{S}\frac{\partial V}{\partial \xi}\,,$$

Because the change of value is independent of the Wiener process, dB_t, the portfolio is instantaneously riskless. Hence $dV = r\,\Pi\, dt$ and we end up with

$$\frac{\partial V}{\partial t} + (\sigma^2\xi - \rho_t)\frac{\partial V}{\partial \xi} + \frac{1}{2}\sigma^2 S^2\frac{\partial^2 V}{\partial S^2} + \frac{1}{2}\,\sigma^2\xi^2\frac{\partial^2 V}{\partial \xi^2} - \sigma^2\xi S\frac{\partial^2 V}{\partial S\,\partial \xi} = r\left(V - S\frac{\partial V}{\partial S} + \xi\frac{\partial V}{\partial \xi}\right)\,, \tag{2.19}$$

with payoff

$$\begin{aligned} V(S,\xi,T) &= \max\left(\int_0^T S_u\,du - K\,,0\right) = S\max\left(\frac{\int_0^T S_u\,du - K}{S}\,,0\right) \\ &= S\max\left(-\xi\,,0\right) = S\,\phi(\xi,T)\,, \end{aligned}$$

at time $t = T$. From the latter equation we observe that the value of the option can be written in terms of an auxiliary function ϕ which depends only on two variables ξ and t. This is true as in this case the similarity variable ξ is consistent with the payoff for the fixed-strike Asian call option. We set $V = S\,\phi(\xi,t)$ into equation (2.19),

$$\frac{\partial \phi}{\partial t} + \frac{1}{2}\,\sigma^2\xi^2\frac{\partial^2 \phi}{\partial \xi^2} - (\rho_t + r\,\xi)\,\frac{\partial \phi}{\partial \xi} = 0\,, \tag{2.20}$$

with payoff

$$\phi(\xi,T) = \max(-\xi\,,0)\,,$$

for a 'fixed strike' Asian call option.

If ρ takes the value -1 then the above equation is identical to (2.5), whereas if ρ takes the value 1, and by setting $\phi(\xi,t) = \exp\left(-r(T-t)\right)\widehat{\phi}(\xi,t)$ we end up having equation

(2.8),

$$\frac{\partial \widehat{\phi}}{\partial t} + \frac{1}{2}\sigma^2 \xi^2 \frac{\partial^2 \widehat{\phi}}{\partial \xi^2} - (\rho_t + r\,\xi)\,\frac{\partial \widehat{\phi}}{\partial \xi} + r\,\widehat{\phi} = 0\,.$$

The above PDE is a two dimensional parabolic differential equation with respect to time and its solution gives the value of the Asian call option.

2.3 The effect of Transaction Costs

In the case where transaction costs are involved a similar PDE for the underlying can be formed. As in section 2.1, we construct a portfolio $\Pi = V - \Delta S$ and fix Δ at time t. If we transact with v shares during the time step $t \to t + dt$ the change in the portfolio is

$$d\Pi = \Pi(S + \delta S, t + \delta t) - \Pi(S, t) = dV - \Delta dS - k|v|S\,,$$

where k is given as the percentage cost of transactions, v is the number of shares traded at a price S and $|v|$ is whether we are buying or selling the shares.
To remove the risk in the portfolio we choose $\Delta = \left(\frac{\partial V}{\partial S}\right)_{\text{at time}\,t}$ and we have

$$dV(I, S, t) = \left(\frac{\partial V}{\partial t} + S\frac{\partial V}{\partial I} + \frac{1}{2}\sigma^2 S^2 \frac{\partial^2 V}{\partial S^2}\right) dt - k|v|S\,,$$

at time $t \to t + dt$. v was found to be approximately equal to $v \simeq \sigma S\,\frac{\partial^2 V}{\partial S^2}\,\delta X$, where $\delta X = \epsilon\,\delta t^{1/2}$, Wilmott [74], and $|v| \simeq \sigma S \left|\frac{\partial^2 V}{\partial S^2}\right| |\delta X|$. By taking the expectation of the transaction costs and taking into account that as $\delta t \to 0$, $\delta t = dt$, we have

$$\mathbb{E}(\delta\Pi) = \left(\frac{\partial V}{\partial t} + S\frac{\partial V}{\partial I} + \frac{1}{2}\sigma^2 S^2 \frac{\partial^2 V}{\partial S^2} - k_1 \sigma S^2 \left|\frac{\partial^2 V}{\partial S^2}\right|\right) dt\,,$$

where $k_1 = k\sqrt{\frac{2}{\pi \delta t}}$ and k is defined such that k_1 is independent of time as $\delta t \to 0$.
For no arbitrage we set this equal to

$$r\Pi dt = r\left(V - S\frac{\partial V}{\partial S}\right) dt\,.$$

For continuous time we end up with a non-linear PDE

$$\frac{\partial V}{\partial t} + S\frac{\partial V}{\partial I} + \frac{1}{2}\sigma^2 S^2 \frac{\partial^2 V}{\partial S^2} - k_1 \sigma S^2 \left|\frac{\partial^2 V}{\partial S^2}\right| = r\left(V - S\frac{\partial V}{\partial S}\right)\,. \tag{2.21}$$

If $\frac{\partial^2 V}{\partial S^2}$ has a definite sign, we end up solving the Black-Scholes equation with a modified volatility, otherwise the full non-linearity of (2.21) has to be dealt with. The effect of the transaction costs depend on the second derivative of the option price with respect to the underlying asset. This derivative is called gamma and is a measure of by how much or how often one needs to re-hedge in order to keep a delta-neutral position[3] (e.g. Wilmott [74]). The delta hedging leaves a small risk proportional to the gamma. In equation (2.21) we have subtracted off the extra gamma term which corresponds to the transaction costs. This causes the value of the option to drop.

Writing the equation in terms of the similarity variable R, we set $V(S,I,t) = SH(R,t)$, where $R = I/S$,

$$\frac{\partial H}{\partial t} + \frac{1}{2}\sigma^2 R^2 \frac{\partial^2 H}{\partial R^2} + (1-rR)\frac{\partial H}{\partial R} - k_1\sigma \left| R^2 \frac{\partial^2 H}{\partial R^2} \right| = 0\,, \tag{2.22}$$

and by setting $t^* = T - t$ we have

$$\frac{\partial H}{\partial t^*} = \frac{1}{2}\sigma^2 R^2 \frac{\partial^2 H}{\partial R^2} + (1-rR)\frac{\partial H}{\partial R} - k_1\sigma \left| R^2 \frac{\partial^2 H}{\partial R^2} \right| . \tag{2.23}$$

Equation (2.23) will be solved numerically later using the finite difference method (chapter 8).

The equivalent equation with the effect of transaction costs for the similarity $U = \frac{1}{S}(K_1 - I)$ applied in equation (2.2) is

$$\frac{\partial V_1}{\partial t^*} = \frac{1}{2}\sigma^2 U^2 \frac{\partial^2 V_1}{\partial U^2} - (1+rU)\frac{\partial V_1}{\partial U} - k_1\sigma \left| U^2 \frac{\partial^2 V_1}{\partial U^2} \right| , \tag{2.24}$$

with $t^* = T - t$ and $V(S,I,t) = S\,V_1(U,t)$.

From the last two equations for R and U, both similarity variables are consistent under the presence of transaction costs. This can be observed by looking at the term inside the modulus being simply one term. The single term inside the modulus involves the gamma only, $\frac{\partial^2 V_2}{\partial U^2}$, and attention needs to be given in determining its sign. Whether the call/put is long or short the sign of the gamma is positive or negative and it will have an effect on the volatility. So for a long position of a call/put the costs are incorporated in the volatility which will be less than the actual volatility. The opposite will happen for a short position. Further on in the thesis we will study analytically ways of determining the sign of the gamma term for different payoffs.

[3] When there is a position where the delta of the option is zero it is called delta neutral. The Delta of an option, Δ, is given as the first derivative of the option price with respect to the underlying asset price and measures the sensitivity to the price (e.g. Hull [39]).

3. CONTINUOUS MONITORING BARRIER

In this chapter we examine the effects of double barriers in the Black-Scholes framework. In the majority of the research done for barrier options the barriers are assumed to be constant throughout the life of the option. However there have been numerous occasions where the barrier changes in time, Roberts and Shortland [61], Kunitomo and Ikeda [46], Kolkiewicz [44].

We work with time $t_1 = T - t$, so $t_1 > 0$ measures the amount of time from the payoff $t_1 = 0$ $(t = T)$. We assume that the boundary is in the shape of a wedge which gets narrower and narrower as t_1 approaches zero. The cross-section of the wedge at a fixed time being a fixed region of the asset values e.g. $S_{-2} < S < S_2$ for fixed t_1. Later when we consider options on many assets this cross-section may be elliptical or spherical in N-dimensions. The geometry of these wedge shaped regions is such that at time $t > T$ they tend to a point such that $S = S_0$ i.e. $x = \ln(\frac{S}{S_0})$ in the coordinate system to be used later. Hence at time $t_1 = 0$ $(t = T)$ the cross-section of the wedge region is finite i.e. $x_{-2} = \ln(\frac{S_{-2}}{S_0}) < 0 < x_2 = \ln(\frac{S_2}{S_0})$.

3.1 Framework of the concept

We consider the single-asset Black-Scholes equation with no dividends or transaction costs on the underlying

$$\frac{\partial V}{\partial t} + \frac{1}{2}\sigma^2 S^2 \frac{\partial^2 V}{\partial S^2} + rS\frac{\partial V}{\partial S} - rV = 0\,, \tag{3.1}$$

which can be written in the form of the heat equation

$$\frac{\partial W}{\partial t_1} = \frac{\partial^2 W}{\partial x^2}\,, \tag{3.2}$$

by using the transformations

$$V(S,t) = \exp\left(-r(T-t)\right) U(S,t)\,, \quad \tau = T - t\,, \quad \bar{S} = \frac{S}{S_0}\,, \quad x = \log \bar{S}\,,$$

$$U = \exp(\alpha x + \beta\tau) W(x,\tau)\,, \quad \alpha = \frac{1}{2} - \frac{r}{\sigma^2}\,, \quad \beta = -\frac{\sigma^2}{8} - \frac{r^2}{2\sigma^2} + \frac{r}{2}\,, \quad t_1 = \frac{\sigma^2}{2}\tau\,,$$

where σ and r are constants.

We choose a transformation such that equation (3.2) can be written in terms of one variable. We introduce a similarity variable of the form

$$W = W(\eta)\,, \quad \text{where} \quad \eta = \frac{|x - x_0|}{\sqrt{t_1 + t_0}}\,, \tag{3.3}$$

where the $|x|$ means that it is symmetric about x_0, $|x'| = |x - x_0|$. The similarity variable η for the single asset option represents two lines reflected about the x-axis which get closer as t_1 approaches zero. The two lines play the role of a double barrier the area of which allows the underlying asset to move freely. The cross-section at fixed time t_1 is two points situated symmetrically about the x-axis taking negative values as well. The negative values make the one-dimensional problem a special case of the multi-dimensional problems introduced later, where the values remain positive. Expressing equation (3.2) in terms of the similarity variable η we have

$$-\frac{\eta}{2}\frac{dW}{d\eta} = \frac{d^2W}{d\eta^2}\,. \tag{3.4}$$

We assume that the barrier is at $\eta = \gamma_2$, say, figure 3.1. Then the value of the option

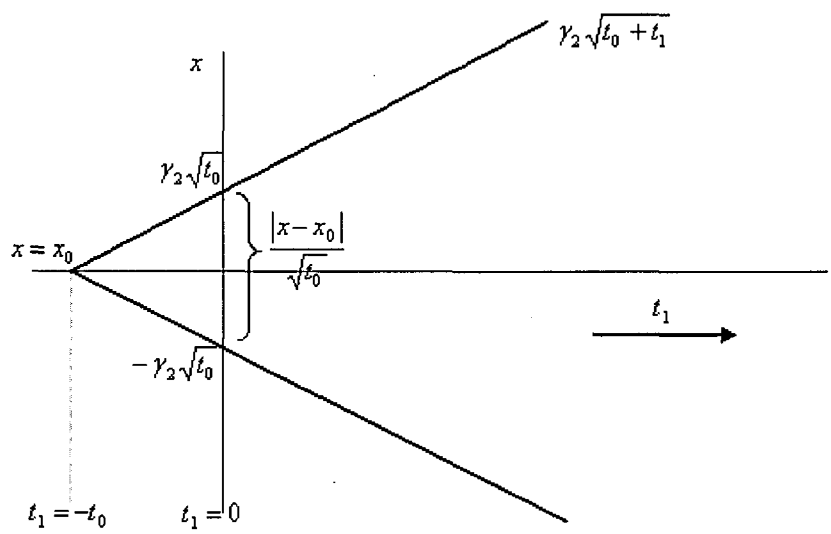

Fig. 3.1: Wedge shaped barrier.

when the barrier is hit is zero, $W = 0$, and $|x - x_0| = \gamma_2\sqrt{t_1 + t_0}$ will be the level of the moving barrier for any time t_1. The solution to equation (3.4) at the barrier $\eta = \gamma_2$

will have the form

$$\frac{dW}{d\eta} = A_1 \exp\left(-\frac{\eta^2}{4}\right) \Rightarrow W = A_1 \int_{\eta}^{\gamma_2} \exp\left(-\frac{s^2}{4}\right) ds\,.$$

Moreover, when $t_1 = 0$ $(t = T)$, $\eta < \gamma_2$ and $|x - x_0| < \gamma_2\sqrt{t_0}$. So $|x - x_0|$ will take initial values between $-\gamma_2\sqrt{t_0}$ and $\gamma_2\sqrt{t_0}$ at $t_1 = 0$ $(t = T)$.

By choosing the constant A_1 to be equal to $A_1 = \frac{1}{\int_0^{\gamma_2} \exp\left(-\frac{s^2}{4}\right)ds}$, the price of the option will be one, $W = 1$, at $x = x_0$ $(\eta = 0)$. In terms of the original variables, the value $W = 1$ corresponds to the value $V(S,t) = \exp\left(-r(T-t)\right)\left(\frac{S}{S_0}\right)^{\frac{1}{2}-\frac{r}{\sigma^2}}$ $\exp\left[\left(-\frac{\sigma^2}{8} - \frac{r^2}{2\sigma^2} + \frac{r}{2}\right)(T-t)\right]$. The analytical solution of the one-dimensional wedge barrier at $\pm\gamma_2$, say W_2, will then be

$$W_2(\eta, t_1) = \frac{\int_{\eta}^{\gamma_2} \exp\left(-\frac{s^2}{4}\right)ds}{\int_0^{\gamma_2} \exp\left(-\frac{s^2}{4}\right)ds}\,, \tag{3.5}$$

where $\eta = \frac{|x-x_0|}{\sqrt{t_1+t_0}}$. Equation (3.5) can be written in terms of error functions as

$$W_2(\eta, t_1) = 1 - \frac{\operatorname{erf}(\frac{\eta}{2})}{\operatorname{erf}(\frac{\gamma_2}{2})}\,. \tag{3.6}$$

Assume there is another boundary in the shape of a wedge which gets narrower and narrower as t_1 approaches zero, figure 3.2. The cross-section of the wedge at a

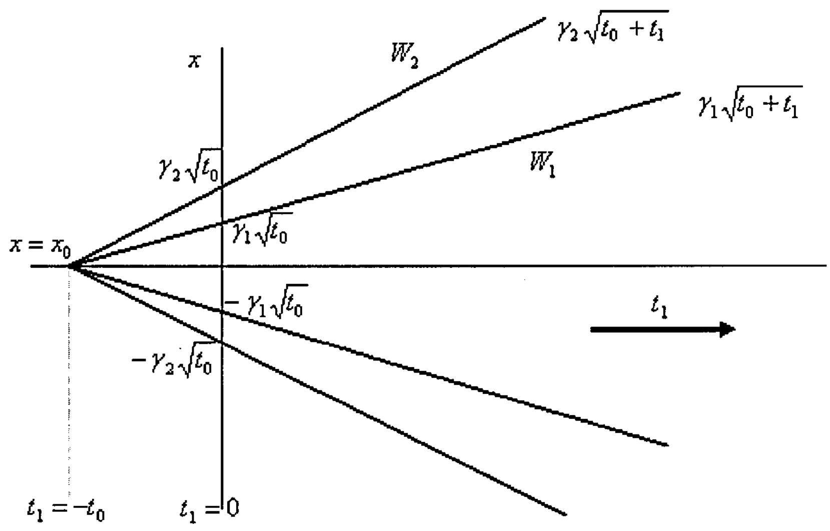

Fig. 3.2: Double wedge shaped barrier.

fixed time is a fixed region of the asset values e.g. $S_{-1} < S < S_1$, for fixed t_1, with $S_{-2} < S_{-1} < S < S_1 < S_2$. The geometry of the new wedge, say W_1, is such that at time $t > T$ it tends to the same point as the W_2 wedge such as $S = S_0$ i.e. $x = \ln\left(\frac{S}{S_0}\right)$ in the coordinate system we use. Hence the W_1 wedge will play the role of the inner barrier and the W_2 wedge will play the role of the outer barrier. We assume that the inner barrier occurs at the point $\eta = \gamma_1$, say. Then the value of the option when the barrier is hit is zero, $W = 0$, and $|x'| = |x - x_0| = \gamma_1\sqrt{t_1 + t_0}$ for any time t_1. The inner wedge for the single-asset problem will have the shape of two symmetric lines narrowing as t_1 approaches zero. The analytic equation for the one-dimensional inner wedge barrier at $\pm\gamma_1$ will similarly be

$$W_1(\eta, t_1) = \frac{\int_\eta^{\gamma_1} \exp\left(-\frac{s^2}{4}\right) ds}{\int_0^{\gamma_1} \exp\left(-\frac{s^2}{4}\right) ds} = 1 - \frac{\operatorname{erf}(\frac{\eta}{2})}{\operatorname{erf}(\frac{\gamma_1}{2})}, \tag{3.7}$$

and the payoff for the two wedge barriers will be

$$W_2(|x'|, 0) = \frac{\int_{\frac{|x'|}{\sqrt{t_0}}}^{\gamma_2} \exp\left(-\frac{s^2}{4}\right) ds}{\int_0^{\gamma_2} \exp\left(-\frac{s^2}{4}\right) ds}, \quad W_1(|x'|, 0) = \frac{\int_{\frac{|x'|}{\sqrt{t_0}}}^{\gamma_1} \exp\left(-\frac{s^2}{4}\right) ds}{\int_0^{\gamma_1} \exp\left(-\frac{s^2}{4}\right) ds}. \tag{3.8}$$

In terms of the original variable S the payoff corresponding to the outer wedge will have the form

$$V_2(S, T) = \left(\frac{S}{S_0}\right)^{\frac{1}{2} - \frac{r}{\sigma^2}} \left(1 - \frac{\operatorname{erf}(\frac{\log(S/S_0)}{2\sqrt{t_0}})}{\operatorname{erf}(\frac{\gamma_2}{2})}\right),$$

and will look like in figure 3.3. This is a particular payoff created by the outer wedge. The inner wedge will also create a payoff different from the one just mentioned. Depending on the form of the similarity variable used, the nature of the problem and the shape of the wedge barrier, one can have different kinds of payoff.

Both wedges will create two barriers symmetrically reflected around the x-axis giving a total of four single barriers. The growing region created by the two expanding barriers will be the area where the asset can move freely. The underlying can move either in the upper area created by the two wedges or in the lower, figure 3.2. If the underlying hits either of these barriers the option will expire worthless.

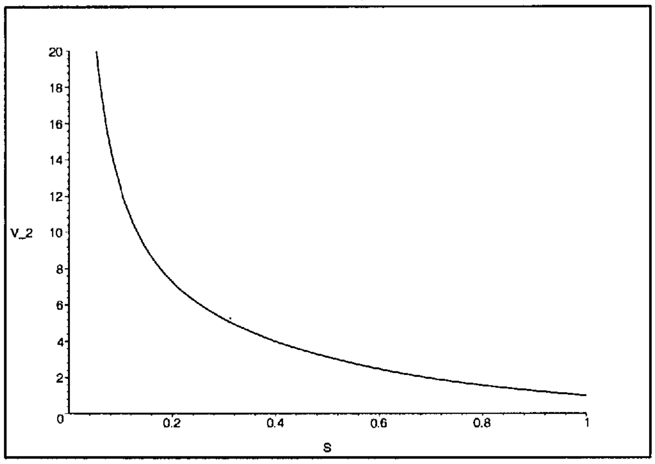

Fig. 3.3: Plot of the payoff V_2 against the original variable of the underlying asset S.

3.2 N-Dimensions

We extend the problem of the wedge in N-dimensions. The underlying assets S_i move freely under the effect of an N-dimensional wedge which shrinks as t_1 approaches zero. The wedge plays the role of a barrier which if hit by the underlying will expire worthless. The cross section of the wedge at a fixed time t_1 depends on the nature of the variable η as well as on the dimensionality of the problem. Taking the similarity variable η to be defined as

$$\sum_{i=1}^{N} \frac{x_i'^2}{\eta + \alpha_i} = t_1 + t_0 \,, \tag{3.9}$$

will produce cross-sections in the shape of ellipses in 2-dimensions or an ellipsoïd in higher dimensions, with α_i being a parameter determining the growth of the ellipsoid. When the parameter α_i is zero, the cross-section will have the shape of a circle in 2-dimensions or the shape of a sphere in higher dimensions. The similarity variable will then look like

$$\sum_{i=1}^{N} \frac{x_i'^2}{\eta} = t_1 + t_0 \,. \tag{3.10}$$

As time evolves, the wedge will take on a cone-like shape with cross-sections being ellipsoïdal or spherical.

Assume we have a European option with N underlying assets S_i and maturity date T. We consider the Black-Scholes framework and assume the underlying assets follow the log-normal random walk

$$dS_i = \mu_i S_i dt + \sigma_i S_i dX_t\,, \quad i = 1, \cdots, N\,,$$

where S_i is the price of the ith asset, μ_i and σ_i are the drift and the volatility of that asset respectively. dX_t is the increment of a Weiner process drawn from a normal distribution with mean zero and standard deviation $dt^{1/2}$ such that $\mathbf{E}[dX_i] = 0$, $\mathbf{E}[dX_i^2] = dt$ and the two Brownian increments, dX_i and dX_j are correlated, $\mathbf{E}[dX_i dX_j] = \rho_{ij}\, dt$. Applying the Itô's lemma in a multi-dimensional range, as done for a one-dimensional case in section 2.1, we have the following multi-asset version of Black-Scholes equation,

$$\frac{\partial V}{\partial t} + \frac{1}{2}\sum_{i=0}^{N}\sum_{j=0}^{N}\sigma_i\sigma_j\rho_{ij}S_iS_j\frac{\partial^2 V}{\partial S_i \partial S_j} + r\sum_{i=0}^{N} S_i\frac{\partial V}{\partial S_i} - rV = 0\,. \tag{3.11}$$

Using similar change of variables as for the one dimensional case we have

$$\frac{\partial W}{\partial t_1} = \frac{1}{2}\sum_{i=0}^{N}\sum_{j=0}^{N}\sigma_i\sigma_j\rho_{ij}\frac{\partial^2 W}{\partial \xi_i \partial \xi_j}\,, \tag{3.12}$$

where

$$V(S_i, S_j; t) = \exp\left(-r(T-t)\right)U(S_i, S_j; t)\,, \quad t_1 = T - t\,, \quad \bar{S}_i = \frac{S_i}{S_0}\,, \quad \xi_i = \log \bar{S}_i\,,$$

$$U(\xi_i, \xi_j; t_1) = \exp\left(\sum_i^N \alpha\xi_i + \beta t_1\right)W(\xi_i, \xi_j; t_1)\,, \quad \text{with} \quad \alpha_i = \sum_j Q_{ij}^{-1}F_i\,,$$

$$\beta = -\frac{1}{2}\sum_i\sum_j F_i Q_{ij}^{-1}F_j\,,\ Q_{ij} = \sigma_i\sigma_j\rho_{ij}\,,\ F_j = \frac{Q_{jj}}{2} - r\,.$$

Call $A_{ij} = \frac{1}{2}Q_{ij}$ where i and j are not summed. So equation (3.12) takes the form

$$\frac{\partial W}{\partial t_1} = \sum_{i=0}^{N}\sum_{j=0}^{N}A_{ij}\frac{\partial^2 W}{\partial \xi_i \partial \xi_j}\,.$$

We diagonalise matrix A_{ij} by using the transformation and summing over repeated indices (i and j)

$$x_s = B_{si}\,\xi_i\,, \quad x_p = B_{pj}\,\xi_j\,,$$

where B_{si} is the transition matrix from the ξ coordinates to the standard ones and the boundary is an ellipse in the x variable. We convert the ξ_i basis to an orthonormal one, x_i. Summing over repeated indices equation (3.12) becomes

$$\frac{\partial W}{\partial t_1} = B_{si} A_{ij} B_{pj} \frac{\partial^2 W}{\partial x_s \partial x_p} \,. \tag{3.13}$$

We want to diagonalise matrix A_{ij} so we choose B_{si} (symmetric, $B_{si} = B_{is}$) such that

$$\sum_{i,j=0}^{N} B_{si} A_{ij} B_{pj} = \delta_{sp} = \begin{cases} 0 & , \text{if } s \neq p \\ 1 & , \text{if } s = p \end{cases} \,.$$

This is done by choosing B_{si} ($B = (X_1, X_2, X_3 \dots X_N)$, where $X_1, X_2, X_3 \dots X_N$ are orthogonal) as a matrix of the eigenvectors of A_{ij} (the eigenvectors of A_{ij} will be the columns of the B_{si} matrix). Hence, if $s = p$,

$$\sum_{i,j=0}^{N} B_{pi} A_{ij} B_{pj} = A \,,$$

where A is the diagonal matrix with the eigenvalues at its diagonal.

$$AB = A_{ij} B_{jp} = A(X_1\, X_2 \dots X_N) = (\lambda_1 X_1\ \lambda_2 X_2 \dots \lambda_N X_N) \,,$$

and so

$$B^T AB = B^T(\lambda_1 X_1\ \lambda_2 X_2 \dots \lambda_N X_N) = \begin{pmatrix} \lambda_1 & \cdots & 0 \\ \vdots & \ddots & \vdots \\ 0 & \cdots & \lambda_N \end{pmatrix}$$

Therefore equation (3.13) becomes

$$\frac{\partial W}{\partial t_1} = \sum_{p=0}^{N} \frac{\partial^2 W}{\partial x_p \partial x_p} \lambda_p^2 \,. \tag{3.14}$$

Returning back to the original coordinates, ξ_i we have

$$\sum_s B_{js} x_s = \sum_s B_{js} B_{si} \xi_i = \delta_{ji} \xi_i = \xi_j \,,$$

since $x_s = \sum_i B_{si} \xi_i$ and $B_{si} B_{js} = \delta_{ij}$ (B is symmetric, $BB^T = I$, $B^{-1} = B^T$). Hence when $i = j$, we have $\xi_j = B_{js} x_s$.

In equation (3.14) we can move the origin of the x_p's by setting $x'_p = \frac{x_p - x_{op}}{\lambda_p}$

$$\frac{\partial W}{\partial t_1} = \sum_{p=0}^{N} \frac{\partial^2 W}{\partial x'_p \partial x'_p} \,. \tag{3.15}$$

Now that the original multi-asset Black-Scholes PDE is reduced to an N-dimensional heat equation we can introduce the similarity method approach.
We now look for solutions of (3.15) as a function of the similarity variable η introduced earlier, $W(\eta)$, where

$$\sum_{i=1}^{N} \frac{x_i'^2}{\eta + \alpha_i} = t_1 + t_0 \,. \tag{3.16}$$

We implicitly change the variables to η by writing equation (3.15) as follows

$$\frac{dW}{d\eta}\frac{\partial \eta}{\partial t_1} = \sum_{p=1}^{N} \frac{\partial^2 \eta}{\partial x_p'^2}\frac{dW}{d\eta} + \sum_{p=1}^{N}\left(\frac{\partial \eta}{\partial x'_p}\right)^2 \frac{d^2 W}{d\eta^2} \,, \tag{3.17}$$

where

$$\frac{\partial \eta}{\partial t_1} = -\frac{1}{\sum_{i=1}^{N} \frac{x_i^{\prime 2}}{(\eta+\alpha_i)^2}} = -\frac{1}{Q}, \quad \frac{\partial \eta}{\partial x'_p} = \frac{1}{Q}\frac{2x'_p}{\eta + \alpha_p}, \quad \frac{\partial^2 \eta}{\partial x_p'^2} = \frac{1}{Q}\sum_{p=1}^{N}\frac{2}{\eta+\alpha_p} \,.$$

Hence (3.17) becomes

$$\frac{d^2 W}{d\eta^2} + \frac{1}{2}\sum_{p=1}^{N}\frac{1}{\eta+\alpha_p}\frac{dW}{d\eta} + \frac{1}{4}\frac{dW}{d\eta} = 0 \,. \tag{3.18}$$

Set $u = \frac{dW}{d\eta}$, then

$$u' + \frac{1}{2}\sum_{p=1}^{N}\frac{1}{\eta+\alpha_p}u + \frac{1}{4}u = 0 \,,$$

and

$$\ln(u) = \log\left[\prod_{p=1}^{N}(\eta+\alpha_p)\right]^{-\frac{1}{2}} - \frac{1}{4}\eta + c \,.$$

So

$$u = \frac{dW}{d\eta} = A\left[\prod_{p=1}^{N}(\eta + a_p)\right]^{-\frac{1}{2}} \exp\left(-\frac{\eta}{4}\right), \quad \text{where} \quad A = \exp(c).$$

Therefore the solution for the N-dimensional expanding barrier will be

$$W_2 = A\int_{\eta}^{\eta_2} \frac{\exp\left(-\frac{\eta'}{4}\right)}{(\eta' + \alpha_1)^{\frac{1}{2}}(\eta' + \alpha_2)^{\frac{1}{2}}\dots(\eta' + \alpha_N)^{\frac{1}{2}}}\, d\eta', \tag{3.19}$$

where $\eta = \eta_2$ is the barrier and

$$\sum_{i=1}^{N} \frac{x_i'^2}{\eta + \alpha_i} = t_1 + t_0 .$$

Since the barrier is of a knock-out nature, W_2 will be zero at $\eta = \eta_2$. For all time during the life of the option the expanding barrier will form a cone for all time with each cross-section at a fixed time t_1 forming an ellipsoid. If the underlying does not trigger the barrier the option reaches expiry with payoff at $t_1 = 0$ $(t = T)$,

$$W_2 = A\int_{\eta}^{\eta_2} \frac{\exp\left(-\frac{\eta'}{4}\right)}{(\eta' + \alpha_1)^{\frac{1}{2}}(\eta' + \alpha_2)^{\frac{1}{2}}\dots(\eta' + \alpha_N)^{\frac{1}{2}}}\, d\eta', \tag{3.20}$$

where

$$\sum_{i=1}^{N} \frac{x_i'^2}{\eta + \alpha_i} = t_0 .$$

As an example of the N-dimensional ellipsoidal similarity variable is the case where the parameter α_i is zero. Then each cross-section at a fixed time t_1 will form an N-dimensional sphere and the N-dimensional equation (3.18) will take the form

$$\frac{d^2W}{d\eta^2} + \frac{1}{2}\sum_{p=1}^{N}\frac{1}{\eta}\frac{dW}{d\eta} + \frac{1}{4}\frac{dW}{d\eta} = 0, \tag{3.21}$$

with solution

$$W_2 = A\int_{\eta}^{\eta_2} \frac{\exp\left(-\frac{\eta'}{4}\right)}{\eta'^{N/2}}\, d\eta', \tag{3.22}$$

at the barrier $\eta = \eta_2$ and

$$\frac{\sum_{i=1}^{N} x_i'^2}{\eta} = t_1 + t_0 .$$

For the multi-asset problems for convenience we change the cartesian coordinates to polar. In the N-dimensional Euclidean space the coordinates are r, θ_{N-2} ... θ_1, ϕ, with $0 \leq \phi \leq 2\pi$ and $0 \leq \theta_i \leq \pi$. The relation between the polar coordinates and the Cartesian coordinates $x_1, \ldots, x_N$ is:

$$\begin{aligned}
x_1 &= r\cos\phi\sin\theta_1\sin\theta_2\ldots\sin\theta_{N-2} \\
x_2 &= r\sin\phi\sin\theta_1\sin\theta_2\ldots\sin\theta_{N-2} \\
x_3 &= r\cos\theta_1\sin\theta_2\ldots\sin\theta_{N-2} \\
&\vdots \\
x_i &= r\cos\theta_{i-2}\sin\theta_{i-1}\ldots\sin\theta_{N-2} \\
x_N &= r\cos\theta_{N-2} .
\end{aligned}$$

Because we have assumed that it is symmetric the new variables will be independent from the θ angles. Hence we are interested in the part of the Laplacian which is a function of r alone. Therefore equation (3.15) takes the form

$$\frac{\partial W}{\partial t_1} = \frac{\partial^2 W}{\partial r^2} + \frac{N-1}{r}\frac{\partial W}{\partial r} . \tag{3.23}$$

The two similarity variables for the elliptical and spherical cross-sections in terms of the polar coordinates, respectively, take the form

$$\sum_{i=1}^{N} \frac{r^2}{\eta + a_i} = t_1 + t_0 , \quad \text{and} \quad \frac{r^2}{\eta} = t_1 + t_0 . \tag{3.24}$$

We assume that at time $t = T$ the wedge has created two barriers r_L, for the lower barrier, and r_U, for the upper barrier, with $r_L < r_U$. We also assume that the initial asset values lie between the two barriers. The payoff at time $t = T$ will be equal to the value of the expanding barrier at that time. For the N-dimensional payoff in terms of the original variables one has to map the ξ_i variables to the original variables S_i. The two barriers are in a form of a wedge which in the case of one-dimension they are just two lines, in the case of two-dimensions they are cylinders, whereas in the case of three-dimensions they are spheres.

3.2.1 Two-Dimensional Example

As an example of the N-dimensional case consider when there are two underlying assets $S_1 = \exp(\xi_1)$ and $S_2 = \exp(\xi_2)$, in the coordinate system used. For the two-asset basket option we can use the similarity used in the one-dimensional problem (3.3) by rotating $|x - x_0|$ about the x-axis. The rotation will create a radial barrier in the shape of a circle with radius $r = |x - x_0| = |x'|$ taking positive values between $r_1 < r < r_2$ as opposed to the negative values the barrier was taking in the one-dimensional case. Hence the two-dimensional wedge will have the form of a cone for all time with cross-section at fixed time t_1 being a circle. The cone-shaped boundary will act as a double barrier in the two-dimensional problem. The barrier in the single-asset case will become a double radial barrier for positive r in the case of two-dimensions. The similarity variable η will have the form

$$\eta = \frac{r}{\sqrt{t_1 + t_0}}\,. \tag{3.25}$$

where r is the variable for the polar coordinate system which in terms of the cartesian and original coordinates is equal to $r^2 = x_1^2 + x_2^2$.
We use the N-dimensional radial PDE (3.23) for $N = 2$,

$$\frac{dW}{dt_1^2} = \frac{dW}{dr^2} + \frac{1}{r}\frac{dW}{dr}\,, \tag{3.26}$$

and change the dimensionality to a single variable equation

$$\frac{dW}{d\eta^2} + \frac{1}{\eta}\frac{dW}{d\eta} + \frac{1}{4}\frac{dW}{d\eta} = 0\,. \tag{3.27}$$

The analytical solution for the two-dimensional wedge will be

$$W(\eta) = A\int_{\eta}^{\gamma} s^{-1}\exp(-s/4)ds\,, \tag{3.28}$$

at the barrier $\eta = \gamma$.

3.2.2 Three-Dimensional Example

Another example is the case where we have a basket option with three underlying assets. We take the similarity variable to be

$$\frac{\sum_{i=1}^{3} x_i'^2}{\eta} = t_1 + t_0\,, \quad \text{or} \quad \frac{r^2}{\eta} = t_1 + t_0\,, \tag{3.29}$$

where each cross-section at fixed time t_1 has the shape of a sphere with radius $r^2 = x_1'^2 + x_2'^2 + x_3'^2$. The wedge has the shape of a cone and shrinks as t_1 approaches zero. The cross-section of the wedge at a fixed time t_1 will be a fixed spherical region of the asset values e.g. $r < r_O$. The wedge acts as a barrier for the option and expires worthless when triggered. The price of such an option is given by setting $N = 3$ in the N-dimensional ODE (3.18) in terms of the spherical variable η, (3.29). The equation will take the form

$$\frac{d^2W}{d\eta^2} + \frac{3}{2\eta}\frac{dW}{d\eta} + \frac{1}{4}\frac{dW}{d\eta} = 0\,. \tag{3.30}$$

the solution of which will give the analytic form for the spherical moving barrier

$$W(\eta) = A\int_{\eta}^{\eta_O} s^{-3/2}\exp\left(-\frac{s}{4}\right)ds\,, \tag{3.31}$$

satisfying the boundary condition at the barrier $\eta = \eta_O$ to be zero. We take the constant A to be such that the price of the option at $\eta = 0$ ($x_i = x_0$) is equal to one, i.e. that

$$W(\eta) = \frac{\int_{\eta}^{\eta_O} s^{-3/2}\exp\left(-\frac{s}{4}\right)ds}{\int_{0}^{\eta_O} s^{-3/2}\exp\left(-\frac{s}{4}\right)ds}\,. \tag{3.32}$$

Assume we have another three-dimensional wedge of the same nature as the one described shrinking as time to maturity $t_1 = 0$ ($t = T$) approaches. The cross-section of the wedge at a fixed time t_1 will be a fixed spherical region of the asset values e.g. $r > r_I$ with $r_I < r_O$. The two spheres are concentric and act as a double barrier to the option. Both are of knock-out nature i.e. if either of the barriers is triggered the option expires worthless. The underlying assets move along time in the area created by the two spherical barriers. If the underlying manages to avoid hitting either barrier during the life of the option, the option will expire taking the value of the payoff. For the case where the two concentric barriers are knock-out an analytic solution for the double wedge barrier cannot be found.

If the inner wedge is a knock-in barrier and the outer wedge a knock-out barrier then an analytic solution can be written for the two barriers of the form

$$W(\eta, t_1) = \frac{\int_{\eta}^{\eta_O} s^{-3/2}\exp\left(-\frac{s}{4}\right)ds}{\int_{\eta_I}^{\eta_O} s^{-3/2}\exp\left(-\frac{s}{4}\right)ds}\,, \tag{3.33}$$

for all time t_1 and with η given by (3.29).

3.2.3 Five-Dimensional Example

In this section we approach the five-dimensional example by taking the radial problem introduced by Firth and Dewynne [21]. Suppose we have an option with five underlying assets and assume we have a single barrier in the form of a wedge (shrinking as time t_1 approaches zero) i.e. of the form $r^2 = \eta(t_1 + t_0)$ with $r^2 = \sum_{i=1}^{5} x_i'^2$ where x_i are the number of assets of the option. The option moves outside the barrier and when the barrier is hit it gives the value one. At infinity the value of the option is zero. The similarity variable for the five dimensions is

$$\frac{\sum_{i=1}^{5} x_i'^2}{\eta} = t_1 + t_0\,, \quad \text{or} \quad \frac{r^2}{\eta} = t_1 + t_0\,, \tag{3.34}$$

with the corresponding ODE for $N = 5$ taking the form

$$\frac{d^2W}{d\eta^2} + \frac{5}{2\eta}\frac{dW}{d\eta} + \frac{1}{4}\frac{dW}{d\eta} = 0\,, \tag{3.35}$$

and the corresponding radial PDE given by

$$\frac{dW}{dt_1} = \frac{d^2W}{dr^2} + \frac{4}{r}\frac{dW}{dr}\,. \tag{3.36}$$

The solution of (3.35) will be equal to

$$W(\eta) = A\int_{\eta}^{\infty} s^{-5/2}\exp\left(-\frac{s}{4}\right)ds\,, \tag{3.37}$$

satisfying the boundary condition at infinity, $W(\infty) = 0$. We choose the constant A such that the boundary condition at the barrier $\eta = \gamma$ is satisfied, $W(\gamma) = 1$. The analytical solution for the single expanding barrier will then be

$$W(\eta) = \frac{\int_{\eta}^{\infty} s^{-5/2}\exp\left(-\frac{s}{4}\right)ds}{\int_{\gamma}^{\infty} s^{-5/2}\exp\left(-\frac{s}{4}\right)ds}\,, \tag{3.38}$$

subject to the boundary conditions

$$W(\gamma, t_1) = 1\,, \quad W(\infty, t_1) = 0\,, \tag{3.39}$$

and payoff consistent with (3.38) with $\eta = \frac{r^2}{t_0}$.
The solution (3.38) can be written in terms of error functions

$$W(\eta) = C\left[\sqrt{\pi}\left(\operatorname{erf}\frac{\sqrt{\eta}}{2} - 1\right) + 2\eta^{-1/2}\exp\left(-\eta/4\right)\left(1 - \frac{2}{\eta}\right)\right]\,, \tag{3.40}$$

where $C = -\frac{1}{6}[\frac{\sqrt{\pi}}{6}(1 - \operatorname{erf}\frac{\sqrt{\gamma}}{2}) - \frac{1}{3}\frac{2}{\sqrt{\gamma}}\exp(-\gamma/4)(\frac{1}{2} - \frac{1}{\gamma})]^{-1}$.

As mentioned in the previous section for the three-dimensional example, we can write the problem of Firth and Dewynne [21] as follows,

$$\frac{dW}{dt_1} = \frac{d^2W}{dr^2} + \frac{4}{r}\frac{dW}{dr},$$

subject to the following boundary conditions

$$W(\eta_I) = 1\,, \quad W(\eta_O) = 0\,. \tag{3.41}$$

Taking the outer boundary condition at $\eta = \eta_O$ to be zero with η_O being large, matches the boundary at infinity given by Firth and Dewynne. The analytical solution to the problem will then be

$$W(\eta, t_1) = \frac{\int_{\eta}^{\eta_O} s^{-5/2}\exp\left(-\frac{s}{4}\right)ds}{\int_{\eta_I}^{\eta_O} s^{-5/2}\exp\left(-\frac{s}{4}\right)ds}, \tag{3.42}$$

with payoff consistent with the similarity variable solution (3.42).

4. BLACK SCHOLES EQUATION WITH STEP BARRIER

In this chapter we price a European option under the effect of a continuous double barrier. We work with time $t_1 = T - t$, so $t_1 > 0$ measures the amount of time from the payoff $t_1 = 0$ ($t = T$). We assume there is a barrier in the form shown in figure 4.1. The actual barrier is that described for $x' > x_0$ by the shaped barrier $A_2B_1B_2C_1C_2D_1D_2$ together with its image in the $x' = x_0$ axis. This shaped barrier lies between two straight lines $A_1B_1C_1D_1$ and $A_2B_2C_2D_2$ with similar images in $x' < x_0$. The solution for the stepped barrier is effected via Fourier series between the upper and lower barriers, both sets being knock out. Special care needs to be taken between steps as the Fourier series is reconstructed e.g. for $t_1 > t_1^{**}$ and $t_1 < t_1^{**}$, etc.

For a single asset option, the two wedges will have the shape of four lines narrowing as t_1 approaches zero and will act as bounds to the step barrier. If the option has two assets, then the wedges will form a double barrier. The Fourier series step barrier will have the shape of a cylinder of constant radius with a circle as the cross-section at fixed time t_1. When the jump occurs the cylinder will shrink to a smaller one of smaller radius which will remain constant till the next jump.

In this section we examine the case where the wedge is one-dimensional and more specifically the behavior of the step barrier option compared with that of an inner and outer wedge barrier. We verify that the outer wedge barrier acts as an upper bound to the step barrier.

We consider a European option with the value given by the Black-Scholes equation

$$\frac{\partial V}{\partial t} + \frac{1}{2}\sigma^2 S^2 \frac{\partial^2 V}{\partial S^2} + rS\frac{\partial V}{\partial S} - rV = 0\,, \tag{4.1}$$

where S, S_L, S_U are scaled on S_0 and the above equation can be written in the form of the heat equation

$$\frac{\partial W}{\partial t_1} = \frac{\partial^2 W}{\partial x^2}\,, \tag{4.2}$$

by using the transformations

$$V(S,t) = \exp\left(-r(T-t)\right) U(S,t)\,, \quad \tau = T - t\,, \quad x = \log S\,,$$

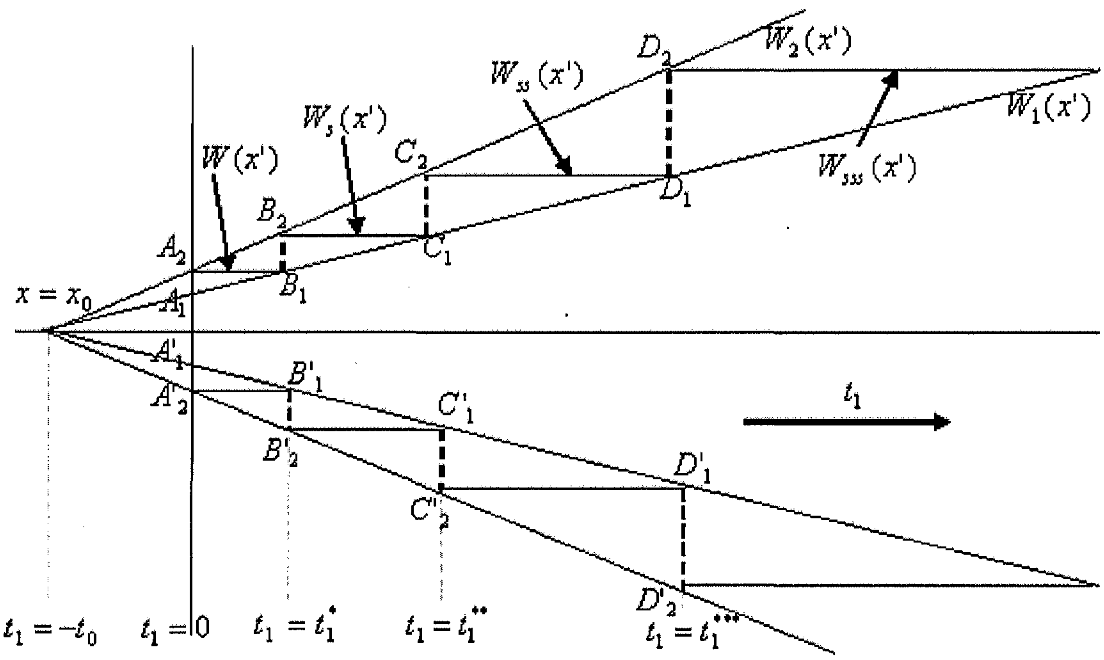

Fig. 4.1: Jump of the barrier at times $t = t_1^*$, $t = t_1^{**}$ and $t = t_1^{***}$.

$$U = \exp(\alpha x + \beta\tau) W(x,\tau)\,, \quad \alpha = \frac{1}{2} - \frac{r}{\sigma^2}\,, \quad \beta = -\frac{\sigma^2}{8} - \frac{r^2}{2\sigma^2} + \frac{r}{2}\,, \quad t_1 = \frac{\sigma^2}{2}\tau\,.$$

We return to the heat equation (4.2) and move the origin by setting $x' = x - x_0$. The equation now will be

$$\frac{\partial W}{\partial t_1} = \frac{\partial^2 W}{\partial x'^2}\,. \tag{4.3}$$

Applying separation of variables we can write the solution of the above equation in the form

$$W(x', t_1) = \exp(-k^2 t_1)(a\cos(kx') + b\sin(kx'))\,.$$

For the payoff at $t_1 = 0$ ($t = T$) we go back to the expanding barrier mentioned in chapter 3. At $t_1 = 0$ the step barrier given by the Fourier series solution will be the same as the solution for the expanding barrier evaluated at $t_1 = 0$. Note that the Fourier series method can deal with any payoff. At that time the width of the barrier is equal to $\eta = \frac{|x'|}{\sqrt{t_0}}$ and so the boundary conditions at the barrier will be

$$W_2 = 0\,, \quad \text{when} \quad \eta = \gamma_2 \Rightarrow |x'| = \gamma_2\sqrt{t_0} \quad \text{or} \quad x' = \pm\gamma_2\sqrt{t_0}\,.$$

Since we have assumed that the barriers expand symmetrically about x_0, the slopes will be symmetric around the x-axis. The initial condition to the problem is an even function which makes the resulting series for the step barrier a cosine series with general term

$$W(x', t_1) = a \exp\left(-k^2 t_1\right) \cos\left(k x'\right). \tag{4.4}$$

At the barrier $\pm\gamma_2\sqrt{t_0}$, $W = 0$ and the value of k will be equal to $k \equiv k_N = \frac{(2N+1)\pi}{2\gamma_2\sqrt{t_0}}$, where k_N are the eigenvalues. Hence the solution takes the form

$$W(x', t_1) = \sum_{N=0}^{\infty} a_N \exp\left(-\frac{(2N+1)^2\pi^2}{4\gamma_2^2 t_0} t_1\right) \cos\left(\frac{(2N+1)\pi}{2\gamma_2\sqrt{t_0}} x'\right), \tag{4.5}$$

where the barrier condition is automatically satisfied.
At $t_1 = 0$ equation (4.5) becomes

$$W(x', 0) = \sum_{N=0}^{\infty} a_N \cos\left(\frac{(2N+1)\pi}{2\gamma_2\sqrt{t_0}} x'\right), \tag{4.6}$$

where the function $W(|x'|, 0)$ is the payoff at time $t_1 = 0$, equation (3.8), i.e.

$$W_2(|x'|, 0) = W(|x'|, 0) = \frac{\int_\eta^{\gamma_2} \exp\left(-\frac{s^2}{4}\right) ds}{\int_0^{\gamma_2} \exp\left(-\frac{s^2}{4}\right) ds} = 1 - \frac{\operatorname{erf}\left(\frac{|x'|}{2\sqrt{t_0}}\right)}{\operatorname{erf}\left(\frac{\gamma_2}{2}\right)}, \tag{4.7}$$

where $\eta = \frac{|x'|}{\sqrt{t_0}}$. In terms of the original variable S the payoff will have the form

$$V_2(S, T) = \left(\frac{S}{S_0}\right)^{\frac{1}{2} - \frac{r}{\sigma^2}} \left(1 - \frac{\operatorname{erf}\left(\frac{\log(S/S_0)}{2\sqrt{t_0}}\right)}{\operatorname{erf}\left(\frac{\gamma_2}{2}\right)}\right),$$

and will look like in figure 3.3.
To determine the Fourier series coefficient a_N we multiply equation (4.6) by $\cos\left(\frac{(2M+1)\pi}{2\gamma_2\sqrt{t_0}} x'\right)$ and integrate with respect to x' from $-\gamma_2\sqrt{t_0}$ to $\gamma_2\sqrt{t_0}$,

$$\begin{aligned}
&\int_{-\gamma_2\sqrt{t_0}}^{\gamma_2\sqrt{t_0}} W(|x'|, 0) \cos\left(\frac{(2M+1)\pi}{2\gamma_2\sqrt{t_0}} x'\right) dx' \\
&= \sum_{N=0}^{\infty} a_N \int_{-\gamma_2\sqrt{t_0}}^{\gamma_2\sqrt{t_0}} \cos\left(\frac{(2M+1)\pi}{2\gamma_2\sqrt{t_0}} x'\right) \cos\left(\frac{(2N+1)\pi}{2\gamma_2\sqrt{t_0}} x'\right) dx'.
\end{aligned}$$

Using the orthogonality condition

$$\int_{-\gamma_2\sqrt{t_0}}^{\gamma_2\sqrt{t_0}} \cos\left(\frac{(2M+1)\pi}{2\gamma_2\sqrt{t_0}}x'\right)\cos\left(\frac{(2N+1)\pi}{2\gamma_2\sqrt{t_0}}x'\right)dx'$$
$$= \begin{cases} 0 & \text{, if } M \neq N \\ \int_{-\gamma_2\sqrt{t_0}}^{\gamma_2\sqrt{t_0}} \left[\cos\left(\frac{(2N+1)\pi}{2\gamma_2\sqrt{t_0}}x'\right)\right]^2 dx' & \text{, if } M = N \end{cases},$$

for $M = N$ we have

$$a_N = \frac{\int_{-\gamma_2\sqrt{t_0}}^{\gamma_2\sqrt{t_0}} W(|x'|,0)\cos\left(\frac{(2N+1)\pi}{2\gamma_2\sqrt{t_0}}x'\right)dx'}{\int_{-\gamma_2\sqrt{t_0}}^{\gamma_2\sqrt{t_0}} \left[\cos\left(\frac{(2N+1)\pi}{2\gamma_2\sqrt{t_0}}x'\right)\right]^2 dx'} = \frac{\int_{0}^{\gamma_2\sqrt{t_0}} W(x',0)\cos\left(\frac{(2N+1)\pi}{2\gamma_2\sqrt{t_0}}x'\right)dx'}{\int_{0}^{\gamma_2\sqrt{t_0}} \left[\cos\left(\frac{(2N+1)\pi}{2\gamma_2\sqrt{t_0}}x'\right)\right]^2 dx'},$$

or equivalently

$$a_N = \frac{4}{(2N+1)\pi^{3/2}\sqrt{t_0}\,\mathrm{erf}\left(\frac{\gamma_2}{2}\right)} \int_0^{\gamma_2\sqrt{t_0}} \exp\left(-\frac{x'^2}{4t_0}\right)\sin\left(\frac{(2N+1)\pi}{2\gamma_2\sqrt{t_0}}x'\right)dx'. \quad (4.8)$$

In order to numerically evaluate the Fourier coefficients we choose the outer barrier to be equal to $\gamma_2 = 2.0$ and the time where the wedge starts growing to be $t_0 = 0.2$. The computations are implemented using Maple V 8.00 and are fast and accurate. The computation becomes costly after the barrier has jumped a number of times. This is because of the number of nested integrals required to be solved in order to compute the Fourier coefficient. In table 4.1 we have listed the first 30 terms of the coefficient a_N corresponding to these values for γ_2 and t_0.

Values of a_N		
$a_0 = 0.7113763244$	$a_{10} = 0.002410676422$	$a_{20} = 0.0006385924265$
$a_1 = 0.1564700605$	$a_{11} = 0.002096716859$	$a_{21} = 0.0005936503987$
$a_2 = 0.04080012711$	$a_{12} = 0.001706250958$	$a_{22} = 0.0005306115373$
$a_3 = 0.02404243980$	$a_{13} = 0.001516345435$	$a_{23} = 0.0004964121563$
$a_4 = 0.01283352767$	$a_{14} = 0.001270935976$	$a_{24} = 0.0004478731469$
$a_5 = 0.009415706921$	$a_{15} = 0.001147436151$	$a_{25} = 0.0004212476311$
$a_6 = 0.006220976538$	$a_{16} = 0.0009832396767$	$a_{26} = 0.0003830807630$
$a_7 = 0.004992541420$	$a_{17} = 0.0008984567600$	$a_{27} = 0.0003619477706$
$a_8 = 0.003662412022$	$a_{18} = 0.0007832365889$	$a_{28} = 0.0003313958261$
$a_9 = 0.003087605355$	$a_{19} = 0.0007225357306$	$a_{29} = 0.0003143426361$
		$a_{30} = 0.0002895071013$

Tab. 4.1: Values of the Fourier coefficient a_N for $N = 0..30$.

So far we have found the Fourier series solution (4.5) of the step barrier using the value of the expanding barrier W_2 as the payoff. We are interested in plotting the Fourier series solution for different values of $x' > 0$ as a function of time t_1. For this purpose we take four different values for x', $0 < x' < \gamma_2\sqrt{t_0} = 0.8944271910$, e.g. $x_1 = 0.2$, $x_2 = 0.4$, $x_3 = 0.6$ and $x_3 = 0.8$ (close to the wedge barrier). With a_N taking the values shown in table 4.1, the behavior of the solution (4.5) in time t_1 can be seen in figure 4.2. When the underlying is closer to the barrier (lower dotted line), the value of the option becomes cheaper because the asset has more chances of hitting the barrier and expiring worthless. As we move further away from the barrier the value of the option becomes more expensive, as the chances of hitting the barrier have decreased and the holder of the option has better chances of reaching maturity and exercising the option. Moving away from maturity makes the value of the option decrease exponentially. For the cases where $x' = 0.4$ (upper dotted line), $x' = 0.6$ (lower solid line) and $x' = 0.8$ (lower dotted line) when the underlying is close to maturity the value drops since there are still chances of hitting the barrier. For $x' = 0.2$ (upper solid line) the price of the option has a normal behavior (increasing exponentially till reaching a maximum value obtained at the payoff) as it is far away from the barrier and hence not effected by it.

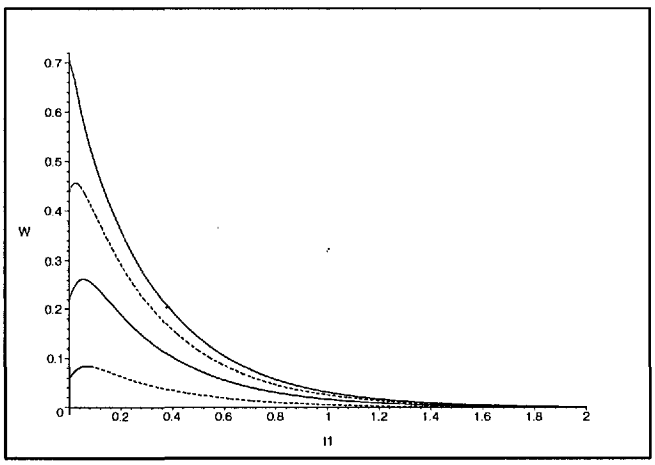

Fig. 4.2: Plot of the Fourier series solution $W(x', t_1)$ against time t_1. From top to bottom, for $x' = 0.2$ (upper solid line), $x' = 0.4$ (upper dotted line), $x' = 0.6$ (lower solid line) and for $x' = 0.8$ (lower dotted line).

In terms of the variable x and real time t the solution will become

$$\begin{aligned} V(x,t) &= \exp\left(-r(T-t)\right)\exp\left[\left(\frac{1}{2}-\frac{r}{\sigma^2}\right)x-\left(\frac{\sigma^2}{8}+\frac{r^2}{2\sigma^2}-\frac{r}{2}\right)(T-t)\right] \qquad (4.9) \\ & \sum_{N=0}^{\infty} a_N \exp\left[-\frac{(2N+1)^2\pi^2\sigma^2}{8\gamma_2^2 t_0}(T-t)\right]\cos\left[\frac{(2N+1)\pi}{2\gamma_2\sqrt{t_0}}(x-x_0)\right]. \end{aligned}$$

Writing the full solution in terms of the original variables S and t will give

$$V(S,t) = \exp\left(-r(T-t)\right) S^{\frac{1}{2}-\frac{r}{\sigma^2}} \exp\left[-\left(\frac{\sigma^2}{8}+\frac{r^2}{2\sigma^2}-\frac{r}{2}\right)(T-t)\right] \tag{4.10}$$
$$\sum_{N=0}^{\infty} a_N \exp\left[-\frac{(2N+1)^2\pi^2\sigma^2}{8\gamma_2^2 t_0}(T-t)\right] \cos\left[\frac{(2N+1)\pi}{2\gamma_2\sqrt{t_0}}\ln\left(\frac{S}{S_0}\right)\right].$$

The corresponding plots for the same values of x for S will look like in figure 4.3 with the barriers taking values $\exp(\pm\gamma_2\sqrt{t_0})$ (taking $\gamma_2 = 2$, $t_0 = 0.2$, $T = 100$, $r = 0.05$ and $S_0 = 1$). Note that S is scaled on the initial asset value S_0. From the transformation in time $t_1 = \frac{\sigma^2}{2}(T-t)$ the time to maturity depends on what value the volatility takes. For our problem we have chosen σ to take value 0.2 and maturity T to be 100 days, or around 0.3 years, (leaving the variable t_1 to take values, $0 < t_1 < 2$). So in real time the life of the option goes from 0 to 100, whereas in the t_1 variable it will take values from 0 to 2. Similarly as we discussed for the previous figure when we are away from maturity the value of the option is very small almost zero, for large values of time. As we move towards the payoff, the price of the option increases to reach the final value it will take at expiry. At $S = \exp(0.2)$ (top solid line), the asset is far away from the barrier and has very little chances of hitting the wedge, giving the holder of the option the benefit to profit when reaching the payoff. As we move closer to the shrinking barrier, the chances for the underlying of hitting it increase making the value of the option to drop just before reaching the expiry date.

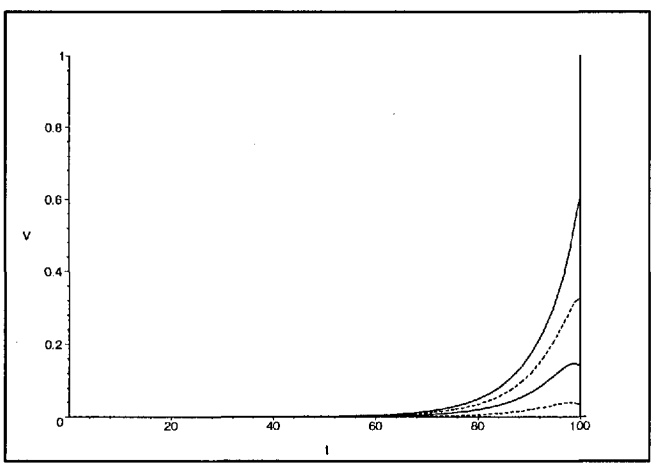

Fig. 4.3: Plot of the Fourier series solution $V(S,t)$ against time t for $S = \exp(0.2)$ (top solid line), $S = \exp(0.4)$ (top dotted line), $S = \exp(0.6)$ (lower solid line) and for $S = \exp(0.8)$ (lower dotted line).

The Fourier series barrier moves in time t_1 till it reaches the inner wedge W_1 ($\pm\gamma_1\sqrt{t_1^*+t_0}$) at time t_1^* say. When the inner wedge is hit, the barrier jumps till it hits the outer wedge W_2 ($\pm\gamma_2\sqrt{t_1^*+t_0}$) at B_2, B_2' and continues it's course at that level. This can be seen in the sketch at the beginning of this chapter, figure 4.1. The point where the Fourier series solution barrier hits the inner barrier W_1 is at $(\gamma_1\sqrt{t_0+t_1^*}=\gamma_2\sqrt{t_0}, t_1^*)$ (point B_1 in the sketch) and it jumps to meet the outer wedge at the point $(\gamma_2\sqrt{t_0+t_1^*}, t_1^*)$ (point B_2). The width of the new barrier $\pm\gamma_2\sqrt{t_0+t_1^*}$ will be $\frac{|x'|}{\sqrt{t_0+t_1^*}}$ and the boundary condition will become

$$W_s = 0 \quad \text{at} \quad \eta = \frac{|x'|}{\sqrt{t_0+t_1^*}} \Rightarrow |x'| = \gamma_2\sqrt{t_0+t_1^*}.$$

Note that the notation used for the value of the option (W_s, V_s, W_{ss}, V_{ss}, W_{sss}, V_{sss}) is not the derivative of the option with respect to the underlying asset S, but actually the value of the step barrier option for every jump.
At the point B_2 the solution for the new step barrier is of the form

$$W_s(x', t_1) = \sum_{N=0}^{\infty} b_N \exp\left(-\frac{(2N+1)^2\pi^2}{4\gamma_2^2(t_0+t_1^*)}t_1\right)\cos\left(\frac{(2N+1)\pi}{2\gamma_2\sqrt{t_0+t_1^*}}x'\right), \tag{4.11}$$

with corresponding eigenvalues $k_N = \frac{(2N+1)\pi}{2\gamma_2\sqrt{t_0+t_1^*}}$. Note that γ_1 and γ_2 correspond to the two wedges W_1 and W_2 respectively. To find the value of γ_1, we fix the point $t_1 = t_1^*$ where the step of the barrier will occur, say $t_1^* = 0.3$, and equate the equation of the inner wedge W_1 with the Fourier series solution (4.5) at time t_1^*. From that we find that the value of γ_1 is 1.264911064 making the point at A_1 have value equal to $\gamma_1\sqrt{t_0} = 0.5656854249$. At B_1 the value of x' will be equal to $\gamma_1\sqrt{t_0+t_1^*} = \gamma_2\sqrt{t_0} = 0.8944271910$ and at B_2 it will be equal to $\gamma_2\sqrt{t_0+t_1^*} = 1.414213562$.
At $t_1 = t_1^*$ the following equality holds

$$W_s(x', t_1^*) = \sum_{N=0}^{\infty} b_N \exp\left(-\frac{(2N+1)^2\pi^2}{4\gamma_2^2(t_0+t_1^*)}t_1^*\right)\cos\left(\frac{(2N+1)\pi}{2\gamma_2\sqrt{t_0+t_1^*}}x'\right). \tag{4.12}$$

Where the left-hand-side is the 'payoff', equal to the Fourier series solution (4.5) evaluated at t_1^*,

$$W(x', t_1^*) = \sum_{N=0}^{\infty} a_N \exp\left(-\frac{(2N+1)^2\pi^2}{4\gamma_2^2 t_0}t_1^*\right)\cos\left(\frac{(2N+1)\pi}{2\gamma_2\sqrt{t_0}}x'\right), \tag{4.13}$$

valid for $-\gamma_2\sqrt{t_0} < x' < \gamma_2\sqrt{t_0}$ and zero for $-\gamma_2\sqrt{t_0+t_1^*} < x' < -\gamma_2\sqrt{t_0}$ ($B_2'B_1'$) and $\gamma_2\sqrt{t_0} < x' < \gamma_2\sqrt{t_0+t_1^*}$ (B_1B_2).

To find b_N we multiply equation (4.12) by $\cos\left(\frac{(2M+1)\pi}{2\gamma_2\sqrt{t_0+t_1^*}}\,x'\right)$ and integrate with respect to x' from $-\gamma_2\sqrt{t_0+t_1^*}$ to $\gamma_2\sqrt{t_0+t_1^*}$,

$$\int_{-\gamma_2\sqrt{t_0}}^{\gamma_2\sqrt{t_0}} W(x',t_1^*)\cos\left(\frac{(2M+1)\pi}{2\gamma_2\sqrt{t_0+t_1^*}}\,x'\right)dx' = \sum_{N=0}^{\infty} b_N \exp\left(-\frac{(2N+1)^2\pi^2}{4\gamma_2^2(t_0+t_1^*)}\,t_1^*\right)$$
$$\int_{-\gamma_2\sqrt{t_0+t_1^*}}^{\gamma_2\sqrt{t_0+t_1^*}} \cos\left(\frac{(2N+1)\pi}{2\gamma_2\sqrt{t_0+t_1^*}}\,x'\right)\cos\left(\frac{(2M+1)\pi}{2\gamma_2\sqrt{t_0+t_1^*}}\,x'\right)dx'\,.$$

Using the orthogonality relation

$$\int_{-\gamma_2\sqrt{t_0+t_1^*}}^{\gamma_2\sqrt{t_0+t_1^*}} \cos\left(\frac{(2N+1)\pi}{2\gamma_2\sqrt{t_0+t_1^*}}\,x'\right)\cos\left(\frac{(2M+1)\pi}{2\gamma_2\sqrt{t_0+t_1^*}}\,x'\right)dx'$$
$$= \begin{cases} 0 & \text{, if } M \neq N \\ \int_{-\gamma_2\sqrt{t_0+t_1^*}}^{\gamma_2\sqrt{t_0+t_1^*}} \left[\cos\left(\frac{(2N+1)\pi}{2\gamma_2\sqrt{t_0+t_1^*}}\,x'\right)\right]^2 dx' & \text{, if } M = N \end{cases},$$

the formula for calculating the coefficients b_N is

$$c_N = b_N \exp\left(-\frac{(2N+1)^2\pi^2}{4\gamma_2^2(t_0+t_1^*)}\,t_1^*\right) = \frac{\int_{-\gamma_2\sqrt{t_0}}^{\gamma_2\sqrt{t_0}} W(x',t_1^*)\cos\left(\frac{(2N+1)\pi}{2\gamma_2\sqrt{t_0+t_1^*}}\,x'\right)dx'}{\int_{-\gamma_2\sqrt{t_0+t_1^*}}^{\gamma_2\sqrt{t_0+t_1^*}} \left[\cos\left(\frac{(2N+1)\pi}{2\gamma_2\sqrt{t_0+t_1^*}}\,x'\right)\right]^2 dx'},$$

or

$$c_N = \frac{\int_{-\gamma_2\sqrt{t_0}}^{\gamma_2\sqrt{t_0}} \left[\sum_{N=0}^{\infty} a_N \exp\left(-\frac{(2N+1)^2\pi^2}{4\gamma_2^2 t_0}\,t_1^*\right)\cos\left(\frac{(2N+1)\pi}{2\gamma_2\sqrt{t_0}}\,x'\right)\right]\cos\left(\frac{(2N+1)\pi}{2\gamma_2\sqrt{t_0+t_1^*}}\,x'\right)dx'}{\int_{-\gamma_2\sqrt{t_0+t_1^*}}^{\gamma_2\sqrt{t_0+t_1^*}} \left[\cos\left(\frac{(2N+1)\pi}{2\gamma_2\sqrt{t_0+t_1^*}}\,x'\right)\right]^2 dx'}\,.$$

Hence the solution for the step barrier B_1B_2 will be

$$W_s(x',t_1) = \sum_{N=0}^{\infty} c_N \exp\left(-\frac{(2N+1)^2\pi^2}{4\gamma_2^2(t_0+t_1^*)}\,(t_1-t_1^*)\right)\cos\left(\frac{(2N+1)\pi}{2\gamma_2\sqrt{t_0+t_1^*}}\,x'\right), \quad (4.14)$$

where the coefficient c_N for $\gamma_2 = 2$, $t_0 = 0.2$, $t_1^* = 0.3$ takes values given in table 4.2. At $t_1 = t_1^*$ the value of the outer wedge W_2 will be equal to the value of the Fourier

Values of c_N		
$c_0 = 0.2065682433$	$c_{11} = 0.0007045306754$	$c_{21} = -0.00009294362029$
$c_1 = 0.08622632873$	$c_{12} = -0.0008719099476$	$c_{22} = -0.0002103282783$
$c_2 = -0.006339344017$	$c_{13} = 0.00009339482748$	$c_{23} = 0.0002336363109$
$c_3 = -0.009555237236$	$c_{14} = 0.0005818874146$	$c_{24} = 0.000003597084514$
$c_4 = 0.006399201682$	$c_{15} = -0.0004823119608$	$c_{25} = -0.0002010750970$
$c_5 = 0.0003231152512$	$c_{16} = -0.0001050884504$	$c_{26} = 0.0001474337726$
$c_6 = -0.003203206373$	$c_{17} = 0.0004536626238$	$c_{27} = 0.00006219576835$
$c_7 = 0.001765751756$	$c_{18} = -0.0002445516252$	$c_{28} = -0.0001742638150$
$c_8 = 0.0007529758979$	$c_{19} = -0.0001873174857$	$c_{29} = 0.00007744184769$
$c_9 = -0.001582393805$	$c_{20} = 0.0003360928752$	$c_{30} = 0.00009357835777$
$c_{10} = 0.0005539015719$		

Tab. 4.2: Values of the Fourier coefficient c_N for $N = 0..30$.

series W_s making the outer wedge W_2 the upper bound of the Fourier series solution

$$\begin{aligned} W_2(|x'|, t_1^*) &= \frac{\int_{\eta^*}^{\gamma_2} \exp\left(-\frac{s^2}{4}\right) ds}{\int_0^{\gamma_2} \exp\left(-\frac{s^2}{4}\right) ds} \\ &= \sum_{N=0}^{\infty} b_N \exp\left(-\frac{(2N+1)^2\pi^2}{4\gamma_2^2(t_0+t_1^*)}\, t_1^*\right) \cos\left(\frac{(2N+1)\pi}{2\gamma_2\sqrt{t_0+t_1^*}}\, x'\right), \quad (4.15) \end{aligned}$$

where $\eta^* = \frac{|x'|}{\sqrt{t1^* + t_0}}$. If we take a point situated under the Fourier series step function and evaluate both the wedge solution, W_2, and the Fourier series solution, W_s, at that point, we will find that the value of W_2 is greater than the value of W_s, making the outer wedge an upper bound for the Fourier series. For example taking the point $(x', t_1) = (1.2, 0.5)$ the value of the wedge W_2 is equal to 0.1817907719 which is more expensive than the value of the Fourier series evaluated at that point, $W_s = 0.03190149234$. This is something we expect as we used the outer wedge as the payoff in calculating the original Fourier series solution W (for $A_2B_1/A_2'B_1'$).

In figure 4.4 are shown the plots of the solution (4.14) against time t_1 for different values of $x' > 0$ inside the barrier. We have chosen the volatility to have value $\sigma = 0.2$ and the expiry date having value equal to 100 days. So the range for time for the price of the option will be $0.3 < t_1 < 2.0$ and in real time $0 < t < 85$. If the underlying is far away from the barrier $B_2C_1 = 1.414213562$ (figure 4.1), at $x' = 0.2$, the underlying of the option is too far to be strongly affected by the barrier and has the behavior expected from the solution (upper solid line in figure 4.4). As time gets closer to maturity, the value of the option increases to a maximum value obtained at the time when the jump occurs and continues to increase till it reaches expiry. The buyer of such an option will have to pay more to enter such a beneficial position. As we move closer to the wedge at positions $x' = 0.6$ (middle solid line), $x' = 0.8$ (bottom solid line) and $x' = 1.2$ (bottom dotted line), in figure 4.4, we observe that when the underlying is close to the jump at $t_1 = 0.3$ (closer to the y-axis) the price is strongly affected by the barrier. As the asset moves towards the jump it has more chances of hitting the barrier than avoiding it and successfully entering the shrunken barrier B_1B_1'. Hence at such a position the value of the option drops. Under these circumstances the holder of the option is not in a favorable position as the price of the option has dropped with a strong chance of expiring without profit.

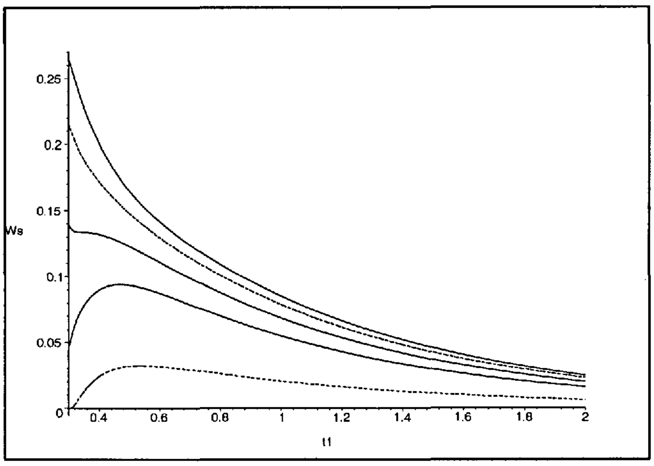

Fig. 4.4: Plot of the step Fourier series solution $W_s(x', t_1)$ against time. From top to bottom, for $x' = 0.2$ (solid line), $x' = 0.4$ (dotted line), $x' = 0.6$ (solid line) $x' = 0.8$ (solid line) and for $x' = 1.2$ (dotted line).

The full solution for the step barrier at $B_2C_1/B_2'C_1' = \pm\gamma_1\sqrt{t_0 + t_1^*}$ in terms of the original variables is

$$\begin{aligned} V_s(S,t) &= \exp\left(-r(T-t)\right) S^{\frac{1}{2}-\frac{r}{\sigma^2}} \exp\left[-\left(\frac{\sigma^2}{8} + \frac{r^2}{2\sigma^2} - \frac{r}{2}\right)(T-t)\right] \qquad (4.16) \\ & \sum_{N=0}^{\infty} c_N \exp\left[-\frac{(2N+1)^2\pi^2}{4\gamma_2^2(t_0+t_1^*)}\frac{\sigma^2}{2}(t^*-t)\right] \cos\left[\frac{(2N+1)\pi}{2\gamma_2\sqrt{t_0+t_1^*}} \ln\left(\frac{S}{S_0}\right)\right], \end{aligned}$$

the graph of which can be viewed in figure 4.5 (S is scaled on the initial asset value S_0). We plot the solution of the step barrier at $B_2C_1/B_2'C_1'$ against time from 0 to 85 where the jump occurs. The time where the jump occurs can be seen from the vertical line at the graph situated at $t^* = 85$ ($t_1^* = 0.3$). The explanation we give for the curves is similar to the one we gave for the curves in figure 4.4. It can be seen that for small values of S far away from the wedge barrier, the price of the option is not affected and does not drop as it approaches the jump (top solid and dashed lines in figure 4.5). When the asset is close to the barrier and near to the time of the jump (middle and bottom solid lines and bottom dashed line in figure 4.5), the price of the option drops dramatically. The possibility of hitting a nullified region increases leaving very little chances for the underlying to fit in the region of the new shrunken barrier.

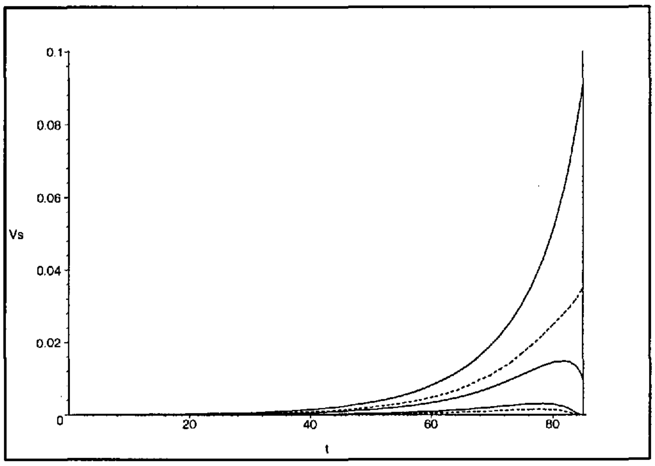

Fig. 4.5: Plot of the step Fourier series solution $V_s(S,t)$ against time t, from top to bottom, for $S = \exp(0.2)$ (solid line), $S = \exp(0.6)$ (dotted line), $S = \exp(0.8)$ (solid line), $S = \exp(1.2)$ (solid line) and for $S = \exp(1.3)$ (dotted line).

Suppose that at time $t_1 = t_1^{**}$, say, the Fourier series solution (4.14) hits the inner wedge W_1 at the point C_1 (at $\gamma_1\sqrt{t_0 + t_1^* + t_1^{**}}$) and jumps to the point C_2 (at $\gamma_2\sqrt{t_0 + t_1^* + t_1^{**}}$) where it meets the outer wedge W_2. The time where the next jump will occur will be at

$$\gamma_2\sqrt{t_0 + t_1^*} = \gamma_1\sqrt{t_0 + t_1^* + t_1^{**}} \Rightarrow t_1^{**} = 0.75\,.$$

At that time, the Fourier series solution for the new barrier ($\pm\gamma_2\sqrt{t_0 + t_1^* + t_1^{**}} = \pm 2.2361$) will be of the form

$$W_{ss}(x', t_1) = \sum_{N=0}^{\infty} d_N \exp\left(-\frac{(2N+1)^2\pi^2}{4\gamma_2^2(t_0 + t_1^* + t_1^{**})}\, t_1\right) \cos\left(\frac{(2N+1)\pi}{2\gamma_2\sqrt{t_0 + t_1^* + t_1^{**}}}\, x'\right), \tag{4.17}$$

with corresponding eigenvalues $k_N = \frac{(2N+1)\pi}{2\gamma_2\sqrt{t_0+t_1^*+t_1^{**}}}$. The width of the new barrier

$\pm\gamma_2\sqrt{t_0+t_1^*+t_1^{**}}$ will be $\frac{|x'|}{\sqrt{t_0+t_1^*+t_1^{**}}}$ and the boundary condition will become

$$W_{ss}=0 \quad \text{at} \quad \eta=\frac{|x'|}{\sqrt{t_0+t_1^*+t_1^{**}}} \Rightarrow |x'|=\gamma_2\sqrt{t_0+t_1^*+t_1^{**}}.$$

At $t_1=t_1^{**}$ the following equality holds

$$\begin{aligned} W_s(x',t_1^{**}) &= W_{ss}(x',t_1^{**}) \\ &= \sum_{N=0}^{\infty} d_N \cos\left(\frac{(2N+1)\pi}{2\gamma_2\sqrt{t_0+t_1^*+t_1^{**}}}\,x'\right)\exp\left(-\frac{(2N+1)^2\pi^2}{4\gamma_2^2(t_0+t_1^*+t_1^{**})}\,t_1^{**}\right), \end{aligned} \tag{4.18}$$

where the left-hand side is given by (4.14) evaluated at $t_1=t_1^{**}$, valid for $-\gamma_2\sqrt{t_0+t_1^*}<x'<\gamma_2\sqrt{t_0+t_1^*}$ and is zero at the regions $-\gamma_2\sqrt{t_0+t_1^*+t_1^{**}}<x'<-\gamma_2\sqrt{t_0+t_1^*}$ $(C_2'C_1')$ and $\gamma_2\sqrt{t_0+t_1^*}<x'<\gamma_2\sqrt{t_0+t_1^*+t_1^{**}}$ (C_1C_2).

We multiply equation (4.18) by $\cos\left(\frac{(2M+1)\pi}{2\gamma_2\sqrt{t_0+t_1^*+t_1^{**}}}\,x'\right)$ and integrate with respect to x' from $-\gamma_2\sqrt{t_0+t_1^*+t_1^{**}}$ to $\gamma_2\sqrt{t_0+t_1^*+t_1^{**}}$. Using the orthogonality condition as before, when $M=N$, equation (4.18) becomes

$$\begin{aligned} &\int_{-\gamma_2\sqrt{t_0+t_1^*}}^{\gamma_2\sqrt{t_0+t_1^*}} W_s(x',t_1^{**})\cos\left(\frac{(2N+1)\pi}{2\gamma_2\sqrt{t_0+t_1^*+t_1^{**}}}\,x'\right)dx' \\ &= d_N\exp\left(-\frac{(2N+1)^2\pi^2}{4\gamma_2^2(t_0+t_1^*+t_1^{**})}\,t_1^{**}\right)\int_{-\gamma_2\sqrt{t_0+t_1^*+t_1^{**}}}^{\gamma_2\sqrt{t_0+t_1^*+t_1^{**}}}\left[\cos\left(\frac{(2N+1)\pi}{2\gamma_2\sqrt{t_0+t_1^*+t_1^{**}}}\,x'\right)\right]^2 dx', \end{aligned}$$

or else

$$e_N=\frac{\int_{-\gamma_2\sqrt{t_0+t_1^*}}^{\gamma_2\sqrt{t_0+t_1^*}} W_s(x',t_1^{**})\cos\left(\frac{(2N+1)\pi}{2\gamma_2\sqrt{t_0+t_1^*+t_1^{**}}}\,x'\right)dx'}{\int_{-\gamma_2\sqrt{t_0+t_1^*+t_1^{**}}}^{\gamma\sqrt{t_0+t_1^*+t_1^{**}}}\left[\cos\left(\frac{(2N+1)\pi}{2\gamma_2\sqrt{t_0+t_1^*+t_1^{**}}}\,x'\right)\right]^2 dx'}, \tag{4.19}$$

where $e_N=d_N\exp\left(-\frac{(2N+1)^2\pi^2}{4\gamma_2^2(t_0+t_1^*+t_1^{**})}\,t_1^{**}\right)$.

Hence the Fourier series solution for the step barrier $\pm\gamma_2\sqrt{t_0+t_1^*+t_1^{**}}$ is

$$W_{ss}(x',t_1)=\sum_{N=0}^{\infty} e_N\exp\left(-\frac{(2N+1)^2\pi^2}{4\gamma_2^2(t_0+t_1^*+t_1^{**})}\,(t_1-t_1^{**})\right)\cos\left(\frac{(2N+1)\pi}{2\gamma_2\sqrt{t_0+t_1^*+t_1^{**}}}\,x'\right), \tag{4.20}$$

where the coefficient e_N for $\gamma_2=2$, $t_0=0.2$, $t_1^*=0.3$ and $t_1^{**}=0.75$ takes values given in table 4.3.

In figure 4.6 are shown the plots of the solution (4.20) against time t_1 $(0.75<t_1<2)$

Values of e_N		
$e_0 = 0.08676198999$	$e_{11} = 0.0002917904919$	$e_{21} = -0.00003850981413$
$e_1 = 0.03650317000$	$e_{12} = -0.0003611459178$	$e_{22} = -0.00008714764096$
$e_2 = -0.002319828039$	$e_{13} = 0.00003868698268$	$e_{23} = 0.00009680629765$
$e_3 = -0.003916151403$	$e_{14} = 0.0002410490672$	$e_{24} = 0.000001490455874$
$e_4 = 0.002638624099$	$e_{15} = -0.0001998086653$	$e_{25} = -0.00008331637588$
$e_5 = 0.0001335031823$	$e_{16} = -0.00004353690026$	$e_{26} = 0.00006109036287$
$e_6 = -0.001324772326$	$e_{17} = 0.0001879528450$	$e_{27} = 0.00002577151126$
$e_7 = 0.0007306768033$	$e_{18} = -0.0001013205887$	$e_{28} = -0.00007220863912$
$e_8 = 0.0003116930022$	$e_{19} = -0.00007760952662$	$e_{29} = 0.00003208930048$
$e_9 = -0.0006551815695$	$e_{20} = 0.0001392528694$	$e_{30} = 0.00003877594374$
$e_{10} = 0.0002293777166$		

Tab. 4.3: Values of the Fourier coefficient e_N for $N = 0..30$.

for different values of $x' > 0$ inside the barrier $[C_2D_1, C_2'D_1']$. Again, for small values of x', the price of the option is high compared to the price it takes when x''s get large. As the x''s get larger, closer to the expanding barrier, the price of the option gets cheaper to become zero for the case where the underlying has reached the jump. The

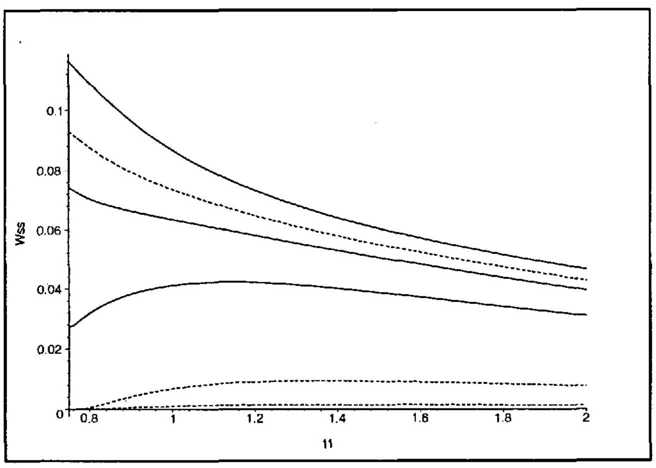

Fig. 4.6: Plot of the step Fourier series solution $W_{ss}(x', t_1)$ against time , from top to bottom, for $x' = 0.2$ (solid line), $x' = 0.6$ (dashed line), $x' = 0.8$ (solid line), $x' = 1.2$ (solid line) and for $x' = 2.0$ (dashed line).

full solution for the step barrier at $\pm\gamma_1\sqrt{t_0 + t_1^* + t_1^{**}}$ in terms of the original variables

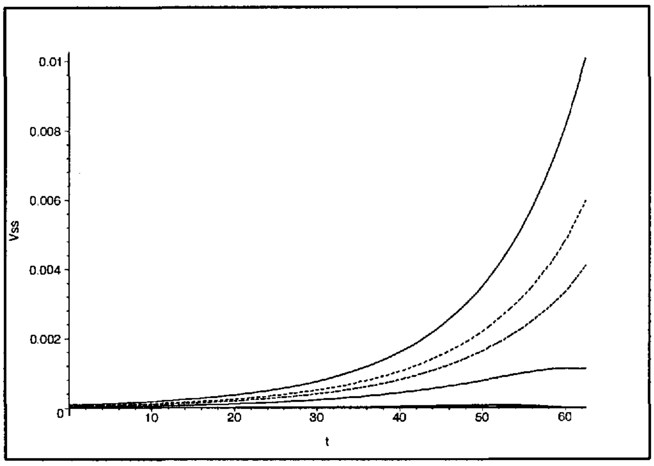

Fig. 4.7: Plot of the step Fourier series solution $V_{ss}(S,t)$ against time , from top to bottom, for $S = \exp(0.2)$ (solid line), $S = \exp(0.6)$ (dashed line), $S = \exp(0.8)$ (dotted line), $S = \exp(1.2)$ (dashed line) and for $S = \exp(2.0)$ (solid line).

will be

$$V_{ss}(S,t) = \exp(-r(T-t))\, S^{\frac{1}{2}-\frac{r}{\sigma^2}} \exp\left[-\left(\frac{\sigma^2}{8}+\frac{r^2}{2\sigma^2}-\frac{r}{2}\right)(T-t)\right] \tag{4.21}$$
$$\sum_{N=0}^{\infty} e_N \exp\left[-\frac{(2N+1)^2\pi^2}{4\gamma_2^2(t_0+t_1^*+t_1^{**})}\frac{\sigma^2}{2}(t^{**}-t)\right]\cos\left[\frac{(2N+1)\pi}{2\gamma_2\sqrt{t_0+t_1^*+t_1^{**}}}\ln\left(\frac{S}{S_0}\right)\right].$$

In figure 4.7 we plot the solution $V_{ss}(S,t)$ for the step barrier $[C_2D_1, C_2'D_1']$ against real time t $(0 < t < 62.5)$. Note that S is scaled on the initial asset value S_0. For large values of S (close to the barrier $C_2D_1/C_2'D_1'$) the value of the option drops significantly.

Next suppose that at $t_1 = t_1^{***}$ the Fourier series (4.20) hits the inner wedge at D_1 (at $\gamma_2\sqrt{t_0+t_1^*+t_1^{**}}$) and jumps to the point D_2 (at $\gamma_2\sqrt{t_0+t_1^*+t_1^{**}+t_1^{***}}$) of the outer wedge. The jump will occur at time

$$\gamma_2\sqrt{t_0+t_1^*+t_1^{**}} = \gamma_1\sqrt{t_0+t_1^*+t_1^{**}+t_1^{***}} \Rightarrow t_1^{***} = 1.875\,.$$

At that time, t_1^{***} the barrier has jumped to values $\pm\gamma_2\sqrt{t_0+t_1^*+t_1^{**}+t_1^{***}}$ and the Fourier series solution will have the form

$$W_{sss}(x',t_1) = \sum_{N=0}^{\infty} f_N \exp\left(-\frac{(2N+1)^2\pi^2}{4\gamma_2^2(t_0+t_1^*+t_1^{**}+t_1^{***})}t_1\right)\cos\left(\frac{(2N+1)\pi}{2\gamma_2\sqrt{t_0+t_1^*+t_1^{**}+t_1^{***}}}x'\right). \tag{4.22}$$

At $t_1 = t_1^{***}$, (4.22) will become

$$W_{sss}(x', t_1^{***}) = \sum_{N=0}^{\infty} f_N \exp\left(-\frac{(2N+1)^2\pi^2}{4\gamma_2^2(t_0+t_1^*+t_1^{**}+t_1^{***})}\, t_1^{***}\right)\cos\left(\frac{(2N+1)\pi}{2\gamma_2\sqrt{t_0+t_1^*+t_1^{**}+t_1^{***}}}\, x'\right), \tag{4.23}$$

where the left-hand-side is equal to (4.20) evaluated at t_1^{***},

$$W_{ss}(x', t_1^{***}) = \sum_{N=0}^{\infty} e_N \exp\left(-\frac{(2N+1)^2\pi^2}{4\gamma_2^2(t_0+t_1^*+t_1^{**})}\,(t_1^{***}-t_1^{**})\right)\cos\left(\frac{(2N+1)\pi}{2\gamma_2\sqrt{t_0+t_1^*+t_1^{**}}}\, x'\right), \tag{4.24}$$

valid for $-\gamma_2\sqrt{t_0+t_1^*+t_1^{**}} < x' < \gamma_2\sqrt{t_0+t_1^*+t_1^{**}}$ $(D_1'D_1)$ and zero in the intervals $-\gamma_2\sqrt{t_0+t_1^*+t_1^{**}+t_1^{***}} < x' < -\gamma_2\sqrt{t_0+t_1^*+t_1^{**}}$ $(D_2'D_1')$ and $\gamma_2\sqrt{t_0+t_1^*+t_1^{**}} < x' < \gamma_2\sqrt{t_0+t_1^*+t_1^{**}+t_1^{***}}$ (D_1D_2).
Multiplying equation (4.23) by $\cos\left(\frac{(2M+1)\pi}{2\gamma_2\sqrt{t_0+t_1^*+t_1^{**}+t_1^{***}}}\, x'\right)$ and integrating with respect to x' from $-\gamma_2\sqrt{t_0+t_1^*+t_1^{**}+t_1^{***}}$ to $\gamma_2\sqrt{t_0+t_1^*+t_1^{**}+t_1^{***}}$ we get

$$g_N = \frac{\int_{-\gamma_2\sqrt{t_0+t_1^*+t_1^{**}}}^{\gamma_2\sqrt{t_0+t_1^*+t_1^{**}}} W_{ss}(x', t_1^{***})\cos\left(\frac{(2N+1)\pi}{2\gamma_2\sqrt{t_0+t_1^*+t_1^{**}+t_1^{***}}}\, x'\right)dx'}{\int_{-\gamma_2\sqrt{t_0+t_1^*+t_1^{**}+t_1^{***}}}^{\gamma\sqrt{t_0+t_1^*+t_1^{**}+t_1^{***}}}\left[\cos\left(\frac{(2N+1)\pi}{2\gamma_2\sqrt{t_0+t_1^*+t_1^{**}+t_1^{***}}}\, x'\right)\right]^2 dx'}, \tag{4.25}$$

using the orthogonality condition (when $M = N$), where
$g_N = e_N \exp\left(-\frac{(2N+1)^2\pi^2}{4\gamma_2^2(t_0+t_1^*+t_1^{**}+t_1^{***})}\, t_1^{***}\right)$.
Hence the Fourier series solution for the step barrier $\pm\gamma_2\sqrt{t_0+t_1^*+t_1^{**}+t_1^{***}}$ is

$$\begin{aligned} W_{sss}(x', t_1) &= \sum_{N=0}^{\infty} e_N \exp\left(-\frac{(2N+1)^2\pi^2}{4\gamma_2^2(t_0+t_1^*+t_1^{**}+t_1^{***})}\,(t_1-t_1^{***})\right) \\ &\quad \cos\left(\frac{(2N+1)\pi}{2\gamma_2\sqrt{t_0+t_1^*+t_1^{**}+t_1^{***}}}\, x'\right), \end{aligned} \tag{4.26}$$

where the coefficient g_N for $\gamma_2 = 2$, $t_0 = 0.2$, $t_1^* = 0.3$, $t_1^{**} = 0.75$ and $t_1^{***} = 1.875$ takes values given in table 4.4.
The full solution for the step barrier at $\pm\gamma_2\sqrt{t_0+t_1^*+t_1^{**}+t_1^{***}}$ in terms of the original

Values of g_N		
$g_0 = 0.03644113456$	$g_{11} = 0.0001225415895$	$g_{21} = -0.00001617280443$
$g_1 = 0.01533277474$	$g_{12} = -0.0001516685038$	$g_{22} = -0.00003659902886$
$g_2 = -0.0009731841039$	$g_{13} = 0.00001624717241$	$g_{23} = 0.00004065534015$
$g_3 = -0.001644500363$	$g_{14} = 0.0001012321951$	$g_{24} = 0.0000006259398367$
$g_4 = 0.001108087526$	$g_{15} = -0.00008391269325$	$g_{25} = -0.00003499003860$
$g_5 = 0.00005606547554$	$g_{16} = -0.00001828398861$	$g_{26} = 0.00002565587354$
$g_6 = -0.0005563505998$	$g_{17} = 0.00007893370621$	$g_{27} = 0.00001082315705$
$g_7 = 0.0003068559987$	$g_{18} = -0.00004255115938$	$g_{28} = -0.00003032517326$
$g_8 = 0.0001308993793$	$g_{19} = -0.00003259333319$	$g_{29} = 0.00001347641678$
$g_9 = -0.0002751522322$	$g_{20} = 0.00005848142910$	$g_{30} = 0.00001628457913$
$g_{10} = 0.00009633036139$		

Tab. 4.4: Values of the Fourier coefficient g_N for $N = 0..30$.

variables will be

$$V_{sss}(S,t) = \exp\left(-r(T-t)\right) S^{\frac{1}{2}-\frac{r}{\sigma^2}} \exp\left[-\left(\frac{\sigma^2}{8}+\frac{r^2}{2\sigma^2}-\frac{r}{2}\right)(T-t)\right] \sum_{N=0}^{\infty} e_N \exp\left[-\frac{(2N+1)^2\pi^2}{4\gamma_2^2(t_0+t_1^*+t_1^{**}+t_1^{***})}\frac{\sigma^2}{2}(t^{***}-t)\right] \cos\left[\frac{(2N+1)\pi}{2\gamma_2\sqrt{t_0+t_1^*+t_1^{**}+t_1^{***}}}\ln\left(\frac{S}{S_0}\right)\right]. \quad (4.27)$$

Note that V_{sss} is the notation for the value of the option after the third jump of the barrier. In figure 4.8 are the plots of the solution (4.27) against time t $(0 < t < 6.25)$ for different values of $S > 0$. The value of the option after the third jump of the barrier is very small, as the underlying has more chances of hitting the barriers and is far away from maturity.

In figure 4.9 we plot the Fourier series solutions for every step barrier occurring during the life of the option from $t = 0$ to expiry $T = 100$ evaluated at $S = \exp(0.4)$ (note that S is scaled on the initial asset value S_0). The position of the point taken can be seen in figure 4.10 at $x' = 0.4$. The times where the jumps occur are at $t^* = 85$, $t^{**} = 62.5$ and $t^{***} = 6.25$. At the expiry date $t = 100$ days, the value of the option, $V(S,t)$ (for $85 < t < 100$), has a certain value which decreases as time moves away from maturity (moving backwards in real time). As the first jump takes place at $t^* = 85$ days, the value of the option $V_s(S,t)$ (for $85 < t < 62.5$) continues to drop exponentially. After the second jump, at $t^{**} = 62.5$, the price of the option $V_{ss}(S,t)$ (for $62.5 < t < 6.25$) becomes even smaller reaching a very small value after the jump at $t^{***} = 6.25$, for $V_{sss}(S,t)$ (for $0 < t < 6.25$). At time far away from maturity the

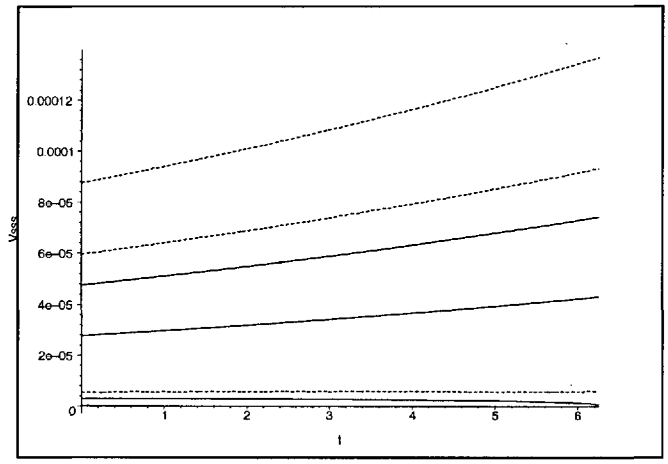

Fig. 4.8: Plot of the step Fourier series solution $V_{sss}(S,t)$ against time, from top to bottom, for $S = \exp(0.2)$ (dotted line), $S = \exp(0.6)$ (dotted line), $S = \exp(0.8)$ (solid line) $S = \exp(1.2)$ (solid line), $S = \exp(2.0)$ (dotted line) and for $S = \exp(2.2)$ (solid line).

value of the option is quite cheap for two reasons. One is because the underlying is far away from the expiry and the other is because the underlying has more time to move and hit the shrinking barrier (wedge), which decreases symmetrically till reaching the values $\pm\gamma_2\sqrt{t_0}$ at maturity.

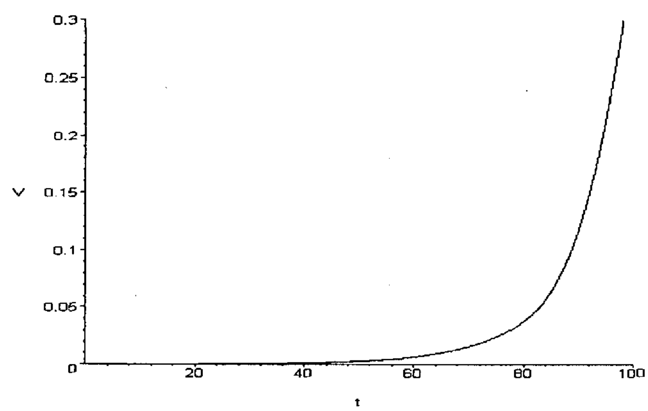

Fig. 4.9: Plot of the step Fourier series solution throughout the life of the option for $S = \exp(0.4)$.

Moving position to $S = \exp(1.0)$ (where S is scaled on S_0), dashed line $x' = 1$ in figure 4.10, one can see the graph for the step barrier in figure 4.11. The value of the step barrier is plotted against real time till 25 days prior to expiry ($0 < t < 85$). This is because at that level the value of the barrier option V (valid for $0 < t < 100$) is zero, as the point taken is outside the barrier region. The figure includes only the other three step barriers, namely V_s (for $62.5 < t < 85$), V_{ss} (for $6.25 < t < 62.5$) and V_{sss} (for $0 < t < 6.25$). The value of the option is cheaper compared to the previous graph since the underlying is further away from expiry, increasing the chances of hitting the barrier. As the option moves towards maturity (towards $t^* = 85$), the value increases reaching a highest value, which is the best possible case scenario for missing the barrier. As soon as that point is bypassed the value drops dramatically, since the underlying has no time before the jump to manoeuvre without hitting the barrier or the nullified region created by the jump ($B_1 B_2 / B_1' B_2'$ in figure 4.10).

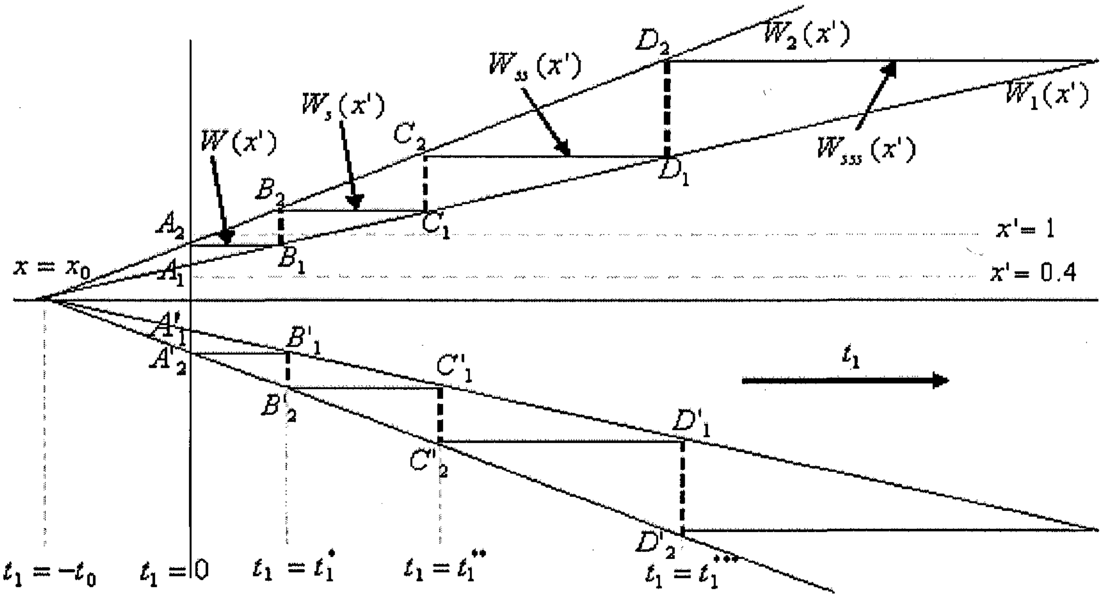

Fig. 4.10: Jump of the barrier at times $t = t_1^*$, $t = t_1^{**}$ and $t = t_1^{***}$.

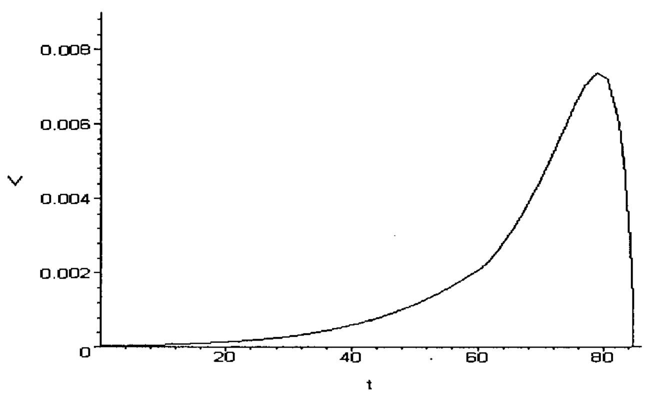

Fig. 4.11: Plot of the step Fourier series solution throughout the life of the option for $S = \exp(1.0)$.

5. N-DIMENSIONAL BLACK SCHOLES EQUATION

Multi-asset options have payoffs depending on the underlying price of more than one asset. These options are also called basket options which are derivatives where the underlying asset is a basket of various financial instruments.

There are certain factors that make the pricing and hedging of multi-asset options difficult. Some of them are the dimensionality, i.e. the number of underlying assets, the existence and derivation of a closed-form solution as well as the path-dependency. The dimensionality refers to the number of underlying assets in an option as well as the number of independent variables. There can be two different types of dimensionality. One is in the case of weak path-dependent contracts, like barrier or basket options, where the dimensionality of the option depends only on the underlying asset and time. The other type of dimensionality is in the case of strong path-dependent options where the price of the option depends on a third independent variable, such as lookback or Asian options. The new variable can be an average of the asset price to date (Asian options) and will be discussed in later chapters.

5.1 N-dimensional Black-Scholes equation

Suppose we have a multi-asset contract in a risk-neutral world. The option has N underlying assets with maturity T. During the life of the option the assets move freely in the area created by two knock-out barriers. If the underlying hits either barrier, the option expires immediately with the value zero otherwise expires at maturity T. The two barriers are fixed in S space. We transform the problem to a radial problem and solve it using the WKB method (named after Wentzel, Kramers and Billouin). We also express the solution in terms of Bessel functions of first and second kind. The two barriers remain fixed in the r space.

We work with $t_1 = T - t$, so $t_1 > 0$ measures the time left to expiry at $t_1 = 0$ ($t = T$). We refer back to the N-dimensional equations stated in section 3.2. The N-dimensional version of the Black-Scholes equation can be written in the form of the heat equation

$$\frac{\partial W}{\partial t_1} = \sum_{p=1}^{N} \frac{\partial^2 W}{\partial x_p'^2}\,, \tag{5.1}$$

subject to the boundary conditions

$$W = 0\,, \qquad \text{at} \qquad x = x_I\,, \tag{5.2}$$

$$W = 0\,, \qquad \text{at} \qquad x = x_O\,, \tag{5.3}$$

where x_I is the inner barrier and x_O the outer barrier. Converting the N-dimensional cartesian heat equation to polar coordinates takes the form

$$\frac{\partial W}{\partial t_1} = \frac{\partial^2 W}{\partial r^2} + \frac{N-1}{r}\frac{\partial W}{\partial r}\,, \tag{5.4}$$

with

$$W = 0\,, \qquad \text{at} \qquad r = r_I\,, \tag{5.5}$$

$$W = 0\,, \qquad \text{at} \qquad r = r_O\,, \tag{5.6}$$

where r_I and r_O are the inner and outer radial barriers respectively. At this stage the shape of the radial barrier is not specified.

Going back to the PDE (5.4) we use separation of variables by setting $W(r, t_1) = R(r)T(t_1)$. The ODE for $R(r)$ has the form

$$\frac{d^2 R}{dr^2} + \frac{N-1}{r}\frac{dR}{dr} + \lambda^2 R = 0\,, \tag{5.7}$$

where λ is the separation variable.
We seek a solution of the form $R(r) = \exp(f(r))R_1(r)$ and the ODE (5.7) takes the form

$$\frac{d^2 R_1}{dr^2} + \left(2f' + \frac{N-1}{r}\right)\frac{dR_1}{dr} + \left(f'' + f'^2 + \frac{N-1}{r}f' + \lambda^2\right)R_1 = 0\,.$$

We choose $f(r)$ to be such that the first derivative disappears,

$$f(r) = -\frac{N-1}{2}\ln(r) + c\,, \quad \text{where} \quad c = 0\,, \tag{5.8}$$

and the equation (5.7) takes the form

$$\frac{d^2R_1}{dr^2} = -\left(\frac{N-1}{2r^2} - \frac{(N-1)^2}{4r^2} + \lambda^2\right). \tag{5.9}$$

The latter equation is of the form

$$\epsilon^2 y'' = Q(x)y\,, \quad Q(x) \neq 0\,, \text{with} \quad \epsilon \quad \text{small}\,,$$

with solution

$$y(x) \sim c_1 Q(x)^{-1/4} \exp\left(\frac{1}{\epsilon}\int_a^x \sqrt{Q(\tau)}\,d\tau\right) + c_2 Q(x)^{-1/4} \exp\left(-\frac{1}{\epsilon}\int_a^x \sqrt{Q(\tau)}\,d\tau\right). \tag{5.10}$$

This is found using the WKB method, e.g. Bender and Orszag [6].
For our case $Q(r) = -\left(\frac{N-1}{2r^2} - \frac{(N-1)^2}{4r^2} + \lambda^2\right)$ and the solution for (5.4) takes the form

$$\begin{aligned} W(r,t_1) &= \sum_{n=1}^{\infty} A_n \exp(-\lambda_n^2 t_1)\, r^{-\frac{N-1}{2}} \left(\frac{N-1}{2r^2} - \frac{(N-1)^2}{4r^2} + \lambda_n^2\right)^{-1/4} \\ &\quad \sin\left(\int_{r_I}^{r} \sqrt{\frac{N-1}{2\tau^2} - \frac{(N-1)^2}{4\tau^2} + \lambda_n^2}\, d\tau\right), \end{aligned} \tag{5.11}$$

where $A = 2i/\sqrt{i}c_1$, $c_2 = -c_1$ and where the lower limit has been chosen such that the boundary condition at $r = r_I$ is satisfied, (5.5). Applying the other boundary condition at the outer barrier, (5.6), we find an equation for the eigenvalues λ_n valid for N dimensions

$$\int_{r_I}^{r_O} \sqrt{\frac{N-1}{2\tau^2} - \frac{(N-1)^2}{4\tau^2} + \lambda_n^2}\, d\tau = n\pi\,, \tag{5.12}$$

where N denotes the dimension and n the numbers of nodes[1]. To determine the values of λ_n we rearrange (5.12) so that it looks like

$$\sqrt{A + \lambda_n^2 r_O^2} - \sqrt{A + \lambda_n^2 r_I^2} + \frac{\sqrt{A}}{2}\ln\left(\frac{\sqrt{A + \lambda_n^2 r_O^2} - \sqrt{A}}{\sqrt{A + \lambda_n^2 r_O^2} + \sqrt{A}}\,\frac{\sqrt{A + \lambda_n^2 r_I^2} + \sqrt{A}}{\sqrt{A + \lambda_n^2 r_I^2} - \sqrt{A}}\right) - n\pi = 0\,, \tag{5.13}$$

where for convenience we have named $A = \frac{N-1}{2\tau^2} - \frac{(N-1)^2}{4\tau^2}$. This equation must be solved numerically.

[1] Nodes are the points of a vibrating string that do not move.

The solution for (5.7) can be written in terms of Bessel functions

$$R(r) = C_1\, r^{1-\frac{N}{2}}\, J_{\frac{N}{2}-1}(\lambda_n r) + C_2\, r^{1-\frac{N}{2}}\, Y_{\frac{N}{2}-1}(\lambda_n r)\,, \tag{5.14}$$

where J and Y are the Bessel functions of first and second kind respectively with argument $\lambda_n r$ and fractional order $\frac{N}{2}-1$. Applying the boundary conditions we have

$$C_1\, r_I^{1-\frac{N}{2}}\, J_{\frac{N}{2}-1}(\lambda_n r_I) + C_2\, r_I^{1-\frac{N}{2}}\, Y_{\frac{N}{2}-1}(\lambda_n r_I) = 0\,, \tag{5.15}$$

and

$$C_1\, r_O^{1-\frac{N}{2}}\, J_{\frac{N}{2}-1}(\lambda_n r_O) + C_2\, r_O^{1-\frac{N}{2}}\, Y_{\frac{N}{2}-1}(\lambda_n r_O) = 0\,. \tag{5.16}$$

which may be written in the form

$$\begin{pmatrix} r_I^{1-\frac{N}{2}}\, J_{\frac{N}{2}-1}(\lambda_n r_I) & r_I^{1-\frac{N}{2}}\, Y_{\frac{N}{2}-1}(\lambda_n r_I) \\ r_O^{1-\frac{N}{2}}\, J_{\frac{N}{2}-1}(\lambda_n r_O) & r_O^{1-\frac{N}{2}}\, Y_{\frac{N}{2}-1}(\lambda_n r_O) \end{pmatrix} \begin{pmatrix} C_1 \\ C_2 \end{pmatrix} = 0\,.$$

For a nontrivial solution we require the determinant of the 2×2 matrix formed by the coefficients of C_1 and C_2 to be equal to zero so that C_1 and C_2 are not identically zero

$$\begin{vmatrix} r_I^{1-\frac{N}{2}}\, J_{\frac{N}{2}-1}(\lambda_n r_I) & r_I^{1-\frac{N}{2}}\, Y_{\frac{N}{2}-1}(\lambda_n r_I) \\ r_O^{1-\frac{N}{2}}\, J_{\frac{N}{2}-1}(\lambda_n r_O) & r_O^{1-\frac{N}{2}}\, Y_{\frac{N}{2}-1}(\lambda_n r_O) \end{vmatrix} = 0\,,$$

or equivalently

$$J_{\frac{N}{2}-1}(\lambda_n r_I)\, Y_{\frac{N}{2}-1}(\lambda_n r_O) - J_{\frac{N}{2}-1}(\lambda_n r_O)\, Y_{\frac{N}{2}-1}(\lambda_n r_I) = 0\,. \tag{5.17}$$

Equation (5.17) gives the formula for finding the eigenvalues of the problem. Using equation (5.15) the solution to the radial ODE (5.7) takes the form

$$R(r) = C_1\, r^{1-\frac{N}{2}} \left[J_{\frac{N}{2}-1}(\lambda_n r) - \frac{J_{\frac{N}{2}-1}(\lambda_n r_I)}{Y_{\frac{N}{2}-1}(\lambda_n r_I)}\, Y_{\frac{N}{2}-1}(\lambda_n r) \right]\,, \tag{5.18}$$

The full solution of the N-dimensional problem in terms of the Bessel functions is

$$W(r,t_1) = \sum_{n=1}^{N} D_n \exp\left(-\lambda_n^2 t_1\right) r^{1-\frac{N}{2}} \left[Y_{\frac{N}{2}-1}(\lambda_n r_I)\, J_{\frac{N}{2}-1}(\lambda_n r) - J_{\frac{N}{2}-1}(\lambda_n r_I)\, Y_{\frac{N}{2}-1}(\lambda_n r) \right]. \tag{5.19}$$

where $D_n = \frac{C_1}{Y_{\frac{N}{2}-1}(\lambda_n r_I)}$.

5.2 Three Dimensional Case

As an example of the multi-asset version of the Black-Scholes we focus our interest on a three-asset basket option. The underlying assets move freely in time under the effect of two barriers which have the shape of a sphere. The two spherical barriers are concentric with radius r_I and r_O for the inner and outer sphere, respectively ($r_I < r_O$). The barriers expand in time $t_1 = T - t$ creating two wedges shaped as cones which shrink as t_1 approaches zero. The barriers are knock-out i.e. if either of the barriers is triggered, the option expires worthless. If the underlying does not hit either of the two barriers it expires with the value of one. We present the solution to the problem in the form of Fourier series and then re-value the option when the two spherical barriers have grown at some time, t_1^* say. Throughout the life of the option the two barriers maintain their knock-out nature.

Recall equation (3.15) for the multi-asset Black-Scholes equation in the form of the N-dimensional heat equation

$$\frac{\partial W}{\partial t_1} = \sum_{p=0}^{N} \frac{\partial^2 W}{\partial x'_p \partial x'_p}, \tag{5.20}$$

which in terms of the polar coordinates takes the form

$$\frac{\partial W}{\partial t_1} = \frac{\partial^2 W}{\partial r^2} + \frac{N-1}{r}\frac{\partial W}{\partial r}, \tag{5.21}$$

subject to

$$\begin{aligned} W(r) &= 0\,, \quad \text{at} \quad r = r_I\,, \\ W(r) &= 0\,, \quad \text{at} \quad r = r_O\,, \end{aligned} \tag{5.22}$$

and with payoff

$$W(r,0) = 1\,. \tag{5.23}$$

where r_I represents the inner spherical barrier and r_O the outer spherical barrier with $r_I < r_O$. For the three dimensional problem the above equation takes the form

$$\frac{\partial W}{\partial t_1} = \frac{\partial^2 W}{\partial r^2} + \frac{2}{r}\frac{\partial W}{\partial r}\,. \tag{5.24}$$

For this particular case (3-dimensional) we can transform the above PDE into the heat equation by applying the transformation $W = U/r$,

$$\frac{\partial U}{\partial t_1} = \frac{\partial^2 U}{\partial r^2}, \tag{5.25}$$

with boundary conditions

$$\begin{aligned} U(r) &= 0, \quad \text{at} \quad r = r_I, \\ U(r) &= 0, \quad \text{at} \quad r = r_O, \end{aligned} \tag{5.26}$$

when the two barriers r_I and r_O are hit and with payoff

$$U(r, 0) = r. \tag{5.27}$$

We now find the Fourier series solution of the three dimensional boundary value problem (5.25) and (5.26).
Using separation of variables for the heat equation (5.25) we have a solution in the form

$$U(r, t_1) = \sum_{n=1}^{\infty} A_n \exp\left(-\lambda_n^2 t_1\right) \sin\left(\lambda_n (r - r_I)\right), \tag{5.28}$$

which satisfies the boundary condition at $r = r_I$. By applying the boundary condition at $r = r_O$ the eigenvalues λ_n are given from the formula

$$\lambda_n = \frac{n\pi}{r_O - r_I}. \tag{5.29}$$

Recall

$$\eta = \frac{r^2}{t_1 + t_0}, \quad \eta_I = \frac{r_I^2}{t_1 + t_0} \quad \text{and} \quad \eta_O = \frac{r_O^2}{t_1 + t_0}. \tag{5.30}$$

For the numerical interpretation we fix η_I and η_O ($\eta_I = 1.0$, $\eta_O = 5.0$, say) and let r_I and r_O vary in time. At $t_1 = 0$, r_I and r_O take values $\sqrt{0.2}$ and 1.0 respectively. Using those values for r_I, r_O and taking $t_0 = 0.2$ we find the eigenvalues λ_n which are given in table 5.1.
Taking into account (5.29) equation (5.28) takes the form

$$U(r, t_1) = \sum_{n=1}^{\infty} A_n \exp\left(-\frac{n^2\pi^2}{(r_O - r_I)^2} t_1\right) \sin\left(\frac{n\pi}{r_O - r_I}(r - r_I)\right), \tag{5.31}$$

and satisfies the heat equation (5.25) along with the boundary conditions (5.26).

n	λ_n	n	λ_n
1	5.683194499	11	62.51513948
2	11.36638900	12	68.19833400
3	17.04958350	13	73.88152848
4	22.73277800	14	79.56472300
5	28.41597250	15	85.24791749
6	34.09916698	16	90.93111198
7	39.78236150	17	96.61430649
8	45.46555599	18	102.2975010
9	51.14875051	19	107.9806955
10	56.83194499	20	113.6638900

Tab. 5.1: Values of λ_n for $n = 1..20$

At time $t_1 = 0$ the following equality holds

$$U(r,0) = \sum_{n=1}^{\infty} A_n \sin\left(\frac{n\pi}{r_O - r_I}(r - r_I)\right), \tag{5.32}$$

where the left-hand side is the payoff given by equation (5.27).

To find the coefficient A_n we multiply equation (5.32) by $\sin\left(\frac{m\pi}{r_O - r_I}(r - r_I)\right)$ and integrate from r_I to r_O with respect to r. Using the orthogonality relation

$$\begin{aligned} &\int_{r_I}^{r_O} \sin\left(\frac{n\pi}{r_O - r_I}(r - r_I)\right) \sin\left(\frac{m\pi}{r_O - r_I}(r - r_I)\right) dr \\ &= \begin{cases} 0 & \text{, if } m \neq n \\ \int_{r_I}^{r_O} \left[\sin\left(\frac{n\pi}{r_O - r_I}(r - r_I)\right)\right]^2 dr & \text{, if } m = n \end{cases}, \end{aligned}$$

when $m = n$ we have

$$A_n = \frac{\int_{r_I}^{r_O} U(r,0) \sin\left(\frac{n\pi}{r_O - r_I}(r - r_I)\right) dr}{\int_{r_I}^{r_O} \left[\sin\left(\frac{n\pi}{r_O - r_I}(r - r_I)\right)\right]^2 dr}, \tag{5.33}$$

where $U(r,0) = r$ for this problem. For the values of t_0, r_I and r_O mentioned earlier, A_n takes values shown in table 5.2.

The full solution to the problem will be

$$W(r,t_1) = \sum_{n=1}^{\infty} A_n \frac{1}{r} \exp\left(-\frac{n^2\pi^2}{(r_O - r_I)^2} t_1\right) \sin\left(\frac{n\pi}{r_O - r_I}(r - r_I)\right). \tag{5.34}$$

In figure 5.1 we have plotted the solution at $t_1 = 0$. The value of the option is trying to adjust to the value of the payoff, 1, creating the shown discontinuity in the function

n	A_n	n	A_n
1	0.9213247898	11	0.08375679907
2	−0.1759573775	12	−0.02932622958
3	0.3071082632	13	0.07087113765
4	−0.08797868875	14	−0.02513676821
5	0.1842649580	15	0.06142165265
6	−0.05865245914	16	−0.02199467218
7	0.1316178271	17	0.05419557585
8	−0.04398934436	18	−0.01955081972
9	0.1023694211	19	0.04849077842
10	−0.03519147551	20	−0.01759573775

Tab. 5.2: Values of A_n for $n = 1..20$.

known as the Gibbs phenomenon effect. The price of the option oscillates around the value 1 between the two barriers at $r_I = \sqrt{0.2} = 0.4472135955$ and $r_O = 1.0$.

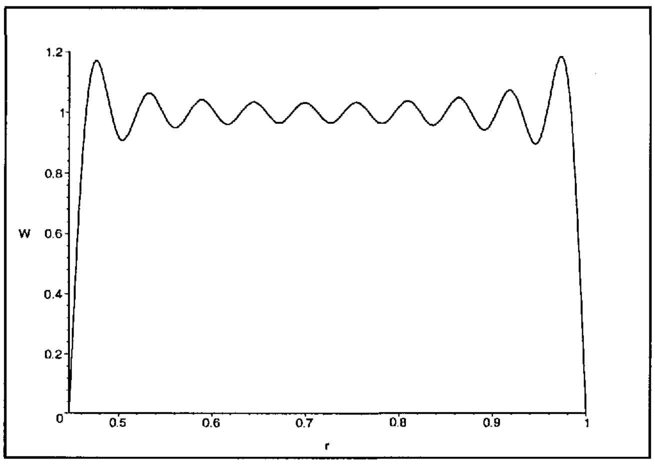

Fig. 5.1: Plot of the series solution $W(r, t_1)$ for $n = 20$, at $t_1 = 0$ against r.

To correct this effect, we can take the Fejer sums[2] and write the solution (5.34) as

$$W(r, t_1) = \frac{1}{N} \sum_{n=1}^{N} a_n \,, \tag{5.35}$$

where

$$a_n = A_n \frac{1}{r} \exp\left(-\frac{n^2\pi^2}{(r_O - r_I)^2} t_1\right) \sin\left(\frac{n\pi}{r_O - r_I}(r - r_I)\right).$$

[2] In 1900 Fejer published his fundamental summation theorem for Fourier series stating that the arithmetic means of the partial sums of Fourier series of a continuous function converge to the function.

Using this formulation, we plot in figure 5.2 the solution $W(r, t_1)$ at $t_1 = 0$ with the discontinuity corrected.

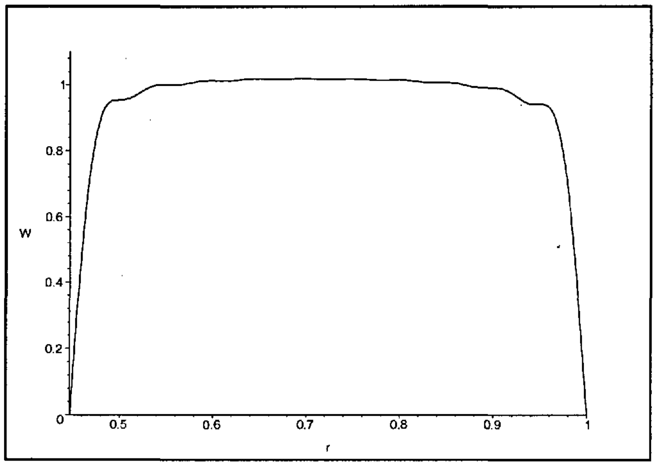

Fig. 5.2: Plot of the series solution $W(r, t_1)$ using the Fejer sums for $n = 20$, at $t_1 = 0$ against r.

In figure 5.3 we plot the solution $W(r, t_1)$ against r for $t_1 = 0.0001$ (dotted line), $t_1 = 0.001$ (dash dotted line) and $t_1 = 0.01$ (solid line). After a very small lapse of time at $t_1 = 0.0001$ the discontinuity has smoothed out and at time $t_1 = 0.001$ even more. At $t_1 = 0.01$ the discontinuity has faded away giving a nice smooth curve for the value of the option when the underlying has moved away from maturity. As we move away from the payoff the value of the option decreases. This happens as the chances of the asset hitting either of the two barriers increase making the value of the option expire worthless. The price of the option takes the shape of a curve after some time has elapsed. This is because as we move towards the middle of the area created by the two barriers the value increases as the chances of hitting any of the two barriers are very small. The holder of the option benefits from this position, as the chances of avoiding any of the two barriers and getting the payoff are good. The buyer will need to pay more for this position as he will have more chances of getting the payoff. The value of the option drops as we approach either barrier as the underlying has greater chances in hitting one of the barriers and the option expiring worthless. Hence the holder of the option can not benefit from this position, as the chances of expiring worthless have increased and hence the value of the option has dropped. On the other hand the buyer of such an option will not need to pay much to get into this position, as the chances of having loss have increased.

In figure 5.4 we plot the value of the option $W(r, t_1)$ against time t_1 when the underlying is situated in different positions between the two barriers. For any position of

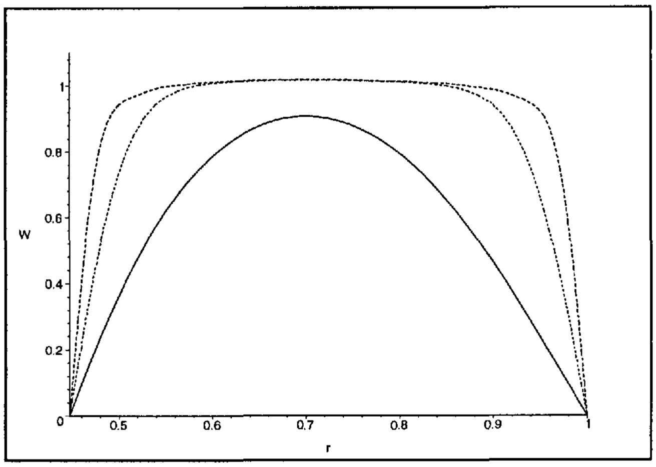

Fig. 5.3: Plot of the series solution $W(r, t_1)$ for $n = 20$, at $t_1 = 0.0001$ (top dotted line), at $t_1 = 0.001$ (middle dotted line) and at $t_1 = 0.01$ (solid line) against r.

the underlying between the two barriers, the price of the option is an exponentially decreasing function of time. Depending where it is positioned the value will be more or less expensive as time progresses.

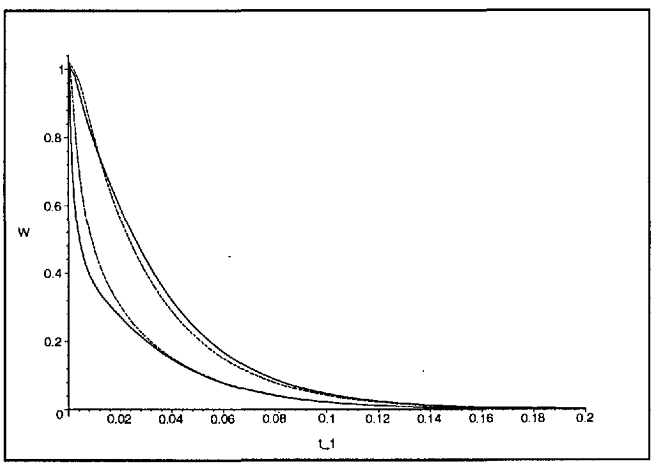

Fig. 5.4: Plot of the series solution $W(r, t_1)$ for $n = 20$ against time t_1 at $r = 0.5$ (lower solid line), $r = 0.6$ (upper solid line), $r = 0.8$ (upper dashed line) and at $r = 0.9$ (lower dashed line).

For example, if we plot the value of the option at $r = 0.5$ (close to the inner barrier r_I, lower solid line) and at $r = 0.6$ (upper solid line), the value of the option for the latter position will be more expensive than for the former position. This happens because at $r = 0.5$, the underlying is close to the inner barrier having substantial chances of hitting it. At $r = 0.6$ the asset is further away from the barrier and will be more expen-

r	$t_1 = 0.0001$	$t_1 = 0.001$	$t_1 = 0.01$
0.5	0.9439849996	0.7374440854	0.3653299405
0.6	1.012259836	1.007899021	0.7860396351
0.8	1.013426249	1.010905559	0.7946772530
0.9	0.9869813161	0.9400179000	0.4621932264

Tab. 5.3: Values of $W(r, t_1)$ for different values of r and t_1.

sive since the chances of hitting the barrier are reduced. Moving away from expiry will result in the value of the option dropping exponentially and tending asymptotically to zero. This is because the different values of r affects the value of the solution for small time. For large time, the exponential term will make this change of r insignificant. The buyer of such an option in early time will purchase the contract at a very low price since the asset has the time to manoeuvre and as a result hit either of the barriers. As time to maturity approaches the value of the option will increase giving less time for the asset to move and consequently the option will expire giving the holder the payoff. If the underlying is situated at $r = 0.8$ (upper dashed line) or at $r = 0.9$ (close to the upper barrier r_O, lower dashed line) the price of the option for the former position will be more expensive than the one for the latter position. When the asset is close to any of the two barriers the buyer of the option will pay little for this position. The chances of hitting either barrier become high and hence the buyer will get no profit from his purchase. On the contrary when the asset is further away from the two barriers (towards the middle of the area), the buyer will need to pay more to enter the contract. This happens because the buyer will profit from this position as the asset will have more chances of reaching maturity by missing the two barriers. The option will expire giving the buyer the value of the payoff which is more than what the buyer initially paid to enter the contract. As time to maturity arrives the value of the option increases to reach the price of the payoff, whereas as time grows away from maturity the difference is reduced to become eventually zero for large time.
For convenience in table 5.3 is illustrated the price of the option $W(r, t_1)$ against values of the two variables t_1 and r. These results can be compared with the Monte Carlo simulation to verify the accuracy of the series approximation.

At time $t_1 = t_1^*$. Furthermore we examine what happens to the value of the option when the concentric spherical barriers have expanded at some time $t_1 = t_1^* > 0$. During this time the barrier has grown from values $[r_I, r_O]$ to values $[r_I^*, r_O^*]$ respectively with $r_I < r_I^* < r_O < r_O^*$ (figure 5.5). From the definition of the similarity variables η_I and η_O the two concentric cylinder barriers grow in time t_1 and given values for t_0 and t_1^* we can find the corresponding values for r at those times. Therefore at $t_1^* = 0.01$, say, the values for r_I^*, r_O^* take the values $r_I^* = \sqrt{0.252} = 0.502$, $r_O^* = \sqrt{1.092} = 1.045$, given $\eta_I^* = 1.2$, $\eta_O^* = 5.2$ and $t_0 = 0.2$ (also $r_I = \sqrt{0.2} = 0.4472135955$, $r_O = 1.0$ given $\eta_I = 1.0$, $\eta_O = 5.0$).

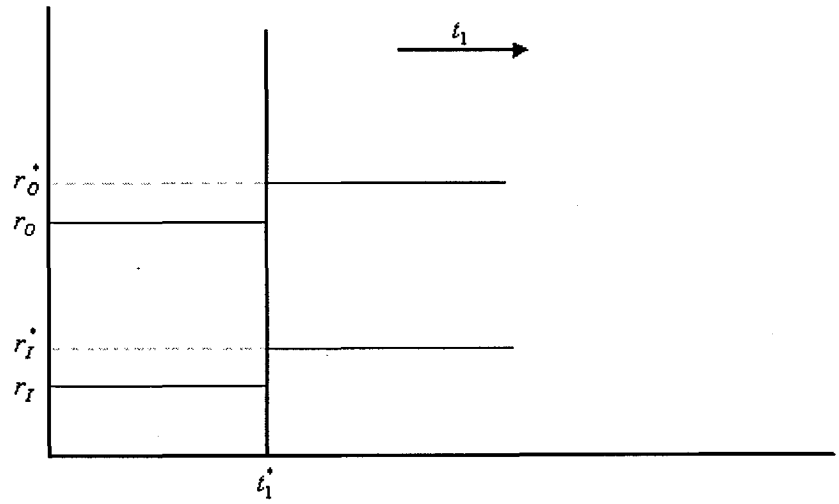

Fig. 5.5: Jump of the double barrier at $t_1 = t_1^*$ for the three-dimensional European option.

As we mentioned at the beginning of this section, the boundary conditions at the two barriers are the same throughout the life of the option. At time t_1^* the value of the option will be given by the same governing heat equation. We call W_1 the value of the option for this problem to distinguish it from the previous one. Hence the equation will look like

$$\frac{\partial W_1}{\partial t_1} = \frac{\partial^2 W_1}{\partial r^2}, \tag{5.36}$$

subject to

$$W_1(r) = 0 \quad \text{at} \quad r = r_I^* \tag{5.37}$$
$$W_1(r) = 0 \quad \text{at} \quad r = r_O^*, \tag{5.38}$$

or in terms of the U function, U_1 for the new barrier option,

$$U_1(r) = 0 \quad \text{at} \quad r = r_I^* \tag{5.39}$$
$$U_1(r) = 0 \quad \text{at} \quad r = r_U^*. \tag{5.40}$$

At t_1^* the value of the option will be discontinuous, i.e. zero for $r_O < r < r_O^*$ and among $r_I^* < r < r_O$ it will have the solution found to be valid for $0 < t_1 < t_1^*$, i.e.

$$U_1(r,t_1^*) = \begin{cases} 0 & \text{, for } r_O < r < r_O^* \\ \sum_{n=1}^{\infty} A_n \exp\left(-\frac{n^2\pi^2}{(r_O-r_I)^2}t_1^*\right)\sin\left(\frac{n\pi}{r_O-r_I}(r-r_I)\right) & \text{, for } r_I^* < r < r_O \end{cases}, \tag{5.41}$$

where r_I, r_O are evaluated at $t_1 = 0$ and r_I^*, r_O^* are evaluated at $t_1 = t_1^*$.
As done earlier in this section, using separation of variables, the Fourier series solution valid for $t_1 > t_1^*$ is equal to

$$U_1(r,t_1) = \sum_{n=1}^{\infty} B_n \exp\left(-\lambda_n^2 t_1\right)\sin\left(\lambda_n(r-r_I^*)\right), \tag{5.42}$$

which is chosen so that the boundary condition at r_I^* is satisfied. To find the eigenvalues λ_n we apply the second boundary condition at $r = r_O^*$,

$$\sin\left(\lambda_n(r_O^* - r_I^*)\right) = 0 \Rightarrow \lambda_n = \frac{n\pi}{r_O^* - r_I^*}. \tag{5.43}$$

Hence the solution to the double barrier for $t_1 > t_1^*$ takes the form

$$U_1(r,t_1) = \sum_{n=1}^{\infty} B_n \exp\left(-\frac{n^2\pi^2}{(r_O^*-r_I^*)^2}t_1\right)\sin\left(\frac{n\pi}{r_O^*-r_I^*}(r-r_I^*)\right), \tag{5.44}$$

valid for $r_I^* < r < r_O^*$ and satisfies the heat equation (5.25) and the boundary conditions (5.39), (5.40).
At $t_1 = t_1^*$ the following equality holds

$$U_1(r,t_1^*) = \sum_{n=1}^{\infty} B_n \exp\left(-\frac{n^2\pi^2}{(r_O^*-r_I^*)^2}t_1^*\right)\sin\left(\frac{n\pi}{r_O^*-r_I^*}(r-r_I^*)\right), \tag{5.45}$$

where the left-hand side is the new 'payoff' given by equation (5.41).
To find the coefficients B_n we multiply (5.45) by $\sin\left(\frac{m\pi}{r_O^*-r_I^*}(r-r_I^*)\right)$ and integrate with respect to r from r_I^* to r_O^*

$$\int_{r_I^*}^{r_O} U(r,t_1^*)\sin\left(\frac{m\pi}{r_O^*-r_I^*}(r-r_I^*)\right)dr =$$
$$\sum_{n=1}^{\infty} B_n \exp\left(-\frac{n^2\pi^2}{(r_O^*-r_I^*)^2}t_1^*\right)\int_{r_I^*}^{r_O^*}\sin\left(\frac{m\pi}{r_O^*-r_I^*}(r-r_I^*)\right)\sin\left(\frac{n\pi}{r_O^*-r_I^*}(r-r_I^*)\right)dr.$$

Using the orthogonality condition,

$$\int_{r_I^*}^{r_O^*} \sin\left(\frac{m\pi}{r_O^* - r_I^*}(r - r_I^*)\right) \sin\left(\frac{n\pi}{r_O^* - r_I^*}(r - r_I^*)\right) dr$$
$$= \begin{cases} 0 & \text{, if } m \neq n \\ \int_{r_I^*}^{r_O^*} \left[\sin\left(\frac{n\pi}{r_O^* - r_I^*}(r - r_I^*)\right)\right]^2 dr & \text{, if } m = n \end{cases}.$$

for $m = n$ the above equation takes the form

$$C_n = \frac{\int_{r_I^*}^{r_O} U(r, t_1^*) \sin\left(\frac{n\pi}{r_O^* - r_I^*}(r - r_I^*)\right) dr}{\int_{r_I^*}^{r_O^*} \left[\sin\left(\frac{n\pi}{r_O^* - r_I^*}(r - r_I^*)\right)\right]^2 dr}, \tag{5.46}$$

where $C_n = B_n \exp\left(-\frac{n^2\pi^2}{(r_O^* - r_I^*)^2} t_1^*\right)$ and $U(r, t_1^*)$ is given by (5.41). The values the coefficient C_n takes for n can be seen in table 5.4.

n	C_n	n	C_n
1	0.6589527492	11	0.009871353079
2	0.1055854100	12	0.01017868655
3	0.004969295440	13	0.01005739416
4	0.06507959625	14	0.007385025171
5	0.003829456199	15	0.009649256561
6	0.03575858227	16	0.005845316662
7	0.007103542810	17	0.008816688782
8	0.02249102638	18	0.005130057895
9	0.008942274486	19	0.007741480278
10	0.01484685061	20	0.004909640716

Tab. 5.4: Values of C_n for $n = 1..20$

Therefore the solution of the double barrier option for $t_1 > t_1^*$ is

$$U_1(r, t_1) = \sum_{n=1}^{\infty} C_n \exp\left(-\frac{n^2\pi^2}{(r_O^* - r_I^*)^2}(t_1 - t_1^*)\right) \sin\left(\frac{n\pi}{r_O^* - r_I^*}(r - r_I^*)\right), \tag{5.47}$$

with $U_1(r_I^*) = 0$, $U_1(r_O^*) = 0$ and in terms of the original problem using the transformation $W_1 = \frac{U_1}{r}$ it becomes

$$W_1(r, t_1) = \sum_{n=1}^{\infty} C_n \frac{1}{r} \exp\left(-\frac{n^2\pi^2}{(r_O^* - r_I^*)^2}(t_1 - t_1^*)\right) \sin\left(\frac{n\pi}{r_O^* - r_I^*}(r - r_I^*)\right), \tag{5.48}$$

subject to $W_1(r_I^*) = 0$, $W_1(r_O^*) = 0$.
As mentioned earlier the value of the option at the jump at time t_1^* is discontinuous.

The discontinuity has a more severe effect on the inner barrier jump. This can be detected on the graph 5.6 where the discontinuity is seen on the wavy behavior of the solution when it is close to the inner barrier $r_I^* = 0.502$ (left side of the curve), whereas when it is close to the outer barrier $r_O^* = 1.045$ the solution is smooth from the series and then zero for $[r_O, r_O^*]$ (right side of the curve). On the interval $[r_I, r_I^*]$ at times $t_1 < t_1^*$ the option takes values given by the Fourier series solution (5.34), whereas at time $t_1 = t_1^*$ the option has no value because of the jump. With the barrier level rising the price of the option attempts to adjust to the jump by producing the wave on the left side of the curve.

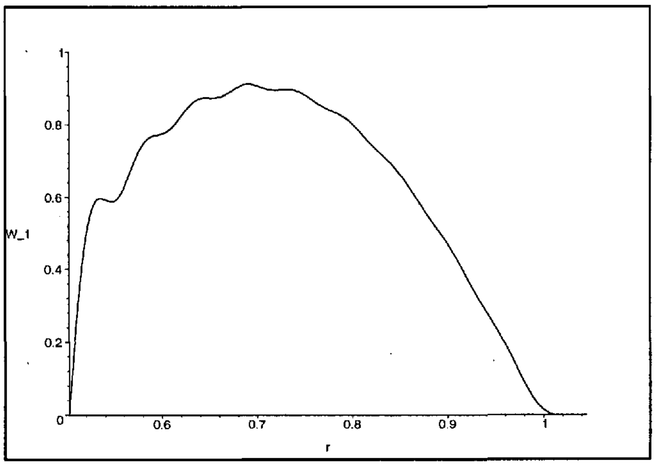

Fig. 5.6: Plot of the series solution $W_1(r,t_1)$ for $n = 20$, at $t_1^* = 0.01$ against r.

We remove this wave in the solution by using the Fejer sums, i.e. by applying the summation used earlier,

$$W_1(r,t_1) = \frac{1}{N}\sum_{n=1}^{N} c_n\,, \tag{5.49}$$

where

$$c_n = C_n \frac{1}{r} \exp\left(-\frac{n^2\pi^2}{(r_O^* - r_I^*)^2}(t_1 - t_1^*)\right) \sin\left(\frac{n\pi}{r_O^* - r_I^*}(r - r_I^*)\right).$$

We can see the smoothed out (corrected) discontinuity in figure (5.7).

In figure 5.8 we plot the price of the option against r at times $t_1 = 0.01$, $t_1 = 0.03$, $t_1 = 0.05$ and $t_1 = 0.08$. After some time, say $t_1 = 0.03$, the curve has smoothed out and is inexpensive. Comparing the curves at $t_1 = 0.01$ (upper dashed curve) and at $t_1 = 0.03$ (upper solid curve) we notice that when the underlying is close to the outer barrier, r_O^*, the price at time $t_1 = 0.03$ is more expensive than the price at time

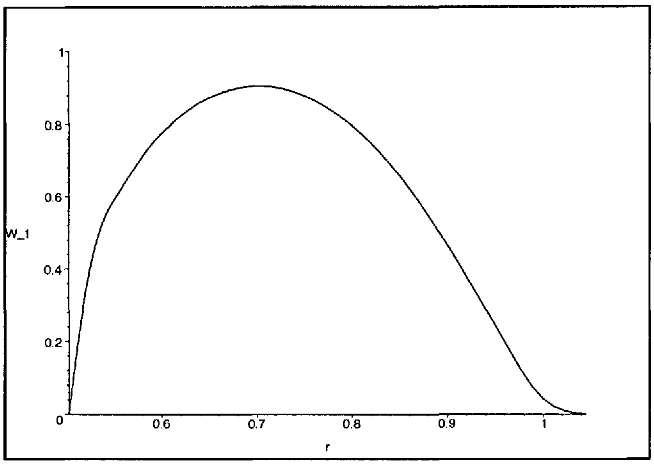

Fig. 5.7: Plot of the series solution $W_1(r, t_1)$ given by (5.49) for $n = 20$, at $t_1^* = 0.01$ against r.

$t_1 = 0.01$. This is because of the jump occurring on the outer barrier. At time t_1^* the value of the option is zero on the interval $[r_O, r_O^*]$. As we go forward in real time towards maturity, just before the jump occurs at t_1^*, the asset is trying to fit in the area created by the two new barriers, $[r_I, r_O]$. The jump allows a much smaller gap than the actual barrier for the underlying to move and this drops the value of the option. Hence the buyer of the option will enter the contract by paying little, since the chances of the asset entering the shrunken area without hitting the barriers are limited. For larger time, say $t_1 = 0.08$ (lower solid line) the price of the option becomes even cheaper. The underlying has more time to expiry and hence more flexibility to move between the barriers.

In figure 5.9 we plot the solution $W(r, t_1)$ against time t_1 evaluated at different points between the two barriers, $r = 0.6$, $r = 0.8$, $r = 0.9$ and $r = 1.0$. The horizontal axis is the time axis t_1 and the solutions are plotted from time $t_1^* = 0.01$ to $t_1 = 0.2$. At $r = 0.6$ (upper solid line), the price of the option is cheaper than at $r = 0.8$ (upper dashed line). This is because when the underlying is at $r = 0.6$ it is more likely to hit the inner barrier than it is when situated at $r = 0.8$. Similarly, the price of the option at $r = 1.0$ (lower dashed line) is much cheaper than the one at $r = 0.9$ (lower solid line) as the former value is closer to the outer barrier than the latter value. For $r = 1.0$ the solution for the option behaves in a slightly different way than for the other values. At the time before the jump occurs the curve for the price behaves in a different way when the asset is close to the outer barrier. As the asset approaches the time where the jump occurs it has two problems to overcome. The increased chances of hitting the upper barrier r_O or the area $[r_O, r_O^*]$ and force the option to expire worthless. In order to get through the previous difficulty it has to slide down and enter the area $[r_I^*, r_O]$

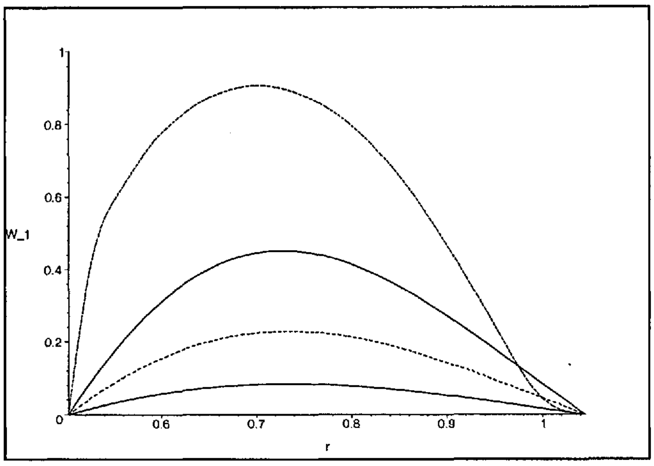

Fig. 5.8: Plot of the series solution $W_1(r, t_1)$ for $n = 20$, for $t_1 = 0.01$ (upper dashed line), $t_1 = 0.03$ (upper solid line), $t_1 = 0.05$ (lower dashed line) and $t_1 = 0.08$ (lower solid line) against r.

of the new barrier and continue till maturity. This causes the value of the option to drop and have the behavior given by the lower dashed curve.

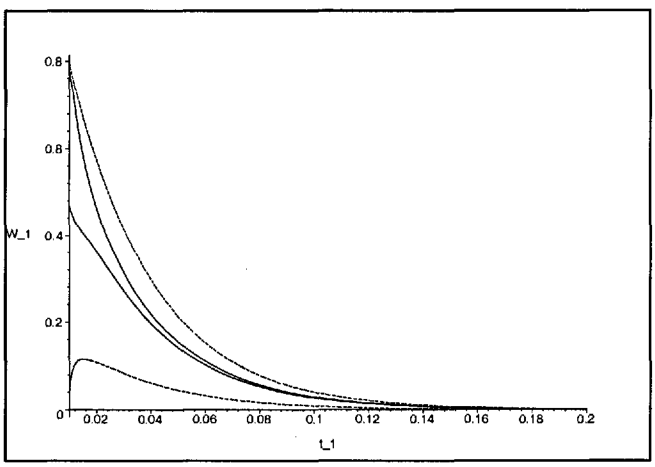

Fig. 5.9: Plot of the series solution $W_1(r, t_1)$ for $n = 20$ against time t_1 for $r = 0.6$ (upper solid line), $r = 0.8$ (upper dashed line), $r = 0.9$ (lower solid line) and $r = 1.0$ (lower dashed line).

In table 5.5 is illustrated the price of the option $W_1(r, t_1)$ against values of the two variables t_1 and r.

r	$t_1 = 0.01$	$t_1 = 0.03$	$t_1 = 0.05$	$t_1 = 0.08$
0.6	0.7784446609	0.3124373624	0.1553355652	0.05665435602
0.8	0.7960994433	0.4141438419	0.2131881370	0.07815857565
0.9	0.4661405042	0.2712374332	0.1422366008	0.05228712646
1.0	0.04230866579	0.08340261177	0.04421570179	0.01627937200

Tab. 5.5: Values of $W_1(r, t_1)$ for different values of r and t_1.

5.3 Three-Dimensional problem with a single barrier

In this section we examine the study of high dimensional radial barrier options based on the work done by Firth and Dewynne [21]. They derive an analytic expression for the multi-asset single barrier option using Laplace transform methods. The single barrier is a knock-in barrier with value one. For the three-dimensional problem the equation used in terms of radial coordinates is given by (5.24),

$$\frac{\partial W}{\partial t_1} = \frac{\partial^2 W}{\partial r^2} + \frac{2}{r}\frac{\partial W}{\partial r}, \tag{5.50}$$

subject to the boundary conditions

$$W(1, t_1) = 1, \tag{5.51}$$
$$W(\infty, t_1) = 0,$$
$$W(r, 0) = 0. \tag{5.52}$$

As done in the previous section we can use a transformation of the form $F = rW$ to reduce the above equation to the heat equation

$$\frac{\partial F}{\partial t_1} = \frac{\partial^2 F}{\partial r^2}, \tag{5.53}$$

subject to the same boundary conditions (5.51). The fundamental solution of the heat equation is given by the formula

$$F(r, t_1) = \frac{1}{2\sqrt{\pi t_1}} \exp\left(-\frac{(r - r')^2}{4t_1}\right). \tag{5.54}$$

For $t_1 > 0$ the above equation gives a smooth curve, but at $t_1 = 0$ the limit of the above expression is equal to the delta function,

$$\lim_{t_1 \to 0} F(r, t_1) = \delta(r - r').$$

At $t_1 = 0$, the value of the option is zero for all r, apart from the barrier at $r = 1$ where it takes the value one. This causes the problem to have discontinuity, which we will overcome using the method of images. The method of images will give the option value zero at the barrier. Due to the reflection principle the probability density for down-and-out barrier options is given by the difference of the two normal densities.

Suppose at some time above the barrier $r = a$ is a source $r = r^* > 0$. The image of that source about the barrier $r = a$ is $r = r^* - A$. Then the equation for the source and its image is given by the following equations

$$F_1(r, t_1) = \frac{1}{2\sqrt{\pi t_1}} \exp\left(-\frac{(r - r^*)^2}{4t_1}\right), \tag{5.55}$$

for the source $r = r^*$ and

$$F_2(r, t_1) = \frac{1}{2\sqrt{\pi t_1}} \exp\left(-\frac{(r - r^* + A)^2}{4t_1}\right), \tag{5.56}$$

for the source $r = r^* - A$. When very close to $t_1 = 0$, the limit of the above equations is equal to

$$\lim_{t_1 \to 0} F_1(r, t_1) = \delta(r - r^*), \quad \text{and} \quad \lim_{t_1 \to 0} F(r, t_1) = \delta(r - r^* + A).$$

respectively.
We require the value of the option to be zero at the barrier $r = a$, hence

$$F = F_1 - F_2 = 0, \quad \text{at} \quad r = a.$$

We choose A such that

$$(r - r^*)^2 = (r - r^* + A)^2, \quad \text{at} \quad r = a,$$

so

$$A = 2r^* - 2a,$$

since A cannot be zero. The value of the single barrier option at $r = a$ will be the integral from the barrier $r = a$ to infinity of the function F times the payoff, i.e.

$$F(r, t_1) = \int_a^\infty (F_1 - F_2) f(r^*) dr^*. \tag{5.57}$$

For small time t_1 the above integral will be

$$\begin{aligned}\lim_{t_1\to 0} F(r,t_1) &= \lim_{t_1\to 0}\int_a^\infty (F_1-F_2)f(r^*)dr^* \\ &= \int_a^\infty \delta(r-r^*)f(r^*)dr^* - \int_a^\infty \delta(r-r^*+A)f(r^*)dr^* = f(r),\end{aligned}$$

since the function in the second integral takes values outside the integral limits.

Going back to the original problem, we want to make the value of the option zero at the barrier $r=a$. To find the function of r which if added to the solution will satisfy all the boundary conditions, we take the part of the PDE which is time independent. Then the ODE

$$\frac{\partial^2 W}{\partial r^2}+\frac{2}{r}\frac{\partial W}{\partial r}=0,$$

has solution

$$W(r)=\frac{1}{r},$$

satisfying the boundary conditions (5.51). Hence the Firth and Dewynne solution can be written as $W=\frac{1}{r}+\bar{W}$, where $\bar{W}$ is our solution with $\bar{W}=0$ at the barrier $r=a$ and with payoff $\bar{W}=-\frac{1}{r}$ at $t_1=0$. Therefore $\bar{F}=r\bar{W}=-1$ for our problem.
Hence the solution to the single barrier problem will equal to the integral

$$\bar{F}(r,t_1)=\int_a^\infty\left[\frac{1}{2\sqrt{\pi t_1}}\exp\left(-\frac{(r-r^*)^2}{4t_1}\right)-\frac{1}{2\sqrt{\pi t_1}}\exp\left(-\frac{(r-r^*+A)^2}{4t_1}\right)\right]f(r^*)dr^*,$$

where $f(r^*)=-1$, $r=a=1$ and $A=2r^*-2a=2r^*-2$.
Therefore the integral takes the form

$$\bar{F}(r,t_1)=-\frac{1}{2\sqrt{\pi t_1}}\int_1^\infty \exp\left(-\frac{(r-r^*)^2}{4t_1}\right)dr^*+\frac{1}{2\sqrt{\pi t_1}}\int_1^\infty \exp\left(-\frac{(r-r^*+A)^2}{4t_1}\right)dr^*,$$

which gives

$$\bar{F}(r,t_1)=\operatorname{erfc}\left(\frac{r-1}{2\sqrt{t_1}}\right)-1.$$

The solution for the three-dimensional single barrier problem is

$$\bar{W}(r, t_1) = \frac{1}{r} \operatorname{erfc}\left(\frac{r-1}{2\sqrt{t_1}}\right) - \frac{1}{r},$$

and therefore the solution given by Firth and Dewynne is

$$W(r, t_1) = \frac{1}{r} \operatorname{erfc}\left(\frac{r-1}{2\sqrt{t_1}}\right), \tag{5.58}$$

We will extend the three-dimensional single barrier problem to the case where the barrier jumps from $r = 1$ to $r = r_1$, say. We use the theory of images for the step barrier as well. Suppose that at time t_1^* the barrier jumps to the value $r = r_1$. At that time the value of the option will be what we found earlier plus a function of r so that the value at the new barrier is zero, $W_s = \frac{r_1}{r} + \bar{W}_s$, where $\bar{W}_s$ is our solution to the problem and is zero at the new barrier r_1.
So the payoff at time t_1^* will be equal to

$$f(r, t_1^*) = \operatorname{erfc}\left(\frac{r-1}{2\sqrt{t_1^*}}\right) - r_1. \tag{5.59}$$

The value of the step barrier will then be equal to

$$\begin{aligned}
F_s(r, t_1) &= \int_{r_1}^{\infty} f(r^*, t_1^*)(F_1 - F_2)\, dr^* \\
&= \frac{1}{2\sqrt{\pi t_1}} \int_{r_1}^{\infty} \exp\left(-\frac{(r-r^*)^2}{4t_1}\right) \left[\operatorname{erfc}\left(\frac{r^*-1}{2\sqrt{t_1^*}}\right) - r_1\right] dr^* \\
&- \frac{1}{2\sqrt{\pi t_1}} \int_{r_1}^{\infty} \exp\left(-\frac{(r-r^*+A)^2}{4t_1}\right) \left[\operatorname{erfc}\left(\frac{r^*-1}{2\sqrt{t_1^*}}\right) - r_1\right] dr^*.
\end{aligned}$$

Hence the value of the step barrier problem of Firth and Dewynne will be equal to

$$\begin{aligned}
W_s(r, t_1) &= \frac{1}{2\sqrt{\pi t_1}} \frac{1}{r} \int_{r_1}^{\infty} \exp\left(-\frac{(r-r^*)^2}{4t_1}\right) \left[\operatorname{erfc}\left(\frac{r^*-1}{2\sqrt{t_1^*}}\right) - r_1\right] dr^* \\
&- \frac{1}{2\sqrt{\pi t_1}} \frac{1}{r} \int_{r_1}^{\infty} \exp\left(-\frac{(r-r^*+A)^2}{4t_1}\right) \left[\operatorname{erfc}\left(\frac{r^*-1}{2\sqrt{t_1^*}}\right) - r_1\right] dr^* + \frac{r_1}{r}.
\end{aligned}$$

5.4 One Dimensional Case

In this section we examine the Black-Scholes model with one underlying asset only. The asset moves under the effect of two barriers $[r_1, r_2]$ starting at $t_1 = 0$ and expanding forward in time t_1. The two barriers are knock-out giving zero value when triggered.

We find the Fourier series solution for pricing this single asset option with payoff being equal to 1. At time $t_1 = t_1^*$ both barriers jump equivalently to a higher position $[r_3, r_4]$ with $r_1 < r_3 < r_2 < r_4$, figure 5.10. We examine how this jump effects the Fourier series solution valid for time $t_1 > t_1^* > 0$ and comment on the corresponding graphs.

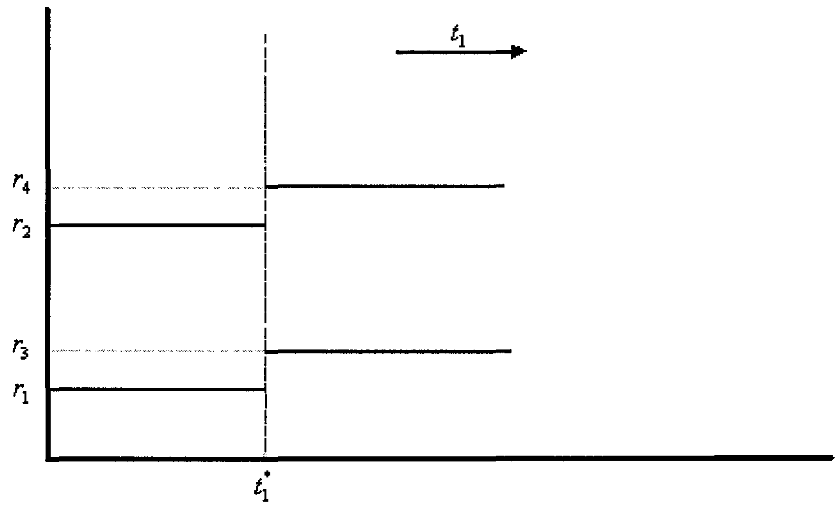

Fig. 5.10: Jump of the double barrier at $t_1 = t_1^*$ for the single asset European option.

For the case of the single asset Black-Scholes model we recall the N-dimensional radial PDE,

$$\frac{\partial W}{\partial t_1} = \frac{\partial^2 W}{\partial r^2} + \frac{N-1}{r}\frac{\partial W}{\partial r}, \tag{5.60}$$

which for $N = 1$ takes the form of the heat equation

$$\frac{\partial W}{\partial t_1} = \frac{\partial^2 W}{\partial r^2}, \tag{5.61}$$

with payoff

$$W(r, 0) = 1, \tag{5.62}$$

and with boundary conditions

$$W(r_1, t_1) = 0 \quad \text{and} \quad W(r_2, t_1) = 0. \tag{5.63}$$

The payoff in terms of the original variable S, given by the transformations performed at the beginning of chapter 4, is equal to

$$V(S,T) = \left(\frac{S}{S_0}\right)^{\frac{1}{2}-\frac{r}{\sigma^2}}.$$

Using separation of variables to solve the above heat equation we end up with a Fourier series of the form

$$W(r,t_1) = \sum_{n=1}^{\infty} A_n \exp\left(-\lambda_n^2 t_1\right) \sin\left(\lambda_n (r - r_1)\right),$$

satisfying the boundary condition at $r = r_1$. By applying the boundary condition at r_2 we find the eigenvalues equal to $\lambda_n = \frac{n\pi}{r_2 - r_1}$. Hence the series solution will take the form

$$W(r,t_1) = \sum_{n=1}^{\infty} A_n \exp\left(-\frac{n^2\pi^2}{(r_2 - r_1)^2} t_1\right) \sin\left(\frac{n\pi}{r_2 - r_1}(r - r_1)\right), \tag{5.64}$$

satisfying the boundary conditions (5.63).

At $t_1 = 0$ equation (5.64) becomes

$$W(r,0) = \sum_{n=1}^{\infty} A_n \sin\left(\frac{n\pi(r - r_1)}{r_2 - r_1}\right), \tag{5.65}$$

where the left-hand-side is the payoff given by (5.62). To find the coefficients of the Fourier series solution we multiply equation (5.65) by $\sin\left(\frac{m\pi(r-r_1)}{r_2-r_1}\right)$ and integrate with respect to r from r_1 to r_2. Using the orthogonality condition, for $m = n$ the above equation becomes

$$A_n = \frac{\int_{r_1}^{r_2} W(r,0) \sin\left(\frac{n\pi(r-r_1)}{r_2-r_1}\right) dr}{\int_{r_1}^{r_2} \left[\sin\left(\frac{n\pi(r-r_1)}{r_2-r_1}\right)\right]^2 dr} \tag{5.66}$$

Similarly with the three-dimensional case for the numerical interpretation of the solution we take the same values for t_0, r_1 and r_2 ($t_0 = 0.2$, $r_1 = \sqrt{0.2}$ and $r_2 = 1$). The values for A_n corresponding to these values are shown in table 5.6.

The solution (5.64) is plotted for the first 20 terms of the series against r in figure 5.11 for $t_1 = 0$, $t_1 = 0.0001$, $t_1 = 0.001$ (curves are very close together as the values of t_1 are very small) and for $t_1 = 0.01$ (dashed line). The value of the option is zero at the two barriers and takes the value 1.0 for any other $r_1 < r < r_2$ at time $t_1 = 0$. To avoid the discontinuity at $t_1 = 0$ (top dashed curve) we use the Fejer sums as mentioned earlier in page 83. Moving away from expiry the value of the option gets cheaper. The

n	A_n	n	A_n
1	1.273239545	11	0.1157490495
2	$0.2085390651 \times 10^{-17}$	12	$0.2564123853 \times 10^{-17}$
3	0.4244131814	13	0.09794150346
4	$-0.2312028640 \times 10^{-15}$	14	$0.1048140179 \times 10^{-14}$
5	0.2546479090	15	0.08488263631
6	$-0.8468268982 \times 10^{-15}$	16	$-0.8572890043 \times 10^{-15}$
7	0.1818913635	17	0.07489644379
8	$-0.5720547493 \times 10^{-15}$	18	$-0.1117179353 \times 10^{-14}$
9	0.1414710605	19	0.06701260760
10	$0.3012618478 \times 10^{-15}$	20	$-0.6903917350 \times 10^{-16}$

Tab. 5.6: Values of A_n for $n = 1..20$

underlying has more time to move with chances of hitting the barriers and expiring worthless. As the asset moves from one barrier to the other the price of the option increases giving the holder of the option more chances in reaching expiry and gaining profit.

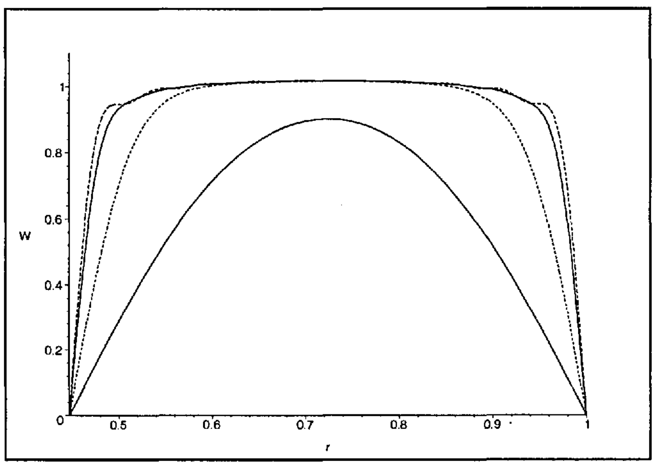

Fig. 5.11: Plot of the series solution $W(r, t_1)$ for $n = 20$ using the Fejer sums, at $t_1 = 0$ (upper dashed line), $t_1 = 0.0001$ (upper solid line), $t_1 = 0.001$ (lower dashed line) and at $t_1 = 0.01$ (lower solid line) against r.

In figure 5.12 we plot the solution (5.64) against time t_1 for $r = 0.5$ (lower solid line), $r = 0.6$ (lower dashed line), $r = 0.8$ (upper dashed line) and $r = 0.9$ (upper solid line). For any value of r the price of the option takes the value 1 at $t_1 = 0$ and zero when time to maturity is big. When the underlying is closer to the inner barrier $r_1 = \sqrt{0.2} = 0.4472135955$, at $r = 0.5$ (lower solid line), the value of the option is much cheaper than when it is further away, say at $r = 0.6$ (lower dashed line). This is because at $r = 0.5$, the asset is more likely to hit the barrier and expire worthless,

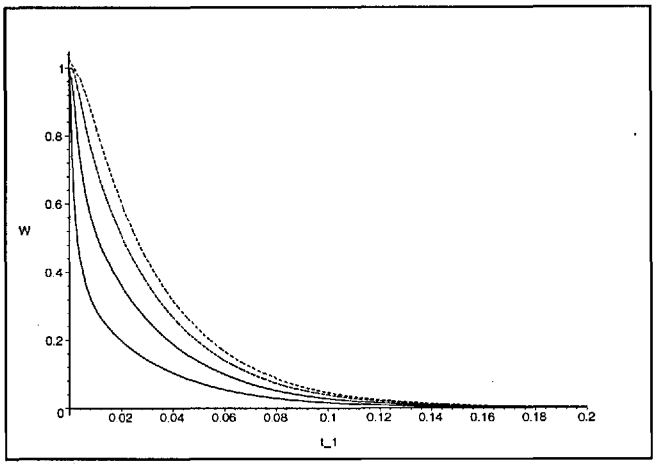

Fig. 5.12: Plot of the series solution $W(r,t_1)$ for $n=20$, at $r=0.5$ (lower solid line), $r=0.6$ (lower dashed line), $r=0.8$ (upper dashed line) and at $r=0.9$ (upper solid line) against t_1.

whereas at $r=0.6$ it has more chances to avoid hitting the lower barrier and expire getting the payoff and making profit. A similar case occurs for the positions at $r=0.8$ and $r=0.9$. At $r=0.9$ (upper solid line) the underlying has more chances of hitting the upper barrier and nullifying the value of the option. At a position further away from the upper barrier, at $r=0.8$ (upper dashed line), the asset has more chances of avoiding hitting the upper barrier and reach the maturity date and be exercised.

Assume that at time $t_1=t_1^*>0$, the two barriers jump simultaneously at the same distance from values $[r_1,r_2]$ to values $[r_3,r_4]$, with $r_1<r_3<r_2<r_4$ (figure 5.10). We examine the behavior of the price of the option when we start the barrier at time t_1^*. Both barriers are of knock-out nature and the new payoff at t_1^* is the Fourier series found earlier. We name the value of the new problem as W_1 to distinguish it from the original one. We have the same governing equation as before,

$$\frac{\partial W_1}{\partial t_1}=\frac{\partial^2 W_1}{\partial r^2}, \tag{5.67}$$

subject to the new boundary conditions at the new barriers

$$W_1(r_3)=0 \quad \text{and} \quad W_1(r_4)=0. \tag{5.68}$$

The payoff to this problem is

$$W(r,t_1^*) = \begin{cases} 0 & , \text{for } r_1 < r < r_3 \\ \sum_{n=1}^{\infty} A_n \exp\left(-\frac{n^2\pi^2}{(r_2-r_1)^2} t_1^*\right) \sin\left(\frac{n\pi}{r_2-r_1}(r-r_1)\right) & , \text{for } r_3 < r < r_2 \\ 0 & , \text{for } r_2 < r < r_4 \end{cases} , \tag{5.69}$$

The solution to the above boundary value problem as stated before is of the form

$$W_1(r,t_1) = \sum_{n=1}^{\infty} B_n \exp\left(-\frac{n^2\pi^2}{(r_4-r_3)^2} t_1\right) \sin\left(\frac{n\pi(r-r_3)}{r_4-r_3}\right). \tag{5.70}$$

At $t_1 = t_1^*$ equation (5.70) becomes

$$W_1(r,t_1^*) = W(r,t_1^*) = \sum_{n=1}^{\infty} B_n \exp\left(-\frac{n^2\pi^2}{(r_4-r_3)^2} t_1^*\right) \sin\left(\frac{n\pi(r-r_3)}{r_4-r_3}\right), \tag{5.71}$$

where the left-hand-side is the payoff given by (5.69).
We multiply equation (5.71) by $\sin\left(\frac{m\pi(r-r_3)}{r_4-r_3}\right)$ and integrate with respect to r from r_3 to r_4 and by using the orthogonality condition for $m = n$ the coefficients of the series are given by the equation

$$C_n = \frac{\int_{r_3}^{r_2} W(r,t_1^*) \sin\left(\frac{n\pi(r-r_3)}{r_4-r_3}\right) dr}{\int_{r_3}^{r_4} \left[\sin\left(\frac{n\pi(r-r_3)}{r_4-r_3}\right)\right]^2 dr}, \tag{5.72}$$

where $C_n = B_n \exp\left(-\frac{n^2\pi^2}{(r_4-r_3)^2} t_1^*\right)$ and therefore the full solution to the problem takes the form

$$W_1(r,t_1) = \sum_{n=1}^{\infty} C_n \exp\left(-\frac{n^2\pi^2}{(r_4-r_3)^2} (t_1 - t_1^*)\right) \sin\left(\frac{n\pi(r-r_3)}{r_4-r_3}\right). \tag{5.73}$$

The corresponding values of r_1, r_2, evaluated at $t_1 = 0$ and r_3, r_4 evaluated at $t_1 = t_1^* = 0.01$, given that $\eta_i = \frac{r_i^2}{t_0+t_1^*}$, are $r_1 = \sqrt{0.2}$, $r_2 = 1$ and $r_3 = \sqrt{0.252}$, $r_4 = \sqrt{1.092}$ (with $\eta_1 = 1$, $\eta_2 = 1.2$, $\eta_3 = 5$, $\eta_4 = 5.2$ and $t_0 = 0.2$). Given these values the first twenty terms of the series are given in table 5.7.
In figure 5.13 we plot the series solution (5.73) against r for different values of time t_1. The upper solid line corresponds to the value of the option at time $t_1 = t_1^* = 0.01$. The option is zero at the lower barrier $r_3 = 0.5019960159$ and reaches a maximum value at the middle of the interval before decreasing to take the value zero at $r_4 = 1.044988038$. At that time when the curve is close to the upper barrier r_4, the value of the option is

n	C_n	n	C_n
1	0.8943964867	11	0.01621525771
2	0.2032247712	12	0.01621853428
3	0.03241827009	13	0.01576297167
4	0.09248291964	14	0.01225964825
5	0.01536115308	15	0.01478060172
6	0.05148575832	16	0.009968895381
7	0.01559383306	17	0.01340209880
8	0.03320761218	18	0.008775110320
9	0.01610450424	19	0.01180854446
10	0.02269092133	20	0.008248747251

Tab. 5.7: Values of C_n for $n = 1..20$

cheaper as the solution is trying to overcome the discontinuity and become zero (since it is zero in the interval $[r_2, r_4]$).

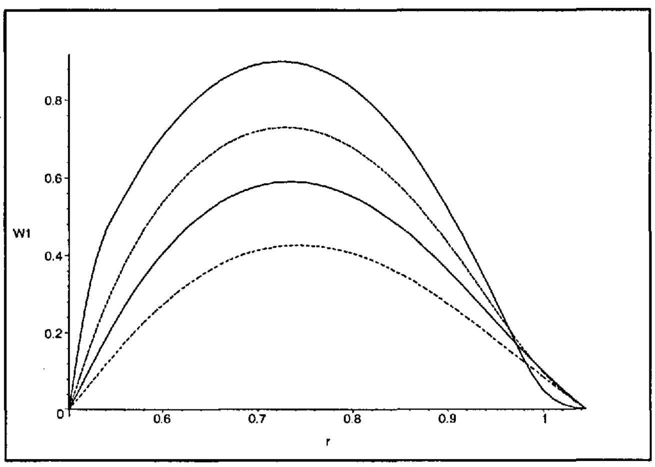

Fig. 5.13: Plot of the series solution $W_1(r, t_1)$ for $n = 20$ using the Fejer sums, for $t_1 = 0.01$ (upper solid line), $t_1 = 0.03$ (upper dashed line), $t_1 = 0.05$ (lower solid line) and at $t_1 = 0.08$ (lower dashed line) against r.

As time moves away from the jump, the value of the option gets cheaper because the underlying is further away and in addition has more chances of hitting the barriers (curves for $t_1 = 0.03$ upper dashed line, $t_1 = 0.05$ lower solid line and $t_1 = 0.08$ lower dashed line). As the underlying moves from one barrier to the other the price of the option is more expensive towards the side of the lower barrier. This is because the holder of the option has more chances in reaching the gap $[r_3, r_2]$ and entering the area of the new barrier without hitting the barriers r_3 and r_2. Moving forward in real time closer to $t_1 = t_1^*$ the value of the option increases as the underlying has to overcome the possibility of entering the $[r_2, r_4]$ region in order to be better off and enter the $[r_3, r_2]$

region. In this case we have taken the values of r_2 and r_4 to be pretty close to each other, reducing the area of the option being zero and increasing the area of 'escape' to get a better value.

In figure 5.14 we plot (5.73) against time t_1 with r taking different values between the two barriers r_3 and r_4. Depending on where we position the asset between the two barriers it will follow a different path. At $r = 0.6$ (solid line) the value of the option when t_1 is large is zero. As we move towards $t_1^* = 0.01$ the value of the option increases to take the value it will have when reaching the jump. At $r = 0.8$ (upper dashed line) the asset is further away from the lower barrier and has more freedom to move around. This beneficial position makes the price more expensive as the chances of the asset managing to enter the area $[r_3, r_2]$ have increased. At $r = 1.0$ (lower dashed line) as time t_1^* approaches the underlying has very little chances of overcoming the gap $[r_2, r_4]$ and enter the new barrier $[r_1, r_2]$. This drops the value of the option dramatically as the holder of the option is in a disadvantaged position.

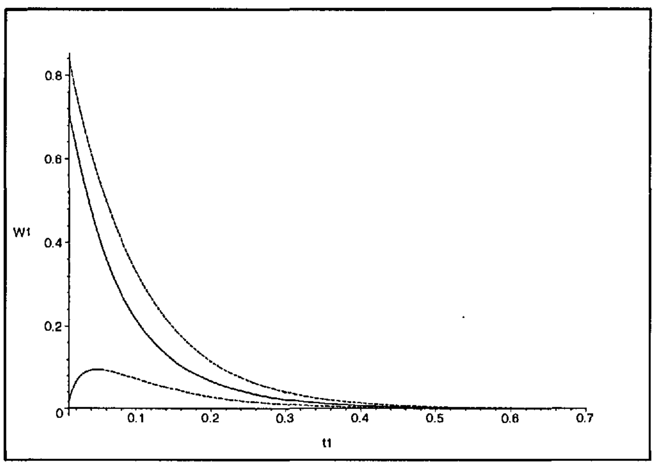

Fig. 5.14: Plot of the series solution $W_1(r, t_1)$ for $n = 20$, for $r = 0.6$ (solid line), $r = 0.8$ (upper dashed line) and at $r = 1.0$ (lower dashed line) against t_1.

5.5 Five-Dimensional double barrier

We apply the multi-asset Black-Scholes equation with barriers in the case where we have five dimensions using the Fourier series method. The problem is solved in radial coordinates $r = \sum_{i=1}^{N} x_i^2$ and the solution we seek for the five-dimensional problem will be radially symmetric, depending on r and time $t_1 = T - t$. The underlying assets move freely under the effect of two radial barriers r_I and r_O with $r_I < r_O$ which become smaller and smaller as t_1 approaches zero.

The multi-dimensional problem for a single radial barrier has been studied by Firth and Dewynne [21]. They study radial barrier options in one, three and five dimensions by solving the problem

$$\frac{\partial u}{\partial \tau} = \frac{\partial^2 u}{\partial \rho^2} + \frac{n-1}{\rho}\frac{\partial u}{\partial \rho}, \tag{5.74}$$

subject to the conditions

$$u(1,\tau) = 1, \quad u(\infty,\tau) = 0, \quad u(\rho,0) = 0. \tag{5.75}$$

They solve the problem where the sphere of radius $\rho = 1$ is a knock-in barrier giving the value 1 when triggered. The option moves outside the spherical barrier and at large values of ρ the option is zero. In time $\tau = \frac{\sigma^2}{2}(T-t)$ the option starts initially with value zero, i.e. with payoff zero at $\tau = 0$.

We take the problem of Firth and Dewynne [21] for the case where there are two radial barriers. The inner barrier at $r = r_I = 1$ takes the value 1 when triggered (knock-in barrier) and the outer barrier at $r = r_O = 10$ is placed far away from the inner barrier and is zero when hit (knock-out barrier). The payoff, i.e. the region between the two barriers is initially zero and will develop as time grows. The radial problem we solve is

$$\frac{\partial W}{\partial t_1} = \frac{\partial^2 W}{\partial r^2} + \frac{n-1}{r}\frac{\partial W}{\partial r}, \tag{5.76}$$

which for the five dimensional problem equation (5.76) takes the form

$$\frac{\partial W}{\partial t_1} = \frac{\partial^2 W}{\partial r^2} + \frac{4}{r}\frac{\partial W}{\partial r}, \tag{5.77}$$

subject to the conditions

$$W(r_I,t_1) = 1, \quad W(r_O,t_1) = 0, \quad W(r,0) = 0. \tag{5.78}$$

To make the value of the option at the two barriers zero we seek a function of r by solving the following ODE

$$\frac{\partial^2 W}{\partial r^2} + \frac{4}{r}\frac{\partial W}{\partial r} = 0,$$

with solution

$$W(r) = \frac{r^{-3} - r_O^{-3}}{r_I^{-3} - r_O^{-3}}, \tag{5.79}$$

satisfying the boundary conditions

$$W(r_I) = 1 \quad \text{and} \quad W(r_O) = 0 .$$

In equation (5.77) we apply separation of variables by taking the solution to be of the form $W(r, t_1) = R(r)\,T(t_1)$. The solution in time will be $T(t_1) = c\exp\left(-\lambda^2 t_1\right)$, where λ^2 is the separation variable and for the radial variable, $R(r)$, we have the following ordinary differential equation

$$R''(r) + \frac{4}{r}R'(r) + \lambda^2 R(r) = 0 , \tag{5.80}$$

which has solution of the form

$$R(r) = C_1\frac{1}{r^3}\left[r\lambda\cos\left(\lambda r\right) - \sin\left(\lambda r\right)\right] + C_2\frac{1}{r^3}\left[r\lambda\sin\left(\lambda r\right) + \cos\left(\lambda r\right)\right], \tag{5.81}$$

subject to

$$R(r_I) = 0 , \quad R(r_O) = 0 . \tag{5.82}$$

Hence the solution to the PDE (5.77) is given by the equation

$$\begin{aligned} W(r, t_1) &= \sum_{n=1}^{\infty} A_n \exp\left(-\lambda_n^2 t_1\right)\frac{1}{r^3}\left\{C_{n1}\left[r\lambda_n\cos\left(\lambda_n r\right) - \sin\left(\lambda_n r\right)\right]\right. \\ &+ \left. C_{n2}\left[r\lambda_n\sin\left(\lambda_n r\right) + \cos\left(\lambda_n r\right)\right]\right\} + \frac{r^{-3} - r_O^{-3}}{r_I^{-3} - r_O^{-3}}, \end{aligned} \tag{5.83}$$

subject to

$$W(r_I, t_1) = 1 , \quad W(r_O, t_1) = 0 , \quad W(r, 0) = -\frac{r^{-3} - r_O^{-3}}{r_I^{-3} - r_O^{-3}} . \tag{5.84}$$

Applying the boundary conditions at the inner and outer barriers in the solution (5.81) we have the following system of equations

$$C_1\frac{1}{r_I^3}\left[r_I\lambda\cos(\lambda r_I)-\sin(\lambda r_I)\right]+C_2\frac{1}{r_I^3}\left[r_I\lambda\sin(\lambda r_I)+\cos(\lambda r_I)\right] = 0 \tag{5.85}$$

$$C_1\frac{1}{r_O^3}\left[r_O\lambda\cos(\lambda r_O)-\sin(\lambda r_O)\right]+C_2\frac{1}{r_O^3}\left[r_O\lambda\sin(\lambda r_O)+\cos(\lambda r_O)\right] = 0\,. \tag{5.86}$$

For a nontrivial solution we require the determinant of the 2×2 matrix formed by the coefficients of C_1 and C_2 to be equal to zero so that C_1 and C_2 are not identically zero

$$\begin{vmatrix} \frac{1}{r_I^3}\left[r_I\lambda\cos(\lambda r_I)-\sin(\lambda r_I)\right] & \frac{1}{r_I^3}\left[r_I\lambda\sin(\lambda r_I)+\cos(\lambda r_I)\right] \\ \frac{1}{r_O^3}\left[r_O\lambda\cos(\lambda r_O)-\sin(\lambda r_O)\right] & \frac{1}{r_O^3}\left[r_O\lambda\sin(\lambda r_O)+\cos(\lambda r_O)\right] \end{vmatrix} = 0\,.$$

The above determinant when calculated simplifies to

$$\tan\left[\lambda(r_O-r_I)\right]=\frac{\lambda(r_O-r_I)}{r_Ir_O\lambda^2+1}\,.$$

The latter formula can provide the values for the eigenvalues λ_n. Because the angle of tan is a function of the variable λ which is to be determined, we set $\bar{\lambda}=\lambda(r_O-r_I)$ and the above equation can be rewritten as

$$\tan(\bar{\lambda})=\frac{(r_O-r_I)^2\bar{\lambda}}{r_Ir_O\bar{\lambda}^2+(r_O-r_I)^2} \quad \text{or} \quad \bar{\lambda}_n=\arctan\left[\frac{(r_O-r_I)^2\bar{\lambda}}{r_Ir_O\bar{\lambda}^2+(r_O-r_I)^2}\right]+n\pi\,.$$

Hence the eigenvalues are given by the formula

$$\lambda_n(r_O-r_I)=\arctan\left[\frac{\lambda_n(r_O-r_I)}{r_Ir_O\lambda_n^2+1}\right]+n\pi\,. \tag{5.87}$$

For values of $r_I=1$, $r_O=10$ the first 20 eigenvalues are given in table (5.8).
Going back to the set of equations we got from applying the boundary conditions, we solve equation (5.85) for C_2 and substitute it in the equation we found for the value of

n	λ_n	n	λ_n
1	0.4522286829	11	3.864981440
2	0.7846562141	12	4.212052583
3	1.118353729	13	4.559409257
4	1.455527457	14	4.906995411
5	1.795607303	15	5.254768497
6	2.137815968	16	5.602695711
7	2.481548956	17	5.950751393
8	2.826382149	18	6.298915210
9	3.172023618	19	6.647170861
10	3.518270942	20	6.995505130

Tab. 5.8: Values of λ_n for $n = 1..20$

the option, (5.83), which becomes

$$W(r,t_1) = \sum_{n=1}^{\infty} C_{1n} \exp(-\lambda_n^2 t_1) \frac{1}{r^3} \tag{5.88}$$
$$\left\{ r\lambda_n \cos(\lambda_n r) - \sin(\lambda_n r) + \frac{\sin(\lambda_n r_I) - r\lambda_n \cos(\lambda_n r_I)}{r\lambda_n \sin(\lambda_n r_I) + \cos(\lambda_n r_I)} [r\lambda_n \sin(\lambda_n r) + \cos(\lambda_n r)] \right\}$$
$$+ \frac{r^{-3} - r_O^{-3}}{r_I^{-3} - r_O^{-3}},$$

or else

$$W(r,t_1) = \sum_{n=1}^{\infty} D_n \exp(-\lambda_n^2 t_1) \frac{1}{r^3} \tag{5.89}$$
$$\left\{ r\, r_I \lambda_n^2 \sin[\lambda_n (r_I - r)] + \lambda_n (r - r_I) \cos[\lambda_n (r_I - r)] + \sin(\lambda_n (r_I - r)) \right\} + \frac{r^{-3} - r_O^{-3}}{r_I^{-3} - r_O^{-3}},$$

satisfying the boundary conditions at r_I and r_O, where $D_n = \frac{C_{1n}}{r\lambda_n \sin(\lambda_n r_I) + \cos(\lambda_n r_I)}$ and is valid for any payoff.
For convenience we can write equation (5.89) as

$$W(r,t_1) = \sum_{n=1}^{\infty} D_n \exp(-\lambda_n^2 t_1) F_n(r) + \frac{r^{-3} - r_O^{-3}}{r_I^{-3} - r_O^{-3}}, \tag{5.90}$$

where $F_n(r) = \frac{1}{r^3} \left\{ r\, r_I \lambda_n^2 \sin[\lambda_n (r_I - r)] + \lambda_n (r - r_I) \cos[\lambda_n (r_I - r)] + \sin(\lambda_n (r_I - r)) \right\}$.

To find the coefficient D_n of the series we need to find an orthogonal function, such that the eigenfunctions form a complete orthonormal set. To find the orthogonal function we take the ODE (5.80) and write in the form of the Sturm-Liouville equation,

$$\frac{d}{dr}[r^4 R'(r)] + \lambda_n^2 r^4 R(r) = 0\,. \tag{5.91}$$

Suppose the above ODE has two solutions, R_n and R_m. Then they both satisfy the equation,

$$\begin{aligned} \frac{d}{dr}[r^4 R_n'(r)] + \lambda_n^2 r^4 R_n(r) &= 0\,, \\ \frac{d}{dr}[r^4 R_m'(r)] + \lambda_m^2 r^4 R_m(r) &= 0\,. \end{aligned}$$

We multiply the first equation by R_m and the second by R_n and subtract

$$R_m \frac{d}{dr}[r^4 R_n'(r)] - R_n \frac{d}{dr}[r^4 R_m'(r)] + (\lambda_n^2 - \lambda_m^2)\, r^4 R_n(r) R_m(r) = 0\,.$$

We integrate the latter equation with respect to r from r_I to r

$$(r^4 R_m R_n' - r^4 R_n R_m') - [r^4(R_m R_n' - R_n R_m')]_{r_I}^{r} = (\lambda_m^2 - \lambda_n^2) \int_{r_I}^{r} r^4 R_n R_m \, dr\,.$$

Set the upper limit equal to the upper (outer) boundary r_O and the term in the square brackets is zero from the boundary conditions and the equation takes the form

$$r^4(R_m R_n' - R_n R_m') = (\lambda_m^2 - \lambda_n^2) \int_{r_I}^{r_O} r^4 R_n R_m \, dr\,.$$

If R_n, R_m belong to different eigenvalues, $\lambda_m \neq \lambda_n$, they are orthogonal. Hence the left hand side which is the Wronskian for R_m, R_n will be zero. The orthogonality relation that holds is

$$(\lambda_m^2 - \lambda_n^2) \int_{r_I}^{r_O} r^4 R_n R_m \, dr = 0\,,$$

for $\lambda_m \neq \lambda_n$ with the weight function being r^4.

At $t_1 = 0$ equation (5.90) takes the form

$$W(r,0) = \sum_{n=1}^{\infty} D_n F_n(r) + \frac{r^{-3} - r_O^{-3}}{r_I^{-3} - r_O^{-3}}\,. \tag{5.92}$$

where the left-hand side is the payoff given by (5.78). This makes the payoff to actually be equal to

$$W(r,0) = -\frac{r^{-3} - r_O^{-3}}{r_I^{-3} - r_O^{-3}}. \qquad (5.93)$$

This payoff causes discontinuity at $t_1 = 0$, as the option takes values given by (5.93) and at the lower barrier takes the value zero.

We multiply equation (5.92) by the orthogonal eigenfunction along with the weight function r^4 and integrate with respect to r from r_I to r_O,

$$\int_{r_I}^{r_O} W(r,0)\, r^4 F_m(r)\, dr = \sum_{n=1}^{\infty} D_n \int_{r_I}^{r_O} r^4 F_n(r) F_m(r)\, dr\,,$$

where the right-hand side is zero when $m \neq n$. Hence for $m = n$

$$D_n = \frac{\int_{r_I}^{r_O} W(r,0)\, r^4 F_n(r)}{\int_{r_I}^{r_O} r^4 [F_n(r)]^2\, dr}.$$

For $r_I = 1$ and $r_O = 10$ the coefficients D_n are given in table 5.9.

n	D_n	n	D_n
1	0.3921011774	11	0.003585152088
2	0.1667798641	12	0.002800239107
3	0.08484442029	13	0.002226789179
4	0.04751200158	14	0.001798655808
5	0.02864253895	15	0.001472880536
6	0.01833996068	16	0.001220795047
7	0.01234097006	17	0.001022799215
8	0.008652331926	18	0.0008651999997
9	0.006277141370	19	0.0007382437952
10	0.004686557397	20	0.0006348604834

Tab. 5.9: Values of D_n for $n = 1..20$

With coefficients given by table 5.9 the first 20 terms of the series solution (5.89) are plotted against the radial variable r in figure 5.15. For the correction of the discontinuity occurring at the lower barrier at $t_1 = 0$, the Fejer sums are used. We use the same formula as stated back in the three-dimensional case (page 83). As we move further away from the payoff, t_1 grows and the exponential becomes smaller leaving the linear term to eventually dominate the price of the option.

In figure 5.15 for any time t_1 the solution takes the value one at the inner barrier r_I and decreases exponentially to take the value zero at the outer barrier r_O. The curve corresponding to the maturity at $t_1 = 0$ (lower dashed line) is very steep as the

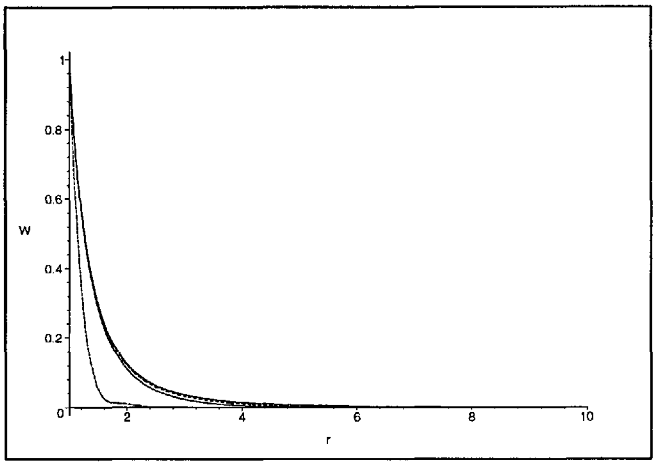

Fig. 5.15: Plot of the series solution $W(r, t_1)$ for $n = 20$, using the Fejer sums at $t_1 = 0$ (lower dashed line), $t_1 = 2$ (lower, solid line), $t_1 = 5$ (dotted line) against r. The upper solid like is the graph of the extra term $W(r)$ against r given by (5.79)

solution is trying to take the value zero at the payoff and at the same time satisfy the conditions at the two boundaries. As we move away from the payoff with time t_1 increasing, the value of the option becomes more expensive and the curves are more smooth. The further we move away from the payoff, the larger t_1 becomes and the Fourier series term gets very small leaving the price of the option to take the maximum value given by the extra term of the solution, (5.79), upper solid line in figure 5.15. In figure 5.16 we plot the solution $W(r, t_1)$ against time t_1 for different fixed values of r. As t_1 approaches zero, the asset has more chances of hitting the inner barrier and expiring with the value of one and at the same time has the same chances of missing the barrier and expire worthless. The closer we are to the inner barrier, at $r = 2$, the more expensive the price of the option will be as the underlying has more chances of hitting the barrier and expiring with a better payoff. When we are positioned far away from the inner barrier, at $r = 3, 4$ or 5, the price of the option drops as the chances of hitting the inner barrier have been reduced and the asset has more chances of expiring worthless.

We take the problem of Firth and Dewynne [21] who have the same governing equation as (5.77) subject to the conditions (5.75). The solution to the five-dimensional problem is given by the formula

$$U(\rho, \tau) = \frac{1}{\rho^3}\left[\operatorname{erfc}\frac{(\rho-1)}{2\sqrt{\tau}} + (\rho - 1)\exp(\rho - 1 + \tau)\operatorname{erfc}\left(\sqrt{\tau} + \frac{(\rho-1)}{2\sqrt{\tau}}\right)\right]. \qquad (5.94)$$

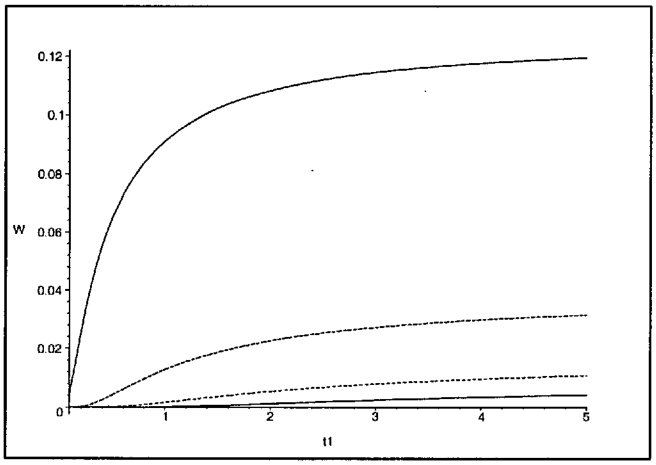

Fig. 5.16: Plot of the series solution $W(r, t_1)$ given by (5.89) against t_1 for $n = 20$. Upper solid line for $r = 2$, middle dashed line for $r = 3$, lower dashed line for $r = 4$ and lower solid line for $r = 5$.

For fixed time and letting r vary, the plots of (5.89) and (5.94) are identical, making the Fourier series solution of our boundary problem a very good approximation to Firth and Dewynne's boundary problem solution.

5.5.1 *The effect of a single expanding barrier*

Suppose there is a moving barrier in the shape of a five-dimensional wedge which narrows as time $t_1 = T - t$ approaches zero, sketch 5.17. The cross-section of the wedge at fixed time t_1 has the shape of a spheroid. The value at the barrier is one and at infinity zero, making it a single barrier, as in the problem of Firth and Dewynne [21]. The underlying moves freely above the expanding barrier. The analytic equation for a multi-dimensional expanding barrier is given in chapter 3. For the five-dimensional wedge the equation will take the form

$$W_W(\eta) = \frac{\int_\eta^\infty \exp{(-s/4)} s^{-5/2} \, ds}{\int_\gamma^\infty \exp{(-s/4)} s^{-5/2} \, ds}, \tag{5.95}$$

where $\frac{\sum_i^N x_i'^2}{\eta} = t_1 + t_0$, $\eta = \gamma$ is the barrier and t_0 $(t > T)$ is the time where the wedge tends to a point such that $S = S_0$, i.e. $x' = \ln{(\frac{S}{S_0})}$, $\sum_{i=1}^N x_i'^2 = r^2$ in the coordinate system used. At $t_1 = 0$, $(t = T)$, the cross-section of the wedge is finite with value

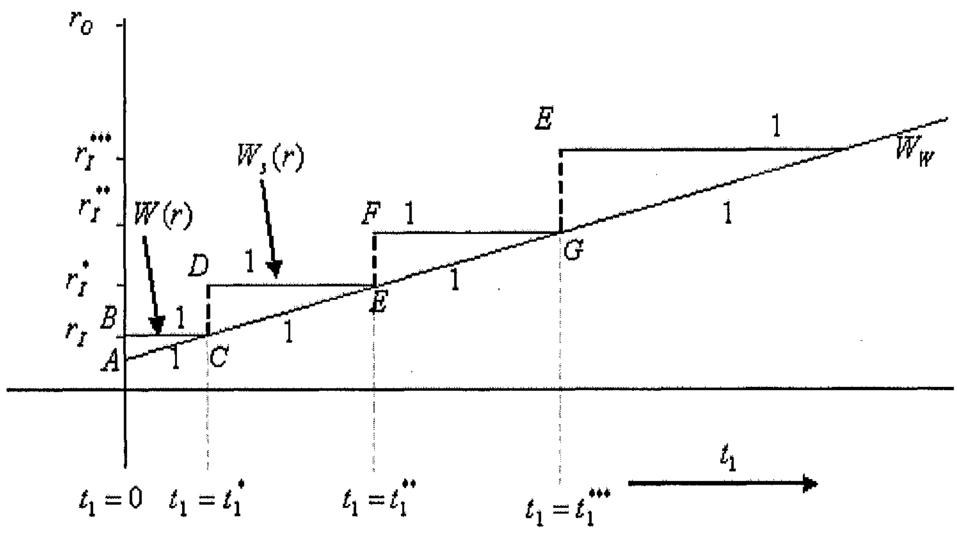

Fig. 5.17: Single expanding barrier.

$\sqrt{\gamma t_0}$. The equation for the moving barrier in terms of the variable r will be

$$W_W(r, t_1) = \frac{\int_{r^2/(t_1+t_0)}^{\infty} \exp(-s/4) s^{-5/2}\, ds}{\int_{\gamma}^{\infty} \exp(-s/4) s^{-5/2}\, ds}. \tag{5.96}$$

At $t_1 = 0$ ($t = T$), the finite value of the single wedge barrier (point A in sketch 5.17, at $r = \sqrt{\gamma t_0}$) is positioned lower than the inner barrier of the Fourier series (point B at $r_I = 1$). Because of this the wedge will act as a lower bound to the Fourier series solution. To test this we take a point above the Fourier series barrier between $0 < t_1 < t_1^*$, say $(r, t_1) = (1.5, 0.3)$, and evaluate the analytic solution of the wedge ($W_W = 0.05689086887$) and the Fourier series solution at that point ($W = 0.2049571051$). The value found from the analytic solution is less than the value found from the Fourier series solution, which verifies that the wedge acts as a lower bound to the Fourier series barrier. As time t_1 grows away from the payoff, $t < T$, the lower barrier of the Fourier series solution remains constant with value $r = r_I$. At time t_1^*, say, the barrier r_I hits the wedge at the point $C(t_1^*, \sqrt{\gamma(t_1^* + t_0)})$. At that point the following equality holds

$$r_I = \sqrt{\gamma(t_1 + t_0)} \Rightarrow \gamma = \frac{r_I^2}{t_1 + t_0}, \tag{5.97}$$

n	k_n	n	k_n
1	0.4686405009	11	4.331171038
2	0.8378061064	12	4.722926924
3	1.216588223	13	5.114825178
4	1.600839994	14	5.506835984
5	1.988012635	15	5.898937268
6	2.376855894	16	6.291112356
7	2.766726224	17	6.683348421
8	3.157267415	18	7.075635432
9	3.548268830	19	7.467965446
10	3.939598779	20	7.860332076

Tab. 5.10: List of the eigenvalues of k_n for the step barrier r_I^* for $n = 1..20$.

which for given time t_1 and t_0 we can find the value of the wedge barrier γ. If we take $t_1^* = 0.5$ to be the time where the first jump occurs and $t_0 = 0.2$ the time where the wedge tends to a point, then the value of γ is equal to $\gamma = 1.428571429$. From the point C the Fourier series barrier jumps to another higher value $r_I^* > r_I$ at the point D of the diagram. For the new step barrier, the Fourier series solution has a similar form, as given in the previous section,

$$W_s(r,t_1) = \sum_{n=1}^{N} E_n \exp\left(-k_n^2 t_1\right) F_n(r, r_I^*) + \frac{r^{-3} - r_O^{-3}}{r_I^{*-3} - r_O^{-3}}\,, \tag{5.98}$$

where

$$F_n(r, r_I^*) = \frac{1}{r^3}\left[r\, r_I^* k_n^2 \sin\left[k_n\left(r_I^* - r\right)\right] + k_n(r - r_I^*)\cos\left[k_n\left(r_I^* - r\right)\right] + \sin\left(k_n\left(r_I^* - r\right)\right)\right]\,, \tag{5.99}$$

and subject to the boundary conditions

$$W_s(r_I^*, t_1) = 1\,, \quad W_s(r_O, t_1) = 0\,. \tag{5.100}$$

Note that W_s is notational and does not imply a derivative. The extra term is added so that the value at the barrier is made zero. The corresponding eigenvalues for the step barrier solution are given by the same formula as found in the previous section, i.e.

$$k_n(r_O - r_I^*) = \arctan\left[\frac{k_n(r_O - r_I^*)}{r_I^* r_O k_n^2 + 1}\right] + n\pi\,. \tag{5.101}$$

For values of $r_I^* = 2$, $r_O = 10$ the first 20 eigenvalues are given in table (5.10).

At t_1^* equation (5.98) takes the form

$$W_s(r, t_1^*) = \sum_{n=1}^{N} E_n \exp\left(-k_n^2 t_1^*\right) F_n(r, r_I^*) + \frac{r^{-3} - r_O^{-3}}{r_I^{*-3} - r_O^{-3}}, \tag{5.102}$$

where the left-hand side is the payoff equal to the Fourier series solution (5.89) evaluated at t_1^*,

$$W(r, t_1^*) = \sum_{n=1}^{\infty} D_n \exp\left(-\lambda_n^2 t_1^*\right) \frac{1}{r^3} \tag{5.103}$$

$$\left\{r\, r_I \lambda_n^2 \sin\left[\lambda_n \left(r_I - r\right)\right] + \lambda_n (r - r_I) \cos\left[\lambda_n \left(r_I - r\right)\right] + \sin\left(\lambda_n \left(r_I - r\right)\right)\right\} + \frac{r^{-3} - r_O^{-3}}{r_I^{-3} - r_O^{-3}},$$

valid for $r_I^* < r < r_O$ and zero at $r_I < r < r_I^*$ and where the values for D_n are given from table 5.9. We multiply equation (5.102) by $r^4 F_m(r, r_I^*)$ and integrate with respect to r from r_I^* to r_O and using the orthogonality condition we have

$$G_n = \frac{\int_{r_I^*}^{r_O} W(r, t_1^*)\, r^4 F_n(r, r_I^*)\, dr - \int_{r_I^*}^{r_O} \frac{r^{-3} - r_O^{-3}}{r_I^{*-3} - r_O^{-3}}\, r^4 F_n(r, r_I^*)\, dr}{\int_{r_I^*}^{r_O} r^4 [F_n(r, r_I^*)]^2\, dr}, \tag{5.104}$$

for $m = n$, where $G_n = E_n \exp\left(-k_n^2 t_1^*\right)$. The values for the first twenty coefficients G_n of the step barrier series solution for $r_I^* = 2$ and $r_O = 10$ are given in table 5.11.

n	G_n	n	G_n
1	2.099010109	11	0.005694749703
2	0.5920888549	12	0.004398466791
3	0.2267004527	13	0.003467054978
4	0.1060022742	14	0.002780791003
5	0.05693277258	15	0.002264124643
6	0.03377839344	16	0.001867788084
7	0.02158031234	17	0.001558724704
8	0.01459064654	18	0.001314195549
9	0.01031278320	19	0.001118211564
10	0.007553027246	20	0.0009593083019

Tab. 5.11: Values of the coefficient G_n for the step barrier for $n = 1..20$

The solution for the step barrier $r = r_I^*$ will eventually take the form

$$W_s(r, t_1) = \sum_{n=1}^{N} G_n \exp\left(-k_n^2 (t_1 - t_1^*)\right) F_n(r, r_I^*) + \frac{r^{-3} - r_O^{-3}}{r_I^{*-3} - r_O^{-3}}, \tag{5.105}$$

where

$$F_n(r, r_I^*) = \frac{1}{r^3} \left[r\, r_I^* k_n^2 \sin\left[k_n\left(r_I^* - r\right)\right] + k_n(r - r_I^*) \cos\left[k_n\left(r_I^* - r\right)\right] + \sin\left(k_n\left(r_I^* - r\right)\right)\right] . \tag{5.106}$$

At t_1^* the jump causes a discontinuity to the solution which can be smoothed out by using the Fejer sums. In figure 5.18 we plot the solution (5.105) against r for fixed time $t_1 \geq t_1^*$. At time $t_1 = 0.5$ when the jump occurs, the curve of the Fourier series solution is very steep as it takes the value one at the inner barrier $r_I^* = 2$ and the value zero at the outer barrier $r_O = 10$. Moving away from the jump, $t_1 > t_1^*$, the curves for the solution smooth out and are more expensive as the effect of the extra cubic term takes place. As time grows the exponential term becomes smaller and smaller leaving the extra term to dominate the solution for large time. The corresponding graphs plotted for the Fourier series barrier $r = r_I$ are cheaper than the ones plotted for the step barrier $r = r_I^*$. This happens as the barrier widens with the effect of the jump when time t_1 approaches zero. The jump reduces the possibilities of the underlying of hitting the inner barrier and expiring with a better value. This increases the chances of the asset entering the wider area which allows the underlying to move and hit the lower barrier r_I.

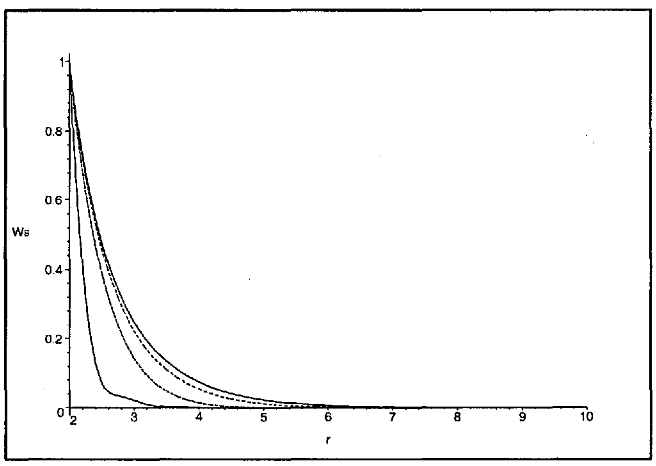

Fig. 5.18: Plot of the series solution $W_s(r, t_1)$ for $n = 20$, using the Fejer sums at $t_1 = 0.5$ (lower solid line), $t_1 = 1$ (lower dashed line), $t_1 = 2$ (upper dashed line) and $t_1 = 3$ (upper solid line) against r.

By letting time vary and keeping r fixed (figure 5.19) we observe that for the underlying positioned close to the jump and close to the inner barrier r_I^* the price of the option falls because the chances of the asset hitting the r_I^* barrier are small (not much time left for the asset to move in order to hit the barrier). The underlying has little time left to move and hit the inner barrier, increasing the chances of the asset to enter the wider barrier area. Moving away from the jump $t_1 > t_1^*$, the value of the option increases as the asset will have more time and will increase the chances of hitting the inner barrier and gaining profit. Taking higher values for r, the price of the option drops considerably. Moving away from the jump the value of the option increases as the underlying has more space and time to move and hit the barrier r_I^* returning a profit to the holder of the option.

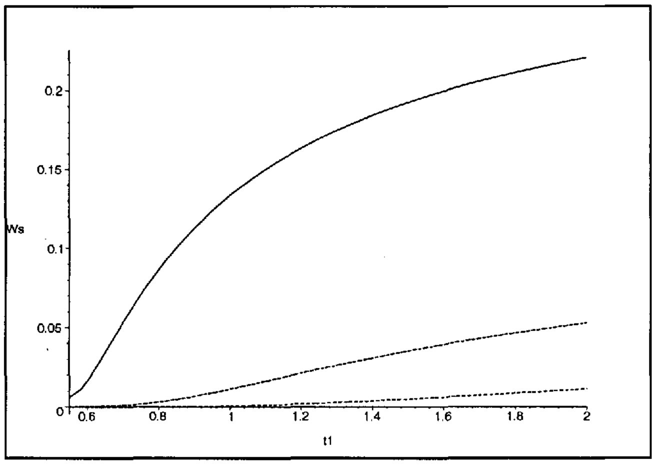

Fig. 5.19: Plot of the series solution $W_s(r, t_1)$ for $n = 20$, for $r = 3$ (solid line), $r = 4$ (top dashed line) and $r = 5$ (bottom dashed line) against time t_1.

6. DOUBLE BARRIER ASIAN OPTIONS

In this chapter we discuss the effects of double barriers on European type Asian options. The nature of the problem can be described as follows.

Suppose there are two barriers parallel to each other remaining constant throughout the life of the option. The value of the option depends on the average price of the asset during time $[0, T]$, the price of the asset and time. At time $t = T$ the two barriers are positioned at levels $S = S_L$ and $S = S_U$, with $S_L < S < S_U$, letting the underlying move freely in the area created between the boundaries (figure 6.1). The initial asset value is assumed to be positioned in the middle of the two barriers. The two barriers are of knock-out nature, meaning that the option will expire worthless if one of the two barriers is triggered.

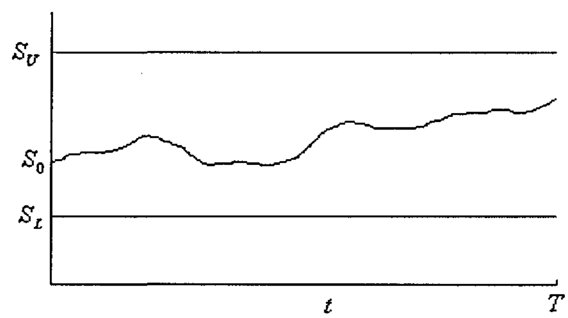

Fig. 6.1: Path of an asset with the effect of double barriers.

Assume there are two constant barriers S_{WL} and S_{WU} which at some time $t = t^* < T$ change symmetrically up and down to take the corresponding values S_L, S_U till expiry, with $S_L < S_{WL} < S_{WU} < S_U$. This change results in a wider area between the two barriers S_L, S_U leaving more space for the underlying to move freely (figure 6.4). The effect on the value of the double barrier Asian option is explored later in section 6.1.1. Suppose we have a slightly different problem where at time $t = t^* < T$ two barriers, S_{SL} and S_{SU} move symmetrically inwards to values S_L, S_U, with $S_{SL} < S_L < S_U < S_{SU}$, making the area between the barriers smaller than before (figure

6.7). This problem is discussed further in section 6.1.2. For both problems the barriers retain their knock-out nature.

We seek a solution to all three problems using the PDE method. More precisely we construct a one-dimensional partial differential equation as part of the boundary value problem, which we solve using the WKB method (named after Wentzel, Kramers and Billouin). Using the WKB solution to the problem along with the properties of Fourier series and orthonormal sets of eigenfunctions, we express the price of the option in series form. We discuss how the price is affected by the two barriers, the jumps and the time to maturity. For the payoff we take a linear function of the asset S forming a triangle between the two barriers S_L and S_U.

The price for any path-dependent option whose value depends on the running average I, the price of the underlying S and time t is given by the following partial differential equation

$$\frac{\partial V}{\partial t} + S\,\frac{\partial V}{\partial I} + \frac{1}{2}\,\sigma^2 S^2\,\frac{\partial^2 V}{\partial S^2} + rS\,\frac{\partial V}{\partial S} - rV = 0\,. \tag{6.1}$$

To investigate the fair price of such an option we consider the payoff to be of the general form

$$V(S,I,T) = \exp\left(\alpha I(T)\right)F(S)\,, \tag{6.2}$$

where $F(S)$ is a function of S, α is a constant and I is the running sum $I = \int_0^t S_u\,du$. If α is considered complex then we get the characteristic function of the average. This is important as it helps one to price payoffs different and more complicated than the one considered later in section 6.3 (e.g. Carr and Madan [10]).
The boundary conditions are

$$V(S,I,t) = 0\,, \quad \text{at} \quad S = S_L\,,\; S = S_U\,. \tag{6.3}$$

where S_L is the lower barrier, S_U is the upper barrier and $S_L < S < S_U$.

Because of the form of the payoff we can reduce the dimension of the equation and remove the average term by using the transformation

$$V(\bar{S},\bar{I},t) = \exp\left(\alpha_1 \bar{I}(t)\right)U(\bar{S},t)\,, \tag{6.4}$$

where $\bar{S} = \frac{S}{S_0}$, $\bar{I} = \frac{I}{S_0}$ and $\alpha_1 = \alpha\,S_0$; S_0 being the initial asset value. Equation (6.1) becomes

$$\frac{\partial U}{\partial t} + \frac{1}{2}\,\sigma^2 \bar{S}^2\,\frac{\partial^2 U}{\partial \bar{S}^2} + r\bar{S}\,\frac{\partial U}{\partial \bar{S}} + (\alpha_1 \bar{S} - r)U = 0\,. \tag{6.5}$$

Note that throughout this chapter $\bar{S} = S/S_0$, $\bar{S}_L = S_L/S_0$, $\bar{S}_U = S_U/S_0$, $\bar{S}_{WL} = S_{WL}/S_0$, $\bar{S}_{WU} = S_{WU}/S_0$, $\bar{S}_{SL} = S_{SL}/S_0$ and $\bar{S}_{SU} = S_{SU}/S_0$ so that the equation is independent of the initial value of the underlying asset, with $0 < \bar{S}_L < 1$ and $\bar{S}_U > 1$.

$$\frac{\partial U}{\partial t} + \frac{1}{2}\sigma^2 \bar{S}^2 \frac{\partial^2 U}{\partial \bar{S}^2} + r\bar{S}\frac{\partial U}{\partial \bar{S}} + (\alpha_1 \bar{S} - r)U = 0\,. \tag{6.6}$$

We set $t_1 = T - t$, then

$$\frac{\partial U}{\partial t_1} = \frac{1}{2}\sigma^2 \bar{S}^2 \frac{\partial^2 U}{\partial \bar{S}^2} + rS\frac{\partial U}{\partial \bar{S}} + (\alpha_1 \bar{S} - r)U\,. \tag{6.7}$$

We change the variable by setting $\bar{S} = \exp(\bar{x})$ and (6.7) takes the form

$$\frac{\partial U}{\partial t_1} = \frac{\sigma^2}{2}\frac{\partial^2 U}{\partial \bar{x}^2} + \left(r - \frac{\sigma^2}{2}\right)\frac{\partial U}{\partial \bar{x}} + (\alpha_1 \exp(\bar{x}) - r)U\,, \tag{6.8}$$

with boundary conditions

$$U(\bar{x}, t_1) = 0\,, \quad \text{at} \quad \bar{x} = \bar{x}_L \quad \text{and} \quad \bar{x} = \bar{x}_U\,, \tag{6.9}$$

where x_L is the lower barrier, $\bar{x}_L < 0$, and $\bar{x}_U$ is the upper barrier, $\bar{x}_U > 0$. We next set $U(\bar{x}, t_1) = \exp(\beta t_1 + \gamma \bar{x})\, U_1(\bar{x}, t_1)$, and choose β and γ such that

$$\frac{\partial U_1}{\partial t_1} = \frac{\sigma^2}{2}\frac{\partial^2 U_1}{\partial \bar{x}^2} + \alpha_1 \exp(\bar{x}) U_1\,,$$

thus $\beta = -\frac{\sigma^2}{8} - \frac{r}{2} - \frac{r^2}{2\sigma^2}$, $\gamma = \frac{1}{2} - \frac{r}{\sigma^2}$ and by setting $t_2 = \frac{\sigma^2}{2}t_1$ we end up having

$$\frac{\partial U_1}{\partial t_2} = \frac{\partial^2 U_1}{\partial \bar{x}^2} + \alpha_2 \exp(\bar{x}) U_1\,, \tag{6.10}$$

where $\alpha_2 = \frac{2\alpha_1}{\sigma^2}$ and with

$$U_1(\bar{x}, t_2) = 0\,, \quad \text{at} \quad \bar{x} = \bar{x}_L \quad \text{and} \quad \bar{x} = \bar{x}_U\,. \tag{6.11}$$

We move the origin by setting $\bar{x} = \tilde{x} + \bar{x}_L$; then equation (6.10) becomes

$$\frac{\partial U_1}{\partial t_2} = \frac{\partial^2 U_1}{\partial \tilde{x}^2} + \alpha_3 \exp(\tilde{x}) U_1\,, \tag{6.12}$$

where $\alpha_3 = \alpha_2 \exp(\bar{x}_L)$ and with boundary condition at the two barriers

$$U_1(0) = U_1(\bar{x}_U - \bar{x}_L) = 0\,. \tag{6.13}$$

In order to solve this one-dimensional parabolic PDE, (6.12), we use separation of variables by letting

$$U_1(\tilde{x}, t_2) = X(\tilde{x})\, T(t_2)\,,$$

and we end up having the equation

$$\frac{T'}{T} = \frac{X''}{X} + \alpha_3 \exp(\tilde{x}) = -k^2\,,$$

where k^2 is the separation variable.
From the above equation we get a system of equations

$$\begin{aligned} T' + k^2\, T &= 0\,, && (6.14)\\ X''(\tilde{x}) + (\alpha_3 \exp(\tilde{x}) + k^2)X(\tilde{x}) &= 0\,. && (6.15)\end{aligned}$$

From the first equation we have

$$T(t_2) = A\, \exp(-k^2 t_2)\,, \tag{6.16}$$

where A is the integrating constant.
The exact solution of equation (6.15) can be written in terms of a conjugate pair of Bessel functions of the first kind,

$$X(\tilde{x}) = C_1\Gamma(1-2ik)J_{-2ik}(2\sqrt{\alpha_3 \exp(\tilde{x})}) + C_2\Gamma(1+2ik)J_{2ik}(2\sqrt{\alpha_3 \exp(\tilde{x})})\,. \tag{6.17}$$

For real X we assume that the constants are complex conjugates, $C_1 = a + ib$, $C_2 = a - ib$ where a and b are real. Hence the equation becomes

$$\begin{aligned} X(\tilde{x}) &= a\,\Re[\Gamma(1-2ik)J_{-2ik}(2\sqrt{\alpha_3 \exp(\tilde{x})}) + \Gamma(1+2ik)J_{2ik}(2\sqrt{\alpha_3 \exp(\tilde{x})})]\\ &+ ib\,\Im[\Gamma(1-2ik)J_{-2ik}(2\sqrt{\alpha_3 \exp(\tilde{x})}) - \Gamma(1+2ik)J_{2ik}(2\sqrt{\alpha_3 \exp(\tilde{x})})]\end{aligned}$$

Applying the boundary conditions (6.13) in the above solution gives us a system of equations

$$\begin{aligned} &a\, \underbrace{\Re[\Gamma(1-2ik)J_{-2ik}(2\sqrt{\alpha_3}) + \Gamma(1+2ik)J_{2ik}(2\sqrt{\alpha_3})]}_{\alpha} \\ &\quad + ib\, \underbrace{\Im[\Gamma(1-2ik)J_{-2ik}(2\sqrt{\alpha_3}) - \Gamma(1+2ik)J_{2ik}(2\sqrt{\alpha_3})]}_{\beta} = 0\,, \end{aligned} \tag{6.18}$$

$$a\,\underbrace{\Re[\Gamma(1-2ik)J_{-2ik}(2\sqrt{\alpha_3\exp(\bar{x}_U-\bar{x}_L)})+\Gamma(1+2ik)J_{2ik}(2\sqrt{\alpha_3\exp(\bar{x}_U-\bar{x}_L)})]}_{\gamma} \qquad (6.19)$$
$$+\,ib\,\underbrace{\Im[\Gamma(1-2ik)J_{-2ik}(2\sqrt{\alpha_3\exp(\bar{x}_U-\bar{x}_L)})-\Gamma(1+2ik)J_{2ik}(2\sqrt{\alpha_3\exp(\bar{x}_U-\bar{x}_L)})]}_{\delta}=0\,,$$

which can be written in the form

$$\begin{pmatrix}\alpha & \beta\\ \gamma & \delta\end{pmatrix}\begin{pmatrix}a\\ ib\end{pmatrix}=0\,.$$

For a nontrivial solution we require the determinant of the 2×2 matrix to be equal to zero so that a and b are not identically zero

$$\begin{vmatrix}\alpha & \beta\\ \gamma & \delta\end{vmatrix}=0\,.$$

This gives

$$\begin{aligned}&\Re[\Gamma(1-2ik)J_{-2ik}(2\sqrt{\alpha_3})+\Gamma(1+2ik)J_{2ik}(2\sqrt{\alpha_3})]\\ &\qquad\Im[\Gamma(1-2ik)J_{-2ik}(2\sqrt{\alpha_3\exp(\bar{x}_U-\bar{x}_L)})-\Gamma(1+2ik)J_{2ik}(2\sqrt{\alpha_3\exp(\bar{x}_U-\bar{x}_L)})]\\ &-\Im[\Gamma(1-2ik)J_{-2ik}(2\sqrt{\alpha_3})-\Gamma(1+2ik)J_{2ik}(2\sqrt{\alpha_3})] \qquad (6.20)\\ &\qquad\Re[\Gamma(1-2ik)J_{-2ik}(2\sqrt{\alpha_3\exp(\bar{x}_U-\bar{x}_L)})+\Gamma(1+2ik)J_{2ik}(2\sqrt{\alpha_3\exp(\bar{x}_U-\bar{x}_L)})]=0\,.\end{aligned}$$

In order to find the solution of the above equation for k, we have to find the zeros of the Bessel functions. This is a difficult task as the separation variable k is involved in the order of the Bessel function. Because of this complication in finding the values of k, we will use the WKB method to find the eigenvalues k and eigenfunctions $X(\tilde{x})$ which satisfy the boundary conditions and determine the orthogonality of the latter. The eigenfunctions will enable us to fit the boundary conditions in a series form and hence determine a good approximation to the exact solution (see section A).
The above ODE, (6.15), can be rewritten as

$$\frac{d^2X}{d\tilde{x}^2}+k^2\left(1+\frac{\alpha_3}{k^2}\exp(\tilde{x})\right)X(\tilde{x})=0\,,$$

or

$$\frac{1}{k^2}\frac{d^2X}{d\tilde{x}^2}+\left(1+\frac{\alpha_3}{k^2}\exp(\tilde{x})\right)X(\tilde{x})=0\,,\quad \text{as } k\to\infty\,,$$

which is of the form

$$\epsilon^2 y'' = Q(x)y\,, \quad Q(x) \neq 0\,, \tag{6.21}$$

when ϵ is small ($\epsilon \to 0$). Equation (6.21) is the Schrödinger equation whose approximate solution for ϵ small can be found using the WKB method; that is

$$y(x) \sim C_1 Q(x)^{-1/4} \exp\left(\tfrac{1}{\epsilon}\textstyle\int_a^x \sqrt{Q(t)}\,dt\right) + C_2 Q(x)^{-1/4} \exp\left(-\tfrac{1}{\epsilon}\textstyle\int_a^x \sqrt{Q(t)}\,dt\right), \quad \text{as } \epsilon \to 0\,, \tag{6.22}$$

where C_1 and C_2 are constants to be determined from the initial or boundary conditions and a is an arbitrary but fixed integration point, e.g. Bender and Orszag [6].

Equation (6.15) can be written in the form of (6.21)

$$\frac{1}{k^2}\frac{d^2X}{d\tilde{x}^2} = -\left(1 + \frac{\alpha_3}{k^2}\exp(\tilde{x})\right) X(\tilde{x})\,, \tag{6.23}$$

where $Q(\tilde{x}) = -(1 + \frac{\alpha_3}{k^2}\exp(\tilde{x}))$, with boundary conditions

$$X(0) = X(\tilde{x}_U - \tilde{x}_L) = 0\,.$$

Therefore the general solution to equation (6.23) using the WKB method is

$$X(\tilde{x}) \sim C_1 Q(\tilde{x})^{-1/4} \exp\left(\int_0^{\tilde{x}} \sqrt{Q(\tau)}\,d\tau\right) + C_2 Q(\tilde{x})^{-1/4} \exp\left(-\int_0^{\tilde{x}} \sqrt{Q(\tau)}\,d\tau\right).$$

Hence the general solution for equation (6.12) is given by the series

$$U_1(\tilde{x}, t_2) = \sum_{n=1}^{\infty} A_n \exp(-k_n^2 t_2)(\alpha_3 \exp(\tilde{x}) + k_n^2)^{-1/4} \sin\left(\int_0^{\tilde{x}} \sqrt{\alpha_3 \exp(\tau) + k_n^2}\,d\tau\right), \tag{6.24}$$

where k_n is given by applying the other boundary condition at $\tilde{x} = \tilde{x}_U - \tilde{x}_L$ which requires that

$$\int_0^{\tilde{x}_U - \tilde{x}_L} \sqrt{\alpha_3 \exp(\tau) + k_n^2}\,d\tau = n\pi\,. \tag{6.25}$$

For the case where k_n is large the solution is shown as an example in section A.

In order to determine the constant coefficient A_n of the series, we need to check the orthogonality of the eigen-solutions. The orthogonality condition that needs to hold is

$$\int_0^{\bar{x}_U-\bar{x}_L} X_n X_m \, d\tilde{x} = 0\,, \quad \text{when } n \neq m\,,$$

where the weight function is equal to 1 (see section A).
At expiry $t_2 = 0$ $(t = T)$ the general solution (6.24) takes the form

$$U_1(\tilde{x},0) = \sum_{n=0}^{\infty} A_n X_n(\tilde{x})\,, \tag{6.26}$$

where the left-hand side is the payoff. To test the accuracy of the WKB method, we take the payoff to be the function

$$U_1(S,0) = \bar{S}^{-\frac{1}{2}+\frac{r}{\sigma^2}} \begin{cases} \frac{\bar{S}_U-\bar{S}}{\bar{S}_U-\bar{S}_L} & , \frac{\bar{S}_U+\bar{S}_L}{2} < \bar{S} < \bar{S}_U \\ \frac{\bar{S}-\bar{S}_L}{\bar{S}_U-\bar{S}_L} & , \bar{S}_L < \bar{S} < \frac{\bar{S}_U+\bar{S}_L}{2} \end{cases}\,, \tag{6.27}$$

in terms of $\bar{S}$,

$$X(\bar{x}) = U_1(\bar{x},0) = \exp\left[-\left(\frac{1}{2}-\frac{r}{\sigma^2}\right)\bar{x}\right] \begin{cases} \frac{\bar{S}_U-\exp(\bar{x})}{\bar{S}_U-\bar{S}_L} & , \ln\left(\frac{\bar{S}_U+\bar{S}_L}{2}\right) < \bar{x} < \ln(\bar{S}_U) \\ \frac{\exp(\bar{x})-\bar{S}_L}{\bar{S}_U-\bar{S}_L} & , \ln(\bar{S}_L) < \bar{x} < \ln\left(\frac{\bar{S}_U+\bar{S}_L}{2}\right) \end{cases}\,, \tag{6.28}$$

in terms of $\bar{x}$, and

$$U_1(\tilde{x},0) = \exp\left[-\left(\frac{1}{2}-\frac{r}{\sigma^2}\right)(\tilde{x}-\bar{x}_L)\right] \begin{cases} \frac{\bar{S}_U-\bar{S}_L\exp(\tilde{x})}{\bar{S}_U-\bar{S}_L} & , \ln\left(\frac{\bar{S}_U+\bar{S}_L}{2\bar{S}_L}\right) < \tilde{x} < \ln\left(\frac{\bar{S}_U}{\bar{S}_L}\right) \\ \frac{\bar{S}_L\exp(\tilde{x})-\bar{S}_L}{\bar{S}_U-\bar{S}_L} & , 0 < \tilde{x} < \ln\left(\frac{\bar{S}_U+\bar{S}_L}{2\bar{S}_L}\right) \end{cases}\,, \tag{6.29}$$

in terms of $\tilde{x}$. The coefficient A_n can be derived by multiplying equation (6.26) by $X_m(\tilde{x})$ and integrating with respect to $\tilde{x}$ from 0 to $\bar{x}_U - \bar{x}_L$.

$$\int_0^{\bar{x}_U-\bar{x}_L} U_1(\tilde{x},0)X_m(\tilde{x})\,d\tilde{x} = \sum_{n=1}^{\infty} A_n \int_0^{\bar{x}_U-\bar{x}_L} X_n(\tilde{x})X_m(\tilde{x})\,d\tilde{x}\,.$$

Using the orthogonality relation

$$\int_0^{\bar{x}_U-\bar{x}_L} X_n(\tilde{x})X_m(\tilde{x})\,d\tilde{x} = \begin{cases} 0 & , \text{if } m \neq n \\ \int_0^{\bar{x}_U-\bar{x}_L} [X_n(\tilde{x})]^2\,d\tilde{x} & , \text{if } m = n \end{cases}\,, \tag{6.30}$$

for $m = n$, A_n will take the form

$$A_n = \frac{\int_0^{\bar{x}_U - \bar{x}_L} U_1(\tilde{x}, 0) X_n(\tilde{x})\, d\tilde{x}}{\int_0^{\bar{x}_U - \bar{x}_L} [X_n(\tilde{x})]^2\, d\tilde{x}}, \tag{6.31}$$

and the eigenfunctions

$$X_n(\tilde{x}) = (\alpha_3 \exp(\tilde{x}) + k_n^2)^{-1/4} \sin\left(\int_0^{\tilde{x}} \sqrt{\alpha_3 \exp(\tau) + k_n^2}\, d\tau \right), \tag{6.32}$$

form a complete orthonormal set. Hence taking into account the payoff (6.29) the coefficient A_n will take the form

$$A_n = \frac{\int_{\ln\left[\frac{1}{2\bar{S}_L}(\bar{S}_U + \bar{S}_L)\right]}^{\ln\left(\frac{\bar{S}_U}{\bar{S}_L}\right)} \frac{\bar{S}_U - \bar{S}_L \exp(\tilde{x})}{\bar{S}_U - \bar{S}_L} X_n(\tilde{x})\, d\tilde{x} + \int_0^{\ln\left[\frac{1}{2\bar{S}_L}(\bar{S}_U + \bar{S}_L)\right]} \frac{\bar{S}_L \exp(\tilde{x}) - \bar{S}_L}{\bar{S}_U - \bar{S}_L} X_n(\tilde{x})\, d\tilde{x}}{\int_0^{\ln\left(\frac{\bar{S}_U}{\bar{S}_L}\right)} [X_n(\tilde{x})]^2\, d\tilde{x}}. \tag{6.33}$$

In table 6.1 we show the first ten coefficients of the series calculated for the payoff (6.29). The solution in terms of the variables $\tilde{x}$ and t_2 is

n	Values for k_n	Values for A_n for payoff (6.29)
1	2.139038725	0.7200689427
2	5.392424381	−0.1969075802
3	8.364169122	−0.04748087769
4	11.27823615	0.09143567646
5	14.17016471	−0.03130769161
6	17.05120432	−0.03284260703
7	19.92607330	0.03942528206
8	22.79710426	−0.005234976555
9	25.66558440	−0.02359201220
10	28.53228267	0.01402482217

Tab. 6.1: Values of k_n and A_n for $n = 1..10$ given from the formula (6.33) with payoff given by (6.29).

$$\begin{aligned} U(\tilde{x}, t_2) &= \exp\left(-\left(\frac{r}{\sigma^2} + \frac{1}{4} + \frac{r^2}{\sigma^4} \right) t_2 + \left(\frac{1}{2} - \frac{r}{\sigma^2} \right) (\tilde{x} + \bar{x}_L) \right) \\ &\quad \sum_{n=1}^{\infty} A_n \exp(-k_n^2 t_2)(\alpha_3 \exp(\tilde{x}) + k_n^2)^{-1/4} \sin\left(\int_0^{\tilde{x}} \sqrt{\alpha_3 \exp(\tau) + k_n^2}\, d\tau \right), \end{aligned} \tag{6.34}$$

where $\alpha_3 = \alpha_2 \exp(\bar{x}_L) = \frac{2}{\sigma^2} \alpha_1 \bar{S}_L$. For the numerical interpretation of the problem we take $r = 0.05$, $\sigma = 0.5$, $\alpha_1 = 0.5$ and $T = 1$. In figure 6.2 we plot the first ten terms of the series (6.34) against $\tilde{x}$ evaluated at different times $t_2 = 0$ (payoff, top dotted line), $t_2 = 0.025$ (top solid line), $t_2 = 0.0625$ (middle dotted line), $t_2 = 0.1$ (bottom dotted line) and $t_2 = 0.125$ (bottom solid line). We can see that the solution becomes zero as soon as the value of the option hits one of the barriers, $\bar{x}_L = 0$ and $\bar{x}_U = \ln\left(\frac{\bar{S}_U}{\bar{S}_L}\right) = 1.098612289$ and at the payoff the peak of the graph occurs at $\tilde{x} = \ln\left(\frac{\bar{S}_U+\bar{S}_L}{2\bar{S}_L}\right) = 0.6931471806$.

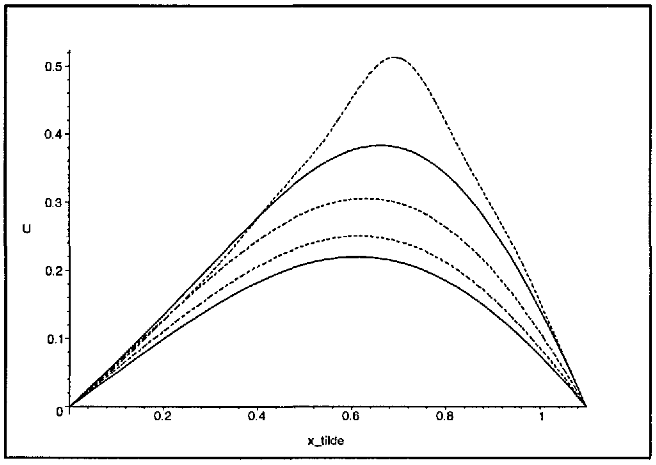

Fig. 6.2: Plot of the WKB solution (6.34) for $n = 10$ against $\tilde{x}$; from top to bottom, at $t_2 = 0$ (dotted line), $t_2 = 0.025$ (solid line), $t_2 = 0.0625$ (dotted line), $t_2 = 0.1$ (dotted line) and $t_2 = 0.125$ (solid line).

In terms of the original variables $\bar{S}$ and real time t the solution takes the form

$$\begin{aligned} U(\bar{S},t) &= \exp\left(-\left(\frac{r^2}{2\sigma^2}+\frac{\sigma^2}{8}+\frac{r}{2}\right)(T-t)\right)\bar{S}^{\left(\frac{1}{2}-\frac{r}{\sigma^2}\right)} \\ &\quad \sum_{n=1}^{\infty} A_n \exp\left(-\frac{\sigma^2}{2}k_n^2(T-t)\right)\left(\frac{2\alpha_1}{\sigma^2}\bar{S}+k_n^2\right)^{-1/4} \sin\left(\int_1^{\bar{S}/\bar{S}_L}\sqrt{\frac{2\alpha_1}{\sigma^2}\bar{S}_L\tau+k_n^2}\,\frac{d\tau}{\tau}\right). \end{aligned} \tag{6.35}$$

The plot of the solution in terms of the original variable $\bar{S}$ and real time t for $n = 10$ is shown in figure 6.3 for $t = 1$ (payoff), $t = 0.8$, 0.5, 0.2 and 0. Similarly the barriers occur at $\bar{S}_L = 0.5$ and $\bar{S}_U = 1.5$, and at $\bar{S} = 1$ the value at expiry is 0.5.
We can see from the figure that as time moves away from expiry (top dash-dotted line), the value of the option drops and becomes cheaper (lines under the top one), as the chances for the underlying asset hitting one of the barriers increases.

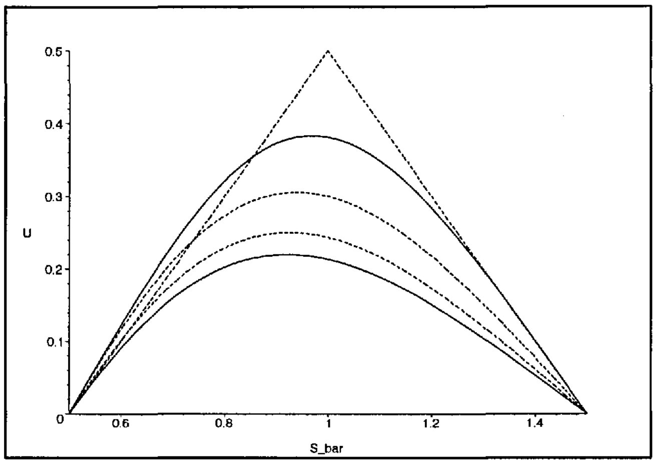

Fig. 6.3: Plot of the WKB solution (6.35) for $n = 10$ against S at real time t; from top to bottom, $t = 1$ (payoff, dotted line), $t = 0.8$ (solid line), $t = 0.5$ (dotted line), $t = 0.2$ (dotted line) and $t = 0$ (solid line).

6.1 Jump of the barrier

6.1.1 When it widens

In this section we assume that the double barrier at some time, t^* say, jumps from initial values $\bar{S}_{WL}$ and $\bar{S}_{WU}$ to values $\bar{S}_L$ and $\bar{S}_U$ ($\bar{S}_L < \bar{S}_{WL} < \bar{S}_{WU} < \bar{S}_U$). Both lower and upper barriers are widened symmetrically from $\bar{S}_{WL} = 0.7$ and $\bar{S}_{WU} = 1.3$ to $\bar{S}_L = 0.5$ and $\bar{S}_U = 1.5$, respectively. The nature of the problem is demonstrated in figure 6.4.

During the analysis we will be going forward in time t_2 ($t_2 = \frac{\sigma^2}{2}(T - t)$) and backward in real time t. For time t_2, suppose that at time $t_2 = t_2^*$, the barrier shrinks to $\bar{S}_{WL}$ and $\bar{S}_{WU}$, $\bar{S}_L < \bar{S}_{WL} < \bar{S}_{WU} < \bar{S}_U$ (going from $t_2 = 0$ to $t_2 = t_2^*$). For $0 < t_2 < t_2^*$ the solution that holds in terms of the variable $\tilde{x}$ was found earlier to satisfy the equation (6.34).

For time $t_2 > t_2^*$ the value of the option will be governed by the same equation we had for the double barrier

$$\frac{\partial U_1}{\partial t_2} = \frac{\partial^2 U_1}{\partial \bar{x}^2} + \alpha_2 \exp(\bar{x}) U_1 , \tag{6.36}$$

with boundary conditions

$$U_1(\bar{x}, t_2) = 0 , \quad \text{at} \quad \bar{x} = \bar{x}_{WL} = \bar{x}_{WU} .$$

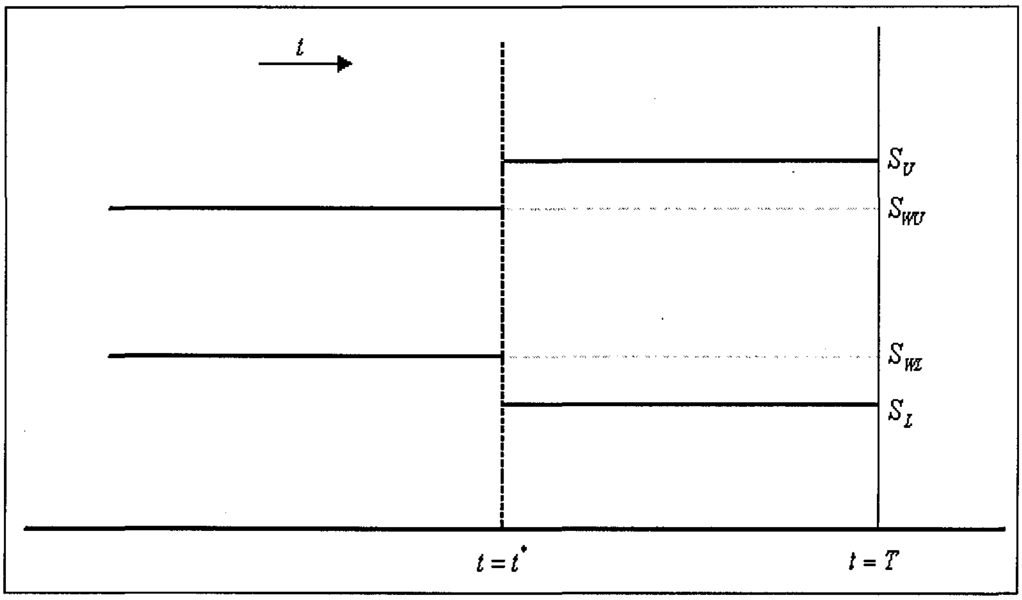

Fig. 6.4: Jump of the barrier at $t = t^*$.

After doing separation of variables we end up having

$$T(t_2) = A \exp(-\lambda^2 t_2),$$

and

$$X_W''(\hat{x}) + (\alpha_5 \exp(\hat{x}) + \lambda^2) X_W(\hat{x}) = 0, \tag{6.37}$$

with boundary conditions $X_W(0) = X_W(\bar{x}_{WU} - \bar{x}_{WL}) = 0$, where $\bar{x} = \hat{x} + \bar{x}_{WL}$, $\alpha_5 = \alpha_2 \exp(\bar{x}_{WL})$ and λ is the separation variable.
The solution of the above equation, (6.37), as found earlier is given by

$$X_W(\hat{x}) = \sum_{n=1}^{\infty} B_n (\alpha_5 \exp(\hat{x}) + \lambda_n^2)^{-1/4} \sin\left(\int_0^{\hat{x}} \sqrt{\alpha_5 \exp(\tau) + \lambda_n^2}\, d\tau \right), \tag{6.38}$$

which satisfies the boundary condition at $\hat{x} = 0$ and where the eigenvalues λ_n are given by applying the boundary condition at $\hat{x} = \bar{x}_{WU} - \bar{x}_{WL}$,

$$\int_0^{\bar{x}_{WU} - \bar{x}_{WL}} \sqrt{\alpha_5 \exp(\tau) + \lambda_n^2} = n\pi, \tag{6.39}$$

which for $\bar{x}_{WL} = 0.7$, $\bar{x}_{WU} = 1.3$ and $\alpha_5 = \alpha_2 \bar{S}_{WL} = 2.8$, (since $\alpha_2 = 4$) give the values shown in table 6.2.

Values for λ_n
$\lambda_1 = 4.677900485$
$\lambda_2 = 9.957139456$
$\lambda_3 = 15.09700435$
$\lambda_4 = 20.20408609$
$\lambda_5 = 25.29824090$
$\lambda_6 = 30.38596979$
$\lambda_7 = 35.47003768$
$\lambda_8 = 40.55182143$
$\lambda_9 = 45.63208409$
$\lambda_{10} = 50.71128279$

Tab. 6.2: Values of λ_n for $n = 1..10$

The solution for $t_2 > t_2^*$ of the PDE (6.36) in terms of the new variable $\hat{x}$ will take the form

$$\begin{aligned} U_{1W}(\hat{x}, t_2) &= \sum_{n=1}^{\infty} B_n \exp\left(-\lambda_n^2 t_2\right)(\alpha_5 \exp(\hat{x}) + \lambda_n^2)^{-1/4} \sin\left(\int_0^{\hat{x}} \sqrt{\alpha_5 \exp(\tau) + \lambda_n^2}\, d\tau\right) \\ &= \sum_{n=1}^{\infty} B_n \exp\left(-\lambda_n^2 t_2\right) X_{Wn}(\hat{x}) . \end{aligned} \tag{6.40}$$

where B_n is the series coefficient which will be determined by applying the normalization condition.
At $t_2 = t_2^*$ the following equality holds

$$U_{1W}(\hat{x}, t_2^*) = \sum_{n=1}^{\infty} B_n \exp\left(-\lambda_n^2 t_2^*\right) X_{Wn}(\hat{x}) , \tag{6.41}$$

where the left-hand-side is the 'new payoff' which is equal to the value of the option found for the barrier at $\bar{x}_L$ and $\bar{x}_U$ evaluated at time t_2^*,

$$U_{1W}(\tilde{x}, t_2^*) = \sum_{n=1}^{\infty} A_n \exp\left(-k_n^2 t_2^*\right)(\alpha_3 \exp(\tilde{x}) + k_n^2)^{-1/4} \sin\left(\int_0^{\tilde{x}} \sqrt{\alpha_3 \exp(\tau) + k_n^2}\, d\tau\right) . \tag{6.42}$$

valid for $\bar{x}_{WL} - \bar{x}_L < \tilde{x} < \bar{x}_{WU} - \bar{x}_L$, where A_n was found to have the values shown in table 6.1. Equation (6.42) in terms of the new variable $\hat{x}$ ($\tilde{x} = \hat{x} + \bar{x}_{WL} - \bar{x}_L$) takes the form

$$U_{1W}(\hat{x}, t_2^*) = \sum_{n=1}^{\infty} A_n \exp(-k_n^2 t_2^*)(\alpha_3 \exp(\hat{x} + \bar{x}_{WL} - \bar{x}_L) + k_n^2)^{-1/4} \sin\left(\int_0^{\hat{x}+\bar{x}_{WL}-\bar{x}_L} \sqrt{\alpha_3 \exp(\tau) + k_n^2}\, d\tau\right), \tag{6.43}$$

valid for $0 < \hat{x} < \bar{x}_{WU} - \bar{x}_{WL}$.

In order to find the coefficients B_n we multiply equation (6.41) by $X_{Wm}(\hat{x})$ and integrate with respect to $\hat{x}$ from 0 to $\bar{x}_{WU} - \bar{x}_{WL}$

$$\int_0^{\bar{x}_{WU}-\bar{x}_{WL}} U_{1W}(\hat{x}, t_2^*) X_{Wm}\, d\hat{x} = \sum_{n=1}^{\infty} B_n \exp(-\lambda_n^2 t_2^*) \underbrace{\int_0^{\bar{x}_{WU}-\bar{x}_{WL}} X_{Wm} X_{Wn}\, d\hat{x}}_{=0,\ \text{unless } m=n}.$$

So for $m = n$ the equation becomes

$$C_n = \frac{\int_0^{\bar{x}_{WU}-\bar{x}_{WL}} U_{1W}(\hat{x}, t_2^*)\, X_{Wn}(\hat{x})\, d\hat{x}}{\int_0^{\bar{x}_{WU}-\bar{x}_{WL}} [X_{Wn}(\hat{x})]^2\, d\hat{x}}, \tag{6.44}$$

where $C_n = B_n \exp(-\lambda_n^2 t_2^*)$, $U_{1W}(\hat{x}, t_2^*)$ is given by (6.43) and $X_{Wn}(\hat{x})$ is given by (6.40). The values of C_n are shown in table 6.3.

n	λ_n	Values for C_n using (6.43)
1	4.677900485	0.8425839615
2	9.957139456	0.09778211922
3	15.09700435	0.3313676954
4	20.20408609	0.06990330878
5	25.29824090	0.2508257942
6	30.38596979	0.05699282296
7	35.47003768	0.2106556363
8	40.55182143	0.04932363552
9	45.63208409	0.1853014203
10	50.71128279	0.04410133861

Tab. 6.3: Values of C_n for $n = 1..10$, using the discontinuous payoff function (6.43).

Hence the solution is

$$U_W(\hat{x}, t_2) = \exp\left[-\left(\frac{r}{\sigma^2} + \frac{1}{4} + \frac{r^2}{\sigma^4}\right) t_2 + \left(\frac{1}{2} - \frac{r}{\sigma^2}\right)(\hat{x} + \bar{x}_{WL})\right] \sum_{n=1}^{\infty} C_n \exp(-\lambda_n^2 (t_2 - t_2^*)) X_{Wn}(\hat{x}) \tag{6.45}$$

where $X_{Wn}(\hat{x})$ is given by (6.40). In figure 6.5 we have plotted the solution (6.45) for the payoff (6.43) with the coefficients found in table 6.3. Whatever the effect of the discontinuity the solution has at the payoff, $t_2 = 0.0625$, it is corrected as soon as a very small time has elapsed. This can be seen from the upper solid line which corresponds to the time just after the jump occurs, $t_2 = 0.075$. As time increases to $t_2 = 0.1$ and 0.125, the value of the option falls, as it has moved further away from the payoff (figure 6.5).

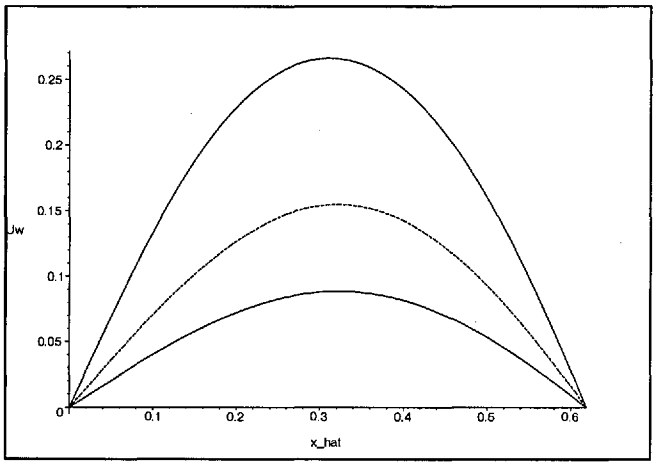

Fig. 6.5: Plot of the series solution $U_W(\hat{x}, t_2)$ for $n = 10$ against the variable $\hat{x}$ for time $t_2 = 0.075$ (top solid line), $t_2 = 0.1$ (dotted line) and $t_2 = 0.125$ (bottom solid line).

The value of the option in terms of the original variables $\bar{S}$ and real time t will look like

$$U_W(\bar{S}, t) = \exp\left[-\left(\frac{r}{2} + \frac{\sigma^2}{8} + \frac{r^2}{2\sigma^2}\right)(T - t)\right]\bar{S}^{\left(\frac{1}{2} - \frac{r}{\sigma^2}\right)} \tag{6.46}$$
$$\sum_{n=1}^{\infty} C_n \exp\left(-\frac{\sigma^2}{2}\lambda_n^2(t^* - t)\right)\left(\frac{2\alpha_1}{\sigma^2}\bar{S} + \lambda_n^2\right)^{-1/4} \sin\left(\int_1^{\bar{S}/\bar{S}_{WL}} \sqrt{\frac{2\alpha_1}{\sigma^2}\bar{S}_{WL}\,\tau + \lambda_n^2}\,\frac{d\tau}{\tau}\right),$$

and is plotted against the original variable $\bar{S}$ for $t = 0.4$, $t = 0.2$ and $t = 0$ in figure 6.6, with $r = 0.05$, $\sigma = 0.5$, $\alpha_1 = 0.5$ and $T = 1$.

The graph of $U(S, t)$ in figure 6.6 shows how the value of the option in terms of the original variable S evolves when the barrier has jumped from $[S_{WL}, S_{WU}]$ to $[S_L, S_U]$ in real time t ($t < t^*$). At $t = 0$ the value of the option is cheap since it is far away from maturity. As time grows the value of the option becomes more expensive ($t = 0.2$, bottom solid line) as it moves closer to maturity. At the jump, $t = t^* = 0.5$, the value of the option will become more expensive as the holder of the option has benefited from this sudden change of luck after managing to avoid hitting any of the barriers.

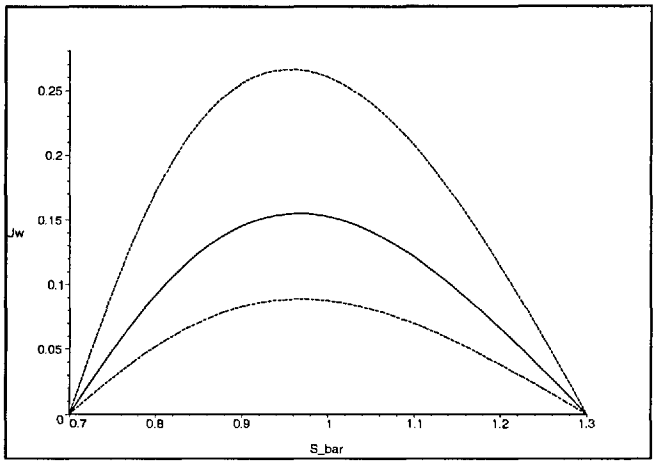

Fig. 6.6: Plot of the series solution $U_W(\bar{S},t)$ for $n = 10$, for time $t = 0.4$ (top dotted line), $t = 0.2$ (solid line) and $t = 0$ (bottom dotted line) in terms of the variable $\bar{S}$.

Because the value of the option before the jump $t = t^*$ diffuses backwards in real time t, the holder of the option is aware of the fact that soon he will benefit from the jump of the two barriers and so the value of the option will be more expensive than it was before. For $t > t^*$ the possibilities of the underlying hitting one of the new barriers have decreased and as the time to maturity approaches, the value of the option increases to reach a value at the exercise date (figure 6.3).

When the value of the option reaches the time $t = t^*$ just before the barrier widens, i.e. forward in real time, say at time $t^* - \epsilon$ ($\epsilon \ll 1$), the option has some value (it's not zero as it hasn't hit any barrier) different to the one occurring at time $t^* + \epsilon$. At $t^* - \epsilon < t < t^* + \epsilon$ the function is discontinuous, since it only takes values equal to $U_{1W}(\hat{x}, t^*)$ for $\bar{S}_{WL} < \hat{x} < \bar{S}_{WU}$ and zero for values $\bar{S}_L < \hat{x} < \bar{S}_{WL}$, $\bar{S}_{WU} < \hat{x} < \bar{S}_U$. The holder of the option at $t^* + \epsilon$ is in much better position than the holder at $t^* - \epsilon$, because he has less chances in hitting the barriers. As a consequence, the value of the option increases from position $t^* - \epsilon$, before the jump, to the position $t^* + \epsilon$, after the jump.

6.1.2 When it shrinks

Assume that the double barrier at some time, t^* say, shrinks from initial values S_{SL} and $\bar{S}_{SU}$ to values $\bar{S}_L$ and $\bar{S}_U$, respectively ($\bar{S}_{SL} < \bar{S}_L < \bar{S}_U < \bar{S}_{SU}$) (going from $t = t^*$ to $t = T$). The values we take for these barriers are $\bar{S}_{SL} = 0.3$, $\bar{S}_L = 0.5$, $\bar{S}_U = 1.5$ and $\bar{S}_{SU} = 1.7$. The nature of the problem is demonstrated in the picture 6.7.
Here we use the same equations as in the case when the barrier widens but with some minor changes.

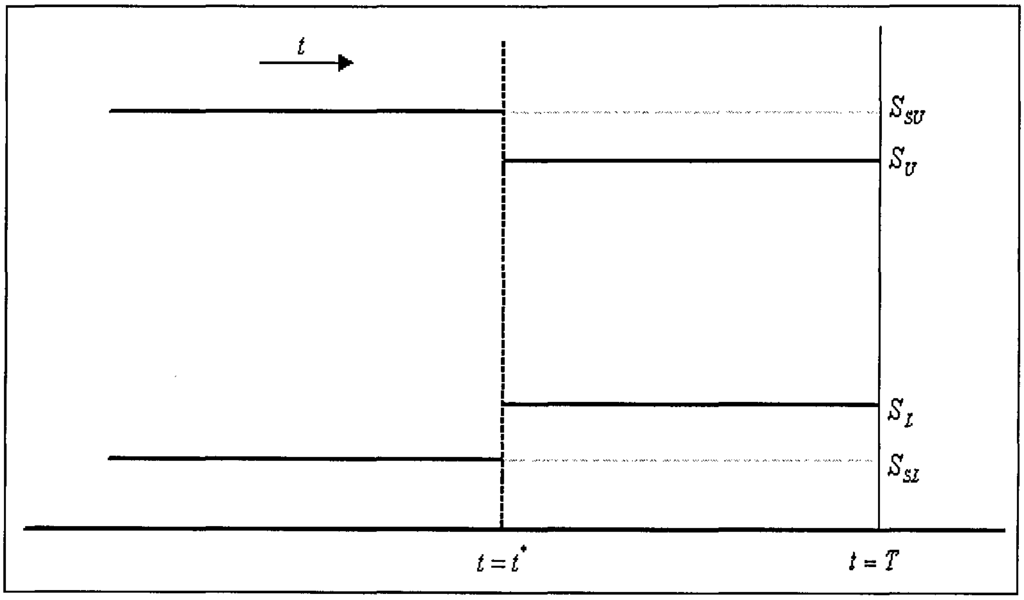

Fig. 6.7: Jump of the barrier at $t = t^*$.

Again throughout this section we will be going backwards in time, i.e. from $t_2 = 0$ to $t_2 = t_2^*$ and the solution of the double barrier option is given by (6.34). The governing equation of the double barrier option up to time t_2^* is the same and by doing separation of variables we have the following system of equations

$$\begin{cases} T(t_2) = A\exp\left(-\lambda^2 t_2\right) \\ X_S''(\bar{x}) + (\alpha_2 \exp(\bar{x}) + \lambda^2)X_S(\bar{x}) = 0 \end{cases}, \tag{6.47}$$

with boundary conditions

$$X_S(\bar{x}_{SL}) = X_S(\bar{x}_{SU}) = 0\,.$$

By moving the origin setting $\bar{x} = \hat{x} + \bar{x}_{SL}$ the second equation of the system becomes

$$X_S''(\hat{x}) + (\alpha_6 \exp(\hat{x}) + \lambda^2)X_S(\hat{x}) = 0\,, \tag{6.48}$$

where $\alpha_6 = \alpha_2 \exp(\bar{x}_{SL}) = \alpha_2 \bar{S}_{SL}$, λ is the separation variable, and satisfies the boundary conditions

$$X_S(0) = X_S(\bar{x}_{SU} - \bar{x}_{SL}) = 0\,. \tag{6.49}$$

The solution to equation (6.48) as found earlier is

$$X_S(\hat{x}) = \sum_{n=1}^{\infty} D_n(\alpha_6 \exp(\hat{x}) + \lambda_n^2)^{-1/4} \sin\left(\int_0^{\hat{x}} \sqrt{\alpha_6 \exp(\tau) + \lambda_n^2}\, d\tau\right), \tag{6.50}$$

which satisfies the boundary condition at $\hat{x} = 0$ and where the eigenvalues are given by applying the boundary condition at $\hat{x} = \bar{x}_{SU} - \bar{x}_{SL}$,

$$\int_0^{\bar{x}_{SU}-\bar{x}_{SL}} \sqrt{\alpha_6 \exp(\tau) + \lambda_n^2}\, d\tau = n\pi \quad \text{for} \quad n = 1, 2, 3, \cdots. \tag{6.51}$$

which for $\bar{x}_{SL} = \ln(0.3)$, $\bar{x}_{SU} = \ln(1.7)$ and $\alpha_6 = 1.2$ gives the values shown in table 6.4.

Values for λ_n
$\lambda_1 = 0.4760406767$
$\lambda_2 = 3.152523996$
$\lambda_3 = 5.129735834$
$\lambda_4 = 7.019015719$
$\lambda_5 = 8.876045484$
$\lambda_6 = 10.71746714$
$\lambda_7 = 12.55011286$
$\lambda_8 = 14.37732426$
$\lambda_9 = 16.20093391$
$\lambda_{10} = 18.02203223$

Tab. 6.4: Values of λ_n for $n = 1..10$ for the new barrier $[\bar{S}_{SL}, \bar{S}_{SU}]$

The solution for $t_2 > t_2^*$ will take the form

$$\begin{aligned} U_{1S}(\hat{x}, t_2) &= \sum_{n=1}^{\infty} D_n \exp(-\lambda_n^2 t_2)(\alpha_6 \exp(\hat{x}) + \lambda_n^2)^{-1/4} \sin\left(\int_0^{\hat{x}} \sqrt{\alpha_6 \exp(\tau) + \lambda_n^2}\, d\tau\right) \\ &= \sum_{n=1}^{\infty} D_n \exp(-\lambda_n^2 t_2) X_{Sn}(\tilde{x}), \end{aligned} \tag{6.52}$$

where D_n is the series coefficient which will be found by applying the orthogonality condition at $t_2 = t_2^*$.

At $t_2 = t_2^*$ the following equality holds

$$U_{1S}(\hat{x}, t_2^*) = \sum_{n=1}^{\infty} D_n \exp(-\lambda_n^2 t_2^*) X_{Sn}(\hat{x}), \tag{6.53}$$

where the left-hand-side is the 'new payoff' at time t_2^* which is equal to the value of the option found for the double barrier $[\bar{x}_L, \bar{x}_U]$,

$$U_{1S}(\tilde{x}, t_2^*) = \sum_{n=1}^{\infty} A_n \exp(-k_n^2 t_2^*)(\alpha_3 \exp(\tilde{x}) + k_n^2)^{-1/4} \sin\left(\int_0^{\tilde{x}} \sqrt{\alpha_3 \exp(\tau) + k_n^2}\, d\tau\right). \tag{6.54}$$

which in terms of the new variable $\hat{x}$ ($\tilde{x} = \hat{x} + \bar{x}_{SL} - \bar{x}_L$) takes the form,

$$\begin{aligned} U_{1S}(\hat{x}, t_2^*) &= \sum_{n=1}^{\infty} A_n \exp(-k_n^2 t_2^*)(\alpha_3 \exp(\hat{x} + \bar{x}_{SL} - \bar{x}_L) + k_n^2)^{-1/4} \\ & \quad \sin\left(\int_0^{\hat{x}+\bar{x}_{SL}-\bar{x}_L} \sqrt{\alpha_3 \exp(\tau) + k_n^2}\, d\tau\right), \end{aligned} \tag{6.55}$$

valid for $\bar{x}_L - \bar{x}_{SL} < \hat{x} < \bar{x}_U - \bar{x}_{SL}$ and is zero at the intervals $[\bar{x}_{SL}, \bar{x}_L]$ and $[\bar{x}_U, \bar{x}_{SU}]$, where A_n was found to have the values shown in table 6.1.

Multiplying equation (6.53) by X_{Sm} and integrating over $\hat{x}$ from 0 to $\bar{x}_{SU} - \bar{x}_{SL}$ we have

$$\int_{\bar{x}_L-\bar{x}_{SL}}^{\bar{x}_U-\bar{x}_{SL}} U_{1S}(\hat{x}, t_2^*) X_{Sm}\, d\hat{x} = \sum_{n=1}^{\infty} D_n \exp(-\lambda_n^2 t_2^*) \underbrace{\int_0^{\bar{x}_{SU}-\bar{x}_{SL}} X_{Sm} X_{Sn}\, d\hat{x}}_{=0,\, \text{unless}\, m=n},$$

since

$$\begin{aligned} \int_{\bar{x}_{SL}}^{\bar{x}_{SU}} (\ldots)\, d\bar{x} &= \underbrace{\int_{\bar{x}_{SL}}^{\bar{x}_L} (\ldots)\, d\bar{x}}_{=0} + \int_{\bar{x}_L}^{\bar{x}_U} (\ldots)\, d\bar{x} + \underbrace{\int_{\bar{x}_U}^{\bar{x}_{SU}} (\ldots)\, d\bar{x}}_{=0} \\ &= \int_{\bar{x}_L}^{\bar{x}_U} (\ldots)\, d\bar{x} = \int_{\bar{x}_L-\bar{x}_{SL}}^{\bar{x}_U-\bar{x}_{SL}} (\ldots)\, d\hat{x}, \quad \text{since} \quad \hat{x} = \bar{x} - \bar{x}_{SL}. \end{aligned}$$

Hence when $m = n$ we have

$$E_n = D_n \exp(-\lambda_n^2 t_2^*) = \frac{\int_{\bar{x}_L-\bar{x}_{SL}}^{\bar{x}_U-\bar{x}_{SL}} U_{1S}(\hat{x}, t_2^*) X_{Sn}(\hat{x})\, d\hat{x}}{\int_0^{\bar{x}_{SU}-\bar{x}_{SL}} (X_{Sn}(\hat{x}))^2\, d\hat{x}}. \tag{6.56}$$

The values of E_n for the first ten terms of the series are given in table 6.5.

Therefore the full solution to the problem becomes

$$\begin{aligned} U_S(\hat{x}, t_2) &= \exp\left[-\left(\frac{r}{\sigma^2} + \frac{1}{4} + \frac{r^2}{\sigma^4}\right) t_2 + \left(\frac{1}{2} - \frac{r}{\sigma^2}\right)(\hat{x} + \bar{x}_{SL})\right] \qquad (6.57) \\ & \sum_{n=1}^{\infty} E_n \exp(-\lambda_n^2 (t_2 - t_2^*))(\alpha_6 \exp(\hat{x}) + \lambda_n^2)^{-1/4} \sin\left(\int_0^{\hat{x}} \sqrt{\alpha_6 \exp(\tau) + \lambda_n^2}\, d\tau\right), \end{aligned}$$

n	Values for λ_n	Values for E_n given by (6.5)
1	0.4760406767	0.2782360162
2	3.152523996	−0.1699091131
3	5.129735834	−0.09048394086
4	7.019015719	0.07882120570
5	8.876045484	−0.01334710795
6	10.71746714	0.04897786562
7	12.55011286	−0.02901824368
8	14.37732426	0.007569492839
9	16.20093391	−0.02644970783
10	18.02203223	0.009274073020

Tab. 6.5: Values of k_n and E_n for $n = 1..10$ with payoff the function (6.55).

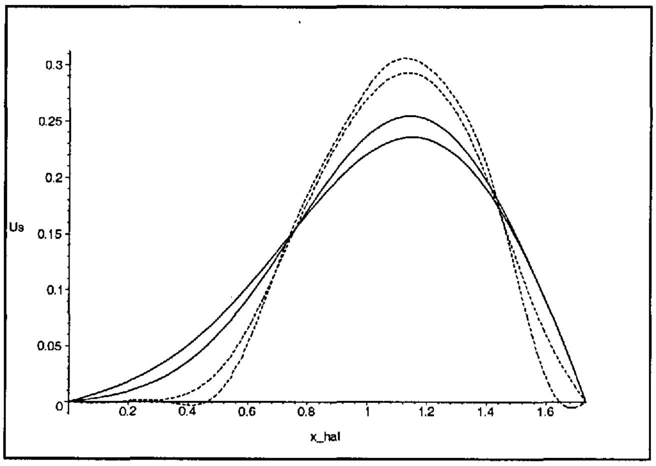

Fig. 6.8: Plot of the series solution $U_S(\hat{x}, t_2)$ for $n = 10$, at time $t_2 = 0.0625$ (payoff, top dashed line), $t_2 = 0.07$ (lower dashed line), $t_2 = 0.1$ (upper solid line), $t_2 = 0.125$ (lower solid line) in terms of the variable $\hat{x}$.

the plot of which for the first 10 terms of the series, as time grows, looks like in figure 6.8 (note that the values taken for σ, r and T are as in the previous section).
In terms of the $\tilde{x}$ variable, the solution above becomes,

$$\begin{aligned} U_S(\tilde{x}, t_2) &= \exp\left[-\left(\frac{r}{\sigma^2} + \frac{1}{4}\right) t_2 + \left(\frac{1}{2} - \frac{r}{\sigma^2}\right)(\tilde{x} + \bar{x}_L)\right] \\ &\quad \sum_{n=1}^{\infty} E_n \exp\left(-\lambda_n^2 (t_2 - t_2^*)\right)(\alpha_6 \exp(\tilde{x} + \bar{x}_L - \bar{x}_{SL}) + \lambda_n^2)^{-1/4} \\ &\quad \sin\left(\int_0^{\tilde{x} + \bar{x}_L - \bar{x}_{SL}} \sqrt{\alpha_6 \exp(\tau) + \lambda_n^2}\, d\tau\right), \end{aligned} \tag{6.58}$$

and in terms of the original variable $\bar{x}$ the solution of the new barrier $[\bar{x}_{SL}, \bar{x}_{SU}]$ looks like

$$U_S(\bar{x}, t_2) = \exp\left[-\left(\frac{r}{\sigma^2} + \frac{1}{4} + \frac{r^2}{\sigma^4}\right) t_2 + \left(\frac{1}{2} - \frac{r}{\sigma^2}\right) \bar{x}\right] \tag{6.59}$$
$$\sum_{n=1}^{\infty} E_n \exp\left(-\lambda_n^2 (t_2 - t_2^*)\right)(\alpha_6 \exp(\bar{x} - \bar{x}_{SL}) + \lambda_n^2)^{-1/4} \sin\left(\int_0^{\bar{x} - \bar{x}_{SL}} \sqrt{\alpha_6 \exp(\tau) + \lambda_n^2}\, d\tau\right),$$

an finally in terms of the original variables $\bar{S}$ and real time t it will look like

$$U_S(\bar{S}, t) = \exp\left[-\left(\frac{r}{2} + \frac{\sigma^2}{8} + \frac{r^2}{2\sigma^2}\right)(T - t)\right] \bar{S}^{\left(\frac{1}{2} - \frac{r}{\sigma^2}\right)} \tag{6.60}$$
$$\sum_{n=1}^{\infty} E_n \exp\left(-\frac{\sigma^2}{2}\lambda_n^2 (t^* - t)\right)\left(\frac{2\alpha_1}{\sigma^2}\bar{S} + \lambda_n^2\right)^{-1/4} \sin\left(\int_1^{\bar{S}/\bar{S}_{SL}} \sqrt{\frac{2\alpha_1}{\sigma^2}\bar{S}_{SL}\,\tau + \lambda_n^2}\, \frac{d\tau}{\tau}\right).$$

The solution (6.60) is plotted against the original variable $\bar{S}$ for $t = 0.5$ (when the jump occurs), $t = 0.2$ and $t = 0$ in figure 6.9.

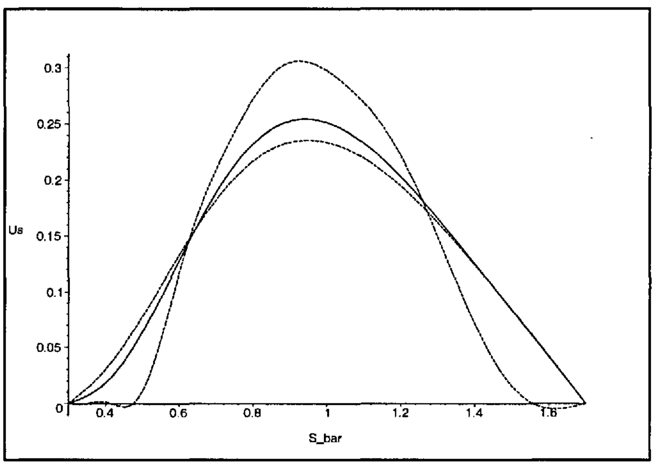

Fig. 6.9: Plot of the series solution $U_S(\bar{S}, t)$ for $n = 10$, for time $t = 0.5$ (top dotted line), $t = 0.2$ (solid line) and $t = 0$ (dashed line) in terms of the variable $\bar{S}$.

The graph of $U(\bar{S}, t)$ (figure 6.9) shows how the value of the option in terms of the original variable S evolves when the barrier has jumped from $[\bar{S}_{SL}, \bar{S}_{SU}]$ to $[\bar{S}_L, \bar{S}_U]$ in real time t. Looking at figures 6.9 and 6.3 we observe that the value of the option at $t = 1$ is quite large compared to the values it takes as it moves away from the payoff. Before the jump occurs at $t = t^*$ the holder of the option is in a better position than after as the underlying has more space to move and is less likely to hit the barrier $[\bar{S}_{SL}, \bar{S}_{SU}]$.

Looking closely at the shape in figure 6.10 we can comment on the behavior of the option throughout this jump. At $t = 0$ the value of the option will be cheap when

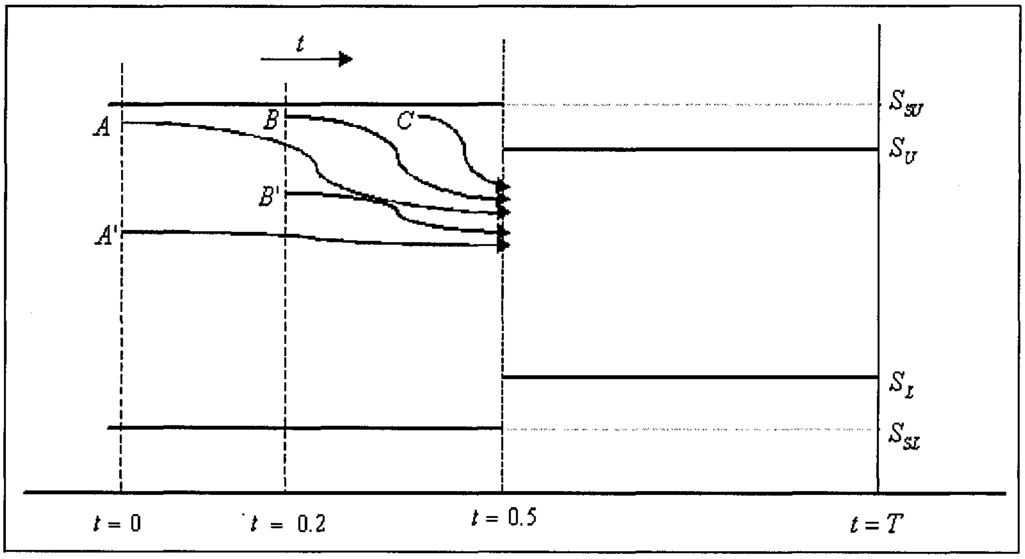

Fig. 6.10: Jump of the barrier backwards in time at $t = t^*$.

the underlying is close to the barriers (position A). As we move away from the two barriers, towards the middle of the interval $[\bar{S}_{SL}, \bar{S}_{SU}]$ (position A'), the value of the option will be increasing and reaching the highest value in the middle, as it will be less likely for the underlying asset to hit any of the two barriers. As time increases, say to time $t = 0.2$, the value of the option when the asset is closer to the barriers (position B) will be less than the corresponding value at time $t = 0$, as the asset is closer time-wise to the jump of the barriers. In the middle the value of the option will be higher from the previous time as time gets closer to expiry (position B'). When the jump occurs at time $t = 0.5$, we can see from the graph 6.9 that something funny is happening to the value of the option. Let us assume that the underlying is close to one of the two barriers (position C in figure 6.10) at time $t^* - \epsilon$. Since the asset has no time to manoeuvre in order to fit into the new barrier the value of the option will be cheaper than if it was situated lower. This is because the underlying is more likely to miss the shrunken area and therefore expire worthless.

In figure 6.11 we plot the values of the three barrier options (equations (6.35), (6.46), (6.60)) at present time.

Looking at the three graphs for the value of the Asian option before and after the jumps have occurred (figures 6.3, 6.6, 6.9) we can draw the following conclusions for the value of the option at time $t = 0$. The value of the three options depends on the size of the barriers. More specifically, the value of the simple barrier at $t = 0$, $[\bar{S}_L, \bar{S}_U]$, is cheaper than the value of the option when the barriers jump inward, $[\bar{S}_{SL}, \bar{S}_{SU}]$, at

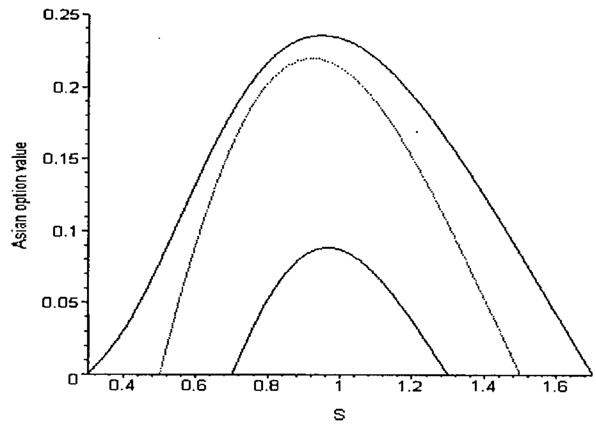

Fig. 6.11: Plot of the solutions $U(\bar{S},t)$ (dashed curve), $U_w(\bar{S},t)$ (lower solid curve), $U_s(\bar{S},t)$ (upper solid curve) at time $t=0$.

that time (figure 6.12). This is because the holder of the option enters the contract having a better position since the two barriers are far away, $[\bar{S}_{SL}, \bar{S}_{SU}]$. Furthermore, the value of the barrier which jumps outwards will be much cheaper than the value of the original barrier, $[\bar{S}_L, \bar{S}_U]$, at that time ($t=0$), as the underlying has more chances of hitting either barrier $[\bar{S}_{WL}, \bar{S}_{WU}]$.

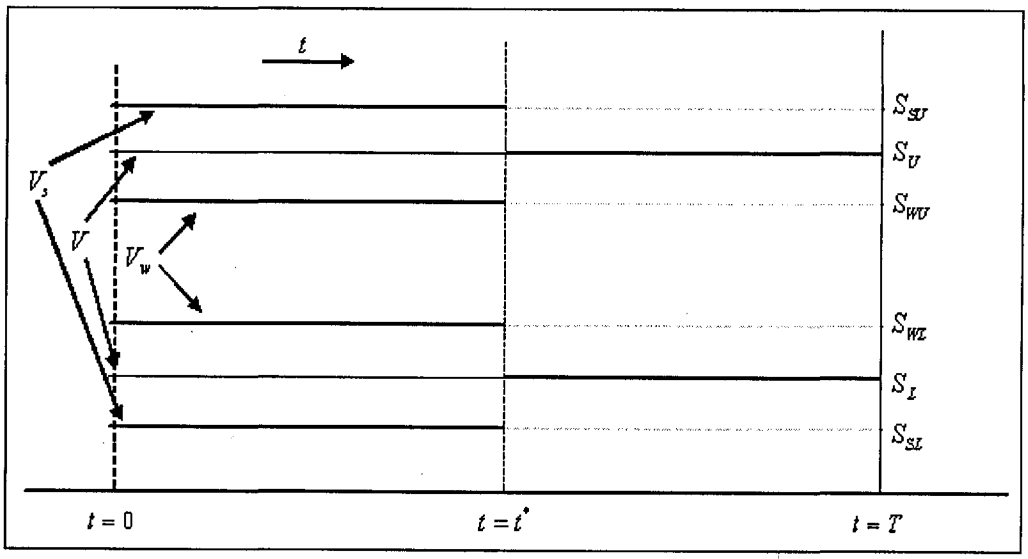

Fig. 6.12: Sketch of the three types of barriers.

6.2 Black-Scholes equation with a single step double barrier

In this section we examine how the problem with the two double barriers (sections 6, 6.1.1 and 6.1.2) which jump inwards and outwards affect the case of a European option. Note that for the numerical interpretation we have used the same values as done in previous sections. Also note that the subscripts used are for notational purposes and not to denote derivatives.

We consider a European option given by the Black-Scholes equation which can be written in the form of the heat equation,

$$\frac{\partial W}{\partial t_1} = \frac{\partial^2 W}{\partial x^2}, \tag{6.61}$$

using the transformations mentioned in chapter 4. The boundary conditions are

$$W = 0, \quad \text{at} \quad x = x_L \quad \text{and} \quad x = x_U. \tag{6.62}$$

The payoff we take is as before

$$U(S, t = T) = \begin{cases} \frac{S_U - S}{S_U - S_L} & , \frac{S_U + S_L}{2} < S < S_U \\ \frac{S - S_L}{S_U - S_L} & , S_L < S < \frac{S_U + S_L}{2} \end{cases}, \tag{6.63}$$

in terms of S, and

$$W(x, t_1 = 0) = \exp\left(-\frac{1}{2} + \frac{r}{\sigma^2}\right) \begin{cases} \frac{S_U - \exp(x)}{S_U - S_L} & , \ln\left(\frac{S_U + S_L}{2}\right) < x < \ln(S_U) \\ \frac{\exp(x) - S_L}{S_U - S_L} & , \ln(S_L) < x < \ln\left(\frac{S_U + S_L}{2}\right) \end{cases}, \tag{6.64}$$

in terms of the x variable.

The solution to the problem in Fourier series is of the form

$$W(r, t_1) = \sum_{n=1}^{\infty} A_n \exp\left(-\frac{n^2\pi^2}{(x_U - x_L)^2} t_1\right) \sin\left(\frac{n\pi}{x_U - x_L}(x - x_L)\right), \tag{6.65}$$

satisfying the boundary conditions (6.62), and where the coefficients are given by the formula

$$A_n = \frac{\int_{x_L}^{x_U} W(x, 0) \sin\left(\frac{n\pi(x - x_L)}{x_U - x_L}\right) dx}{\int_{x_L}^{x_U} \left[\sin\left(\frac{n\pi(x - x_L)}{x_U - x_L}\right)\right]^2 dx}. \tag{6.66}$$

The full solution is given by the equation

$$V_{BS}(S,t) = \exp\left(-r(T-t)\right)\exp\left[\left(-\frac{\sigma^2}{8}-\frac{r^2}{2\sigma^2}+\frac{r}{2}\right)(T-t)\right]S^{\frac{1}{2}-\frac{r}{\sigma^2}} \quad (6.67)$$
$$\sum_{n=1}^{\infty} A_n \exp\left(-\frac{n^2\pi^2}{(x_U-x_L)^2}\frac{\sigma^2}{2}(T-t)\right)\sin\left[\frac{n\pi}{x_U-x_L}\ln\left(\frac{S}{S_L}\right)\right].$$

The above solution can be viewed against S for different times t in figure 6.13. The two barriers take values $S_L = 0.5$ and $S_U = 1.5$. The expiry date has been taken to be $T = 1$ year.

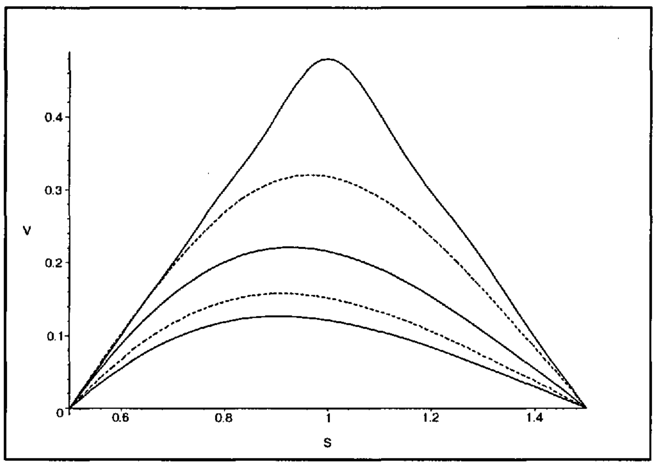

Fig. 6.13: Plot of the series solution $V(S,t)$ against S for $n = 10$ at $t = 1$ (top solid line), $t = 0.8$ (top dotted line), $t = 0.5$ (middle solid line), at $t = 0.2$ (bottom dotted line) and $t = 0$ (bottom solid line).

Comparing the European with the Asian option at time $t = 0$ we observe that the Black-Scholes will act as a bound on the Asian option, figure 6.14. This is because of the extra $\exp(\alpha I)$ term the Asian option has, leaving the European option to vary between values $\exp(\alpha I_{\min})V_{BS}$ and $\exp(\alpha I_{\max})V_{BS}$.

Suppose that at time $t_1 = t_1^* = 0.5$ the two barriers jump outwards from values S_{WL} and S_{WU} to values S_L and S_U, respectively ($S_{WL} < S_L < S_U < S_{WU}$), figure 6.4. For the new barrier the Fourier series is given by

$$W_w(r,t_1) = \sum_{n=1}^{\infty} E_n \exp\left(-\frac{n^2\pi^2}{(x_{WU}-x_{WL})^2}(t_1-t_1^*)\right)\sin\left(\frac{n\pi}{x_{WU}-x_{WL}}(x-x_{WL})\right), \quad (6.68)$$

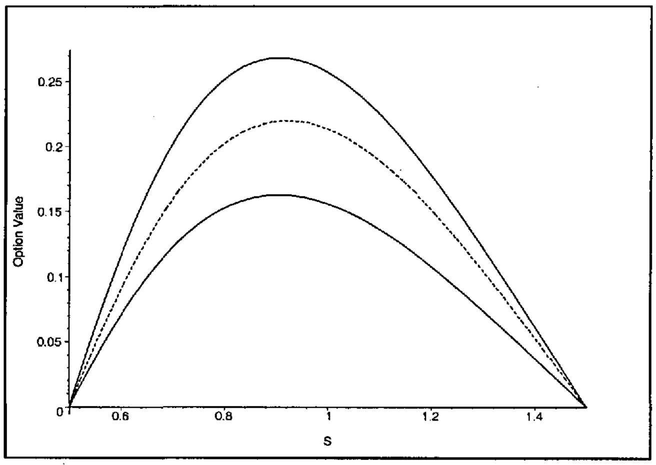

Fig. 6.14: Plot of the Asian (dotted line) and the minimum and maximum values (lower and upper solid lines respectively) of the Black-Scholes equation against S at time $t = 0$.

where the payoff at time $t_1 = t_1^*$ is

$$W(r, t_1^*) = \sum_{n=1}^{\infty} A_n \exp\left(-\frac{n^2\pi^2}{(x_U - x_L)^2} t_1^*\right) \sin\left(\frac{n\pi}{x_U - x_L}(x - x_L)\right), \tag{6.69}$$

valid for $x_L < x < x_U$ and the coefficients E_n are given by

$$E_n = \frac{\int_{x_L}^{x_U} W(x, t_1^*) \sin\left(\frac{n\pi(x - x_{WL})}{x_{WU} - x_{WL}}\right) dx}{\int_{x_{WL}}^{x_{WU}} \left[\sin\left(\frac{n\pi(x - x_{WL})}{x_{WU} - x_{WL}}\right)\right]^2 dx}. \tag{6.70}$$

The full solution for the barrier jumping outwards is given by

$$\begin{aligned} V_w(S, t) &= \exp(-r(T - t)) \exp\left[\left(-\frac{\sigma^2}{8} - \frac{r^2}{2\sigma^2} + \frac{r}{2}\right)(T - t)\right] S^{\frac{1}{2} - \frac{r}{\sigma^2}} \qquad (6.71) \\ & \sum_{n=1}^{\infty} E_n \exp\left(-\frac{n^2\pi^2}{(x_{WU} - x_{WL})^2} \frac{\sigma^2}{2}(t^* - t)\right) \sin\left[\frac{n\pi}{x_{WU} - x_{WL}} \ln\left(\frac{S}{S_{WL}}\right)\right], \end{aligned}$$

and the graphs for the value V_w against S for different times are shown in figure 6.15. The corresponding graphs for the European option acting as a bound for the Asian option for the case where the two barriers jump outwards at $t = 0$ are shown in figure 6.16.

Similarly, suppose that at time $t_1 = t_1^*$ the two barriers jump inwards (in real time) from values S_{SL} and S_{SU} to values S_L and S_U, respectively ($S_{SL} < S_L < S_U < S_{SU}$),

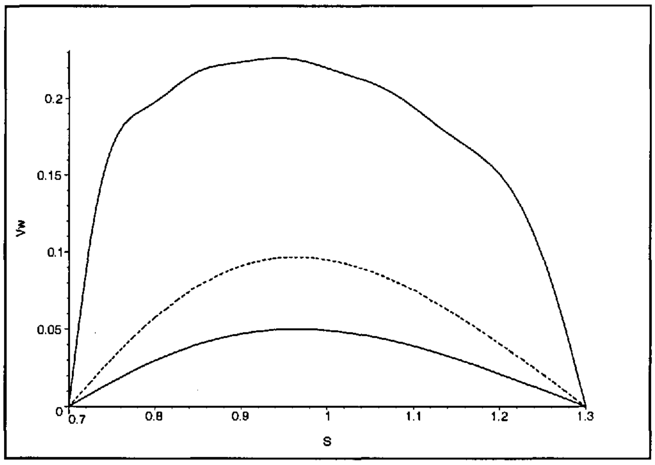

Fig. 6.15: Plot of the series solution $V_w(S,t)$ against S for $n = 10$ at $t = 0.5$ (top solid line), at $t = 0.2$ (dotted line) and at $t = 0$ (bottom solid line).

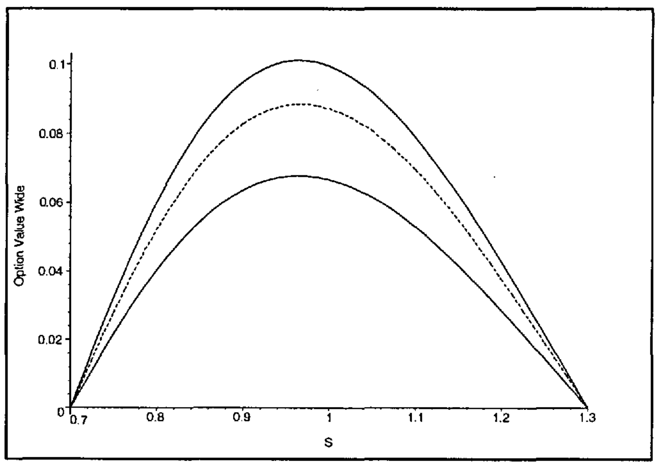

Fig. 6.16: Case where the barriers jump outwards: plots of the Asian option (dotted line), minimum and maximum values (lower and upper solid lines respectively) of the Black-Scholes equation against S at time $t = 0$.

figure 6.7. For the new barrier the Fourier series is given by

$$W_s(r,t_1) = \sum_{n=1}^{\infty} C_n \exp\left(-\frac{n^2\pi^2}{(x_{SU}-x_{SL})^2}(t_1 - t_1^*)\right)\sin\left(\frac{n\pi}{x_{SU}-x_{SL}}(x - x_{SL})\right), \tag{6.72}$$

where the payoff at time $t_1 = t_1^*$ is given by (6.69) valid for $x_L < x < x_U$ and the

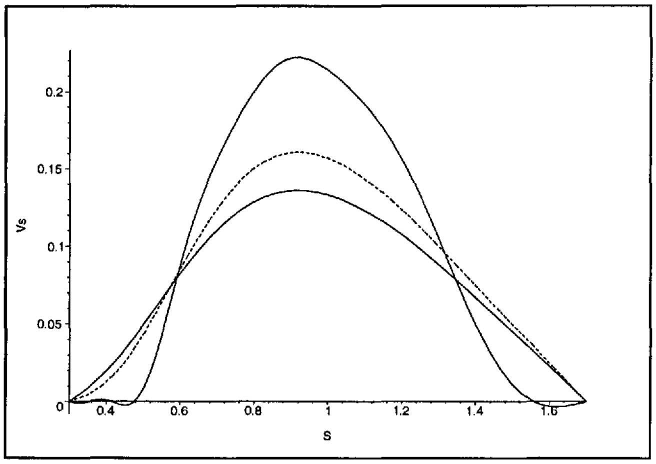

Fig. 6.17: Plot of the series solution $V_s(S,t)$ against S for $n = 10$ at $t = 0.5$ (top solid line), at $t = 0.2$ (dotted line) and at $t = 0$ (bottom solid line).

coefficients C_n are given by

$$C_n = \frac{\int_{x_L}^{x_U} W(x,t_1^*) \sin\left(\frac{n\pi(x-x_{SL})}{x_{SU}-x_{SL}}\right) dx}{\int_{x_{SL}}^{x_{SU}} \left[\sin\left(\frac{n\pi(x-x_{SL})}{x_{SU}-x_{SL}}\right)\right]^2 dx}. \tag{6.73}$$

The full solution for the barrier jumping inwards is given by

$$\begin{aligned} V_s(S,t) &= \exp\left(-r(T-t)\right) \exp\left[\left(-\frac{\sigma^2}{8} - \frac{r^2}{2\sigma^2} + \frac{r}{2}\right)(T-t)\right] S^{\frac{1}{2}-\frac{r}{\sigma^2}} \\ & \sum_{n=1}^{\infty} C_n \exp\left(-\frac{n^2\pi^2}{(x_{SU}-x_{SL})^2}\frac{\sigma^2}{2}(t^*-t)\right) \sin\left[\frac{n\pi}{x_{SU}-x_{SL}} \ln\left(\frac{S}{S_{SL}}\right)\right], \end{aligned} \tag{6.74}$$

and the graphs for the value against S for different times are shown in figure 6.17. The corresponding graphs for the European option acting as a bound for the Asian option for the case where the two barriers jump inwards at $t = 0$ are shown in figure 6.18.

As mentioned at the end of section 6.1.2 a similar observation can be commented for the value of the European option at time $t = 0$. In figure 6.19 we plot the three values V, V_s and V_w against S at time $t = 0$. From figure 6.12 we can observe that at time $t = 0$ the value of the shrinking barrier V_s is more expensive than the original barrier V. Also the value of the expanding barrier V_w is much cheaper than the original barrier V at time $t = 0$.

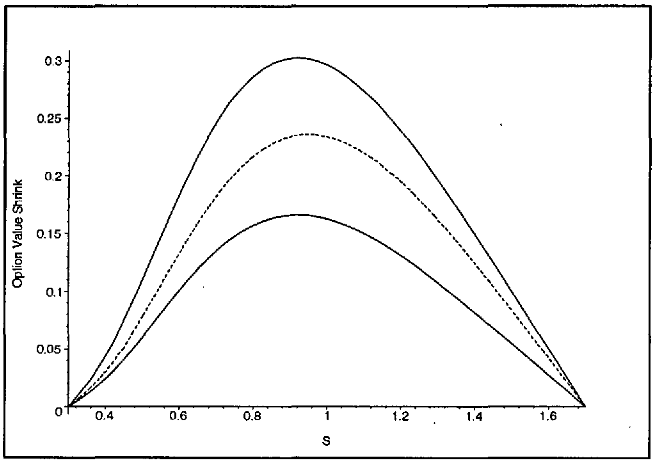

Fig. 6.18: Case where the barriers jump inwards: plots of the Asian option (dotted line), minimum and maximum values (lower and upper solid lines respectively) of the Black-Scholes equation against S at time $t = 0$.

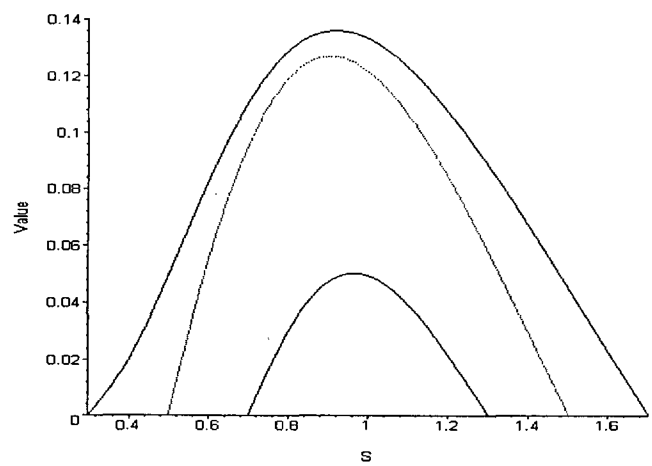

Fig. 6.19: Plots of the value of the options at $t = 0$ when the barriers remain constant, $V(S,t)$ (dotted line), jump inwards $V_S(S,t)$ (top solid line) and outwards $V_W(S,t)$ (bottom solid line) in real time t (figure 6.12 for the shapes of the barriers).

6.3 Example of an Asian option

For the valuation of a double barrier Asian option we have given (at the beginning of chapter 6) a Fourier series solution for a general payoff of the form

$$V(S, I, T) = \exp(\alpha I)\, F(S), \tag{6.75}$$

where $F(S)$ is a function of S which we took to have a triangle shaped payoff at $t = T$ between the two knock-out barriers $S = S_L$ and $S = S_U$. In the previous sections S,

S_L, S_U and I were all scaled on S_0 ($\bar{S} = S/S_0$, $\bar{S}_L = S_L/S_0$, $\bar{S}_U = S_U/S_0$, $\bar{I} = I/S_0$, $\alpha_1 = \alpha/S_0$). The solution was found to be of the form

$$V(\bar{S},\bar{I},t) = \exp(\alpha_1 \bar{I}) \exp\left(-\left(\frac{r^2}{2\sigma^2} + \frac{\sigma^2}{8} + \frac{r}{2}\right)(T-t)\right)\bar{S}^{\left(\frac{1}{2}-\frac{r}{\sigma^2}\right)} \tag{6.76}$$
$$\sum_{n=1}^{\infty} A_n \exp\left(-\frac{\sigma^2}{2}k_n^2(T-t)\right)\left(\frac{2\alpha_1}{\sigma^2}\bar{S} + k_n^2\right)^{-1/4} \sin\left(\int_1^{\bar{S}/\bar{S}_L}\sqrt{\frac{2\alpha_1}{\sigma^2}\bar{S}_L\,\tau + k_n^2}\,\frac{d\tau}{\tau}\right),$$

where

$$A_n = \frac{\int_{\bar{S}_L}^{\bar{S}_U} F(\bar{S})X_n(\bar{S})\,d\bar{S}}{\int_{\bar{S}_L}^{\bar{S}_U}\left[X_n(\bar{S})\right]^2\,d\bar{S}}, \tag{6.77}$$

k_n is given from

$$\int_1^{\bar{S}_U/\bar{S}_L}\sqrt{\alpha_3\bar{S}_L\tau + k_n^2}\,d\tau = n\pi\,. \tag{6.78}$$

and

$$X_n(\bar{S}) = \left(\frac{2\alpha_1}{\sigma^2}\bar{S} + k_n^2\right)^{-1/4}\sin\left(\int_1^{\bar{S}/\bar{S}_L}\sqrt{\frac{2\alpha_1}{\sigma^2}\bar{S}_L\tau + k_n^2}\,\frac{d\tau}{\tau}\right). \tag{6.79}$$

For ordinary European Asian options the payoff for a call option is given by the equation

$$V(S,I,T) = \max\left(\frac{I}{T} - E,\,0\right).$$

For European Asians with barriers we construct a payoff of the form

$$V(S,I,T) = \exp(\alpha I)\left(\frac{I}{T} - S_L\right), \tag{6.80}$$

which is similar to the ordinary value of an Asian call option. In general the strike price, E, is situated between the two barriers at maturity $t = T$. For convenience we have taken the value of the strike E to be equal to the value of the lower barrier S_L. In this example we do not scale S, S_L, S_U and I on S_0. At any time t the average $I(t)$ will take values between $S_L\,t < I(t) < S_U\,t$, where $S_L\,t$ and $S_U\,t$ are the minimum and maximum values the average takes at the two barriers and $I(t) = \int_0^t S_u\,du$. This can be seen in diagram 6.20.

Compared to the normal Asian options, in the case of Asian barrier options the buyer of the option will pay less for the contract he is entering as it will have more chances

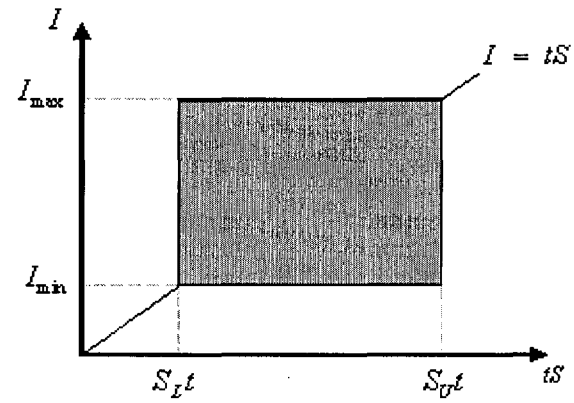

Fig. 6.20: Area (shaded) where the average takes value at time t.

of hitting the lower barrier and expiring worthless.

The payoff (6.80) corresponds to two options. One where the function $F(S)$ is equal to $F(S) = S_L = E$ and the payoff for that option will be

$$V^{(1)}(S, I, T) = S_L \exp(\alpha I), \tag{6.81}$$

and another option where the function $F(S)$ is equal to $F(S) = \frac{1}{T}$ with payoff

$$V(S, I, T) = \frac{1}{T} \exp(\alpha I). \tag{6.82}$$

We use the latter option to differentiate the payoff with respect to α to get an option with payoff

$$V^{(2)}(S, I, T) = \frac{\partial V}{\partial \alpha} = \frac{I}{T} \exp(\alpha I). \tag{6.83}$$

We deal with $V^{(1)}(S, I, T)$ and $V^{(2)}(S, I, T)$ as two different problems. Combining the two payoffs results to the original payoff,

$$V^{(2)}(S, I, T) - V^{(1)}(S, I, T) = \exp(\alpha I) \left(\frac{I}{T} - S_L \right). \tag{6.84}$$

The solution to the first option with payoff (6.81) in terms of the variables $\bar{S} = S/S_0$,

$\bar{I}$ and t will be given by equation (6.76) with coefficient $\bar{S}_L$,

$$V^{(1)}(\bar{S},\bar{I},t) = \bar{S}_L \exp(\alpha_1 \bar{I}) \exp\left(-\left(\frac{r^2}{2\sigma^2}+\frac{\sigma^2}{8}+\frac{r}{2}\right)(T-t)\right)\bar{S}^{\left(\frac{1}{2}-\frac{r}{\sigma^2}\right)} \tag{6.85}$$
$$\sum_{n=1}^{\infty} A_n \exp\left(-\frac{\sigma^2}{2}k_n^2(T-t)\right)\left(\frac{2\alpha_1}{\sigma^2}\bar{S}+k_n^2\right)^{-1/4} \sin\left(\int_1^{\bar{S}/\bar{S}_L}\sqrt{\frac{2\alpha_1}{\sigma^2}\bar{S}_L v + k_n^2}\,\frac{dv}{v}\right),$$

and with coefficients given from equation (6.90), with $F(\bar{S}) = 1$.
For the second option with payoff (6.82) the solution is similarly given by

$$V^{(2)}(\bar{S},\bar{I},t) = \frac{1}{T}\exp(\alpha_1 \bar{I}) \exp\left(-\left(\frac{r^2}{2\sigma^2}+\frac{\sigma^2}{8}+\frac{r}{2}\right)(T-t)\right)\bar{S}^{\left(\frac{1}{2}-\frac{r}{\sigma^2}\right)} \tag{6.86}$$
$$\sum_{n=1}^{\infty} A_n \exp\left(-\frac{\sigma^2}{2}k_n^2(T-t)\right)\left(\frac{2\alpha_1}{\sigma^2}\bar{S}+k_n^2\right)^{-1/4} \sin\left(\int_1^{\bar{S}/\bar{S}_L}\sqrt{\frac{2\alpha_1}{\sigma^2}\bar{S}_L v + k_n^2}\,\frac{dv}{v}\right),$$

with the same coefficients, A_n, as in the first option. Differentiating the latter we get a complicated expression

$$V^{(2)}(\bar{S},\bar{I},t) = \frac{dV}{d\alpha_1} = \exp(\alpha_1 \bar{I}) \exp\left(-\left(\frac{r^2}{2\sigma^2}+\frac{\sigma^2}{8}+\frac{r}{2}\right)(T-t)\right)\bar{S}^{\left(\frac{1}{2}-\frac{r}{\sigma^2}\right)}$$
$$\left[\frac{\bar{I}}{T}\sum_{n=1}^{\infty} A_n \exp\left(-\frac{\sigma^2}{2}k_n^2(T-t)\right)\left(\frac{2\alpha_1}{\sigma^2}\bar{S}+k_n^2\right)^{-1/4} \sin\left(\int_1^{\bar{S}/\bar{S}_L}\sqrt{\frac{2\alpha_1}{\sigma^2}\bar{S}_L v + k_n^2}\,\frac{dv}{v}\right)\right.$$
$$+\ \frac{1}{T}\sum_{n=1}^{\infty} \frac{dA_n}{d\alpha_1} \exp\left(-\frac{\sigma^2}{2}k_n^2(T-t)\right)\left(\frac{2\alpha_1}{\sigma^2}\bar{S}+k_n^2\right)^{-1/4} \sin\left(\int_1^{\bar{S}/\bar{S}_L}\sqrt{\frac{2\alpha_1}{\sigma^2}\bar{S}_L v + k_n^2}\,\frac{dv}{v}\right)$$
$$-\ \frac{\sigma^2(T-t)}{T}\sum_{n=1}^{\infty} A_n k_n \frac{dk_n}{d\alpha_1} \exp\left(-\frac{\sigma^2}{2}k_n^2(T-t)\right)\left(\frac{2\alpha_1}{\sigma^2}\bar{S}+k_n^2\right)^{-1/4}$$
$$\sin\left(\int_1^{\bar{S}/\bar{S}_L}\sqrt{\frac{2\alpha_1}{\sigma^2}\bar{S}_L v + k_n^2}\,\frac{dv}{v}\right) - \frac{1}{2T}\sum_{n=1}^{\infty} A_n \exp\left(-\frac{\sigma^2}{2}k_n^2(T-t)\right)\left(\frac{\bar{S}}{\sigma^2}+k_n\frac{dk_n}{d\alpha_1}\right)$$
$$\left(\frac{2\alpha_1}{\sigma^2}\bar{S}+k_n^2\right)^{-5/4} \sin\left(\int_1^{\bar{S}/\bar{S}_L}\sqrt{\frac{2\alpha_1}{\sigma^2}\bar{S}_L v + k_n^2}\,\frac{dv}{v}\right)$$
$$+\ \frac{1}{T}\sum_{n=1}^{\infty} A_n \exp\left(-\frac{\sigma^2}{2}k_n^2(T-t)\right)\left(\frac{2\alpha_1}{\sigma^2}\bar{S}+k_n^2\right)^{-1/4}$$
$$\left.\cos\left(\int_1^{\bar{S}/\bar{S}_L}\sqrt{\frac{2\alpha_1}{\sigma^2}\bar{S}_L v + k_n^2}\,\frac{dv}{v}\right)\int_1^{\bar{S}/\bar{S}_L}\left(\frac{\bar{S}_L}{\sigma^2}v + k_n\frac{dk_n}{d\alpha_1}\right)\left(\frac{2\alpha_1}{\sigma^2}\bar{S}_L v + k_n^2\right)^{-1/2}\frac{dv}{v}\right],$$

where $\frac{dA_n}{d\alpha_1}$ and $\frac{dk_n}{d\alpha_1}$ are given further down.
The latter expression is proportional to the average I giving a term $\bar{I}\exp(\alpha_1\bar{I})g(\bar{S})$ plus another term of the form $\exp(\alpha_1\bar{I})g(\bar{S})$. The solution to the problem of double

barrier Asian options corresponds to the payoff (6.80).
Therefore the value of the double barrier Asian option will be equal to

$$V(\bar{S},\bar{I},t) = V^{(2)}(\bar{S},\bar{I},t) - V^{(1)}(\bar{S},\bar{I},t)\,. \tag{6.87}$$

For the numerical realization of the problem we take the two barriers to have values $\bar{S}_L = 0.5$, $\bar{S}_U = 1.0$, the volatility $\sigma = 0.5$, the interest rate $r = 0.05$, $\alpha_1 = 0.5$ and maturity $T = 1$ year. The eigenvalues k_n are given from the formula

$$\int_1^{\bar{S}_U/\bar{S}_L} \sqrt{\frac{2\alpha_1}{\sigma^2}\,\bar{S}_L\, v + k_n^2}\,\frac{dv}{v} = n\pi\,. \tag{6.88}$$

The derivative $\frac{dk_n}{d\alpha_1}$ can be found for each k_n by differentiating the integral equation for the eigenvalues with respect to α_1,

$$\begin{aligned}\int_1^{\bar{S}_U/\bar{S}_L} \left(\frac{\bar{S}_L}{\sigma^2}\,v + k_n\frac{dk_n}{d\alpha_1}\right)\left(\frac{2\alpha_1}{\sigma^2}\,\bar{S}_L\, v + k_n^2\right)^{-1/2}\frac{dv}{v} &= 0 \\ \Rightarrow k_n\frac{dk_n}{d\alpha_1} = -\frac{\bar{S}_L}{\sigma^2}\frac{\int_1^{\bar{S}_U/\bar{S}_L}\left(\frac{2\alpha_1}{\sigma^2}\,\bar{S}_L\, v + k_n^2\right)^{-1/2} dv}{\int_1^{\bar{S}_U/\bar{S}_L}\left(\frac{2\alpha_1}{\sigma^2}\,\bar{S}_L\, v + k_n^2\right)^{-1/2}\frac{dv}{v}} &\,.\end{aligned} \tag{6.89}$$

For the values mentioned earlier the first 20 eigenvalues are given in table 6.6. For the

n	k_n	n	k_n
1	3.845453412	11	49.79805474
2	8.740846165	12	54.33524518
3	13.38325832	13	58.87169153
4	17.96960881	14	63.40755349
5	22.53413133	15	67.94294808
6	27.08785801	16	72.47796305
7	31.63544978	17	77.01266545
8	36.17921962	18	81.54710742
9	40.72044675	19	86.08133013
10	45.25989645	20	90.61536648

Tab. 6.6: Values of k_n for $n = 1..20$

coefficients of the series we use the formula

$$A_n = \frac{\int_{\bar{S}_L}^{\bar{S}_U} F(\bar{S})X_n(\bar{S})\,d\bar{S}}{\int_{\bar{S}_L}^{\bar{S}_U}\left[X_n(\bar{S})\right]^2 d\bar{S}}\,, \tag{6.90}$$

where $F(\bar{S}) = 1$ and $X_n(\bar{S})$ is equal to

$$X_n(\bar{S}) = \left(\frac{2\alpha_1}{\sigma^2}\bar{S} + k_n^2\right)^{-1/4} \sin\left(\int_1^{\bar{S}/\bar{S}_L} \sqrt{\frac{2\alpha_1}{\sigma^2}\,\bar{S}_L\, v + k_n^2}\,\frac{dv}{v}\right). \tag{6.91}$$

Differentiating A_n with respect to α_1 will give the derivative of the coefficients with respect to α_1

$$\frac{dA_n}{d\alpha_1} = \frac{\left(\int_{\bar{S}_L}^{\bar{S}_U}[X_n(\bar{S})]^2\,d\bar{S}\right)\int_{\bar{S}_L}^{\bar{S}_U}\frac{d}{d\alpha_1}[X_n(\bar{S})]\,d\bar{S} - \left(\int_{\bar{S}_L}^{\bar{S}_U}X_n(\bar{S})\,d\bar{S}\right)\int_{\bar{S}_L}^{\bar{S}_U}\frac{d}{d\alpha_1}[X_n(\bar{S})]^2\,d\bar{S}}{\left(\int_{\bar{S}_L}^{\bar{S}_U}[X_n(\bar{S})]^2\,d\bar{S}\right)^2}. \tag{6.92}$$

The corresponding coefficients for the first 20 terms of the series (6.87) are given in table table 6.7. To improve the convergence of the Fourier series, more terms can be taken into account.

n	A_n	n	A_n
1	2.161168076	11	0.7120644585
2	−0.7547279312	12	−0.3403120040
3	1.339498104	13	0.6552985006
4	−0.5749187982	14	−0.3153381276
5	1.049984857	15	0.6102224608
6	−0.4766964493	16	−0.2951364526
7	0.8905781868	17	0.5733129549
8	−0.4151258163	18	−0.2783639376
9	0.7866061028	19	0.5423720423
10	−0.3722648084	20	−0.2641516643

Tab. 6.7: Values of A_n for $n = 1..20$

We can find bounds to the Asian option. This can be done by taking three options with payoffs $V_1 = \frac{\partial}{\partial\alpha_1}(\frac{1}{T}\exp(\alpha_1\bar{I})) = \exp(\alpha_1\bar{I})\,\frac{\bar{I}}{T}$, $V_2 = \exp(\alpha_1\bar{I})\,\bar{S}_L$ and $V_3 = \exp(\alpha_1\bar{I})\,\bar{S}_U$. T is the expiry date of 1 year and α_1 is a constant parameter taken to have value equal to 0.5. We expect the value of the option V_1 to lie between the values of the options V_2 and V_3. The graphs that correspond to these options at $t = 0$ are given in figure 6.21.

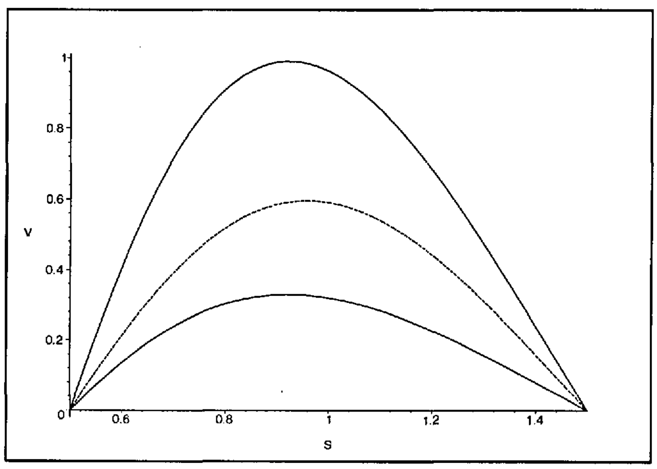

Fig. 6.21: Bounds on the Asian option at time $t = 0$ (V_1, dash curve, V_2 bottom solid curve, V_3 top solid curve).

7. TRANSACTION COSTS

An important effect is the presence of transaction costs when valuing options. Leland [47] considered a model that allows transactions only at discrete times. By adopting a δ-hedging argument, he derived an option price that converges to a Black-Scholes price as transaction costs become arbitrarily small with an adjusted volatility

$$\breve{\sigma}^2 = \sigma^2 \pm 2k\sigma\sqrt{\frac{2}{\pi\delta t}},$$

where σ is the original volatility, k is the proportional transaction cost and δt is the transaction frequency. The plus or minus sign depends in whether the option is held short or long respectively. Barles and Soner [4] applied a utility function approach as well as an asymptotic analysis of a nonlinear PDE under the effect of transaction costs. The presence of transaction costs effect the volatility and therefore the governing equation. Gondzio, Kouwenberg and Vorst [31] propose a stochastic optimization model for hedging contingent claims and take into account the effects of stochastic volatility and transaction costs. Morozovsky [56] constructed a modified Black-Scholes equation with transaction costs and gave a solution to the equation for the case where the option was close to expiry and the case where the transaction costs were small. Dewynne, Whalley and Wilmott [19] constructed a PDE model for valuing exotic options with the possibility of a similarity solution. They used explicit finite differences to overcome the strong nonlinearity caused by the transaction costs term.

7.1 Asian options

We consider the effect of transaction costs for the case of strongly path-dependent options and more precisely for Asian options. We take the case where a similarity variable used by Geman and Yor [29] is introduced in the problem. With transaction costs the partial differential equation valid for any path-dependent option is of the form

$$\frac{\partial V}{\partial t} + S\frac{\partial V}{\partial I} + \frac{1}{2}\sigma^2 S^2 \frac{\partial^2 V}{\partial S^2} - k_1\sigma S^2 \left|\frac{\partial^2 V}{\partial S^2}\right| + rS\frac{\partial V}{\partial S} - rV = 0\,, \tag{7.1}$$

where I is the running average and $k_1 = k\sqrt{\frac{2}{\pi\,\delta t}}$.
We set $V(S,I,t) = \exp\left[-r(T-t)\right] V_1(S,I,t)$ to get an extra rV_1 term in the latter PDE,

$$\frac{\partial V_2}{\partial t} + S\frac{\partial V_2}{\partial I} + \frac{1}{2}\sigma^2 S^2 \frac{\partial^2 V_2}{\partial S^2} - k_1\sigma S^2 \left|\frac{\partial^2 V_2}{\partial S^2}\right| + rS\frac{\partial V_2}{\partial S} + rV_2 = 0\,. \tag{7.2}$$

We then change the variable by introducing the similarity variable

$$U = \frac{1}{S}(K_1 - I)\,, \quad \text{where} \quad K_1 = KT\,, \tag{7.3}$$

K being the strike price and T the maturity date.
Hence equation (7.2) becomes

$$\frac{\partial W}{\partial t_1} = \frac{1}{2}\sigma^2 U^2 \frac{\partial^2 W}{\partial U^2} - (1 + rU)\frac{\partial W}{\partial U} - k_1\sigma\left|U^2\frac{\partial^2 W}{\partial U^2}\right| + rW\,, \tag{7.4}$$

where $V_2 = \frac{S}{T}\,W(U,t)$, $t_1 = T - t$ and with payoff for a fixed-strike Asian call option

$$W(U,0) = \max(-U,0)\,. \tag{7.5}$$

We examine the sign the Greek gamma ($\Gamma = \frac{\partial^2 W}{\partial U^2}$) takes by returning to the PDE (7.4) without the effect of transaction costs and see whether we can draw any conclusion for the sign of the modulus. We have the equation

$$\frac{\partial W}{\partial t_1} = \frac{1}{2}\sigma^2 U^2 \frac{\partial^2 W}{\partial U^2} - (1 + rU)\frac{\partial W}{\partial U} + rW\,.$$

Differentiating the above equation with respect to U gives

$$\frac{\partial \Delta}{\partial t_1} = \frac{1}{2}\sigma^2 U^2 \frac{\partial^2 \Delta}{\partial U^2} + [(\sigma^2 - r)U - 1]\frac{\partial \Delta}{\partial U}\,. \tag{7.6}$$

When $t_1 = 0$,

$$\Delta = \frac{\partial W}{\partial U} = \begin{cases} -1 & , \text{for } U < 0 \\ 0 & , \text{for } U > 0 \end{cases}\,.$$

We differentiate again to get a partial differential equation for Γ,

$$\frac{\partial \Gamma}{\partial t_1} = \frac{1}{2}\sigma^2 U^2 \frac{\partial^2 \Gamma}{\partial U^2} + [(2\sigma^2 - r)U - 1]\frac{\partial \Gamma}{\partial U} + (\sigma^2 - r)\Gamma\,, \tag{7.7}$$

and at time $t_1 = 0$, $\Gamma = \frac{\partial^2 W}{\partial U^2} = 0$ everywhere apart from the point $U = 0$ where Γ is positive but undefined.
We set $\Gamma = \exp\left((\sigma^2 - r)t_1\right)\Gamma_1$ and (7.7) takes the form

$$\frac{\partial \Gamma_1}{\partial t_1} = \frac{1}{2}\sigma^2 U^2 \frac{\partial^2 \Gamma_1}{\partial U^2} + [(2\sigma^2 - r)U - 1]\frac{\partial \Gamma_1}{\partial U}\,.$$

At this stage we still cannot determine the sign of Γ so we multiply the equation by a function of μ which we will find later,

$$\begin{aligned}\mu\frac{\partial \Gamma_1}{\partial t_1} &= \frac{1}{2}\sigma^2 U^2 \mu\frac{\partial^2 \Gamma_1}{\partial U^2} + [(2\sigma^2 - r)U - 1]\mu\frac{\partial \Gamma_1}{\partial U} \\ &= \frac{\partial}{\partial U}\left[\frac{1}{2}\sigma^2 U^2 \mu \frac{\partial \Gamma_1}{\partial U}\right].\end{aligned}$$

Provided

$$\sigma^2 U \mu + \frac{1}{2}\sigma^2 U^2 \frac{\partial \mu}{\partial U} = \mu[(2\sigma^2 - r)U - 1]\,,$$

to hold, which gives

$$\mu = A\,|U|^{\frac{2(\sigma^2 - r)}{\sigma^2}} \exp\left(\frac{2}{\sigma^2 U}\right). \tag{7.8}$$

Substituting into the equation we have

$$|U|^{\frac{2(\sigma^2 - r)}{\sigma^2}} \exp\left(\frac{2}{\sigma^2 U}\right)\frac{\partial \Gamma_1}{\partial t_1} = \frac{\partial}{\partial U}\left[\frac{1}{2}\sigma^2 |U|^{\frac{2(2\sigma^2 - r)}{\sigma^2}} \exp\left(\frac{2}{\sigma^2 U}\right)\frac{\partial \Gamma_1}{\partial U}\right]. \tag{7.9}$$

The above equation is a non-linear diffusion equation with positive coefficients. Therefore as a consequence of (7.9) the gamma for the call option, $\Gamma = \frac{\partial^2 W}{\partial U^2}$, will always be positive. So we can proceed with the valuation of the Asian option with the effect of transaction costs, by removing the modulus sign. Hence equation (7.4) becomes

$$\frac{\partial W}{\partial t_1} = \left(\frac{1}{2}\sigma^2 - k_1\sigma\right)U^2\frac{\partial^2 W}{\partial U^2} - (1 + rU)\frac{\partial W}{\partial U} + rW\,, \tag{7.10}$$

with payoff for a fixed-strike Asian call option

$$W(U, 0) = \max(-U, 0)\,, \tag{7.11}$$

and

$$W(U, 0) = \max(U, 0)\,, \tag{7.12}$$

for a fixed-strike Asian put option. For the case of the similarity variable $R = \frac{I}{S}$ the governing PDE with transaction costs is of the form

$$\frac{\partial H}{\partial t} + \frac{1}{2}\sigma^2 R^2 \frac{\partial^2 H}{\partial R^2} + (1 - rR)\frac{\partial H}{\partial R} - k_1 \sigma \left| R^2 \frac{\partial^2 H}{\partial R^2} \right| + rH = 0\,, \tag{7.13}$$

with payoff for a floating-strike Asian call option

$$H(R,T) = \max\left(1 - \frac{R}{T}, 0\right)\,. \tag{7.14}$$

Applying the above analysis for this problem leads to the diffusion equation

$$|R|^{\frac{2(\sigma^2 - r)}{\sigma^2}} \exp\left(-\frac{2}{\sigma^2 R}\right)\frac{\partial \Gamma_1}{\partial t_1} = \frac{\partial}{\partial R}\left[\frac{1}{2}\sigma^2 |R|^{\frac{2(2\sigma^2 - r)}{\sigma^2}} \exp\left(-\frac{2}{\sigma^2 R}\right)\frac{\partial \Gamma_1}{\partial R}\right]\,. \tag{7.15}$$

The delta of the payoff behaves like

$$\Delta = \frac{\partial H}{\partial R} = \begin{cases} -\frac{1}{T} & , \text{for } R < T \\ 0 & , \text{for } R > T \end{cases}\,,$$

and the gamma of the payoff is zero everywhere apart from the point $R = T$ when it is infinite.

Following the above procedure one can determine the sign of the modulus of the equation for options where the gamma of the payoff is single signed. For the case where the sign of the gamma changes this method cannot be efficient and we are led to solving the problem numerically, see next chapter.

8. NUMERICAL APPROACH

There has been a wide range of literature devoted to path-dependent options and more specifically to Asian options. Unfortunately, no explicit pricing formulae are available for pricing them. This is because the distribution of the geometric average of a set of log-normal distributions is not explicit. This factor has led several authors to approach the problem of valuing Asian options using different methodologies. The most popular approach is numerical. A variety of numerical techniques have been developed to analyze this kind of path-dependent option. Some numerical implementation has been done using a mixed implicit/explicit discretization and Monte Carlo simulation.

A very common numerical method used for pricing options based on the average of the underlying asset is Monte-Carlo simulation. One of the first well-known studies in that area is by Kemna and Vorst [43] who use Monte Carlo simulation to determine the price of an average value-option expressed as a PDE. They show that an out-of-the-money[1] standard option can be expected to be significantly more expensive than an average value option and they find an analytical value for a geometric average option. Monte Carlo simulation was also used by Ritchken, Sankarasubramanian and Vijh [59] to price a number of path-dependent contracts, average and lookback[2] option values, and Rogers and Shi [62] provided numerical results for the PDE with very good accuracy.

Another way to approach this kind of problem numerically is by using finite difference methods. Benhamou and Duguet [7] derive a PDE for the Asian option which they solve quite efficiently with the standard Crank-Nicholson method. Zvan, Forsyth and Vetzal [77] explore the pricing of Asian options numerically by solving a one-dimensional similarity variable PDE and a two-dimensional PDE using finite differences. The two-dimensional PDE that rises for the case of the Asian option can be reduced to a one-dimensional one by introducing an appropriate similarity variable, Ingersoll [41], Wilmott, Dewynne and Howison [73], Rogers and Shi [62]. This can happen only when the payoff is of a particular form and is consistent with the simi-

[1] An option is said to be out-of-the-money when either in the case of a call option the asset price is less than the strike price, or in the case of a put option the asset price is greater than the strike price (Hull [39]).

[2] Lookback options have a payoff that depends on the realized maximum or minimum of the underlying asset over some period prior to expiry.

larity variable itself. However these kind of PDEs can apply only to European-style options and it is difficult to numerically solve them as the diffusion term is very small compared to the values taken on the finite difference grid. Alziary, Décamps and Koehl [2] derived a one-state variable PDE for pricing a European type Asian option (for both fixed and floating-strike) and solved it numerically by applying a modified explicit method (similar to the one used by Hull and White [40]). Fusai, Sanfelici and Tagliani [26] commented on the different numerical schemes used in solving PDEs in finance, mainly focusing on the finite difference and finite element approach. Linetsky [50] provided numerical examples using a series and an integral representation to compute continuously sampled arithmetic Asian options using the Sturm-Liouville problem. Fouque and Han [22] solved with finite differences two one-dimensional partial differential equations using the asymptotic framework for pricing Asian options with stochastic volatility. As the biggest disadvantage of the explicit method is the lack of convergence, Hull and White [40] provided a systematic procedure for implementing a modified version of the method in such a way that convergence is guaranteed when Δt tends to zero.
The finite differences numerical method was used by Meyer [55] who solved the problem for the fixed-strike Asian call. Zhang [75] developed a fast and accurate method of pricing and hedging European average rate Asian options with continuous sampling by constructing a PDE using a similarity variable equivalent to that of Rogers and Shi [62] and solved it numerically using the Crank-Nicolson scheme. Later on Zhang [76] used the perturbation method to write the solution of the governing PDE in a series form and observed numerically that the series solution converges very quickly giving a good approximate value that is more accurate than any other approximate method.

Another method mentioned in earlier sections is the numerical inversion of the Laplace transform. Craddock, Heath and Platen [15] priced Asian options by using various numerical methods to invert the Laplace transform of Geman and Yor [29] after expressing it as a series of the Gamma function. Abate and Whitt [1] suggested numerical methods (Euler and Post-Widder) of inverting the Laplace transform of the probability distribution.

8.1 Explicit finite difference method

We solve the partial differential equations using finite difference methods. More specifically we use the fully explicit method which means that V_i^{n+1} for each i can be calculated explicitly from the quantities that are already known. We use this method as it is easy to implement, since only values at time level n have to be stored to find values at time level $n+1$.

Denote x to be the spatial variable and t the time variable. We choose equally spaced points along both the $x-$ and $t-$ axes.

$$
\begin{aligned}
x_i &= x_0 + i\Delta x\,, \qquad i = 0, 1, \cdots, M \\
t_n &= t_0 + n\Delta t\,, \qquad n = 0, 1, \cdots, N\,.
\end{aligned} \tag{8.1}
$$

Let V_i^n denote $V(x_i, t_n)$. We choose to express the time derivative in a forward differencing form

$$
\left.\frac{\partial V}{\partial t}\right|_{i,n} = \frac{V_i^{n+1} - V_i^n}{\Delta t} + O(\Delta t)\,. \tag{8.2}
$$

This has the advantage that one is able to calculate quantities at the time-step $n+1$ in terms of quantities known in time-step n. For the spatial derivative we use the central differences using the quantities known at time-step n

$$
\left.\frac{\partial V}{\partial x}\right|_{i,n} = \frac{V_{i+1}^n - V_{i-1}^n}{2\Delta x} + O(\Delta x^2)\,, \tag{8.3}
$$

and in a similar way the second order spatial derivative

$$
\left.\frac{\partial^2 V}{\partial x^2}\right|_{i,n} = \frac{V_{i-1}^n - 2V_i^n + V_{i+1}^n}{(\Delta x)^2} + O(\Delta x^2)\,. \tag{8.4}
$$

For the first order spatial derivative a second-order formula can be introduced (Wilmott, Dewynne and Howison [73], Seydel [65]) to avoid spatial oscillations caused when using (8.3),

$$
\left.\frac{\partial V}{\partial x}\right|_{i,n} = \frac{-3V_i^n + 4V_{i+1}^n - V_{i+2}^n}{2\Delta x} + O(\Delta x^2)\,. \tag{8.5}
$$

Before applying the above finite difference formulae in the PDE, the time needs to be changed to $t_1 = T - t$, so that the calculations are done forward in time t_1.
The general algorithm for solving a PDE is of the form

$$
V_i^{n+1} = A_i V_{i-1}^n + A_i V_i^n + C_i V_{i+1}^n\,, \tag{8.6}
$$

with the central difference formula used for the first spatial derivative, where A_i, B_i, C_i are the coefficients which differ depending on the PDE solved each time.
In general this algorithm is easy to derive, takes little storage and executes quickly. This method is easy and simple to implement as the PDE can be solved by the use of the initial condition only without the use of any boundary conditions. Unfortunately

the explicit method contrary to the implicit method is not stable for all step sizes. For this reason we need to make sure that stability restrictions hold. This can easily be done by applying the von Neumann stability analysis to find the condition that can guarantee stability. The von Neumann stability analysis is local in the sense that the coefficients of the difference equation vary so little so that they can be considered to be constant in space and time. In that case the independent solutions of the difference equation will have the form

$$V_i^n = \lambda^n \exp\left(jk\, i\Delta x\right), \tag{8.7}$$

where k is the real spatial wave number taking any value, $\lambda = \lambda(k)$ is a complex number that depends on k and $j^2 = -1$ is the complex identity. If $|\lambda| > 1$ then the system is unstable, whereas for $|\lambda| \leq 1$ stability is ensured. For the classic case of the heat equation

$$\frac{\partial V_i^n}{\partial t_1} = \frac{\partial^2 V_i^n}{\partial x^2}, \tag{8.8}$$

the stability is

$$\frac{\Delta t_1}{(\Delta x)^2} \leq \frac{1}{2}.$$

8.2 Similarity variable R

We seek a numerical solution for the case of the Asian option with the similarity variable R. Recall the PDE of such an option from section 2.2, (2.5), given by the equation

$$\frac{\partial H}{\partial t} + \frac{1}{2}\sigma^2 R^2 \frac{\partial^2 H}{\partial R^2} + (1 - rR)\frac{\partial H}{\partial R} = 0, \tag{8.9}$$

with payoff

$$H(R,T) = \left(1 - \frac{R}{T}, 0\right), \quad \text{for} \quad 0 \leq t \leq T, \quad R \geq 0, \tag{8.10}$$

where

$$R = \frac{I}{S} \quad \text{and} \quad I = \int_0^t S(u)du.$$

To examine the boundary conditions for the similarity variable problem we need to look closely at the behavior of the similarity variable as well as at the resulting PDE, (8.9). As t increases to $t + dt$, the change in the variable R is given by the SDE

$$dR = [1 + R(\sigma^2 - \mu)]\, dt - R\,\sigma\, dX\,. \tag{8.11}$$

The random walk for R hence does not depend on S explicitly. Boundary conditions for the problem need to be posed. From the definition of the similarity variable $R = \frac{I}{S}$ as $R \longrightarrow \infty$, S needs to be zero. In this case the option is not exercised and hence the value will be zero. The boundary condition for large R is therefore

$$H(R,t) = 0\,, \quad \text{as} \quad R \longrightarrow \infty\,. \tag{8.12}$$

For the boundary condition at $R = 0$ we need to examine the behavior of the differential equation. For $R = 0$, from the stochastic differential equation of R, $dR = dt > 0$, implying that R does not remain zero as time moves, but grows taking only positive values ($R > 0$). In equation (8.9), the terms which involve R can be ignored as R is zero, leaving the first order derivatives with respect to R and t to contribute for the value of the option. Hence the behavior of the option at $R = 0$ is given by the hyperbolic PDE

$$\frac{\partial H}{\partial t} + \frac{\partial H}{\partial R} = 0\,, \quad \text{on} \quad R = 0\,. \tag{8.13}$$

Changing the time variable to $t_1 = T - t$ the boundary value problem will take the form

$$\frac{\partial H}{\partial t_1} = \frac{1}{2}\sigma^2 R^2 \frac{\partial^2 H}{\partial R^2} + (1 - rR)\frac{\partial H}{\partial R}\,, \tag{8.14}$$

with payoff

$$H(R,0) = \left(1 - \frac{R}{T}, 0\right)\,, \quad \text{for} \quad t_1 \geq 0\,, \quad R \geq 0\,, \tag{8.15}$$

and boundary conditions

$$\text{at} \quad R = 0\,, \quad \frac{\partial H}{\partial t_1} = \frac{\partial H}{\partial R} \tag{8.16}$$

$$\text{at} \quad R \longrightarrow \infty\,, \quad H(R,t_1) \sim 0\,, \tag{8.17}$$

To numerically solve the above boundary value problem, we use the finite difference formulas for the derivative terms of the option value $H_{i,n}(R,t)$ as mentioned in section 8.1. Substituting the central differences (8.2), (8.3) and (8.4) in equation (8.14) will take the form

$$H_i^{n+1} = A_i^n H_{i-1}^n + B_i^n H_i^n + C_i^n H_{i+1}^n \,, \tag{8.18}$$

where

$$\begin{aligned} A_i^n &= \frac{1}{2}\sigma^2 R^2 \frac{\Delta t_1}{(\Delta R)^2} - (1 - r\,R)\frac{\Delta t_1}{2\,\Delta R}\,, \\ B_i^n &= 1 - \sigma^2 R^2 \frac{\Delta t_1}{(\Delta R)^2}\,, \\ C_i^n &= \frac{1}{2}\sigma^2 R^2 \frac{\Delta t_1}{(\Delta R)^2} + (1 - r\,R)\frac{\Delta t_1}{2\,\Delta R}\,. \end{aligned}$$

For the numerical implementation of the boundary condition at $R = 0$, (8.16), we use the second-order finite-difference formula (8.5) and takes the form

$$H_i^{n+1} = \left(1 - \frac{3}{2}\frac{\Delta t_1}{\Delta R}\right) H_i^n + 2\frac{\Delta t_1}{\Delta R} H_{i+1}^n - \frac{1}{2}\frac{\Delta t_1}{\Delta R} H_{i+2}^n \,, \tag{8.19}$$

with $i = 0$.

To find the condition that will ensure the explicit method to be stable we apply the von Neumann stability analysis by substituting equation (8.7) into the finite difference scheme we formulated for the PDE, (8.18). For stability we require $|\xi| \le 1 \Rightarrow -1 \le \xi \le 1$. The condition for stability will be analogous to the condition used for the heat equation (used locally for the term $\frac{\sigma^2}{2} R^2$). Hence the condition we need to ensure stability for the problem will be proportional to the range of R and is given by

$$(\Delta t_1) R^2 \le \frac{(\Delta R)^2}{\sigma^2}\,. \tag{8.20}$$

To solve the problem we use Visual C++ 6.0 on a Intel Pentium IV. The values we set for this problem are similar to the ones used by Wilmott, Dewynne and Howison [73], $\sigma = 0.8$, $r = 0.05$, with $T = 1$. We take R to take values $0 < R < 2$. We take the asset-step ΔR to be $\Delta R = 0.08$ and the time-step Δt_1 to be $\Delta t_1 = 0.0003$. The payoff of the option at $t_1 = 0$ ($t = T = 1$) is shown in figure 8.1 The value of the option against the similarity variable R at some time before expiry, $t = 0.75$, is shown in figure 8.2.

For the case of the floating-strike Asian put option the put-call parity can be used for convenience. This will be seen further on in section 8.7.1. To compute numerically the value of a floating-strike Asian put option the PDE is the same as (8.14) with

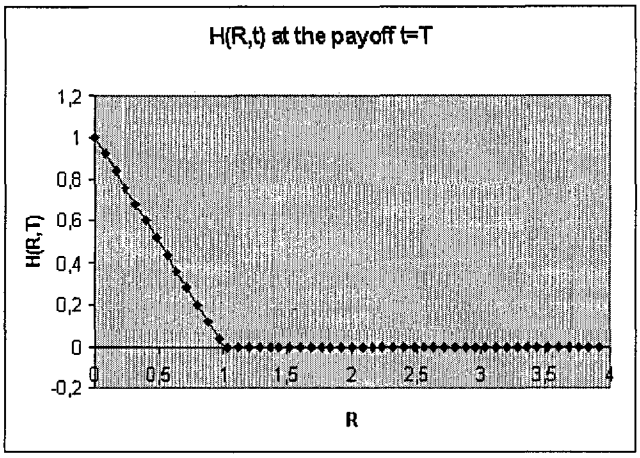

Fig. 8.1: Plot of the solution $H(R,t)$ for the floating-strike Asian call option at the payoff $t=T$.

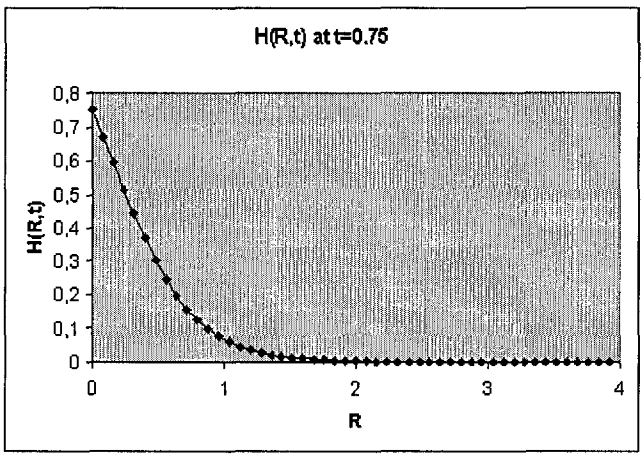

Fig. 8.2: Plot of the solution $H(R,t)$ for the floating-strike Asian call option for $t=0.75$.

payoff

$$H(R,0) = \max\left(\frac{R}{T} - 1,\, 0\right). \tag{8.21}$$

Apart from the boundary condition at $R=0$ a boundary condition for large positive R needs to be considered. For large R the value of the option grows like

$$H(R,t) = \frac{R}{T}\exp\left(-r(T-t)\right), \quad \text{as} \quad R \to \infty. \tag{8.22}$$

This can be observed from the put-call parity formula given in section 8.7.1. Plotting both options, call and put, for a floating-strike Asian options for $r = 0.05$, $\sigma = 0.8$

and $T = 1$, one can see how they evolve in time from maturity to some time $t < T$. In figure 8.3 is the plot of the call and put at maturity. The value of the put is zero for $R < T = 1$ and at $R = 1$ it grows according to the payoff in the form $\frac{R}{T} - 1$. The value of the call starts from one when $R = 0$ and decays to zero at $R = 1$ and remains zero for the rest of the life of the option, when $R > T = 1$.

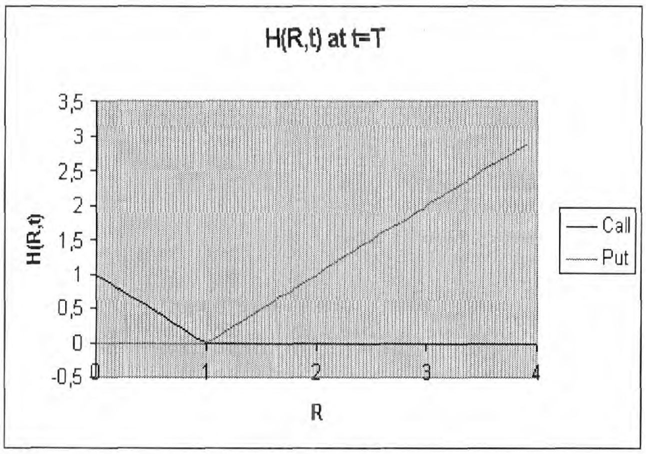

Fig. 8.3: Plot of the call and put value $H(R, t)$ for the floating-strike Asian option at maturity $t = T = 1$.

At some time before expiry, say at time $t = 0.75$, the curves for the call and put have changed slightly, figure 8.4. The value of the call drops, whereas the value of the put grows. At that time the two curves no longer meet at $R = 1$, but at $R = 0.75$. This is the point where both values are equal. This can be verified by using the put-call parity formula, which is given in section 8.7.1, namely

$$H_C(R,t) - H_P(R,t) = \frac{1}{rT}(\exp(-r(T-t)) - 1) - \frac{R}{T}\exp(-r(T-t)) + 1\,. \quad (8.23)$$

To see where the two curves meet, i.e. where $H_C - H_P = 0$, we write the put-call parity formula for small r;

$$H_C(R,t) - H_P(R,t) = 1 - \frac{T-t}{T} - \frac{R}{T} + \cdots\,, \quad \text{for } r \text{ small}\,. \quad (8.24)$$

Therefore at any time $T - t$ the point where the put and call values are equal is at $R = T - t$. This corresponds to the way the curves look on the graphs 8.4 and 8.5.

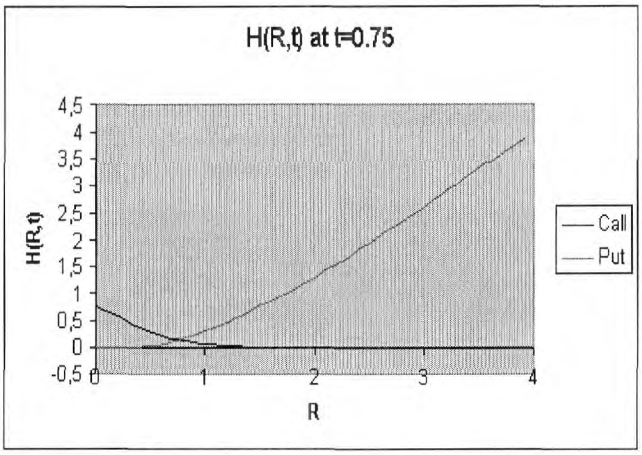

Fig. 8.4: Plot of the price, $H(R,t)$, of a call and put for the floating-strike Asian option at $t = 0.75$.

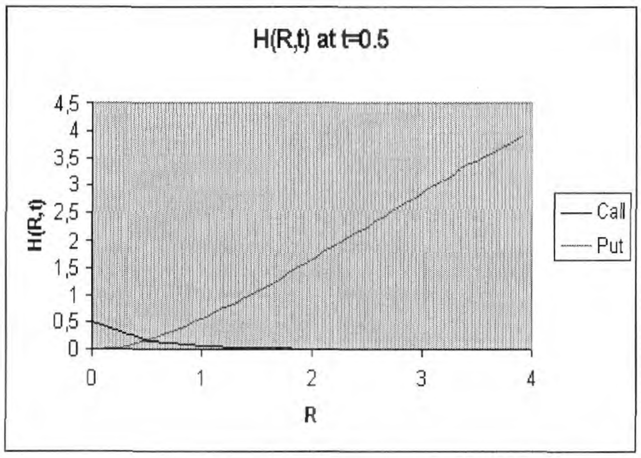

Fig. 8.5: Plot of the price, $H(R,t)$, of a call and put for the floating-strike Asian option at $t = 0.5$.

8.3 Similarity variable U

We value numerically the price of an Asian option using the similarity variable U. Recall the PDE from section 2.2, given by equation 2.10,

$$\frac{\partial W}{\partial t} + \frac{1}{2}\sigma^2 U^2 \frac{\partial^2 W}{\partial U^2} - (1 + r\,U)\frac{\partial W}{\partial U} = 0\,, \tag{8.25}$$

with payoff for a call option

$$W(U,T) = \max(-U, 0)\,, \quad \text{for} \quad 0 \le t \le T\,, \quad -\infty \le U \le \infty\,, \tag{8.26}$$

where

$$U = \frac{1}{S}(K_1 - I)\,, \quad K_1 = KT \quad \text{and} \quad I = \int_0^t S(u)du\,.$$

The payoff implies that for negative values of U the price of the option is equal to U, whereas for positive values of U the price of the option is zero. The option takes value $-U$ for $I > K_1$ and when $S = 0$, the option has no payoff since $I = 0$ at $t = 0$.
Write equation (8.25) as a forward equation in time $t_1 = T - t$,

$$\frac{\partial W}{\partial t_1} = \frac{1}{2}\sigma^2 U^2 \frac{\partial^2 W}{\partial U^2} - (1 + r\,U)\frac{\partial W}{\partial U}\,, \tag{8.27}$$

with payoff

$$W(U, 0) = \max(-U,\, 0)\,, \quad \text{for} \quad t_1 \geq 0\,, \quad -\infty \leq U \leq \infty\,. \tag{8.28}$$

Using central differences (equations (8.2)-(8.4)), equation (8.27) takes the form

$$W_i^{n+1} = A_i^n W_{i-1}^n + B_i^n W_i^n + C_i^n W_{i+1}^n\,, \tag{8.29}$$

where

$$\begin{aligned}
A_i^n &= \frac{1}{2}\sigma^2 U^2 \frac{\Delta t_1}{(\Delta U)^2} + (1 + r\,U)\frac{\Delta t_1}{2\,\Delta U}\,, \\
B_i^n &= 1 - \sigma^2 U^2 \frac{\Delta t_1}{(\Delta U)^2}\,, \\
C_i^n &= \frac{1}{2}\sigma^2 U^2 \frac{\Delta t_1}{(\Delta U)^2} - (1 + r\,U)\frac{\Delta t_1}{2\,\Delta U}\,.
\end{aligned}$$

The only boundary condition required for this problem is for large and negative values for U. This can be found by doing the following analysis. In equation (8.27) set $W(U, t_1) = \exp(-rt_1) W_1(U, t_1)$ to take the form

$$\frac{\partial W_1}{\partial t_1} = \frac{1}{2}\sigma^2 U^2 \frac{\partial^2 W_1}{\partial U^2} - (1 + r\,U)\frac{\partial W_1}{\partial U} + r\,W_1\,. \tag{8.30}$$

For the latter equation we seek a solution of the form $W_1 = -U\,f(t_1) + g(t_1)$ in relation to the payoff $\max(-U,\, 0)$. The PDE then takes the form of an ODE in time t_1,

$$-Uf' + g' = f + rg\,,$$

we want $f(t_1)$ to be constant since the option at large negative U behaves like $-U$. Hence $f(t_1) = f_0 =$ constant and assume also that the value of the constant is one so that it is consistent with the payoff. Therefore the ODE simplifies to one for g only with solution

$$g = \frac{1}{r}\left(\exp\left(rt_1\right) - 1\right), \quad \text{with} \quad g(0) = 0\,.$$

Hence for large negative U the boundary condition needed is

$$W_1(U, t_1) \sim -U + \frac{1}{r}\left(\exp\left(rt_1\right) - 1\right), \tag{8.31}$$

which gives $-U$ at $t_1 = 0$. In terms of the function $W(U, t_1)$ we have

$$W(U, t_1) \sim -U \exp\left(-rt_1\right) + \frac{1}{r}\left(1 - \exp\left(-rt_1\right)\right). \tag{8.32}$$

The stability condition will be the same used for the similarity variable R,

$$(\Delta t_1) U^2 \leq \frac{(\Delta U)^2}{\sigma^2}\,. \tag{8.33}$$

For the numerical interpretation we take the same numbers for σ, r, T, $\sigma = 0.8$, $r = 0.05$ and $T = 1$. We let U vary between $-10 < U < 10$. The payoff as well as the value of the option at time far away from expiry expiry, e.g. at $t = 0$, is shown in figure 8.6.

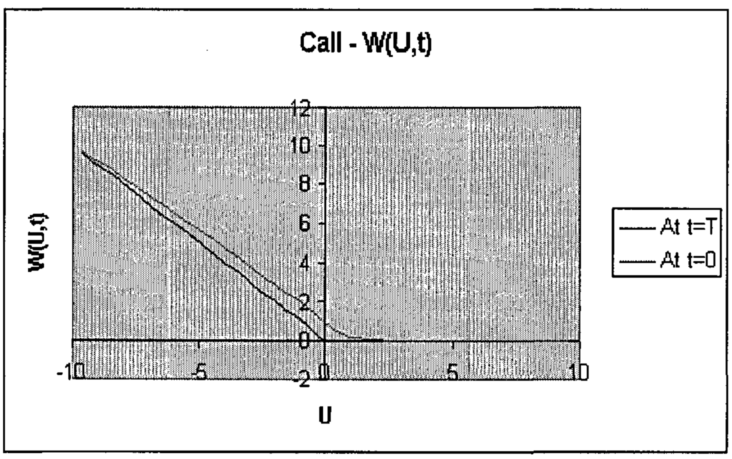

Fig. 8.6: Plot of the solution $W(U, t)$ for the fixed-strike Asian call option at the payoff $t = T$ and at $t = 0$.

For the case of a put option the payoff will be

$$W(U, 0) = \max(U,\, 0)\,, \quad \text{for} \quad t_1 \geq 0\,, \quad -\infty \leq U \leq \infty\,, \tag{8.34}$$

and by doing a similar analysis to the one done for the call option, the boundary condition for large positive U is given by the formula

$$W(U,t_1) \sim U \exp(-rt_1) + \frac{1}{r}(\exp(-rt_1) - 1) . \tag{8.35}$$

The value for a fixed-strike Asian put option at time $t = T$ and time $t = 0$ can be seen in figure 8.7.

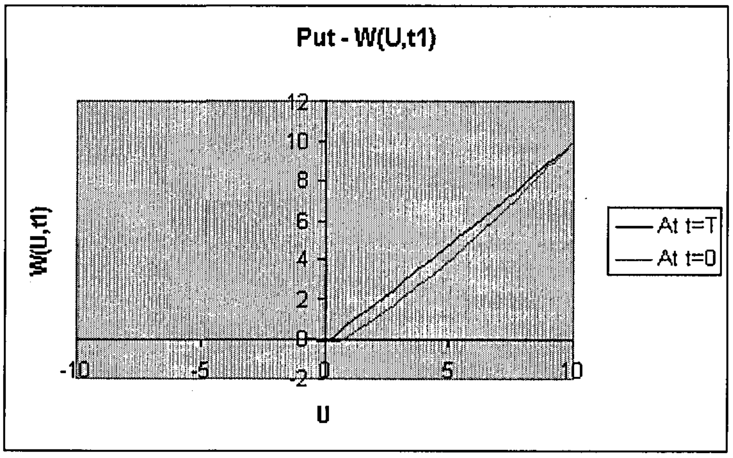

Fig. 8.7: Plot of the solution $W(U, t)$ for the fixed-strike Asian put option at time $t = T$ and $t = 0$.

8.4 Formulation by Geman and Yor

In this section we derive a PDE for Geman and Yor's problem, [29], and compare it with our version of the similarity variable U explored in the previous section. Geman and Yor valued fixed-strike Asian options expressing the price in terms of Laplace transform. The value of the Asian option under their notation can be summarised as follows

$$C_{t,T}(k) = \frac{\exp(-r(T-t))}{T-t_0} \frac{4S(t)}{\sigma^2} C^{(\nu)}(h,q) , \tag{8.36}$$

where

$$\nu = \frac{2\,r}{\sigma^2} - 1 ; \quad h = \frac{\sigma^2}{4}(T-t) ; \quad q = \frac{\sigma^2}{4\,S(t)} \left\{ k(T-t_0) - \int_{t_0}^{t} S(u)\,du \right\} , \tag{8.37}$$

and $C^{(\nu)}(h,q)$ is given by

$$\int_0^{\infty} C^{(\nu)}(h,q)\exp(-\lambda h)\,dh = \frac{\int_0^{1/2q}\exp(-x)x^{(\mu-\nu)/2-2}(1-2qx)^{(\mu+\nu)/2+1}}{\lambda(\lambda-2-2\nu)\Gamma((\mu-\nu)/2-1)}, \quad (8.38)$$

where $\mu=\sqrt{2\lambda+\nu^2}$, λ is the Laplace transform variable and Γ is the gamma function. We construct the corresponding PDE for the Geman and Yor problem by taking the PDE valid for any average value option

$$\frac{\partial V}{\partial t}+S\frac{\partial V}{\partial I}+rS\frac{\partial V}{\partial S}+\frac{1}{2}\sigma^2S^2\frac{\partial^2 V}{\partial S^2}-rV=0, \quad (8.39)$$

with payoff

$$V(S,I,T)=\max\left(\frac{I}{T}-K\,,0\right). \quad (8.40)$$

Looking at the form of the solution in equation (8.36) we use the transformation

$$V(S,I,t)=\exp(-r(T-t))V_1(S,I,t),$$

and the general PDE takes the form

$$\frac{\partial V_1}{\partial t}+S\frac{\partial V_1}{\partial I}+rS\frac{\partial V_1}{\partial S}+\frac{1}{2}\sigma^2S^2\frac{\partial^2 V_1}{\partial S^2}=0. \quad (8.41)$$

The payoff (8.40) can be written as

$$V(S,I,T)=\frac{S}{T}\max\left(\frac{I-KT}{S}\,,0\right)=\frac{4}{\sigma^2}\frac{S}{T}\max(-U,0),$$

where U is the similarity variable introduced by Geman and Yor and is equal to

$$U_{GY}=\frac{\sigma^2}{4}\frac{1}{ST}(K_1-I), \quad (8.42)$$

where $K_1=KT$, $I=\int_0^t S(u)\,du$ and $t_0=0$.
Since the payoff has the above form we can write the value of the option V_1 to be $V_1(S,I,t)=S\,V_2(S,I,t)$ and $V_2(S,I,t)=\frac{4}{\sigma^2 T}V_3(U_{GY},t)$. Then equation (8.41) takes the form

$$\frac{\partial V_3}{\partial t}+\frac{1}{2}\sigma^2U_{GY}^2\frac{\partial^2 V_3}{\partial U_{GY}^2}-(1+rU_{GY})\frac{\partial V_3}{\partial U_{GY}}+rV_3=0, \quad (8.43)$$

with payoff

$$V_3(U_{GY}, T) = \max(-U_{GY}\,, 0) \tag{8.44}$$

Hence

$$V(S, I, t) = \frac{\exp\left(-r(T-t)\right)}{T} \frac{4S}{\sigma^2} V_3(U_{GY}, t)\,. \tag{8.45}$$

Equation (8.43) is the same equation with (8.30) when $t_1 = T - t$.
Hence we can write the Geman and Yor problem in terms of our similarity variable problem as

$$V_{GY} = \frac{S}{T} \exp\left(-r(T-t)\right) \frac{4}{\sigma^2} W_1(U, t)\,, \tag{8.46}$$

where W_1 is the solution of the problem with the similarity variable $U = \frac{1}{S}(K_1 - I)$. Therefore the Geman and Yor solution is $\frac{4}{\sigma^2}$ times our solution $W_1(U,t)$, i.e.

$$V_3(U_{GY}, t) = \frac{4}{\sigma^2} W_1(U, t)\,. \tag{8.47}$$

If $\sigma^2 = 4$ then both solutions are equivalent.

8.5 Transaction Costs with the similarity variable R

For the numerical valuation of Asian options under the effect of the transaction costs we take as an example the case of the similarity variable R. As mentioned in section 7.1 the general PDE for any path-dependent option with the effect of transaction costs is given by

$$\frac{\partial V}{\partial t} + S\frac{\partial V}{\partial I} + \frac{1}{2}\sigma^2 S^2 \frac{\partial^2 V}{\partial S^2} - k_1 \sigma S^2 \left|\frac{\partial^2 V}{\partial S^2}\right| + rS\frac{\partial V}{\partial S} - rV = 0\,, \tag{8.48}$$

where I is the running average and $k_1 = k\sqrt{\frac{2}{\pi \delta t}}$. Setting $R = \frac{I}{S}$ and $V(S, I, t) = S\,H(R, t)$ the above PDE takes the form

$$\frac{\partial H}{\partial t} + \frac{1}{2}\sigma^2 R^2 \frac{\partial^2 H}{\partial R^2} - k_1 \sigma \left|R^2 \frac{\partial^2 H}{\partial R^2}\right| + (1 - rR)\frac{\partial H}{\partial R} = 0\,. \tag{8.49}$$

For the case of a floating-strike Asian call option with payoff

$$H(R, T) = \max\left(1 - \frac{R}{T}\right)\,, \quad \text{with} \quad R \geq 0\,, \tag{8.50}$$

the maximum value the payoff can take is one.

According to the analysis done in section 7.1 the sign of the transaction cost term will remain positive whether the option is a call or a put. This is because during the life of the option in neither case does the sign of the gamma, $\frac{\partial^2 H}{\partial R^2}$, change. Therefore we can safely remove the modulus and write equation (8.49) with a modified volatility. The PDE will take the form

$$\frac{\partial H}{\partial t} + \left(\frac{1}{2}\sigma^2 - k_1\sigma\right) R^2 \frac{\partial^2 H}{\partial R^2} + (1 - rR)\frac{\partial H}{\partial R} = 0 . \tag{8.51}$$

In figure 8.8 we plot the value of the option $H(R,t)$ given by (8.51) at time $t = 0.5$ for different volatilities. We take $r = 0.05$ and $k_1 = \sigma/4$. Under the effect of transaction costs the value of the option with a more volatile underlying asset is more costly than the one with a smaller volatility. Similarly for a put option the corresponding curves

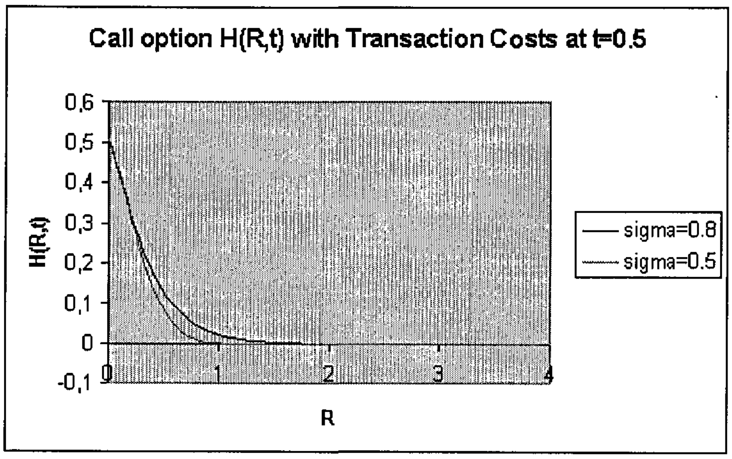

Fig. 8.8: Plot of the solution $H(R,t)$ for the floating-strike Asian call option with transaction costs at time $t = 0.5$.

for different values in the volatility can be seen in figure 8.9. From figures 8.8 and 8.9 we see that the value of the option in both cases is more expensive when the volatility is high and cheaper when the volatility drops.

8.6 Transaction Costs with the similarity variable U

As in the previous section we set $U = \frac{1}{S}(K_1 - I)$ and $V(S,I,t) = \frac{S}{T}W(U,t)$ in equation (8.48) to get

$$\frac{\partial W}{\partial t} + \frac{1}{2}\sigma^2 U^2 \frac{\partial^2 W}{\partial U^2} - k_1\sigma \left| U^2 \frac{\partial^2 W}{\partial U^2} \right| - (1 + rU)\frac{\partial W}{\partial U} = 0 , \tag{8.52}$$

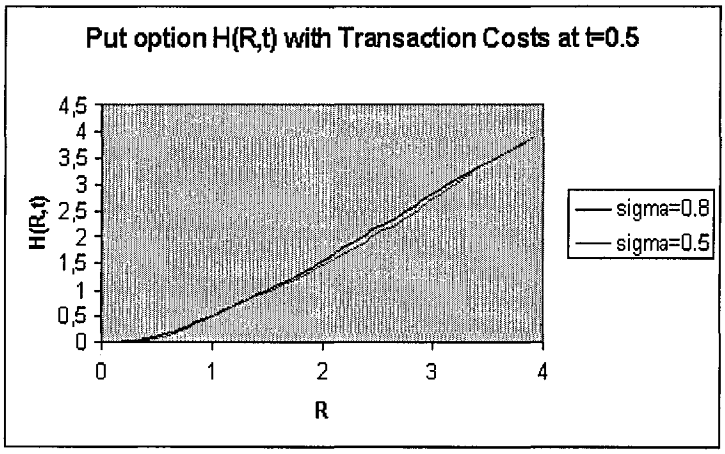

Fig. 8.9: Plot of the solution $H(R,t)$ for the floating-strike Asian put option with transaction costs at time $t = 0.5$.

which is the PDE for the option with the similarity variable U with the effect of transaction costs.

With the effect of the transaction costs the only aspect in which the PDE will be of any difference is the volatility. To go ahead and compute the above equation one needs to know the sign of the modulus of the gamma term. This depends on the payoff which in the case of a fixed-strike call option is

$$W(U,T) = \max(-U, 0)\,, \tag{8.53}$$

and for a fixed-strike put option is

$$W(U,T) = \max(U, 0)\,. \tag{8.54}$$

Following the analysis introduced in the previous chapter, 7.1, in both cases the sign of the modulus is positive. Therefore for the call option the PDE to be solved is

$$\frac{\partial W}{\partial t} + \left(\frac{1}{2}\sigma^2 - k_1\sigma\right) U^2 \frac{\partial^2 W}{\partial U^2} - (1 + rU)\frac{\partial W}{\partial U} = 0\,. \tag{8.55}$$

The numerical interpretation of this problem can be done in a similar way as done in the previous section for the similarity variable R.

8.7 Put-Call parity

In this section we will examine the put-call parity for a European style Asian option with fixed-strike and floating-strike payoff. The two different kinds of payoffs generate two different similarity variables seen in earlier chapters, namely R and U.

Assume in general we have a portfolio of one European average strike call held long and one put held short. The payoff of the portfolio at time $t = T$ is

$$\max(A - K, 0) - \max(K - A, 0)\,, \tag{8.56}$$

where A is the average.

8.7.1 Put-Call parity for similarity variable R

For an Asian option with a floating-strike payoff the payoff for the portfolio will equal to

$$V_C(S, I, T) - V_P(S, I, T) = S \max\left(1 - \frac{R}{T}, 0\right) - S \max\left(\frac{R}{T} - 1, 0\right). \tag{8.57}$$

Whether R takes greater or smaller values than T at maturity, the value of the option will then be

$$S - S\frac{R}{T}.$$

The value of the portfolio will consist of an asset and a financial product whose value at expiry is equal to

$$-S\frac{R}{T}. \tag{8.58}$$

In order to value such a product we seek a solution for the PDE (8.9) in the form

$$H(R, t) = a(t) + R\,b(t)\,, \tag{8.59}$$

where a and b take values at maturity $t = T$, $a(T) = 0$ and $b(T) = -\frac{1}{T}$, from the form equation (8.58) has. Substituting equation (8.59) into the PDE (8.9) we get the equation

$$a'(t) + b(t) + (b(t) - rb(t))R = 0\,,$$

which when taking the coefficients of order of R and using the boundary conditions for a and b at $t = T$ we get that

$$a(t) = \frac{1}{rT}(\exp(-r(T - t)) - 1)\,, \quad \text{and} \quad b(t) = -\frac{1}{T}\exp(-r(T - t))\,. \tag{8.60}$$

Therefore

$$H(R,t) = \frac{1}{rT}(\exp(-r(T-t)) - 1) - \frac{1}{T}\exp(-r(T-t))\,R + 1\,,$$

and hence the put-call parity relation will be given by the formula

$$\begin{aligned} V_C(S,I,t) - V_P(S,I,t) &= S - S\frac{R}{T} \qquad (8.61)\\ &= S - \frac{S}{rT}(1 - \exp(-r(T-t))) - \frac{I}{T}\exp(-r(T-t))\,, \end{aligned}$$

where V_C and V_P are the values of the Asian floating-strike option call and put respectively.

8.7.2 Put-Call parity for similarity variable U

Similarly for the case of an Asian option with a fixed-strike payoff the payoff for the portfolio will equal to

$$V_C(S,I,T) - V_P(S,I,T) = \frac{S}{T}\max(-U,\,0) - \frac{S}{T}\max(U,\,0)\,. \qquad (8.62)$$

Whether U takes positive or negative values at expiry $t = T$, the value of the option and hence of the portfolio will be identical to a financial product whose value at maturity is equal to

$$-\frac{S}{T}U\,. \qquad (8.63)$$

In order to value such a product we seek a solution for the PDE (8.25) in the form

$$H(U,t) = a(t) + U\,b(t)\,, \qquad (8.64)$$

where a and b take values at maturity $t = T$, $a(T) = 0$ and $b(T) = -1$, from the form equation (8.63) has. Substituting equation (8.64) into the PDE (8.25) we get the equation

$$a'(t) - b(t) + (b'(t) - rb(t))U = 0\,,$$

which when taking the coefficients of order of U and using the boundary conditions for a and b at $t = T$ we get that

$$a(t) = \frac{1}{r}(1 - \exp(-r(T-t)))\,, \quad \text{and} \quad b(t) = -\exp(-r(T-t))\,. \qquad (8.65)$$

Therefore

$$W(U,t) = \frac{1}{r}(1 - \exp(-r(T-t))) - \exp(-r(T-t))\, U\,,$$

and hence the put-call parity relation will be given by the formula

$$V_C(S,I,t) - V_P(S,I,t) = \frac{S}{rT}\,(1 - \exp(-r(T-t))) - \frac{K\,T - I}{T}\,\exp(-r(T-t))\,, \tag{8.66}$$

where V_C and V_P are the values of the Asian fixed-strike option call and put respectively.

9. CONCLUSIONS

Throughout this thesis the valuation of exotic options and in particular European and Asian barrier options were studied.

A moving barrier was introduced which grows symmetrically in time creating a wedge which acts as a double barrier to the underlying (chapter 3). Analytical solutions for the moving barrier were presented in N-dimensions with examples in two, three and five dimensions.

Attention was focused in chapter 4 on double knock-out step barrier options in the Black-Scholes framework for single-asset options and we showed that a wedge barrier acts as an upper bound to the step barrier. A Fourier series approach was used to value the option. We assumed there is another expanding barrier inside the wedge so that the step barrier moves between the two expanding barriers. The step barrier which intersects the two wedges (figure 4.1) was valued and numerical evidence was given for how the value of the option changes in time.

The problem with the double knock-out barrier was extended to the case where there are N underlying assets in the option, chapter 5. A Fourier series approach expressed the solution in terms of Bessel functions of first and second kind and we show that the WKB method can also be used to value the option accurately. As an example a basket option with three underlying assets is valued by transforming to the classic heat equation (section 5.2). For the case where there are five underlying assets the Fourier series approach was applied (section 5.5).

The effect of a double knock-out barrier for the three- and five-dimensional problem in which the upper barrier is far away from the lower barrier has also been studied. This problem structure is equivalent to the single knock-in barrier problem treated by Firth and Dewynne [21]. For the three-asset option the method of images is applied to deduce the solution given by Firth and Dewynne [21] and extended to the problem where the barrier jumps (section 5.3). In the five-asset option the Fourier series solution method is also applied to the problem of Firth and Dewynne [21] (section 5.5.1). An example of the latter problem is considered where an expanding barrier plays the role of the lower bound to the Fourier series step solution. Numerical evidence is given for that bound as well as for the value during the life of the option.

European style Asian options with double knock-out barriers using the PDE method

were valued in chapter 6. Using a general payoff of the form $V(S, I, T) = \exp(\alpha I(T))F(S)$, the WKB method was applied and numerical results presented. The accuracy of the WKB solution against the exact solution of the PDE, which can be written in terms of a conjugate pair of Bessel functions of first kind, appears in section A of the thesis. The problem was extended to the case where the two barriers jump simultaneously and symmetrically inwards and outwards, sections 6.1.1 and 6.1.2. It is noted that the value of the double barrier option at present time, $t = 0$, is cheaper than the value of the shrunken barrier at that time and more expensive than the value of the widened barrier. The results were compared with the corresponding European options and in particular the Black-Scholes equation. The solution of the Black-Scholes equation proved to be a good lower and upper bound for the value of the double barrier Asian option at present time.
A more realistic payoff for the Asian option of the form $V(S, I, T) = \exp(\alpha I)(\frac{I}{T} - S_L)$ was constructed, where S_L is the lower barrier and we found lower and upper bounds for the option.

The study of the pricing of Asian options with the effect of transaction costs is given in chapter 7. As shown in section 2.2, a one-dimensional similarity variable PDE for the case of a fixed- and floating-strike Asian option can be formed. Hence a method to determine the sign of the gamma term according to the nature of the problem was introduced. The method was shown to be useful in the case where the payoff was single valued. For the case where the sign of the gamma of the payoff changed, a numerical method was suggested to solve the problem, section 8.

The numerical method used to solve the PDEs was the finite difference method and particularly the explicit scheme. The framework for the numerical scheme utilised to value some of the problems mentioned throughout the thesis is provided in chapter 8. The PDEs used, value Asian options with the use of similarity variables with and without the effect of transaction costs. A put-call parity formula was derived and used to price the Asian options with a similarity variable.

BIBLIOGRAPHY

[1] Abate, J., Whitt, W. (1995): "Numerical inversion of Laplace transforms of probability distributions" *ORSA Journal on Computing*, **7**, pp. 36–43.

[2] Alziary, B., Décamps, J.P., Koehl, P.F. (1997): "A P.D.E. approach to Asian options: analytical and numerical evidence", *Journal of Banking and Finance*, **21**, pp.613–640.

[3] Atkinson, C., Fusai, G. (2005): "The discrete estrema of the Brownian Motion and pricing of lookback options" *Quantitative notebooks of the Department of Economic Sciences and Methods (SEMEQ)*, 86/04.

[4] Barles, G., Soner, H.M. (1998): "Option pricing wuth transaction costs and a nonlinear Black-Scholes equation", *Finance and Stochastics*, **2**, pp.369–397.

[5] Barucci, E., Polidoro, S., Vespri, V. (2001): "Some results on partial differential equations and Asian options", *Mathematical Models and Methods in Applied Sciences*, **11**, pp.475–497.

[6] Bender, C.M., Orszag, S.A. (1978): "Advanced mathematical methods for scientists and engineers", International Student Edition, McGraw-Hill,Inc.

[7] Benhamou, E., Duguet, A. (2003): "Small dimension PDE for discrete Asian options" *Journal of Economic Dynamics and Control*, **27**, pp. 2095–2114.

[8] Black, F., Scholes, M. (1973): "The pricing of options and corporate liabilities" *The Journal of Political Economy*, **81**, pp. 637–654.

[9] Broadie, M., Glasserman, P., Kou, S.G. (1999): "Connecting discrete and continuous path-dependent options", *Finance and Stochastics*, **3**, pp.55–82.

[10] Carr,P., Madan,D.B. (2004): "Option valuation using the fast Fourier transform", *Journal of Computational Finance*, **2**, pp. 61–73.

[11] Carr,P., Schröder,M. (2003): "Bessel processes, the integral of geometric Brownian motion, and Asian options", *to appear in Theory of Probability and its Applications.*

[12] Carr,P., Schröder,M. (2000): "On the valuation of arithmetic-average Asian options: the Geman-Yor Laplace transform revisited", *Mannheim and New York, December 2000.*

[13] Carverhill,A., Clewlow,L. (1990): "Flexible convolution", *RISK*, **3**, pp. 25–29.

[14] Costabile, M., (2002): "Extending the Cox-Ross-Rubinstein" *Proceedings of ALGORITMY 2002*, Conference on Scientific Computing, pp. 23–32.

[15] Craddock,M., Heath,D., Platen,E. (2000): "Numerical inversion of Laplace transforms: a survey of techniques with applications to derivative pricing", *Journal of Computational Finance*, **4**, pp. 57–81.

[16] Dahl, L.O., Benth, F.E. (2001): "Fast evaluation of the Asian basket option by singular value decomposition.", *Pure Mathematics*, preprint 8, ISBN 82-553-1286-2.

[17] Davydov, D., Linetsky, V. (2001/2002): "Structuring, pricing and hedging double-barrier step options", *Journal of Computational Finance*, **5**, pp. 55–87.

[18] Davydov, D., Linetsky, V. (2003): "Pricing Options on Scalar Diffusions: An Eigenfunction Expansion Approach" *Operations Research*, **51**, pp. 185–209.

[19] Dewynne, J.N., Whalley, A.E., Wilmott, P. (1994): "Path-dependent options and transaction costs" *Philosophical Transactions of The Royal Society London*, **A347**, pp. 317–529.

[20] Donati-Martin, C., Ghomrasni, R., Yor, M.(2001): "On certain Markov processes attached to exponential functionals of Brownian motion; application to Asian options" *Revista Mathe-matica Iberoamericana*, **17**, pp. 179–193.

[21] Firth, N.P., Dewynne, J.N. (2004): "High dimensional radial barrier options", *OCIAM*, Mathematical Institute, University of Oxford, Not published.

[22] Fouque, J.P., Han, C.H. (2003): "Pricing Asian options with stochastic volatility", *Quantitative Finance*, **3**, pp.353–362.

[23] Fu,M.C., Madan,D.B., Wang,T.(1998/99): "Pricing continuous Asian options: a comparison of Monte Carlo and Laplace transform inversion methods", *Journal of Computational Finance*, **2**, pp. 49–74.

[24] Fusai,G. (2004): "Pricing Asian options via Fourier and Laplace transforms", *Journal of Computational Finance*, **7**, pp. 1–20.

[25] Fusai,G., Tagliani,A. (2002): "An accurate valuation of Asian options using moments", *International Journal of Theoretical and Applied Finance*, **5**, pp. 147–169.

[26] Fusai, G., Sanfelici, S., Tagliani, A. (2002): "Practical problem in the numerical solution of PDE's in finance" *Rendiconti per gli Studi Economici Quantitativi dell'Università di Venezia*, pp. 105–132.

[27] Geman, H., Eydeland, A. (1995): "Domino effect: inverting the Laplace transform" *RISK*, **8**, pp. 65–67.

[28] Geman, H., Karoui, N., Rochet, J.C. (1995): "Changes of numeraire, changes of probability measure and option pricing" *Journal of Applied Probability*, **32**, pp. 443–458.

[29] Geman, H., Yor, M. (1993): "Bessel processes, Asian options, and perpetuities", *Mathematical Finance*, **3**, pp. 349–375.

[30] Geman, H., Yor, M. (1996): "Pricing and hedging double-barrier options: a probabilistic approach", *Mathematical Finance*, **6**, pp. 365–378.

[31] Gondzio, J., Kouwenberg, R., Vorst, T. (2003): "Hedging options under transaction costs and stochastic volatility", *Journal of Economic Dynamics and Control*, **27**, pp. 1045–1068.

[32] Haug, E.G. (1999): "Barrier put-call transformations", Working paper Tempus Financial Engineering. Presented at the Danske Bank Symposium on Securities with Embedded Options 1998.

[33] Henderson, V., Wojakowski, R. (2001): "On the equivalence of floating and fixed-strike Asian options" *Journal of Applied Probability*, **39**, pp. 391–394.

[34] Heritage, J.P. (2002): "Pricing moving average barrier options" *Journal of Computational Finance*, **5**, pp. 51–67.

[35] Hugger, J. (2003): "The boundary value formulation of the Asian call option" *Numerical Mathematics and Advanced Applications. ENUMATH 2001*, Springer-Velrag Italia, Milano, pp. 409–418.

[36] Hui,C.H. (1996): "One touch double barrier binary option values", *The Applied Financial Economics*, **6**, pp. 343–346.

[37] Hui,C.H. (1997): "Time-dependent barrier option values", *The Journal of Futures Markets*, **17**, pp. 667–688.

[38] Hui, C.H., Lo, C.F., Yuen, P.H. (2000): "Comment on 'Pricing Double barrier options using Laplace transforms' by Antoon Pelsser", *Finance and Stochastics*, **4**, pp. 105–107.

[39] Hull, J.C. (2000): "Options, futures, & other derivatives", Prentice-Hall, Inc.

[40] Hull, J., White, A. (1990): "Valuing derivative securities using the explicit difference method", *Journal of Financial and Quantitative Analysis*, **25**, pp.87–100.

[41] Ingersoll, J.E. (1987): "Theory of financial decision making", Rowman and Littlefield Publishining, Inc.

[42] Ju, N. (2002): "Pricing Asian and basket options via Taylor expansion", *Journal of Computational Finance*, **5**, pp.79–103.

[43] Kemna, A.G.Z., Vorst, A.C.F. (1990): "A pricing method for options based on average asset values", *Journal of Banking and Finance*, **14**, pp.113–129.

[44] Kolkiewicz, A.W. (2002): "Pricing and hedging more general double-barrier options", *Journal of Computational Finance*, **5**, pp. 1–26.

[45] Kou, S.G. (2003): "Pricing options with curved boundaries", *Statistica Sinica*, **13**, pp. 955–964.

[46] Kunitomo, N., Ikeda, M. (1992): "Pricing options with curved boundaries", *Mathematical Finance*, **2**, pp. 275–298.

[47] Leland, H.E. (1985): "Option pricing and replication with transaction costs", *The Journal of Finance*, **40**, pp.1283–1301.

[48] Linetsky, V. (1998): "The path integral approach to financial modeling and options pricing", *Computational Economics*, **11**, pp.129–163.

[49] Linetsky, V. (2002): "Exotic spectra", *RISK* pp. 85–89.

[50] Linetsky, V. (2004): "Spectral expansions for Asian (average price) options", *Operations Research*, **52**, pp.856–867.

[51] Lipton, A. (2004): "Similarities via self-similarities", *RISK*, , pp.101–105.

[52] Lo, C.F., Yuen, P.H., Hui, C.H. (2001): "Pricing barrier options square root process", *International Journal of Theoretical and Applied Finance*, **4**, pp. 805–818.

[53] Marcozzi, M.D. (2003): "On the valuation of Asian options by variational methods", *Journal on Scientific Computing*, **24**, pp. 1124–1140.

[54] Matacz, A. (2002/03): "Path-dependent option pricing: the path integral partial averaging method", *Journal of Computational Finance*, **6**, pp. 79–103.

[55] Meyer, G.H. (2001): "On pricing American and Asian options with PDE methds", *Acta Mathematica Universitatis Comenianae*, LXX, pp.153–165.

[56] Morozovsky, A. (2000): "A new volatility term in the theory of options with transaction costs", *ArXiv Physics e-prints.*

[57] Pelsser, A., "Pricing Double Barrier Options: An Analytical Approach", *Society for Computational Economics, Computing in Economics and Finance 1997* No. 130.

[58] Pelsser, A. (2000): "Pricing Double barrier options using Laplace transforms", *Finance and Stochastics*, **4**, pp. 95–104.

[59] Ritchken, P., Sankarasubramanian, L., Vijh, A.M. (1993): "The valuation of path dependent contracts on the average" *Management Science*, **39**, pp. 1202–1213.

[60] Ritchken, P. (1995): "On pricing barrier options", *Journal of Derivatives*, 3, pp. 19–28.

[61] Roberts, G.O., Shortland, C.F. (1997): "Pricing barrier options with time-dependent coefficients", *Mathematical Finance*, 7, pp. 83–93.

[62] Rogers, L.C.G., Shi, Z. (1995): "The value of an Asian option", *Journal of Applied Probability*, 32, pp.1077–1088.

[63] Rogers, L.C.G., Zane, O. (1997): "Valuing moving barrier options", *Journal of Computational Finance*, 1, pp.5–11.

[64] Schröder, M. (2000): "On the valuation of double-barrier options: computational aspects", *Journal of Computational Finance*, 3, pp. 5–33.

[65] Seydel, R. (2004): "Tools for computational finance", Springer.

[66] Sidenius, J. (1998): "Double barrier options: valuation by path counting", *Journal of Computational Finance*, **1**, pp. 63–79.

[67] Thompson, G.W.P. (2002): "Bounds on the value of barrier options with curved boundaries", *Judge Institute of Management Working Papers* WP10.

[68] Thompson, G.W.P. (2002): "Fast narrow bounds on the value of Asian options", *Judge Institute of Management Working Papers* WP09.

[69] Turnbull, S.M., Wakeman, L.M. (1991): "A quick algorithm for pricing European average options" *Journal of Financial and Quantitative Analysis*, **26**, pp. 377–389.

[70] Večeř, J. (2001): "A new PDE approach for pricing arithmetic average Asian options", *Journal of Computational Finance*, **4**, pp. 105–113.

[71] Večeř, J. (2001): "New pricing of Asian options", *Preprint, Columbia University*, pp. 1–8.

[72] Večeř, J., Xu, M (2004): "Pricing Asian options in a semimartingale model", *Quantitative Finance*, **4**, pp. 170–175.

[73] Wilmott, P., Dewynne, J.N., Howision, S.D. (1993): "Option Pricing: mathematical models and computation", Oxford Financial Press.

[74] Wilmott, P. (2001): "Paul Wilmott introduces quantitative finance", John Wiley & Sons Ltd.

[75] Zhang, J.E. (2001): "A semi-analytical method for pricing arithmetic average rate options" *Journal of Computational Finance*, **5**, pp. 59–79.

[76] Zhang, J.E. (2003): "Pricing continuously sampled Asian options with perturbation method" *Journal of Futures Markets*, **23**, pp. 535–560.

[77] Zvan, R., Forsyth, P.A., Vetzal, K. (1998): "Robust numerical methods for PDE models of Asian options", *Journal of Computational Finance*, 1, pp.39–78.

[78] Zvan, R., Vetzal, K.R., Forsyth, P.A. (2000): "PDE methods for pricing barrier options", *Journal of Computational Dynamics and Control*, **24**, pp. 1563–1590.

APPENDIX

A. DOUBLE BARRIER ASIAN OPTION

We approach this problem by taking the equation

$$\frac{\partial V}{\partial t} + S\frac{\partial V}{\partial I} + \frac{1}{2}\sigma^2 S^2 \frac{\partial^2 V}{\partial S^2} + rS\frac{\partial V}{\partial S} - rV = 0\,, \tag{A.1}$$

with payoff of the form

$$V(S, I, T) = \exp(\alpha I)\, U(S, T)\,, \tag{A.2}$$

where $U(S,T)$ is a function of S and T, α is a constant and the boundary conditions at the two barriers are

$$V(S, I, t) = 0\,, \quad \text{at } S = S_1 \text{ and } S = S_2\,. \tag{A.3}$$

Since the payoff is in the form of an exponential of I, we can seek a solution in the form

$$V(S, I, t) = \exp(\alpha I)\, U(S, t)\,,$$

and retrieve a PDE in the form

$$\frac{\partial U}{\partial t} + \alpha S U + \frac{1}{2}\sigma^2 S^2 \frac{\partial^2 U}{\partial S^2} + rS\frac{\partial U}{\partial S} - rU = 0\,, \tag{A.4}$$

which we want to solve subject to

$$U(S_1, t) = 0 = U(S_2, t)\,.$$

Setting $t_1 = T - t$, $S = \exp(x)$ and $U(x, t_1) = \exp(\beta t_1 + \gamma x)\, U_1(x, t_1)$, where $t_2 = \frac{\sigma^2}{2}\, t_1$, $\alpha_1 = \frac{2\alpha}{\sigma^2}$ and $\beta = -\frac{r}{2} - \frac{\sigma^2}{8} - \frac{r^2}{2\sigma^2}$, $\gamma = \frac{1}{2} - \frac{r}{\sigma^2}$ the equation takes the form

$$\frac{\partial U_1}{\partial t_2} = \frac{\partial^2 U_1}{\partial x^2} + \alpha_1 \exp(x) U_1\,, \tag{A.5}$$

with

$$U_1 = 0\,, \quad \text{at} \quad x = x_1 = x_2\,,$$

We use separation of variables to solve equation (A.5) by letting

$$U_1(x, t_2) = X(x)\,T(t_2)\,,$$

and we end up having the following equations

$$T(t_2) = A\,\exp\left(-k^2 t_2\right), \tag{A.6}$$

where A is the integrating constant, k is the separation variable, and

$$X''(\bar{x}) + (\alpha_2 \exp(\bar{x}) + k^2)X(\bar{x}) = 0\,, \tag{A.7}$$

where $x = \bar{x} + x_1$, $\alpha_2 = \alpha_1 \exp(x_1)$. The boundary condition at the two barriers are

$$X(0) = 0 = X(x_2 - x_1)\,. \tag{A.8}$$

The exact solution of equation (A.7) can be written in terms of a conjugate pair of Bessel functions of the first kind,

$$X(\bar{x}) = C_1\Gamma(1-2ik)J_{-2ik}(2\sqrt{\alpha_2 \exp(\bar{x})}) + C_2\Gamma(1+2ik)J_{2ik}(2\sqrt{\alpha_2 \exp(\bar{x})})\,. \tag{A.9}$$

For real X we assume that the constants are complex conjugates, $C_1 = a + ib$, $C_2 = a - ib$ where a and b are real. Hence the equation becomes

$$\begin{aligned} X(\bar{x}) &= a\,\Re[\Gamma(1-2ik)J_{-2ik}(2\sqrt{\alpha_2 \exp(\bar{x})}) + \Gamma(1+2ik)J_{2ik}(2\sqrt{\alpha_2 \exp(\bar{x})})] \\ &+ ib\,\Im[\Gamma(1-2ik)J_{-2ik}(2\sqrt{\alpha_2 \exp(\bar{x})}) - \Gamma(1+2ik)J_{2ik}(2\sqrt{\alpha_2 \exp(\bar{x})})] \end{aligned}$$

Applying the boundary conditions (A.8) at the above solution gives us a system of equations

$$a \underbrace{\Re[\Gamma(1-2ik)J_{-2ik}(2\sqrt{\alpha_2}) + \Gamma(1+2ik)J_{2ik}(2\sqrt{\alpha_2})]}_{\alpha} \\ + ib \underbrace{\Im[\Gamma(1-2ik)J_{-2ik}(2\sqrt{\alpha_2}) - \Gamma(1+2ik)J_{2ik}(2\sqrt{\alpha_2})]}_{\beta} = 0\,, \tag{A.10}$$

$$a \underbrace{\Re[\Gamma(1-2ik)J_{-2ik}(2\sqrt{\alpha_2 \exp{(x2-x1)}}) + \Gamma(1+2ik)J_{2ik}(2\sqrt{\alpha_2 \exp{(x2-x1)}})]}_{\gamma} \\ + ib \underbrace{\Im[\Gamma(1-2ik)J_{-2ik}(2\sqrt{\alpha_2 \exp{(x2-x1)}}) - \Gamma(1+2ik)J_{2ik}(2\sqrt{\alpha_2 \exp{(x2-x1)}})]}_{\delta} = 0\,, \tag{A.11}$$

which can be written in the form

$$\begin{pmatrix} \alpha & \beta \\ \gamma & \delta \end{pmatrix} \begin{pmatrix} a \\ ib \end{pmatrix} = 0\,.$$

For a nontrivial solution we require the determinant of the 2×2 matrix to be equal to zero so that a and b are not identically zero

$$\begin{vmatrix} \alpha & \beta \\ \gamma & \delta \end{vmatrix} = 0\,.$$

The determinant will give us a relationship for the eigenvalues k_n of equation (A.7),

$$\begin{aligned} &\Re[\Gamma(1-2ik)J_{-2ik}(2\sqrt{\alpha_2}) + \Gamma(1+2ik)J_{2ik}(2\sqrt{\alpha_2})] \\ &\quad \Im[\Gamma(1-2ik)J_{-2ik}(2\sqrt{\alpha_2 \exp{(x2-x1)}}) - \Gamma(1+2ik)J_{2ik}(2\sqrt{\alpha_2 \exp{(x2-x1)}})] \\ &-\Im[\Gamma(1-2ik)J_{-2ik}(2\sqrt{\alpha_2}) - \Gamma(1+2ik)J_{2ik}(2\sqrt{\alpha_2})] \\ &\quad \Re[\Gamma(1-2ik)J_{-2ik}(2\sqrt{\alpha_2 \exp{(x2-x1)}}) + \Gamma(1+2ik)J_{2ik}(2\sqrt{\alpha_2 \exp{(x2-x1)}})] = 0\,. \end{aligned} \tag{A.12}$$

In order to find the solution of the above equation for k, we have to find the zeros of the Bessel functions. This is a difficult task as the separation variable k is involved in the order of the Bessel function. Because of this complication in finding the values of k, we will use the WKB method to find the eigenvalues k and eigenfunctions $X(\bar{x})$ and determine the orthogonality of the latter. The eigenfunctions will enable us to fit the boundary conditions in a series form and hence determine a good approximation to the exact solution.

The above ODE can be rewritten as

$$\frac{d^2X}{d\bar{x}^2} + k^2\left(1 + \frac{\alpha_2}{k^2}\exp(\bar{x})\right)X(\bar{x}) = 0 \tag{A.13}$$

or

$$\frac{1}{k^2}\frac{d^2X}{d\bar{x}^2} + \left(1 + \frac{\alpha_2}{k^2}\exp(\bar{x})\right)X(\bar{x}) = 0\,, \quad \text{as } k \to \infty\,,$$

which is of the form

$$\epsilon^2 y'' = Q(x)y\,, \quad Q(x) \neq 0\,, \tag{A.14}$$

when ϵ is small ($\epsilon \to 0$). Equation (A.14) is the Schrödinger equation whose approximate solution for ϵ small can be found using the WKB method; that is

$$y(x) \sim C_1 Q(x)^{-1/4}\exp\left(\tfrac{1}{\epsilon}\textstyle\int_a^x \sqrt{Q(t)}\,dt\right) + C_2 Q(x)^{-1/4}\exp\left(-\tfrac{1}{\epsilon}\textstyle\int_a^x \sqrt{Q(t)}\,dt\right), \quad \text{as } \epsilon \to 0\,, \tag{A.15}$$

where C_1 and C_2 are constants to be determined from the initial or boundary conditions and a is an arbitrary but fixed integration point.
Equation (A.7) can be written in the form of (A.14)

$$\frac{1}{k^2}\frac{d^2X}{d\bar{x}^2} = -\left(1 + \frac{\alpha_2}{k^2}\exp(\bar{x})\right)X(\bar{x})\,, \tag{A.16}$$

where $Q(\bar{x}) = -(1 + \frac{\alpha_2}{k^2}\exp(\bar{x}))$, with boundary conditions

$$X(0) = 0 = X(x_2 - x_1)\,.$$

Therefore the general solution to equation (A.16) using the WKB method is

$$X(\bar{x}) \sim C_1 Q(\bar{x})^{-1/4}\exp\left(\int_0^{\bar{x}} \sqrt{Q(\tau)}\,d\tau\right) + C_2 Q(\bar{x})^{-1/4}\exp\left(-\int_0^{\bar{x}} \sqrt{Q(\tau)}\,d\tau\right).$$

Hence the eigen-solutions behave like a Fourier series and are given by the equation

$$X(\bar{x}) = \sum_{n=1}^{\infty} A_n \underbrace{(\alpha_2\exp(\bar{x}) + k_n^2)^{-1/4}\sin\left(\int_0^{\bar{x}} \sqrt{\alpha_2\exp(\tau) + k_n^2}\,d\tau\right)}_{X_n}, \tag{A.17}$$

Therefore the general solution for equation (A.5) in terms of the variable $\bar{x}$ is given by the series

$$U_1(\bar{x}, t_2) = \sum_{n=1}^{\infty} A_n \exp\left(-k_n^2 t_2\right)\left(\alpha_2 \exp\left(\bar{x}\right) + k_n^2\right)^{-1/4} \sin\left(\int_0^{\bar{x}} \sqrt{\alpha_2 \exp\left(\tau\right) + k_n^2}\, d\tau\right). \tag{A.18}$$

We now apply the other boundary condition at $\bar{x} = x_2 - x_1$ to determine the eigenvalues k_n,

$$\int_0^{x_2 - x_1} \sqrt{\alpha_2 \exp\left(\tau\right) + k_n^2}\, d\tau = n\pi. \tag{A.19}$$

For large values of k_n, the above equation takes the form

$$\int_0^{x_2 - x_1} k_n \left(1 + \frac{\alpha_2 \exp\left(\tau\right)}{2\, k_n^2} + \cdots\right) d\tau = n\pi,$$

which will give an approximate formula for evaluating the eigenvalues k_n

$$k_n \int_0^{x_2 - x_1} 1\, d\tau = n\pi \Rightarrow k_n = \frac{n\pi}{x_2 - x_1}, \quad n = 1, 2, 3, \cdots. \tag{A.20}$$

Therefore the eigen-solutions for large k_n become

$$X(\bar{x}) = A_n \left(\alpha_2 \exp\left(\bar{x}\right) + \frac{n^2\pi^2}{(x_2 - x_1)^2}\right)^{-1/4} \sin\left(\int_0^{\bar{x}} \sqrt{\alpha_2 \exp\left(\tau\right) + \frac{n^2\pi^2}{(x_2 - x_1)^2}}\, d\tau\right). \tag{A.21}$$

The constant A_n in the general solution (A.17) can be found by applying the initial condition

$$X'(0) = 1. \tag{A.22}$$

This condition ensures that the derivative at $\bar{x} = 0$ is never zero and will help us determine a numerical solution for the equation. The solution will be arbitrary to a constant A_n which is found by using (A.22) in equation (A.17),

$$A_n = \left(\alpha_2 + k_n^2\right)^{-1/4}. \tag{A.23}$$

Taking equation (A.19) we solve it for the eigenvalues, k_n ($n = 1, 2, 3, \cdots$), by substituting the values $x_1 = 1$, $x_2 = 2$ and $\alpha_2 = 2$. In table A.1 are calculated the first 10 eigenvalues along with the corresponding values of A_n.

Exact values of k_n	Values for A_n
$k_1 = 2.541104171$	$A_1 = 0.5863989934$
$k_2 = 6.003995301$	$A_2 = 0.4026402223$
$k_3 = 9.240811418$	$A_3 = 0.3270629430$
$k_4 = 12.42894355$	$A_4 = 0.2827393373$
$k_5 = 15.59822191$	$A_5 = 0.2526815948$
$k_6 = 18.75819489$	$A_6 = 0.2305627278$
$k_7 = 21.91288553$	$A_7 = 0.2134022178$
$k_8 = 25.06428736$	$A_8 = 0.1995846850$
$k_9 = 28.21350201$	$A_9 = 0.1881477575$
$k_{10} = 31.36118814$	$A_{10} = 0.1784773814$

Tab. A.1: Values of k_n and A_n for $n = 1..10$

Taking the first node, $n = 1$, the WKB solution becomes

$$X(\bar{x}) = A_1(\alpha_2 \exp(\bar{x}) + k_1^2)^{-1/4} \sin\left(\int_0^{\bar{x}} \sqrt{\alpha_2 \exp(\tau) + k_1^2}\, d\tau\right) . \tag{A.24}$$

and looks like the plot in figure A.1. To see how good the value of k_1, for example

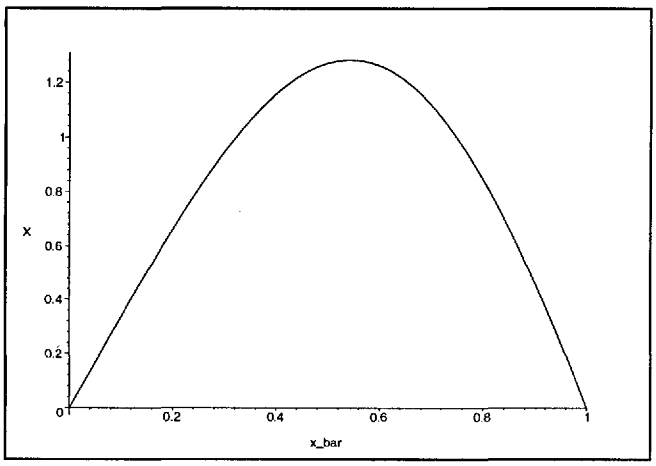

Fig. A.1: Plot of the WKB solution for the first node.

is, we substitute that value in equation (A.7) and solve it by using the boundary and initial condition at the origin

$$X''(\bar{x}) + (\alpha_2 \exp(\bar{x}) + k_1^2)X(\bar{x}) = 0 , \tag{A.25}$$

subject to

$$X(0) = 0 , \quad X'(0) = 1 .$$

We then find the point at which the graph meets the x-axis for the first time which will be a good approximation for the value of $x_2 - x_1$. We then substitute the value of $x_2 - x_1$ into the equation for the eigenvalues, (A.19), and get the corresponding value for k_1. The new value of k_1 should be a good approximation to the one we found initially when we chose the values for x_1 and x_2. The graph cuts the x-axis twice in the interval $[0, 2]$ at $x = 1.002248$ and at $x = 1.819432$. Hence the value of $x_2 - x_1$ for the first node is 1.002248 which we can take as 1.

Substituting the new value found for $x_2 - x_1$ in (A.19) we get a new value for $k_1 = 2.531553503$ ($A_1 = 0.5872418122$), which is a good approximation to the value we found initially when we chose the values for x_1 and x_2 ($k_1 = 2.541104171$, $A_1 = 0.5863989934$). Hence the value $x_2 - x_1 \simeq 1$ can be used in future calculations.

We also check whether the equation for finding k_n for large n, (A.20), is a good approximation to the exact values of k_n found earlier using equation (A.19). In table A.2 we have calculated the values of k_n using both equations.

We observe that as the number of nodes increase, the approximate values for large k_n approach the exact values. On the 20th node the approximate value has grown closer to the exact value and on the 80th node it is identical up to the second decimal place, whereas it takes n to reach the value of 700 in order for the third decimal place to be identical. We observe that as n increases the difference becomes smaller and the approximation for large k_n becomes closer to the exact value.

Returning back to the exact solution we found earlier (A.9), we can check whether the exact values found for $k = k_n$ actually satisfy the equation (A.12), i.e. whether they are solutions of the equation.

For the first node the LHS of equation (A.12) gives a relatively good approximation with the value -0.024902801 and a better for the second node, 0.005777162 (table A.3). From the fourth node and onwards it gives an even better approximation by satisfying the equation up to the fourth decimal place. The larger the node is, the more accurate the values of k_n are when substituted in equation (A.12). Since equation (A.12) is satisfied by all the k_n's given by (A.19), we can consider those values of k_n as the solutions of equation (A.12).

In order to determine the constant coefficient A_n of the series, we need to check the orthogonality of the eigen-solutions.

In general we have the ODE

$$\frac{d^2X}{d\bar{x}^2} = -(\alpha_2 \exp(\bar{x}) + k_n^2)X(\bar{x}),$$

Exact values of k_n using (A.19)	Values for large k_n using (A.20)
$k_1 = 2.541104171$	$k_1 = 3.141592654$
$k_2 = 6.003995301$	$k_2 = 6.283185308$
$k_3 = 9.240811418$	$k_3 = 9.424777962$
$k_4 = 12.42894355$	$k_4 = 12.56637062$
$k_5 = 15.59822191$	$k_5 = 15.70796327$
$k_6 = 18.75819489$	$k_6 = 18.84955592$
$k_7 = 21.91288553$	$k_7 = 21.99114858$
$k_8 = 25.06428736$	$k_8 = 25.13274123$
$k_9 = 28.21350201$	$k_9 = 28.27433389$
$k_{10} = 31.36118814$	$k_{10} = 31.41592654$
$k_{11} = 34.50776393$	$k_{11} = 34.55751919$
$k_{12} = 37.65350768$	$k_{12} = 37.69911185$
$k_{13} = 40.79861181$	$k_{13} = 40.84070450$
$k_{14} = 43.94321363$	$k_{14} = 43.98229716$
$k_{15} = 47.08741377$	$k_{15} = 47.12388981$
$k_{16} = 50.23128765$	$k_{16} = 50.26548246$
$k_{17} = 53.37489291$	$k_{17} = 53.40707512$
$k_{18} = 56.51827437$	$k_{18} = 56.54866777$
$k_{19} = 59.66146741$	$k_{19} = 59.69026043$
$k_{20} = 62.80450030$	$k_{20} = 62.83185308$
$k_{30} = 94.22954645$	$k_{30} = 94.24777962$
$k_{40} = 125.6500318$	$k_{40} = 125.6637062$
$k_{50} = 157.0686934$	$k_{50} = 157.0796327$
$k_{60} = 188.4864432$	$k_{60} = 188.4955592$
$k_{70} = 219.9036721$	$k_{70} = 219.9114858$
$k_{80} = 251.3205754$	$k_{80} = 251.3274123$
$k_{700} = 2199.114076$	$k_{700} = 2199.114858$

Tab. A.2: Exact and approximate values of k_n

which has the solutions $X_m(\bar{x})$ and $X_n(\bar{x})$, say. Then $X_m(\bar{x})$ and $X_n(\bar{x})$ will satisfy the above equation,

$$\frac{d^2X_m}{d\bar{x}^2} = -(\alpha_2 \exp(\bar{x}) + k_m^2)X_m(\bar{x}),$$
$$\frac{d^2X_n}{d\bar{x}^2} = -(\alpha_2 \exp(\bar{x}) + k_n^2)X_n(\bar{x}).$$

Multiplying the first equation by $X_n(\bar{x})$, the second by $X_m(\bar{x})$ and subtracting, we get

$$-(k_m^2 - k_n^2)X_nX_m = X_nX_m'' - X_mX_n'' = \frac{d}{d\bar{x}}(X_nX_m' - X_mX_n').$$

Exact values of k_n	Error approximation of the LHS of (A.12)
$k_1 = 2.541104171$	-0.024902801
$k_2 = 6.003995301$	0.005777162
$k_3 = 9.240811418$	-0.0018935879
$k_4 = 12.42894355$	0.000827504
$k_5 = 15.59822191$	-0.0004306274
$k_6 = 18.75819489$	0.000251449
$k_7 = 21.91288553$	-0.000159191
$k_8 = 25.06428736$	0.0001070308
$k_9 = 28.21350201$	-0.000075327
$k_{10} = 31.36118814$	0.0000550202

Tab. A.3: Error approximation of equation (A.12) for different values of k_n for $n = 1..10$

Integrating over $\bar{x}$ from 0 to $x_2 - x_1$, we obtain

$$\underbrace{\int_0^{x_2-x_1} [X_n X_m'' - X_m X_n''] d\bar{x}}_{[X_n X_m' - X_m X_n']_0^{x_2-x_1}=0, \quad \text{Wronskian}} = -(k_m^2 - k_n^2) \int_0^{x_2-x_1} X_n X_m d\bar{x} \,,$$

where $X_m(0) = X_m(x_2 - x_1) = 0$ are the boundary conditions that hold for any m. The above equality implies that

$$(k_m^2 - k_n^2) \int_0^{x_2-x_1} X_n X_m \, d\bar{x} = 0 \,, \quad \text{unless } k_m^2 = k_n^2 \,.$$

Hence the orthogonality condition that needs to hold is

$$\int_0^{x_2-x_1} X_n X_m \, d\bar{x} = 0 \,, \quad \text{when } n \neq m \,,$$

where the weight function is equal to 1.

The constant A_n of the general solution (A.18) can be found from the normalization condition which we can determine by taking equation (A.17) and multiplying both sides by X_m and integrating over $\bar{x}$ from 0 to $x_2 - x_1$

$$\int_0^{x_2-x_1} X \, X_m \, d\bar{x} = \sum_{n=1}^{\infty} A_n \int_0^{x_2-x_1} X_n X_m \, d\bar{x} \,.$$

The right-hand-side of the above equation is zero unless $m = n$, orthogonality condition:

$$\int_0^{x_2-x_1} X \, X_n \, d\bar{x} = A_n \int_0^{x_2-x_1} (X_n)^2 \, d\bar{x} \,.$$

Hence for different payoffs we can determine the coefficient A_n by using the formula

$$A_n = \frac{\int_0^{x_2-x_1} X\, X_n\, d\bar{x}}{\int_0^{x_2-x_1} (X_n)^2\, d\bar{x}}\,, \tag{A.26}$$

where X is the payoff function. The eigenfunctions now, (A.17), form a complete orthonormal set.

The general solution for the WKB approximation is of the form

$$U_1(\bar{x}, t_2) = \sum_{n=0}^{\infty} \frac{\int_0^{x_2-x_1} X\, X_n\, d\bar{x}}{\int_0^{x_2-x_1} (X_n)^2\, d\bar{x}} \exp\left(-k_n^2 t_2\right) X_n(\bar{x})\,, \tag{A.27}$$

where $X_n(\bar{x})$ is given by equation (A.17).

At expiry $t_2 = 0$ $(t = T)$ the general solution (A.27) takes the form

$$U_1(\bar{x}, 0) = \sum_{n=0}^{\infty} A_n X_n(\bar{x})\,,$$

where the left-hand side is the payoff.

To test the accuracy of the WKB method for the first node $(n = 1)$, we take the payoff to be the function

$$X(\bar{x}) = U_1(\bar{x}, 0) = \begin{cases} 2\bar{x} & , 0 < \bar{x} < \frac{1}{2} \\ -2\bar{x} + 2 & , \frac{1}{2} < \bar{x} < 1 \end{cases}. \tag{A.28}$$

Hence the formula for the coefficient A_n will take the form

$$A_n = \frac{\int_0^1 X X_n(\bar{x})\, d\bar{x}}{\int_0^1 (X_n(\bar{x}))^2\, d\bar{x}} = \frac{\int_0^{\frac{1}{2}} 2\bar{x} X_n(\bar{x})\, d\bar{x} + \int_{\frac{1}{2}}^1 (-2\bar{x} + 2) X_n(\bar{x})\, d\bar{x}}{\int_0^1 (X_n(\bar{x}))^2\, d\bar{x}}\,. \tag{A.29}$$

In table A.4 we show the first ten coefficients of the series calculated for the payoff (A.28).

Hence the solution in terms of the variables $\bar{x}$ and t_2 is

$$\begin{aligned} U(\bar{x}, t_2) \;&=\; \exp\left(-\left(\frac{r}{\sigma^2} + \frac{1}{4} + \frac{r^2}{\sigma^4}\right) t_2 + \left(\frac{1}{2} - \frac{r}{\sigma^2}\right) (\bar{x} + x_1)\right) \qquad \text{(A.30)} \\ &\sum_{n=1}^{\infty} A_n \exp\left(-k_n^2 t_2\right)\left(\alpha_2 \exp(\bar{x}) + k_n^2\right)^{-1/4} \sin\left(\int_0^{\bar{x}} \sqrt{\alpha_2 \exp(\tau) + k_n^2}\, d\tau\right). \end{aligned}$$

As time evolves away from the expiry date (as t_2 gets larger and real time t smaller) the value of the option becomes cheaper. This is illustrated in figure A.2 where we plot the solution for different values of time t_2 by taking $\sigma = 0.5$, $r = 0.05$ and $x_1 = 1$

Values for k_n	Values for A_n for payoff (A.28)
$k_1 = 2.541104171$	$A_1 = 1.433625356$
$k_2 = 6.003995301$	$A_2 = 0.04455112743$
$k_3 = 9.240811418$	$A_3 = -0.2781345140$
$k_4 = 12.42894355$	$A_4 = -0.002947616423$
$k_5 = 15.59822191$	$A_5 = 0.1284327365$
$k_6 = 18.75819489$	$A_6 = 0.001292900196$
$k_7 = 21.91288553$	$A_7 = -0.07749956755$
$k_8 = 25.06428736$	$A_8 = -0.0005280061660$
$k_9 = 28.21350201$	$A_9 = 0.05296101762$
$k_{10} = 31.36118814$	$A_{10} = 0.0002426368150$

Tab. A.4: Values of k_n and A_n for $n = 1..10$ with payoff given by (A.28).

in equation (A.30).

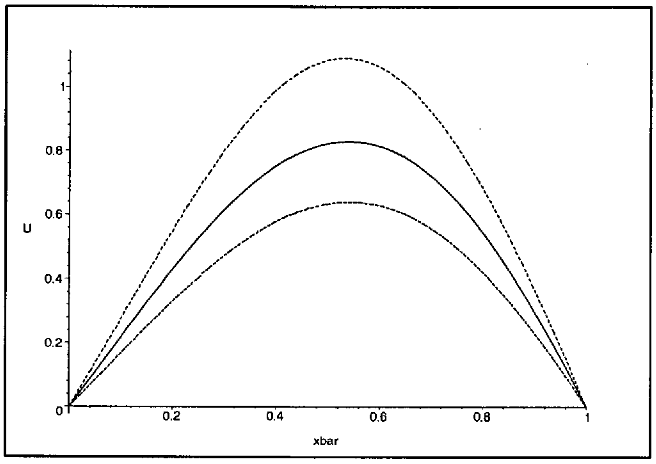

Fig. A.2: Plot of the WKB solution for $n = 5$ at times $t_2 = 0.025$ (dashed line), $t_2 = 0.0625$ (solid line) and $t_2 = 0.1$ (dotted line) .

In terms of the x variable and real time t, the solution takes the form

$$U(x,t) = \exp\left(-\left(\frac{r}{2} + \frac{\sigma^2}{8} + \frac{r^2}{2\sigma^2}\right)(T-t) + \left(\frac{1}{2} - \frac{r}{\sigma^2}\right)x\right) \tag{A.31}$$
$$\sum_{n=1}^{\infty} A_n \exp\left(-\frac{\sigma^2}{2}k_n^2(T-t)\right)(\alpha_2 \exp(x - x_1) + k_n^2)^{-1/4} \sin\left(\int_0^{x-x_1} \sqrt{\alpha_2 \exp(\tau) + k_n^2}\, d\tau\right),$$

and will look like in figure A.3 for $n = 5$ at time $t = T = 1$ and $t = 0.8$.

Going back to the original variable S, the denominator of the coefficient A_n, (A.26),

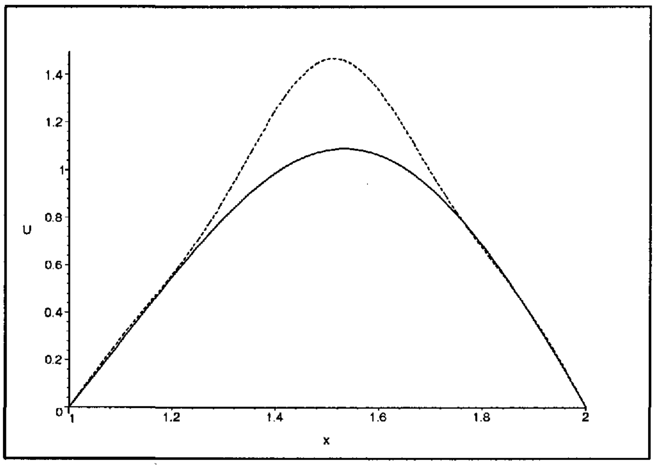

Fig. A.3: Plot of the WKB solution $U(x,t)$ against x for $n = 5$ at the payoff $t = 1$ (dotted line) and $t = 0.8$ (solid line).

will take the form

$$\int_0^{x_2-x_1} (X_n(\bar{x}))^2 \, d\bar{x} = \cdots = \int_{S_1}^{S_2} \frac{1}{S} \left(\alpha_2 \frac{S}{S_1} + k_n^2 \right)^{-1/2} \sin^2 \left(\int_1^{S/S_1} \sqrt{\alpha_2 \, \tau + k_n^2} \, \frac{d\tau}{\tau} \right) dS \, .$$

Using the trigonometric formula for the double angle, $\sin^2 x = \frac{1}{2} - \frac{1}{2}\cos(2x)$, the above equation can be rewritten as

$$\int_{S_1}^{S_2} \frac{1}{2S} \left(\alpha_2 \frac{S}{S_1} + k_n^2 \right)^{-1/2} \left[1 - \cos \left(2 \int_1^{S/S_1} \sqrt{\alpha_2 \, \tau + k_n^2} \, \frac{d\tau}{\tau} \right) \right] dS \, .$$

Hence the coefficient A_n of the WKB solution is given from the formula

$$A_n = \frac{\int_{S_1}^{S_2} \frac{1}{S} \left(\alpha_2 \frac{S}{S_1} + k_n^2 \right)^{-1/4} \sin \left(\int_1^{S/S_1} \sqrt{\alpha_2 \tau + k_n^2} \, \frac{d\tau}{\tau} \right) dS}{\int_{S_1}^{S_2} \frac{1}{2S} \left(\alpha_2 \frac{S}{S_1} + k_n^2 \right)^{-1/2} \left[1 - \cos \left(2 \int_1^{S/S_1} \sqrt{\alpha_2 \, \tau + k_n^2} \, \frac{d\tau}{\tau} \right) \right] dS} \, . \tag{A.32}$$

Hence, the value of the option will be

$$U(S,t) = \exp \left[- \left(\frac{r}{2} + \frac{\sigma^2}{8} + \frac{r^2}{2\sigma^2} \right) (T-t) \right] S^{\frac{1}{2} - \frac{r}{\sigma^2}} \sum_{n=1}^{\infty} A_n \exp \left(-\frac{\sigma^2}{2} \, k_n^2 (T-t) \right) X_n(S) \, , \tag{A.33}$$

and in terms of the average it takes the form

$$V(S,I,t) = \exp\left[\alpha I - \left(\frac{r}{2} + \frac{\sigma^2}{8} + \frac{r^2}{2\sigma^2}\right)(T-t)\right] S^{\frac{1}{2}-\frac{r}{\sigma^2}} \sum_{n=1}^{\infty} A_n \exp\left(-\frac{\sigma^2}{2} k_n^2 (T-t)\right) X_n(S), \quad (A.34)$$

where A_n is given by (A.32) and $X_n(S)$ is given by

$$X_n(S) = \left(\alpha_2 \frac{S}{S_1} + k_n^2\right)^{-1/4} \sin\left(\int_1^{S/S_1} \sqrt{\alpha_2 \tau + k_n^2}\, \frac{d\tau}{\tau}\right).$$

In terms of the original variables S and t, $U(S,t)$ for $t = 1$, $t = 0.8$ and $t = 0.5$ looks like in figure (A.4).

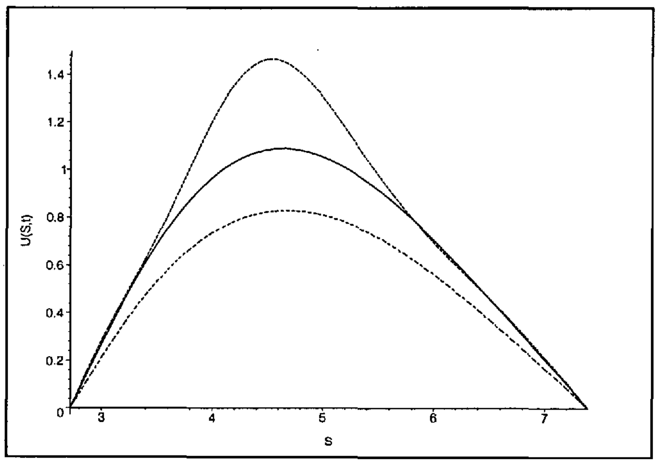

Fig. A.4: Plot of the WKB solution $U(S,t)$ against S for $n = 5$ at the payoff $t = 1$ (dashed line), $t = 0.8$ (solid line) and $t = 0.5$ (dotted line).

We now return to the exact solution (A.9). If we take equation (A.10) and solve it for the constant b

$$b = -\frac{a}{i} \frac{\Re[\Gamma(1-2ik_n)J_{-2ik_n}(2\sqrt{\alpha_2}) + \Gamma(1+2ik_n)J_{2ik_n}(2\sqrt{\alpha_2})]}{\Im[\Gamma(1-2ik_n)J_{-2ik_n}(2\sqrt{\alpha_2}) - \Gamma(1+2ik_n)J_{2ik_n}(2\sqrt{\alpha_2})]},$$

then the exact solution for (A.7) can be written as the sum of all the nodes in terms of the constant coefficient a_n

$$\begin{aligned}
X(\bar{x}) &= \sum_{n=1}^{\infty} a_n \Big(\Re[\Gamma(1-2ik_n)J_{-2ik_n}(2\sqrt{\alpha_2 \exp(\bar{x})}) + \Gamma(1+2ik_n)J_{2ik_n}(2\sqrt{\alpha_2 \exp(\bar{x})})] \\
&- \frac{\Re[\Gamma(1-2ik_n)J_{-2ik_n}(2\sqrt{\alpha_2}) + \Gamma(1+2ik_n)J_{2ik_n}(2\sqrt{\alpha_2})]}{\Im[\Gamma(1-2ik_n)J_{-2ik_n}(2\sqrt{\alpha_2}) - \Gamma(1+2ik_n)J_{2ik_n}(2\sqrt{\alpha_2})]} \\
&\quad \Im[\Gamma(1-2ik_n)J_{-2ik_n}(2\sqrt{\alpha_2 \exp(\bar{x})}) - \Gamma(1+2ik_n)J_{2ik_n}(2\sqrt{\alpha_2 \exp(\bar{x})})] \Big) .
\end{aligned}$$

We can rewrite the above equation as

$$X(\bar{x}) = \sum_{n=1}^{\infty} B_n X_n(\bar{x}) , \tag{A.35}$$

where $B_n = a_n \Re[\Gamma(1-2ik_n)J_{-2ik_n}(2\sqrt{\alpha_2}) + \Gamma(1+2ik_n)J_{2ik_n}(2\sqrt{\alpha_2})]$ and X_n is

$$\begin{aligned}
X_n(\bar{x}) &= \frac{\Re[\Gamma(1-2ik_n)J_{-2ik_n}(2\sqrt{\alpha_2 \exp(\bar{x})}) + \Gamma(1+2ik_n)J_{2ik_n}(2\sqrt{\alpha_2 \exp(\bar{x})})]}{\Re[\Gamma(1-2ik_n)J_{-2ik_n}(2\sqrt{\alpha_2}) + \Gamma(1+2ik_n)J_{2ik_n}(2\sqrt{\alpha_2})]} \\
&- \frac{\Im[\Gamma(1-2ik_n)J_{-2ik_n}(2\sqrt{\alpha_2 \exp(\bar{x})}) - \Gamma(1+2ik_n)J_{2ik_n}(2\sqrt{\alpha_2 \exp(\bar{x})})]}{\Im[\Gamma(1-2ik_n)J_{-2ik_n}(2\sqrt{\alpha_2}) - \Gamma(1+2ik_n)J_{2ik_n}(2\sqrt{\alpha_2})]} .
\end{aligned} \tag{A.36}$$

Hence the solution $U_1(\bar{x}, t_2)$ will look like

$$U_1(\bar{x}, t_2) = \sum_{n=1}^{\infty} B_n \exp(-k_n^2 t_2) X_n(\bar{x}) . \tag{A.37}$$

The constant B_n is determined from equation (A.26)

$$B_n = \frac{\int_0^{x_2-x_1} X X_n \, d\bar{x}}{\int_0^{x_2-x_1} (X_n)^2 \, d\bar{x}} , \tag{A.38}$$

where X is the payoff function.

For the payoff having the form (A.28), the constant B_n takes the values shown in table A.5. In figure A.5 we plot $X(\bar{x}, t_2)$ at time $t_2 = 0.5$ against $\bar{x}$ the WKB solution and

n	Values for k_n	Values for B_n
1	2.541104171	0.3777619415
2	6.003995301	−0.006343438072
3	9.240811418	0.02017037334
4	12.42894355	−0.0004135957651
5	15.59822191	−0.003849954886

Tab. A.5: Values of k_n and B_n for $n = 1..5$

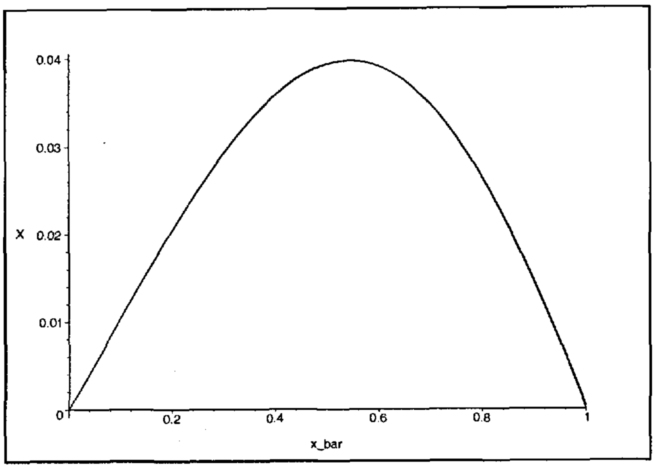

Fig. A.5: Plot of the exact series solution (A.35) and the WKB solution (A.21) for $n = 5$ against $\bar{x}$ at time $t_2 = 0.5$.

the exact solution. We observe that the WKB solution is identical to the exact solution making it an accurate method of solving the problem. Hence the complete solution for the original PDE (A.1) is

$$\begin{aligned} V(S,I,t) &= \exp(\alpha I)\exp\left[-\left(\frac{r}{2}+\frac{\sigma^2}{8}+\frac{r^2}{2\sigma^2}\right)(T-t)\right]S^{\frac{1}{2}-\frac{r}{\sigma^2}} \\ & \sum_{n=1}^{\infty} B_n \exp\left(-\frac{\sigma^2}{2}k_n^2(T-t)\right)X_n(S;S_1), \end{aligned} \tag{A.39}$$

where

$$\begin{aligned} X_n(S;S_1) &= \frac{\Re\left[\Gamma(1-2ik_n)J_{-2ik_n}\left(2\sqrt{\frac{2\alpha}{\sigma^2}S}\right)+\Gamma(1+2ik_n)J_{2ik_n}\left(2\sqrt{\frac{2\alpha}{\sigma^2}S}\right)\right]}{\Re\left[\Gamma(1-2ik_n)J_{-2ik_n}\left(2\sqrt{\frac{2\alpha}{\sigma^2}S_1}\right)+\Gamma(1+2ik_n)J_{2ik_n}\left(2\sqrt{\frac{2\alpha}{\sigma^2}S_1}\right)\right]} \\ &- \frac{\Im\left[\Gamma(1-2ik_n)J_{-2ik_n}\left(2\sqrt{\frac{2\alpha}{\sigma^2}S}\right)-\Gamma(1+2ik_n)J_{2ik_n}\left(2\sqrt{\frac{2\alpha}{\sigma^2}S}\right)\right]}{\Im\left[\Gamma(1-2ik_n)J_{-2ik_n}\left(2\sqrt{\frac{2\alpha}{\sigma^2}S_1}\right)-\Gamma(1+2ik_n)J_{2ik_n}\left(2\sqrt{\frac{2\alpha}{\sigma^2}S_1}\right)\right]}, \end{aligned} \tag{A.40}$$

and B_n is given by

$$B_n = \frac{\int_{S_1}^{S_2} X(S)\, X_n(S)\, \frac{dS}{S}}{\int_{S_1}^{S_2} (X_n(S))^2\, \frac{dS}{S}}. \tag{A.41}$$